

THESIS ON NATURAL AND EXACT SCIENCES B202

**Detection of Psycho- and Bioactive Drugs  
in Different Sample Matrices  
by Fluorescence Spectroscopy and  
Capillary Electrophoresis**

JEKATERINA MAZINA

**TUT**  
PRESS

TALLINN UNIVERSITY OF TECHNOLOGY  
Faculty of Science  
Department of Chemistry

**This dissertation was accepted for the defence of the degree of Doctor of Philosophy in Chemistry on 11<sup>th</sup> of December, 2015.**

**Supervisors:** Prof. Mihkel Kaljurand  
Department of Chemistry, Faculty of Science, Tallinn  
University of Technology, Estonia

PhD Larisa Poryvkina  
NarTest AS, Estonia

**Reviewed by:** PhD Andrus Seiman  
Department of Chemistry, Faculty of Science, Tallinn  
University of Technology, Estonia

**Opponents:** Prof. Boguslaw Buszewski  
Chair of Environmental Chemistry and Bioanalysis,  
Faculty of Chemistry, Nicolaus Copernicus University,  
Poland

Prof. Heli Siren  
Department of Chemistry, Faculty of Science,  
University of Helsinki, Finland

**Defence of the thesis:** 28<sup>th</sup> of January, 2016

Declaration:

*Hereby I declare that this doctoral thesis, my original investigation and achievement, submitted for the doctoral degree at Tallinn University of Technology has not been submitted for doctoral or equivalent academic degree before.*

/Jekaterina Mazina/



Copyright: Jekaterina Mazina, 2016  
ISSN 1406-4723  
ISBN 978-9949-23-888-0 (publication)  
ISBN 978-9949-23-889-7 (PDF)

LOODUS- JA TÄPPISTEADUSED B202

**Psühho- ja bioaktiivsete ainete tuvastamine  
erinevates proovimaatriksites kasutades  
fluoresentsspektroskoopia ja  
kapillaarelektroforeesi meetodeid**

JEKATERINA MAZINA



*Моей семье посвящается...*



## CONTENTS

LIST OF PUBLICATIONS.....	9
THE AUTHOR'S CONTRIBUTION.....	9
ABBREVIATIONS.....	11
INTRODUCTION.....	13
1 LITERATURE OVERVIEW.....	15
1.1 Purity of street drug samples.....	15
1.2 Drugs: health effects and drug addiction.....	17
1.2.1 Cannabis and its metabolites.....	18
1.2.2 $\gamma$ -hydroxybutyric acid.....	22
1.2.3 Herbal medicines and their constituents.....	24
1.3 Regulations and directives for drug detection in bulk seizures and clinical samples.....	25
1.4 On-site detection methods.....	26
1.4.1 Available on-site portable methods for detection of drugs at market.....	27
1.4.2 Spectral fluorescence signature method.....	29
1.4.3 Capillary electrophoresis.....	30
1.5 Pattern recognition techniques for data analysis.....	32
1.5.1 Data preparation.....	32
1.5.2 Unsupervised method.....	33
1.5.3 Supervised methods.....	35
1.6 Validation requirements.....	35
2 AIMS OF THE STUDY.....	37
3 EXPERIMENTAL.....	38
3.1 Reagents and samples.....	38
3.1.1 Samples in Publication I.....	38
3.1.2 Herbal samples in Publication II.....	38
3.1.3 Saliva samples in Publications III and IV.....	38
3.2 Methods.....	38
3.2.1 Spectral fluorescence signature method (EEM spectroscopy) ...	38
3.2.2 Capillary electrophoresis.....	39

3.2.3	HPLC-DAD-MS.....	42
4	RESULTS AND DISCUSSION .....	43
4.1	Spectral Fluorescence Signature method coupled to chemometric techniques as a tool for the rapid and reliable determination of drugs and fingerprints in herbs and solid samples .....	43
4.1.1	Qualitative detection of illegal drugs (cocaine, heroin and MDMA) in seized street samples based on SFS data and ANN: validation of method (Publication I) .....	43
4.1.2	Fluorescence, electrophoretic and chromatographic fingerprints of herbal medicines and their comparative chemometric analysis (Publication II) .....	47
4.2	Capillary electrophoresis as a tool for drug abuse determination in saliva .....	52
4.2.1	Determination of cannabinoids in oral fluid (Publication III)....	52
4.2.2	Determination of $\gamma$ -hydroxybutyric acid in oral fluid (Publication IV).....	56
5	CONCLUSIONS.....	59
	REFERENCES.....	61
	ACKNOWLEDGEMENTS .....	66
	ABSTRACT .....	68
	KOKKUVÖTE.....	69
	LIST OF ORIGINAL PUBLICATIONS .....	74
	CURRICULUM VITAE .....	76
	ELULOOKIRJELDUS.....	78

## LIST OF PUBLICATIONS

This thesis is based on the following publications, which are referred to by Roman numerals within the text:

- I. Mazina, J., Aleksejev, V., Ivkina, T., Kaljurand, M., Poryvkina, L. Qualitative detection of illegal drugs (cocaine, heroin and MDMA) in seized street samples based on SFS data and ANN: validation of method. *Journal of Chemometrics* **2012**, 26, 442–455.
- II. Mazina, J., Vaher, M., Kuhtinskaja, M., Poryvkina, L., Kaljurand, M. Fluorescence, electrophoretic and chromatographic fingerprints of herbal medicines and their comparative chemometric analysis. *Talanta* **2015**, 139, 233–246.
- III. Mazina, J., Špiljova, A., Vaher, M., Kaljurand, M., Kulp, M. Rapid capillary electrophoresis method with LED-induced native fluorescence detection for the analysis of cannabinoids in oral fluid. *Analytical methods* **2015**, 7, 7741–7747.
- IV. Mazina, J., Saar-Reismaa, P., Kulp, M., Poryvkina, L., Kaljurand, M., Vaher, M. Determination of  $\gamma$ -hydroxybutyric acid in saliva by capillary electrophoresis coupled with contactless conductivity and indirect UV absorbance detectors. *Electrophoresis* **2015**, 36, 3042–3049.

## THE AUTHOR'S CONTRIBUTION

The contribution made by the author to the publications included is the following:

- I. The author designed the experiments and carried out all experiments for the validation study of the SFS-ANN method for a qualitative analysis of cocaine, heroin and MDMA. She prepared the libraries for the expert system construction and implementation. The author proposed an approach for evaluation of the uncertainty region for artificial neural networks (ANN) implemented for the binary response “detected/not detected”. The author interpreted the results obtained, wrote the manuscript and is the first and corresponding author.

II. The author was responsible for planning the experiments and carried out all SFS measurements of medical and tea herbs with the aim to develop a rapid and reliable tool for evaluating the quality and authenticity of herbal medicines (HMs) based on their polyphenolic composition “fingerprints”. To achieve better results in the classification of HMs she tested chemometric techniques such as PARAFAC and PCA combined with CA. She conducted the validation of the SFS method and performed comparative analysis of data with those of reference methods like CE and HPLC. The author wrote the manuscript and is the first and corresponding author.

III. The author conducted preliminary experiments and identified a suitable electrophoretic methodology. She was responsible for planning the experiments, participated in the interpretation of the results and analysis of data. She participated in the preparation of the manuscript and is the first author.

IV. The author optimized the experimental setup and carried out part of the experimental work. She conducted the pre-processing of electrophoretic data and interpreted the results. The author wrote the manuscript and is the first and corresponding author.

## ABBREVIATIONS

2C-B – 4-bromo-2,5-dimethoxyphenethylamine  
4-FA – 4-fluoroamphetamine  
5-MeO-DiPT – N,N-Diisopropyl-5-methoxytryptamine  
ABS – absorbance  
ACN – acetonitrile  
AIDS – acquired immune deficiency syndrome  
ANN – artificial neural network  
ATS – amphetamine type stimulants  
BAC – blood alcohol content  
BGE – background electrolyte  
BZP – benzylpiperazine  
C<sup>4</sup>D – capacitively-coupled contactless conductivity detector  
CBD – cannabidiol  
CBDA – cannabidiolic acid  
CC $\beta$  – threshold limit  
CE – capillary electrophoresis  
CHMP – Committee for Medicinal Products for Human Use  
CTAB – cetyltrimethylammonium bromide  
DAD – diode array detector  
DHBA – dihydroxybenzoic acid  
EFSI – Estonian Forensic Science Institute  
EMCDDA – European Monitoring Centre for Drugs and Drugs Addiction  
EOF – electroosmotic flow  
GABA –  $\gamma$ -aminobutyric acid  
GC – gas chromatography  
GHB –  $\gamma$ -hydroxybutyric acid  
HCA – hydroxycinnamic acid-like derivatives  
HM – herbal medicines  
HPLC – high-performance liquid chromatography  
IDL – instrument detection limit  
IMS – ion mobility spectrometry  
Interpol – International Criminal Police Organization  
IQL – instrument quantification limit  
LC – liquid chromatography  
LED – light emitting diode  
LoD – limit of detection  
LoQ – limit of quantification  
LSD – lysergic acid diethylamide  
mCPP – *meta*-chlorophenylpiperazine  
MDA – 3,4-methylenedioxyamphetamine  
MDEA – 3,4-methylenedioxy-N-ethyl-amphetamine  
MDMA – 3,4-methylenedioxyamphetamine  
MDP2P – 3,4-Methylenedioxyphenylpropan-2-one

MDPV – methylenedioxypropylamphetamine  
ME – matrix effect  
MeOH – methanol  
MLP – multilayer perceptron  
MS – mass spectrometry  
NACE – non-aqueous capillary electrophoresis  
NMR – nuclear magnetic resonance  
NSAIDs – nonsteroidal anti-inflammatory drugs  
OF – oral fluid  
PARAFAC – parallel factor analysis  
PCA – principal component analysis  
PMA – *para*-methoxyamphetamine  
PMMA – *para*-methoxy-N-methylamphetamine  
PMPA – pinacolyl methylphosphonic acid  
Rec – recovery  
SFS – spectral fluorescence signature  
SWGDRUG – Scientific Working Group for the Analysis of Seized Drugs  
THC – (-)-*trans*- $\Delta^9$ -tetrahydrocannabinol  
THC-COOH – 11-nor-9-Carboxy-THC  
TFMPP – 3-trifluoromethylphenylpiperazine  
UN – United Nations  
UNODC – United Nations Office on Drugs and Crime  
UV – ultraviolet

# INTRODUCTION

## **Illegal drug trafficking and abuse – a global disaster**

Illegal drug abuse and addiction is a globally recognized phenomenon encountering thousands of victims every year. It is reported that there were estimated 187,100 drug-related deaths only in 2013<sup>1</sup>. According to the related international organizations such as the United Nations Office on Drugs and Crime (UNODC), the European Monitoring Centre for Drugs and Drug Addiction (EMCDDA) and the International Criminal Police Organization (Interpol), drug-related crimes do not stop boosting and have shown an increase over the period of 2003 – 2013<sup>1,2</sup>.

There seems to be no obvious evidence of a decline of the trafficking, production and distribution of illegal drugs. Furthermore, the situation has generally remained stable. Undoubtedly, consumption of a certain drug, for example, heroin, cocaine or marijuana, may decline in one region or part of the world, but boost in another, as happened to opiates, cannabis and cocaine in a number of counties of Western and Central Europe in 2012 in contrast to 2011<sup>2,3</sup>. At the same time, the demand for opiates has grown in South-West Asia, the use of cocaine has expanded in Oceania and the growth was observed in the United States<sup>3</sup>. In addition, the demand for amphetamine-type stimulants (ATS) such as ecstasy (3,4-methylenedioxymethamphetamine (MDMA)), methamphetamine and amphetamine has increased globally<sup>1, 3</sup>. Therefore, the extent of drug production and distribution exhibits its own specificities depending on region or country.

The War on Drug production, trafficking and distribution is ongoing at different international levels, including law enforcement, border control, forensic laboratories and private sector. The related parties need effective and accurate tools to proactively respond to the crimes facilitated by the illicit distribution of drugs. Therefore, the implementation of innovative technologies is beyond doubt.

Generally, drug testing in street seizures and biological samples is conducted on road, at workplaces, border controls, post offices, hospitals and prisons. Gathering evidence of drug production, distribution and trafficking requires analysis of seized samples, searching of drug traces on the hands or clothes of suspected individuals. Biological samples such as blood, urine or oral fluids can be used as an evidence of drug abuse or consumption on the scene of crime, at workplace, hospitals, clubs, schools and other places.

Undoubtedly, analysis of drugs is a complex and sensitive challenge. The conclusion made on drugs abuse or connection to drug distribution/production

may lead to social and economic consequences. The drug testing must eliminate false positive results and reduce false negative ones, leading to the cases that only a guilty person is punished. Therefore, strict requirements and recommendations for drugs testing are set by international organizations.

Considering the above, the development of rapid, sensitive and reliable methods for drugs detection is of utmost importance. This dissertation deals with the development of screening methods for different illegal drugs such as cocaine, heroin and MDMA in seizures by using the spectral fluorescence signature (SFS) method. The artificial intelligence system Artificial Neural Networks (ANN) utilized as an expert system for fluorescent pattern recognition was validated according to the internal requirements and recommendations. Moreover, the working capability of ANN often described as 'black box' was evaluated via an approach to uncertainty regions estimation for qualitative methods and proven to be effective for this task.

The SFS method, which was also applied for fingerprinting analysis of herbal medicines, offered good sensitivity, reproducibility and accuracy.

Moreover, methodologies for determination of abuse of two illegal drugs in oral fluids are proposed. In this study, capillary electrophoresis (CE) instruments combined with different detectors such as light-emitting diode (LED) induced fluorescence detector, capacitively-coupled contactless conductivity detector (C<sup>4</sup>D) and diode array detector were used for cannabis and  $\gamma$ -hydroxybutyric acid (GHB) abuse determination in saliva samples. Furthermore, this is the first study to utilize CE-C<sup>4</sup>D for detection of GHB in saliva samples.

# 1 LITERATURE OVERVIEW

## 1.1 Purity of street drug samples

Illegal drugs are distributed in different forms such as tablets, powders, capsules, crystals, liquids, etc. In case of prescription drugs, the active ingredient or ingredients and diluents are known and the content and proportions are strictly regulated.

Illegal drugs sold in streets can be compared to the “black box” as their composition has often been cut, diluted or adulterated with other compounds. This is done for several reasons. First, dealers are interested in earning more profit. To increase the amount of an illegal drug, diluting its active ingredient, for instance, with glucose, lactose, mannitol, etc. and, therefore, getting more samples available for sale, is one of the ways. Another reason is the desire to enhance the effect of an active ingredient, adding another psychoactive substance or even substances (caffeine, paracetamol, levamisole) to the drug. The final overall effect is sometimes unpredictable and can lead to overdosing or even death. Moreover, the trafficking of illegal drugs across the countries is often associated with smuggling, when the substances are hidden in coffee, soaked in clothes, sealed in plastic bottles, hidden in soap or alcoholic beverages, etc. Finally, the synthesis or purification of by-products has also occurred even in uncut or unadulterated substances. As a consequence, the purity of street samples varies from drug to drug, from dealer to dealer, from country to country.

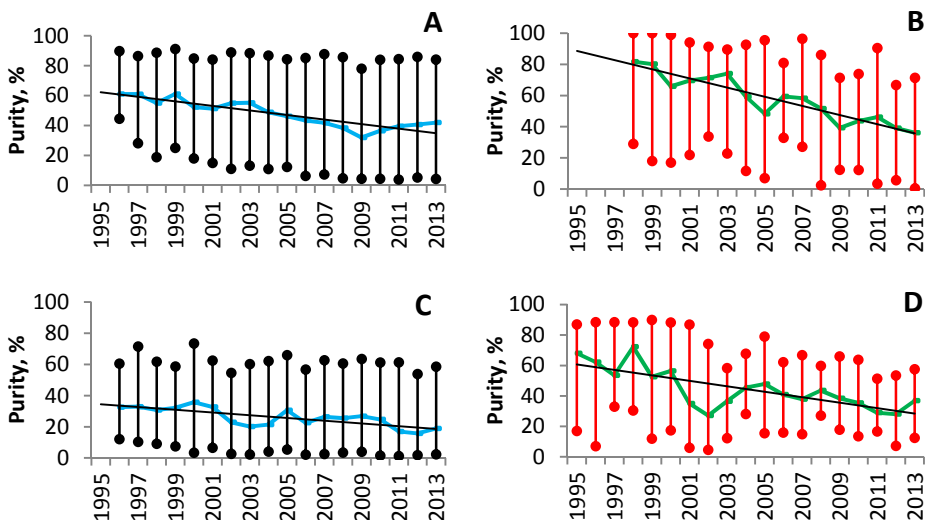


Figure 1. Statistics on purity of drug seizures based on EMCDDA data (mean, max, min) in EU countries: A – cocaine; B – cocaine crack; C – heroin brown; D – heroin white (graphics have been constructed using statistics on EMCDDA<sup>4</sup>).

The seized sample purity statistics is published by EMCDDA every year<sup>4</sup>. Figure 1 shows the statistics on cocaine and heroin seizures during 1995 and 2013. It is clearly observed that there is a tendency of heroin and cocaine purity decrease throughout the years. The reason of purity decrease can be hidden in the shortage of illegal drugs due to the proactive work of law enforcement bodies and international organizations against the drug war. As a consequence, it leads to dilution and adulteration of illegal drug samples at market.

**Table 1. Common cocaine, heroin and MDMA adulterants and diluents (the most common varieties are indicated in bold)**

<b>Cocaine</b> <sup>5,6,7</sup>	<b>Heroin</b> <sup>5,6</sup>	<b>MDMA</b> <sup>8,9</sup>
<i>Adulterants:</i>		
Acetylsalicylic acid	<b>Caffeine</b>	2C-B*
Atropine	Clenbuterol	4-FA*
Benzocaine	Cocaine	4-Methylmethcathinone
<b>Caffeine</b>	Codeine	5-MeO-DiPT*
Creatine	Dextromethorphan	Acetylsalicylic acid
Diclofenac	Diltiazem	Amphetamine
<b>Diltiazem</b>	<b>Griseofulvine</b>	Benocyclidine
Ephedrine	Levamisole	Benzocaine
<b>Hydroxyzine</b>	Lidocaine	BZP*
Ibuprophen	Morphine	<b>Caffeine</b>
<b>Levamisole</b>	<b>Paracetamol</b>	Cocaine
<b>Lidocaine</b>	Phenacetin	Dextromethorphan
Methylephedrine	Phenobarbital	Diphenhydramine
Paracetamol,	Piracetam	Ethylone
<b>Phenacetin</b>	Scopolamine	Guaifenesin
Procaine	Strychnine	<b>Ketamine</b>
Propoxyphene		Lidocaine
Strychnine		LSD*
Tetracaine		mCPP*
		MDA*
<i>Diluents:</i>	<i>Diluents:</i>	MDEA*
Fructose	<b>Glucose</b>	MDP2P*
<b>Glucose</b>	Inositol	MDPV*
<b>Inositol</b>	Lactose	<b>Methamphetamine</b>
<b>Lactose</b>	<b>Mannitol</b>	Methylone
<b>Mannitol</b>	Quinine	<b>Methylsulfonylmethane</b>
Sucrose	Sucrose	Paracetamol
		Phentermine
		Phthalates
		Piracetam
		PMA*
		PMMA*
		<b>Procaine</b>
		Pseudo-/ephedrine
		TFMPP*

\* abbreviations are defined in ABBREVIATIONS list.

The variability of illegal drugs cutting agents and adulterants has been studied by different research groups<sup>5,6</sup>. The common cocaine adulterants are levamisole, lidocaine, procaine, benzocaine, caffeine, boric acid, hydroxyzine, diltiazem and phenacetin. The widespread heroin adulterants are caffeine, paracetamol and griseofulvine. MDMA adulterants are caffeine, ketamine, methamphetamine, methylsulfonylmethane and procaine. Moreover, the mixtures of different adulterants are quite widely spread, especially for MDMA tablets<sup>9</sup>. The common cocaine, heroin and MDMA adulterants and diluents are listed in Table 1.

## 1.2 Drugs: health effects and drug addiction

In medicine, “drug” refers to any substance with the potential to prevent or cure disease or enhance physical or mental welfare. According to the United Nations (UN) Single Convention on Narcotic Drugs of 1961, amended in 1972, “*drug*” means any of the substances in Schedule I and II, whether natural or synthetic<sup>10</sup>.

Generally, drugs are referred to as psychoactive drugs (equivalent to psychotropic drug), altering the mind and processes in the human body and possibly, but not necessarily, producing dependence. The 1971 UN Convention on Psychotropic Substances defined the “*psychotropic*” compound as any substance, natural or synthetic, or any natural material in Schedule I, II, III or IV.

Scheduling varies from country to country and by compound. Examples of Schedule I substances include marijuana, tetrahydrocannabinols (THC, delta-8 THC, delta-9 THC, dronabinol, etc.), heroin (diacetylmorphine, diamorphine),  $\gamma$ -hydroxybutyric acid (GHB), and lysergic acid diethylamide (LSD). Examples of Schedule II substances include cocaine, coca leaves, codeine, fentanyl, amphetamine, and methamphetamine.

Illegal drugs can be divided into synthetic and plant-derived drugs. Common drugs that are obtained from the plants are cocaine and heroin. Moreover, herbal plants such as *Cannabis* products (marijuana, hashish (THC, CBD and other cannabinoids)), *Catha edulis* or khat (cathine and cathinone), *Erythroxylum coca* or coca (cocaine), *Papaver somniferum* or opium poppy (morphine, codeine and other opiates), *Mitragyna speciosa* or kratom (mitragynine), *Salvia divinorum* (salvinorin A), *Ephedra sinica* (ephedrine) and many, many others can be used as illegal drugs. Common synthetic drugs are amphetamine, methamphetamine, ecstasy (MDMA, MDA, MDEA) and fentanyl and its analogues.

Certainly, not always have illegal drugs been unlawful. Historically, these substances have been produced as medicaments for treatment of different disorders in the human body. Moreover, nowadays some of them are still well-recognized prescription medications. For instance, popular prescription medicines are Dronabinol (the main ingredient (-)-*trans*- $\Delta$ 9-

tetrahydrocannabinol or THC) used to treat the loss of appetite that causes weight loss in people with AIDS (Acquired Immune Deficiency Syndrome), Adderall (the main ingredient amphetamine) employed to treat attention deficit hyperactivity disorder (ADHD) and narcolepsy, or Xyrem (sodium  $\gamma$ -hydroxybutyrate) used to treat excessive daytime sleepiness (EDS) or cataplexy associated with narcolepsy and etc. On the one hand, these substances can be effective drugs, on the other hand, scheduled compounds may have several adverse effects and addictive properties.

Nevertheless, psychoactive drugs are divided into groups according to their pharmacological effects. The most known stimulants are amphetamine, cocaine, caffeine and nicotine. Depressants with an opposite effect to the stimulants include such representatives as opioids, barbiturates, benzodiazepines, GHB, and ethanol. MDMA commonly known as Ecstasy, and its analogues MDA and MDEA are euphoriant. LSD and psilocybin are hallucinogens, altering a person's perception of reality.

### **1.2.1 Cannabis and its metabolites**

Cannabis products are the most widely used illegal drugs. According to the EMCDDA report, every 4<sup>th</sup> person in the European Union has tried cannabis at least once in his life. Therefore, the driving impairment under the influence of illegal drugs can be caused with higher probability by use of cannabis. The fatal traffic accidents are thoroughly monitored and the drivers responsible are identified. The drivers are screened for possible alcohol and/or drugs abuse. According to surveys, THC is detected in 4 – 14 % of drivers who have been injured or fatally injured in traffic accidents<sup>11</sup>. Cannabis use significantly impairs motor coordination, judgement, visual functions and reaction time. Furthermore, the use of cannabis together with alcohol is the worst, having additive or even multiplicative effects on conscious control.

Generally, the recognition of cannabis use is carried out in urine or blood tests. But there are also other biological samples such as oral fluids (OFs) that can be utilized to detect recent drug use. One is saliva, the collection of which is less invasive, painless and easier than that of blood or urine. Saliva is a perfect alternative to blood and urine and can be used as a screening sample matrix on-site, giving a more accurate picture of the processes going on in the body. However, saliva is still not well recognized and is underestimated as an evidence matrix. Other sample matrixes are sweat, exhaled breath condensate and hair.

The distribution of different cannabinoids in the body has induced the investigation of their metabolites. Cannabinoids are present in cannabis plants as a mixture of carboxylic acids. Tetrahydrocannabinolic acid (THCA) and cannabidiolic acid (CBDA) are acidic forms of THC and CBD, abundantly found in the plant material. THCA and CBDA decarboxylate naturally over time

slowly or upon heating (smoking, cooking, etc.) quickly to the most psychoactive form, THC, and the non-psychoactive form, CBD, respectively. The efficiency of decarboxylation depends on temperature. The temperature higher than 140 °C is optimal for THCA conversion, while the temperature not higher than 150 °C leads to the formation of a degradation product cannabinol (CBN)<sup>12</sup>. Both THCA and THC are present in saliva via direct absorption into the buccal mucosa during smoking/inhalation. During smoking THC is rapidly transferred from the lungs to the blood and is almost immediately bound to lipoproteins in the blood plasma (90% of THC). During hydroxylation of THC, an active metabolite 11-OH-THC is formed, which is further oxidized to the inactive form THC-COOH. THC-COOH and its glucuronic acid conjugates are excreted in the urine and feces<sup>13,14,15</sup>. The metabolic route of THCA, THC, 11-OH-THC as well as THC-COOH and its glucuronide form is shown in Figure 2.

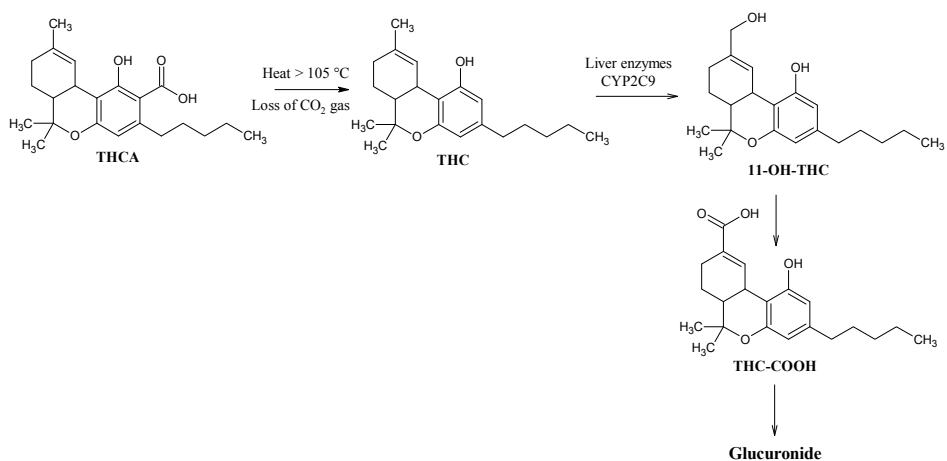


**Figure 2. Metabolic route of THC and its metabolites in the body.**

Experimental studies have shown that the maximal impairment appears during 60 minutes after smoking a joint containing 9 – 18 mg of THC, and vanishes after 3 – 4 hours after use<sup>11</sup>. Peak impairment after THC use is comparable to the alcohol impairment with an alcohol level > 0.05% in the blood. However,, the effects on individuals vary due to the differences in tolerance, smoking techniques and absorption of THC. Moreover, the culpability study<sup>16</sup> showed that the 5 ng/ml THC concentration in the blood is associated with the “odds ratio” (OR) of 1.0, which is equal to the number of car traffic accidents caused by drug free drivers. OR is the ratio of the number of drivers, who are responsible for traffic accidents taken place due to driving under the influence of cannabis, to that of clear drivers. In case of the THC concentration in the blood greater than 5 ng/ml, the OR of 6.6 was established, which is comparable to the blood alcohol content (BAC) of 0.15% (percent by weight). This means that a person is responsible for a traffic accident when driving under the influence of cannabis with a 6.6-fold higher probability than a drug free person.

Moreover, the determination of THC concentration in the drivers' blood reflects more accurately the THC impairment than the metabolite of THC, THC-COOH (11-nor-9-carboxy-THC). In fact, THC-COOH is an inactive carboxy metabolite of THC that can be present in urine or blood for days<sup>17, 18, 19</sup>. Urine THC-COOH correlates neither with the amount of the initial dose nor the time of the last use. Therefore, the impairment or recent cannabis use does not necessarily points to the presence of THC-COOH in urine or blood. Nevertheless, THC-COOH is a preferred marker of THC use determined by screening methods such as immunoassay or by confirmation methods such as LC/MS or GC/MS. Undoubtedly, the occurrence of THC-COOH in the urine can be used for identification of previous or regular drug users among people<sup>19</sup>. This is especially essential at workplaces or doping control where it is important to minimize drug use associated risks and to identify individuals possibly involved.

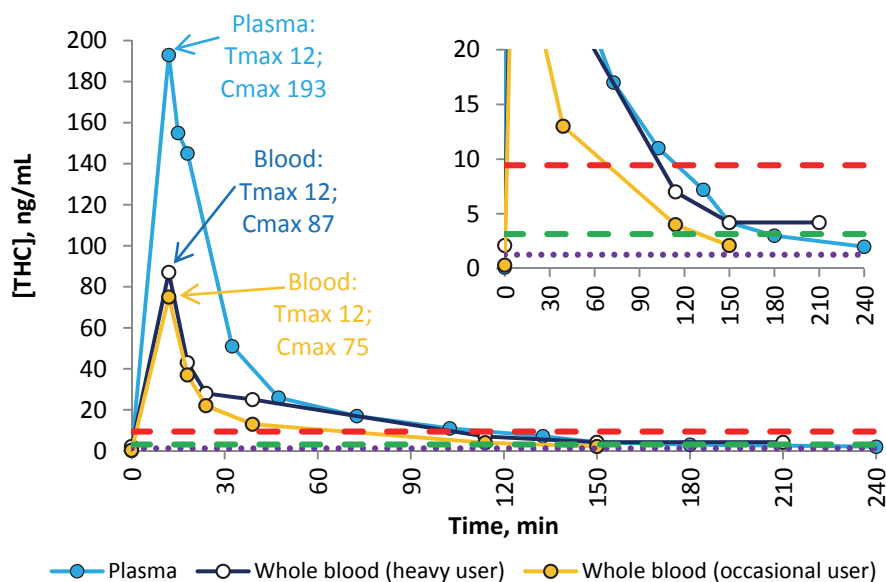


**Figure 3. Excretion patterns of THC in plasma and whole blood levels with THC *per se* limits (whole blood)<sup>20</sup>: purple dotted line – 0.02% BAC; green dashed line – 0.05% BAC; red dashed line – 0.12% BAC. Plasma – smoking of a single cannabis cigarette containing 3.55% THC for heavy smokers (33.8 mg of THC) (data based on <sup>21</sup>); whole blood levels for heavy and occasional users – smoking of an around 0.4 g cannabis cigarette containing 11% THC in Bedrobinol head tops (43 mg of THC) (data based on <sup>22</sup>).**

As discussed above, the impairment after THC use vanished during 3-4 hours depending on the dosage and user. Taking into account the possible impairment cut-off concentration of 5 ng/ml of THC in blood, the excretion time is between 2.0-2.5 hours after smoking (Figure 3). Moreover, the THC concentration level in OFs after 2.0-2.5 hours is around 4.3-3.5 ng/ml (Figure 4). Therefore, the suggestion of impairment must be thoroughly considered and the very low

concentration (< 2 ng/ml) of THC in OF cannot be regarded as a certain impairment and connected to the resulting traffic accident.

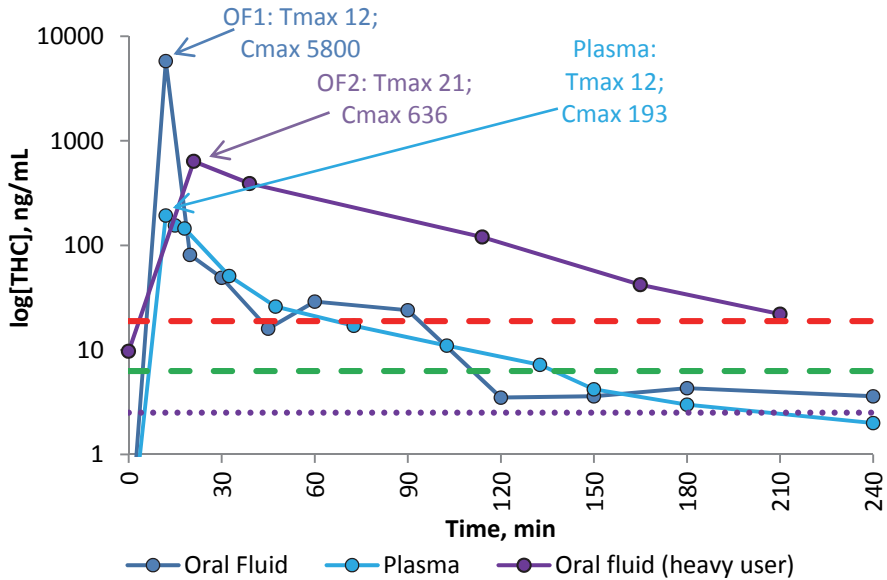


Figure 4. Time profiles of THC in oral fluids and plasma with THC *per se* limits<sup>23</sup> (plasma, ratio plasma: blood = 2<sup>24,25</sup>); purple dotted line – 0.02% BAC; green dashed line – 0.05% BAC; dashed red line – 0.12% BAC. OF1 and plasma – smoking of a single cannabis cigarette containing 3.55% THC for heavy smokers (33.8 mg of THC) (data based on <sup>21</sup>); OF2 – smoking of a 0.4 g cannabis cigarette containing 11% THC in Bedrobinol head tops (43 mg of THC) (data based on <sup>22</sup>).

One of the countries that has linked the concentration of drugs found in blood to impairment comparable to three BAC levels, 0.02, 0.05 and 0.12%, is Norway<sup>26, 20</sup>. The country has set legal limits (*per se* limit) and appropriate punishments depending on THC concentration (Table 2).

Table 2. *Per se* limit<sup>26, 20</sup> of THC in blood equivalent to BAC in blood set in Norway and correlation between THC concentrations in blood and alternative sample matrixes.

BAC, %	Blood, ng/ml	Plasma/serum*, ng/ml	Excretion time in blood (plasma), min <sup>21,22,27</sup>	Saliva, ng/ml <sup>21</sup>	Urine, ng/ml
0.02	1.3	2.5	180-240 (105-210)** <sup>21</sup>	3.6-4.3 (22)**	Not excreted
0.05	3.1	6.3	120-150 (45-210)**	3.5-3.6 (42-122)**	Not excreted
0.12	9.4	18.9	30-45 (45-60) <sup>22</sup>	16-29 (390)**	Not excreted

\* plasma: blood ratio = 2<sup>24, 25</sup>; \*\* for heavy user<sup>21</sup>.

### 1.2.2 $\gamma$ -hydroxybutyric acid

$\gamma$ -Hydroxybutyric acid or GHB is an endogenous neurotransmitter, an analogue to  $\gamma$ -aminobutyric acid (GABA), which was first synthesized by Zaytsev<sup>28</sup> in 1874 and studied for medical purposes as an anesthetic for the first time by Laborit in 1961, but was withdrawn due to undesirable side effects<sup>29</sup>. GHB is used to treat insomnia (sleeplessness), narcolepsy, alcoholism and drug abuse, and as an antidepressant agent<sup>30</sup>.

GHB is a naturally occurring compound found in different tissues (brain, liver) and fluids (urine, blood, saliva and others)<sup>31</sup>. GHB is biologically synthesized from GABA and occurs as an anion,  $\gamma$ -hydroxybutyrate (pKa 4.72), in the human body. The exogenous concentration levels of GHB were studied in blood (0.17 – 1.51 mg/L)<sup>32</sup>, serum (0.62 – 3.24 mg/L)<sup>33</sup>, urine (male: 0.22 – 2.33 mg/L, female: 0.31 – 1.51 mg/L)<sup>34</sup> and saliva (0.15 – 3.33 mg/L)<sup>35</sup>.

GHB is used as a recreational drug known as “Liquid Ecstasy” and is a controlled compound in many European and other countries. In addition, there are several compounds such as 1,4-butanediol (1,4-BD) and  $\gamma$ -butyrolactone (GBL)<sup>36</sup>, which are used as alternative sources of GHB as they convert rapidly to GHB in the human body (Figure 5). GHB is rapidly eliminated from the body (half-life 20-53 minutes<sup>37</sup>).

GHB abuse can be determined using saliva during 2 hours (cut-off limit 5 mg/L), blood during 2 hours (cut-off limit 5 mg/L) and urine during 2.5 hours (cut-off limit 10 mg/L) after consumption<sup>38</sup>. The maximum concentration was detected in saliva in 10 – 30 minutes<sup>38,39</sup>, in blood in 30-50 minutes<sup>40</sup> and in urine in 1-2 hours<sup>36</sup>, depending on GHB dosage.

GHB effects are dose-dependent. Oral doses of 10 mg/kg BW cause short amnesia and hypotonia, 20 – 30 mg/kg BW doses lead to euphoria, drowsiness, disinhibition and driving ability impairment during 1 – 3 hours<sup>41</sup>. Higher GHB oral doses, around 45 mg per kg body weight, produce dissociative, sedating and some stimulant-like effects in humans. Intravenous 50-70 mg/kg GHB dose produces hypnosis and has little analgesic effect. Higher doses of GHB (>60 mg/kg) can result in coma<sup>42</sup>.

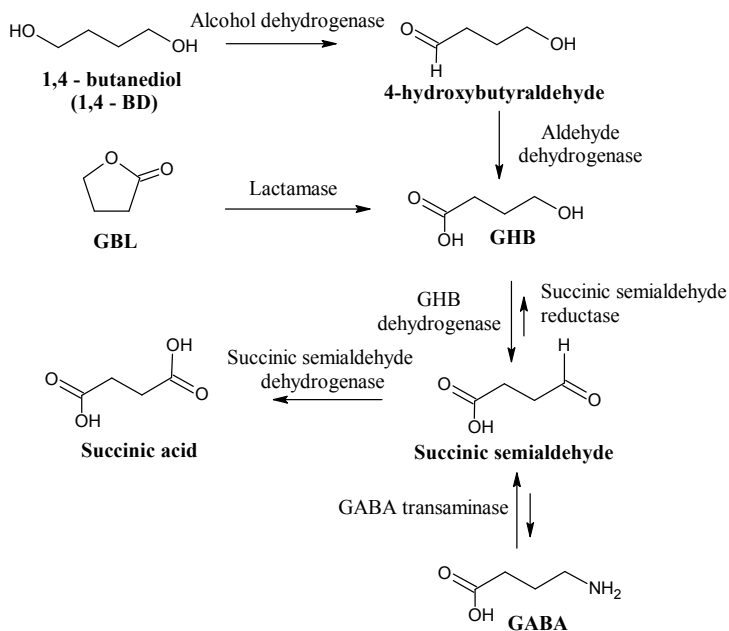


**Figure 5. Biotransformation of GBL, 1,4-BD, and GHB**<sup>43</sup>.

The GHB concentration levels in biological samples depend on the dosage, reflecting the extent of consciousness. For instance, the serum GHB concentration higher than 260 mg/L is associated with deep sleep (comatose), 156-260 mg/L with moderate sleep (asleep but responsive), 52-156 mg/L with light sleep and less than 52 mg/L with wakefulness, respectively<sup>44</sup>. Moreover, the correlation of GHB concentration level in blood (blood:plasma ratio 1:2) with the impairment of driving ability was established and three levels linked to BAC were set<sup>26</sup>. The blood GHB concentration of 10.4 mg/L is linked to 0.02% BAC, 31.2 mg/L to 0.05% BAC and 124.9 mg/L to 0.12% BAC (Table 3). Drivers abusing GHB show generally sedation, impaired balance and irrational behaviour.

**Table 3. *Per se* limit<sup>26, 20</sup> of GHB in blood equivalent to BAC in blood set in Norway and correlation between GHB concentrations in blood and alternative sample matrixes.**

BAC, %	Blood, mg/L	Excretion time in blood, min <sup>45</sup>	Saliva, mg/L <sup>38</sup>	Urine, mg/L <sup>45,36</sup>
0.02	10.4*	30*-150** <sup>41</sup> -300*** <sup>37</sup>	3**-4*** <sup>37</sup>	20-160** <sup>45</sup>
0.05	31.2**	30**-90** <sup>45</sup> -180*** <sup>37</sup>	12**-15*** <sup>37</sup>	30-100** <sup>45</sup> ;
0.12	124.9***	30*** <sup>46</sup> -34*** <sup>41</sup>	40 <sup>37</sup>	15-40** <sup>45</sup>

\* dosage  $\leq 12.5$  mg/kg; \*\* dosage  $\geq 25$  mg/kg; \*\*\* dosage  $\geq 60$ <sup>37</sup>-72 mg/kg<sup>46</sup>

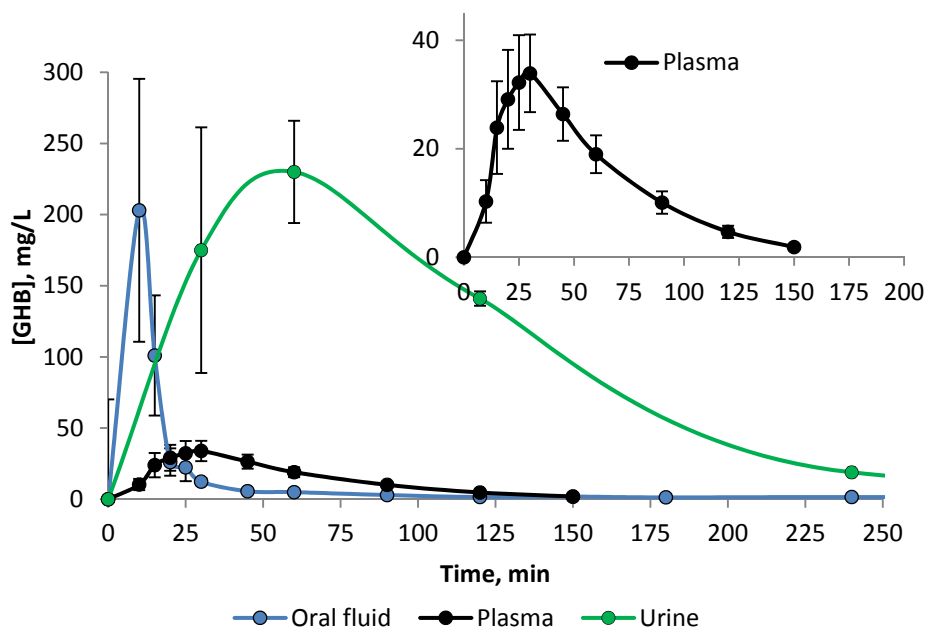


**Figure 6.** Oral fluid (LoD = 0.1 mg/L), plasma (LoD = 0.2 mg/L), and urine (LoD = 0.1 mg/L), profile of GHB after an oral dose of 25 mg GHB per kg b.wt., GHB-naïve subjects (mean  $\pm$  SEM, n = 8) based on reference<sup>38</sup>.

GHB abuse determination depends on the ability of the methodology to differentiate the exogenous and endogenous concentration levels in the human body. GHB not only occurs naturally in the human body, but can also be found in excessive concentration in the physiological fluids, i.e. up to 800-fold in urine and 200-fold in plasma. GHB can be the marker of succinic semialdehyde dehydrogenase deficiency, when GABA is not converted to succinic acid but accumulates as  $\gamma$ -hydroxybutyrate<sup>47</sup>. Therefore, this disorder must be taken into account during the determination of possible impairment. This can be simply eliminated by the continuous analysis of the person under suspicion. The concentration of GHB must decrease in time and not remain high.

### 1.2.3 Herbal medicines and their constituents

For centuries, herbals have been used as medicines and in rituals. Nowadays, herbal medicines (HM) are also very common and are used for treatment of different disorders and to promote health. Some of them are legal, some illegal, such as *Cannabis sativa*, *Catha edulis*, *Erythroxylum coca*, *Papaver somniferum* and others mentioned before. Therefore, the monitoring of HM is of major concern for both forensic scientists and phytochemists.

Nowadays, HM production is a profitable and well-organized business. The major active substances broadly distributed in herbs can be grouped as flavonoids and non-flavanoid polyphenols. The non-flavanoid polyphenols are simple phenols, phenolic acids (derived from cinnamic or benzoic acid) and stilbenoids (resveratrol and its derivatives). Flavonoids include flavones, flavanones, flavan-3-ols, flavonols, isoflavones, anthocyanidins, proanthocyanidins and chalcone. In total, there are more than 8,000 phenolic compounds isolated and described<sup>48</sup>. Indeed, polyphenols are secondary plant metabolites and tend to be water-soluble, as they occur frequently esterified with glucose and other carbohydrates (glycosides) and are usually located in vacuole.<sup>49</sup> But they can also be found as free aglycones that are poorly soluble in water.

Polyphenols have different cellular, molecular, and biochemical actions and are an important source for dietary. There is a huge number of publications describing the different activities of polyphenolic compounds. For example, resveratrol, a representative of stilbenes, is found to have a preventing effect on cancer<sup>50</sup>. Catechins have a significant effect on cell proliferation<sup>51</sup>. Green tea catechins are found to have preventive properties against prostate and liver cancers<sup>52</sup>. Hydroxycinnamic acids have antioxidant properties, and are associated with reduction of the risk of cardiovascular disease, cancer and other chronic diseases<sup>53,54</sup>. Gallic acid, a representative of the hydroxybenzoic acid group, possesses ant-viral, anti-bacterial, anti-inflammatory and anti-oxidant properties. Gallic acid is found to have anti-cancer and chemopreventive properties<sup>55</sup>.

### **1.3 Regulations and directives for drug detection in bulk seizures and clinical samples**

The Scientific Working Group for the Analysis of Seized Drugs (SWGDRUG)<sup>56</sup>, UNODC and the Committee for Medicinal Products for Human Use (CHMP)<sup>57</sup> have worked out the recommendations for operator training, sampling, drug identification in seizures, and requirements for validation.

According to SWGDRUG<sup>57</sup>, analytical tools are divided into three groups according to their diminishing power. At least two uncorrelated methods must be implemented for drugs identification. Moreover, one of them must be classified as Category A method (infrared, NMR, Raman, mass spectrometry, X-ray diffraction) and the other must be either Category A, Category B (CE, GC, ion mobility spectrometry or IMS, LC, thin layer chromatography, microcrystalline tests, pharmaceutical identifiers, micro/macroscopic examination for cannabis only) or Category C technique (colour tests, fluorescence spectroscopy, immunoassay, melting point, ultraviolet spectroscopy). If none of the Category A methods is available, at least two Category B methods and one Category B or Category C method must be utilized in the identification scheme. Therefore, the

combination of GC, HPLC or CE to MS can be suggested as a confirmatory method. The two first combinations, GC-MS and HPLC-MS, are the most widespread techniques used in forensic laboratories.

Drug testing starts with screening, after which confirmatory analysis is performed. Generally, the first analysis is conducted on the place of the crime or incident. Commonly, the screening methods help rapidly to identify the illegal drug occurrence in seizures or provide evidence of drug abuse. Therefore, these tests help law enforcement officers to respond rapidly and stop the possible future crimes.

More and more frequently attention is riveted to biological samples that can be taken noninvasively. Despite the fact that blood and urine are the generally accepted samples for confirmatory drug testing, these sample matrixes have disadvantages. Blood sampling is complex and requires special conditions and the trained and certified personnel. Urine sampling is less invasive and uncomfortable, but produces the psychological discomfort to the person under suspicion. Nowadays, sampling of oral fluids such as saliva, sweat, and exhaled breath condensate are desirable sample matrixes for drug testing on road. This is mainly so due to the easy and friendly sampling procedure. Therefore, the development of sensitive and rapid analytical methodologies for determination of illegal drug abuse in oral fluids is of utmost importance.

During the development of methodologies one must overcome the huge number of issues that can arise during method development, validation and implementation. First of all, the methodology must be specific for an analyte of interest, and reduce the number of false positives. Secondly, the sensitivity of determination of the concentration level in toxicological samples must be archived, eliminating false negatives. The method must be robust under different testing conditions, improve the efficiency of routine testing and minimize the failure of analysis on-site. Finally, the uncertainty of the methodology needs thorough evaluation as this is connected to the decision making on drug abuse.

#### **1.4 On-site detection methods**

Abundant illegal drug production, distribution and abuse require a proactive response of law enforcement bodies, border control officers and others concerned. The illegal drugs analysis is conducted in the forensic laboratory or hospitals by experienced operators. Nevertheless, a critical aspect is time to prevent the possible crime and minimize fatal consequences to the society. The availability of rapid, sensitive and easy-to-use early warning detection tools to be employed on-site is of high importance.

#### 1.4.1 Available on-site portable methods for detection of drugs at market

Drug detection tools can be divided into three major categories: tools for detection of illegal drug seizures, tools for detection of drug abuse in biological samples and tools enabling both. In addition, the detection systems can be contact or non-contact. Portable devices are mainly exploiting Fourier transform infrared spectroscopy (FTIR) (HazMatID), Raman (ICx Fido® Verdict™ Portable Explosives and Narcotics Identifier, Smiths Detection RespondeR™ RCI, Thermo Scientific® FirstDefender RM™, Trunarc Termofisher), ion mobility (IMS) (A Smith Detection Ionscan 400B (Danbury CT) or fluorescence spectroscopy (NarTest NTX2000).

The main disadvantages of portable Raman spectrometers utilizing lasers with a wavelength of 785 nm are low reproducibility and low cut-off levels for drug detection. Moreover, Raman spectroscopy does not work well on the surface of highly fluorescent and/or pigmented objects. Raman scattering can be influenced by background light, leading to spectra of poor quality. Besides, Raman spectroscopy has a limited capability of detecting herbal samples such as cannabis products and heroin as they contain highly fluorescing constituents present in the samples naturally. According to the reports of NFSTC, none of the four commercial Raman spectrometers tested during evaluation (ICx Fido® Verdict™, DeltaNu® ReporteR™, Thermo Scientific® FirstDefender RM™, Smiths Detection RespondeR™ RCI) afforded accurate detection results for a controlled substance in the mixtures of cutting agents and adulterants. The accuracy values were around 50%, except in one case when the accuracy was approximately 70%<sup>58</sup>. Nowadays, IMS is a very widely spread method for detection of explosives and controlled substance traces especially at airports and border controls. However, apart from its advantages such as high sensitivity (<ppb), rapid response (>s) and portability, this technique has also some disadvantages. The main disadvantage is the occurrence of reactions of competitive ion/molecules with matrix molecules, during which the analyte of interest can be lost. Moreover, IMS instruments are extremely sensitive to contamination and have a long clearance time<sup>59</sup>.

Other common screening tests are colour tests utilizing colour chemical reactions or more sophisticated immunoassays (enzyme-multiplied immunoassay technique (EMIT), fluorescence polarization immunoassay (FPIA), immunoturbidimetric assay and radioimmunoassay (RIA))<sup>60</sup>. Colour tests (ODV, Inc. (NarcoPouch®), Sirchie Group (NARK®II), Public Safety, Inc. (NIK®), Lynn Peavey Company (QuickCheck™)) are presumptive and the determination of colour depends on the user's experience. Moreover, colour tests are designed for detection of a family of drugs and are not specific. For example, diphenhydramine and benzphetamine give false positives in Scott's and Marquis colour tests, quinine, lidocaine, phencyclidine in Scott's tests, respectively<sup>61</sup>.

The screening tests that are designed for drug abuse determination in biological samples such as urine and oral fluids are mainly employing immunoassays. The latter are not specific as often declared. Moreover, the sensitivity of immunoassays is similar to or even worse than that of confirmatory methods like GC-MS (LoQ: amphetamine, MDMA, codeine, morphine 20 ng/ml, MDMA 20 ng/mL, THC 1 ng/mL in OF)<sup>62</sup> or UPLC-MS/MS (LoQ: 0.53 ng/mL for THC, amphetamine, MDMA, codeine, morphine, etc.)<sup>63</sup>.

Table 4 summarizes the commercial available immunoassays designed for drug detection in oral fluids. Therefore, there is strong evidence that drug impairment cannot sometimes be determined on-site. As a rule, only a positive sample must be sent to the laboratory for confirmatory tests.

**Table 4. Commercial immunoassay cut-off limits and time of analysis in oral fluids, ng/mL** <sup>64, 65</sup>.

<b>Drug Class Test: Drug under detection</b>	<b>Dräger 5000</b>	<b>DrugWipe ® 5+</b>	<b>Reditest® Oral</b>	<b>MMC DOA Saliva</b>	<b>iScreen Oral</b>	<b>Oratect® III</b>
<i>Amphetamine:</i>						
d-Amphetamine	50	50	50	50	50	25
<i>Benzodiazepines:</i>						
Diazepam	15		15	20		5
Temazepam						
<i>Cocaine:</i>						
Cocaine	20			20		20
Benzoyllecgonine		30	20		20	
<i>Methamphetamine:</i>						
d-Methamphetamine	35	25	50	50	50	25
MDMA				50		
<i>Opiates:</i>						
Morphine	20		40	40	40	10
Codeine		10				
<i>Cannabis:</i>						
9-THC	5	30		12		40
THC-COOH			12		12	
<i>MDMA:</i>						
MDMA		25		50	50	25
<i>Phencyclidine:</i>						
Phencyclidine			10	10	10	10
<i>Methadone:</i>						
Methadone				30		
<b>Time of analysis, min</b>	<b>5 – 10</b>	<b>3 – 10</b>	<b>10</b>	<b>5 – 7</b>	<b>10</b>	<b>5</b>
<b>Drugs per tests</b>	<b>4,5,6</b>	<b>1</b>	<b>6</b>	<b>3,5,6</b>	<b>5,6</b>	<b>6</b>

Immunoassays are designed to recognize a wide range of chemically similar compounds reacting with the antibodies. The main drawback of immunoassays is the possibility of false positive results, when the drug of the same class is detected as the drug of interest. For example, false-positive results for cannabinoids are usually obtained with dronabinol, elavirenz, hemp-containing food, NSAIDs (nonsteroidal anti-inflammatory drugs), proton pump inhibitors and tolmetin. Opioids, opiates and heroin immunoassays can give false positive results in case of dextromethorphan, diphenhydramine quinine, quinolones and others<sup>60,66</sup>. It is also known that cold remedies, pain relievers, hay fever remedies and diet pills can give a false positive for amphetamine use on EMIT. Certain antibiotics such as amoxicillin are claimed to cause a false positive for heroin and cocaine. Therefore, immunoassay cannot be recognized as a confirmatory method. A positive sample always requires the second test for confirmation by another method.

Moreover, European projects such as ROSITA, ROSITA-2 (Roadside Testing Assessment) and DRUID (Driving under the Influence of Drugs, Alcohol and Medicines) during 2006 – 2011 were run to evaluate oral fluid collection devices for detection of controlled substances. Unfortunately, none of the devices were recommended for on-site use as their sensitivity, specificity and accuracy remained below 80% in all separate tests<sup>67</sup>. Other techniques for drug detection utilized in this dissertation are spectral fluorescence signature spectroscopy and capillary electrophoresis coupled to the different detection methods are described below.

#### **1.4.2 Spectral fluorescence signature method**

The spectral fluorescence signature (SFS) method is an advanced mode of excitation emission matrix (EEM) spectroscopy. SFS is based on the ability of compounds under excitation at a specific wavelength to emit light at a specific higher wavelength, i.e. with lower energy.

The difference between EEM and SFS is that Rayleigh scattering is outside the measurement window (Figure 7). It means starting the SFS measurement at  $\lambda_{\text{ex}} = 230$  nm, the emission is recorded with a 20 nm shift to lower energy, i.e.  $\lambda_{\text{em}} = 250$  nm. The shift is repeated at all excitation wavelengths. Therefore, SFS is generated as a parallelogram of fluorescence patterns (Figure 7B). The SFS method can be utilized in two different modes: classical angle fluorescence and front-face. The front-face mode has several advantages in comparison to the classical one. First of all, the front-face mode can deal with very turbid and viscous samples, even solid samples, whereas classical angle fluorescence spectroscopy requires samples dilution or a special pre-treatment procedure to archive the solutions with an absorbance value lower than 0.05<sup>68</sup>. The measurement of a neat or undiluted sample gives awesome advantage. In this

case, the fluorescence fingerprint is not disrupted and the authentic properties of samples of interest are preserved.

The SFS method was developed by Babichenko and Poryvkina and was first introduced for different environmental applications<sup>69</sup>, starting from oil in water detection, phytoplankton type determination<sup>70</sup>, dissolved organic matters (DOM) measurements<sup>70</sup> across the Baltic Sea and petroleum product differentiation. Afterwards, this method was also successfully applied in the forensic science for illegal drug detection<sup>71,72</sup> (Publication I) and in the food industry for apple juice<sup>73</sup> and herbal medicine (Publication II) quality monitoring. Undoubtedly, there is a huge number of other applications where this great technique can be utilized in the future.

### Rayleigh

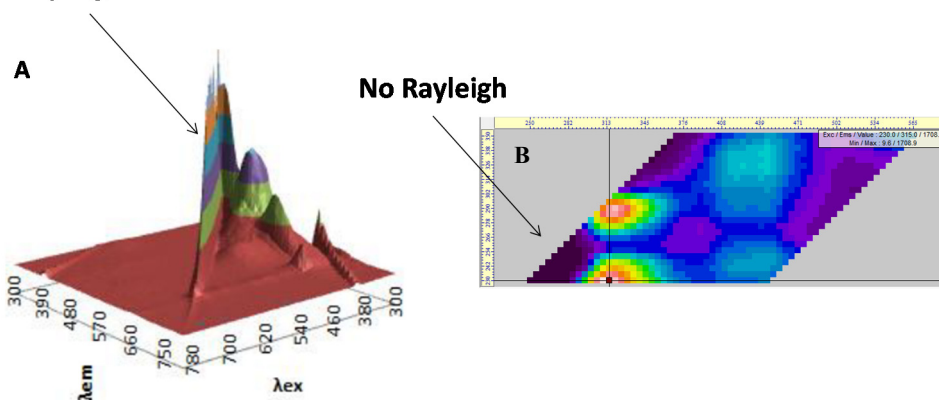


Figure 7. A – conventional EEM spectroscopy; B – SFS method.

### 1.4.3 Capillary electrophoresis

The capillary electrophoresis (CE) technique was first described in 1937 by Tiselius, who won the Nobel Prize in Chemistry in 1948 for the separation of proteins in a U-tube with buffer solutions under applied electric field<sup>74</sup>. Hjerten<sup>75</sup>, Jorgenson and Lukacs<sup>76</sup>, and Terabe<sup>77</sup> made a crucial contribution to the development of capillary electrophoresis into the version we are using today.

CE is a separation method which is based on the difference in migration mobility between charged analytes (solutes) inside the capillary, typically 25 – 100  $\mu\text{m}$  in inner diameter (i.d.), filled with a background electrolyte (BGE), under the influence of an electrical field of intensity  $E$ . The electrophoretic mobility ( $\mu_{ep}$ ) depends on the properties of the analyte such as electric charge, molecular size, and shape, and also on those of BGE like type, ionic strength, pH, viscosity and additives. The electrophoretic velocity ( $v_{ep}$ ) is found according to the following equation (assuming a spherical shape):

$$v_{ep} = \mu_{ep} \times E = \left( \frac{q}{6\pi\eta r} \right) \times \left( \frac{V}{L} \right), \quad (1)$$

where,  $q$  is an effective charge of the solute,  $\eta$  is the viscosity of the electrolyte solution,  $r$  is the Stoke radius of the solute,  $V$  is the applied voltage and  $L$  is the total length of the capillary.

Electrophoretic separation is conducted under a very high electric field (100 – 500 V/cm or even higher) inside the narrow-bore fused silica, borosilicate glass or polytetrafluoroethylene (PTFE) capillary, where the detrimental effects of Joule heating are minimized due to the high electrical resistance of capillaries and heat dissipation over the large surface area-to-volume ratio. The high field strength in narrow-bore capillaries and a suitable BGE for analytes of interest allows achieving very rapid separation with high efficiency and resolution.<sup>78</sup> Another important phenomenon associated with electrophoretic separation is electroosmotic flow (EOF). EOF is the movement of a liquid near a charged surface of the capillary under an electric field. In case of the fused silica capillary covered with silanol groups (SiOH), ionization to SiO<sup>-</sup> starts at pH >2 and at pH >9 the groups are fully ionized, resulting in a negatively charged surface. Therefore, the extent of EOF ( $\mu_{EOF}$ ) depends on the charge on the capillary (zeta potential,  $\zeta$ ), the buffer viscosity ( $\eta$ ) and dielectric constant of BGE<sup>78</sup>.

$$\mu_{EOF} = \left( \frac{\varepsilon\zeta}{\eta} \right), \quad (2)$$

The presence of EOF allows the separation of cations and anions within a single CE run, affecting the overall migration time ( $t$ ) of analytes, whose apparent mobility ( $\mu_{app}$ ) is found<sup>78</sup>:

$$\mu_{app} = \mu_{ep} + \mu_{EOF} = \left( \frac{l \times L}{t \times V} \right), \quad (3)$$

where  $l$  is an effective length of capillary.

CE is a modern analytical separation techniques, and is probably one of the most rapidly expanding in different industries such as the food industry<sup>79</sup>, as well as in environmental<sup>80,81</sup>, military<sup>82</sup>, medical<sup>83</sup>, nanotechnology<sup>84</sup> and forensic applications<sup>85,86,87</sup>. The demand for CE is high due its high efficiency ( $N < 10^5$  to  $10^6$ ), short or even extremely short (in seconds) analysis time, small sample (1 to 50 nL for injection) and reagents/solvents volumes and low mass detection limits. Moreover, there is an outstanding number of CE modes such as capillary zone electrophoresis, micellar electrokinetic capillary chromatography, capillary isotachopheresis, capillary gel electrophoresis, capillary isoelectric focusing, and

non-aqueous capillary electrophoresis.<sup>88</sup> CE modes can be utilized at the same simple instrument, basically just changing the background electrolyte. It enables analysis to be conducted more rapidly and with higher efficiency of separation of analytes of interest than can usually be achieved with HPLC. Generally, CE separation does not require any derivatization of analytes prior to analysis as does GC due to poor volatility (for example, sugars), poor detectability (for example, steroids/ cholesterol), high polar nature (for example, barbiturates) or/and poor thermal stability (for example, THC-COOH, LSD and psilocin, benzodiazepines)<sup>89</sup> of analytes of interest.

Nevertheless, CE has drawbacks like poor sensitivity or/and probability of adsorption of proteins and peptides into the capillary wall. These factors may be especially of concern in the forensic analysis of biological samples (saliva, blood, urine). Though, the sensitivity of CE can be improved by utilizing other sensitive detection techniques such as fluorescence, conductivity, amperometric or mass spectrometry, or applying stacking techniques like isotachopheresis and transient isotachopheresis, high-field stacking, hydrodynamic injection stacking, ACN-salt mixture stacking, etc.<sup>90, 91</sup>.

## **1.5 Pattern recognition techniques for data analysis**

Nowadays, chemometric tools or pattern recognition techniques are highly demanded and also widely used in analytical chemistry. They are especially useful for data pre-processing, chemical fingerprint analysis often via dimensionality reduction of data set and searching for feature vectors (variables that summarize variations) and, therefore, interpretation of hidden similarities/dissimilarities between groups, within samples, buried in high dimensional datasets. These techniques are also used for analysis automatization, utilizing them as a predictor on new samples and embedded into the software.

The pattern recognition techniques can be divided into two groups: unsupervised and supervised methods. The goal of unsupervised methods is to classify observations/samples/chemical fingerprints into groups without prior knowledge of the sample class. The most common are principal component analysis (PCA), parallel factor analysis (PARAFAC) and cluster analysis (CA). Supervised techniques (for example, ANN, partial least squares discriminant analysis (PLS-DA)) are applied when the ‘categories’ of samples are known. It means that the samples are presented with known classification/feature vectors as a training data and the algorithm can reproduce this classification on new unknown samples<sup>92</sup>.

### **1.5.1 Data preparation**

Due to capillary or column aging, the shifting of peaks in time axes may occur in electrophoretic or chromatographic data. Therefore, the analysis and interpretation of this data by chemometric techniques can be affected or even

totally ruined. It means that electrophoretic and chromatographic data may sometimes need the alignment, improving the quality of the final result. The reproducibility of migration time is of importance in CE in order to identify the analyte of interest. Therefore, electropherograms can be corrected prior to the analysis of CE data, using the method proposed by Zhang<sup>93</sup>.

Two internal substance components can be used for correction coefficient evaluation for each electropherogram/chromatogram against the standard, using the following equation:

$$\gamma = \frac{\frac{1}{\hat{t}_I} - \frac{1}{\hat{t}_P}}{\frac{1}{t_I} - \frac{1}{t_P}} \quad (4)$$

The new migration time ( $t_x$ ) is found using the calculated correction coefficient  $\gamma$ :

$$t_x = \left[ \frac{1}{t_I} - \frac{1}{\gamma \left( \frac{1}{\hat{t}_I} - \frac{1}{\hat{t}_P} \right)} \right]^{-1} \quad (5)$$

where  $\gamma$  is the correction coefficient;  $t_I$  and  $t_P$  are migration times of the first and second internal standards, respectively;  $\hat{t}_I$  and  $\hat{t}_P$  are migration times of the first and second internal standards, respectively, in the electropherogram under correction;  $t_x$  is the corrected migration time for the corrected electropherogram and  $\hat{t}_x$  is the migration time of the electropherogram under correction.

## 1.5.2 Unsupervised method

### 1.5.2.1 Principal Component Analysis

Principal Component Analysis (PCA) is one of the most popular traditional methods used for data analysis<sup>94,95</sup>. PCA compresses the size of data by simplifying and extracting and keeping only important information. PCA creates linear combinations of original variables called principal components (PCs) which describe the systematic patterns of variation between the samples. PCs are orthogonal and their number is smaller than or equal to the number of original variables. The first PC has the largest possible variance. PCA is a decomposition of the original 2D-matrix  $X$ , i.e. representation of it as the product of two 2D-matrices  $T$  and  $P$ :

$$X = TP^T + E, \quad (6)$$

where T is a matrix of scores, P is a matrix of loadings and E is a matrix of residuals.

### 1.5.2.2 Parallel factor analysis

PARAFAC is a generalization of PCA to higher order arrays such as EEM/SFS for several samples or any kind of spectra measured chromatographically/electrophoretically for several samples.

For example, SFS data arranged into a 3-way array ( $I \times J \times K$ ) are modelled using PARAFAC<sup>96</sup> as follows:

$$x_{IJK} = \sum_{r=1}^R a_r b_r c_r + e_{IJK} \quad (7)$$

where  $I$  is the number of samples,  $J$  is the number of emission wavelengths,  $K$  is the number of excitation wavelengths, and  $R$  is the number of components applied to the model. PARAFAC decomposes the data into a number of trilinear components where the output results are presented in excitation, emission spectra loadings (vectors  $b$  and  $c$ ) and scores (vector  $a$ ) that are directly related to the relative concentration of each component.

In case of chromatographic or electrophoretic data recorded by DAD, all the chromatograms or electropherograms are segmented. Therefore, each segment is then analysed by PARAFAC. PARAFAC is used to extract process information about the number of chemical components present in the segment, their relative concentrations and pure UV spectra<sup>97</sup>. Non-negativity constraints are often applied to ensure that each model had a physical interpretation.

### 1.5.2.3 Cluster Analysis

Cluster analysis (CA) is an unsupervised pattern recognition technique that can be used instead of PCA or in combination with PCA, PARAFAC or other chemometric techniques. Cluster analysis is divided into two approaches, non-hierarchical and hierarchical algorithms. Furthermore, a large variety of hierarchical algorithms exists, e.g. average linkage, complete linkage, single linkage and Ward's linkage. Ward's linkage algorithm differs from others by utilising the variance approach to evaluate the distance between clusters, instead of using distance metrics or measures of association. Ward's linkage attempts to minimise the sum of squares (SSE) of any two hypothetical clusters that can be formed at each step. The error sum of squares (SSE) is defined as follows:

$$SSE = \sum_{i=1}^K \sum_{j=1}^{n_i} (y_{ij} - \bar{y}_i)^2 \quad (8)$$

where  $y_{ij}$  is the  $j$ th object in the  $i$ th cluster and  $n_i$  is the number of objects in the  $i$ th cluster.

### 1.5.3 Supervised methods

#### 1.5.3.1 ANN

Artificial neural networks (ANN) is a powerful mathematical tool that can be related to biological neural network models. The use of ANN for data processing/interpretation has significantly increased during the last 20 years<sup>92</sup>. ANN is being successfully used to resolve several issues in finance, medical diagnosis<sup>98,99</sup>, process control, weather forecasting, and chemistry<sup>100</sup>. The real advantage of using ANN in spectroscopic data analysis is the option to automatize the analysis.

### 1.6 Validation requirements

The performance characteristics of methods (SFS (Publications I, II), CE (Publications II, III, IV) utilized for detection of illegal drugs in bulk samples and in saliva and for authentication of herbal medicines were evaluated. The number of parameters under evaluation depends on the type of analysis conducted (qualitative or quantitative) (Table 5).

**Table 5. Performance characteristics.**

Type of analysis	Parameters under evaluation
Qualitative <sup>56, 101</sup>	Selectivity/matrix effects (CC $\beta$ , uncertainty region for each of the interferences); limit of detection (LoD) in the mixture of inert matrix; threshold limit (CC $\beta$ ) in the mixture of inert matrix; upper range of application; precision (repeatability, reproducibility); robustness (expressed as reliability% at the threshold value * 1.5)
Quantitative <sup>57</sup>	Selectivity; carry-over effect*; lower limit of quantification (LLOQ) <sup>102</sup> ; calibration curve; linearity range; precision (intra-day and inter-day, (RSD%)); matrix effect% (ME%) <sup>103, 104</sup> ; accuracy (efficacy/extraction recovery); robustness**

\*for clinical samples

\*\*recommended, not obligatory

Nowadays, the application of pattern recognition techniques is widely spread in chemistry. Obviously, an important part of validation is the evaluation of the applied chemometric technique, especially when it is used for routine analysis. The validation must be performed for both unsupervised and supervised techniques. Generally, validation requires an independent set of samples, which have not previously been applied in model construction.

For example, the expert systems utilizing cluster analysis and in combination with other chemometric techniques requires an independent validation. The results of validation clustering are usually compared to those of the training clustering. The accuracy and precision are evaluated using the following equations:

$$Accuracy\% = \frac{True\_positives + True\_negatives}{Total\_positives + Total\_negatives} * 100\% \quad (9)$$

$$Precision\% = \frac{True\_positives}{True\_positives + False\_positives} * 100\% \quad (10)$$

Today more and more chemometric approaches such as ANN and support vector machines (SVM) are implemented for data analysis to make the detection more efficient, therefore, human subjective judgment is replaced by an artificial intelligence system's response. With no doubt, the efficacy of ANN in the classification of unknown samples must be evaluated in the validation procedure. Indeed, there are no special requirements for the artificially intelligent system either in the 2002/657/EC<sup>19</sup> or in the 2007/47/EC. There is a huge number of articles that suggest that the primary parameter for evaluation of prediction performance of an ANN model is a true error on testing the trained network. Generally, the following parameters are evaluated for such as false positive rate, false negative rate, sensitivity and specificity<sup>105</sup>. But none of them defines, rather ANN has an uncertainty region (unreliability region), where its outputs are inconclusive. However, the uncertainty region for ANN's working capability can be estimated as was performed in Publication I.

## 2 AIMS OF THE STUDY

The main goal of the present thesis is to develop on-site screening methodologies for illicit drugs determination in different multicomponent sample matrixes using CE and SFS methods coupled to chemometric techniques.

The specific aims of the current study are the following:

- to further develop the SFS technique combined with the Artificial Neural Networks (ANN) method of analysis for illegal drug detection in street bulk samples;
- to extend the SFS database, to systematize and prepare data for ANN and improve the SFS expert system for analysis of illegal drugs in powders;
- to find out ANN's uncertainty regions;
- to work out the validation plan and perform the validation of the working capability of ANN for the SFS method and device used for illicit drug detection in bulk samples;
- to model and analyze herbal medicine fingerprinting by different chemometric techniques (PARAFAC-PCA/CA) for exploratory analysis,
- to compare herbal medicine fingerprints differentiation by their polyphenolic content by SFS to CE-DAD and HPLC-DAD/MS methods;
- to identify major metabolites in HMs and determine their spectral properties;
- to compare the capabilities of SFS, CE-DAD and HPLC-DAD for detection of polyphenolic compounds HMs;
- to develop approaches for determination of abuse of drugs such as cannabis and GHB in oral fluids by CE;
- to validate CE methodologies according to EMA's recommendations for bioanalytical method validation<sup>57</sup>.

## **3 EXPERIMENTAL**

### **3.1 Reagents and samples**

All reagents were of analytical grade. Ultrapure water (Milli-Q) (resistivity  $\geq 18$  M $\Omega$ cm) was obtained using a Milli-Q integral water purification system (Merck KGaA, Germany).

#### **3.1.1 Samples in Publication I**

3-trifluoromethylphenylpiperazine (TFMPP) with benzylpiperazine (BZP) (1:1), 4-bromo-2,5-dimethoxyphenethylamine (2C-B) (a. 3%) and marijuana (13% THC) were obtained from the Estonian Forensic Science Institute (EFSI) (Tallinn, Estonia) (Table 1, Publication I).

Forensic drug samples were obtained from police departments<sup>72</sup> of North Carolina(NC), USA and from the EFSI, Tallinn, Estonia. The validation was performed in EFSI and the NarTest Laboratory, NC. EFSI performed quantitative analysis of the drug content of samples provided by them, along with identification of additional compounds. Another set of samples seized by the police in North Carolina, USA was analysed by reference methods GC-MS and FT-IR in the laboratory of NarTest Company (NC, USA).

#### **3.1.2 Herbal samples in Publication II**

The air dried samples of HMs harvested in 2011 (three samples of each HM; moisture content 7-8%) were obtained from OÜ Kubja Ürt, Estonia.

HMs grow in a natural environment. Neither mineral nor chemical fertilizers are used. HMs with their respective identification number are listed in Table 1 of Publication II.

#### **3.1.3 Saliva samples in Publications III and IV**

Blank saliva samples were collected from six volunteers (both male and female, age ranging from 25 to 70). Potential endogenous interferences were assessed by the analysis of saliva samples fortified with analytes of interest and the corresponding internal standard (pinacolyl methylphosphonic acid (PMPA) for CE-C<sup>4</sup>D-UV and bicalutamide for CE-LED).

### **3.2 Methods**

#### **3.2.1 Spectral fluorescence signature method (EEM spectroscopy)**

The SFS method was utilized in Publications I and II for measurement of illegal drugs and herbal medicines. All fluorescence measurements were carried out on a portable NarTest™ NTX2000 Drug Analyser (NarTest AS, Estonia)<sup>106</sup>, which generates advanced excitation emission matrixes (EEMs) or SFSs. This is a

compact spectrofluorometer equipped with a 5 W pulsed Xenon lamp and a special 10 ml optical cell with a quartz window at the bottom (Figure 8). The spectrofluorometer generated an SFS, where the Rayleigh scattering was outside the measuring range. One scanning took 2.3 minutes.



**Figure 8. NarTest NTX2000 Drug Analyser® (NarTest AS, Estonia) and an optical cell for the front-face measurement (reproduced by permission of NarTest AS, Estonia).**

SFSs were measured in a front-face optical layout ( $35^\circ$ ) from the surface at room temperature. The experimental parameters were set as follows:  $\lambda_{\text{ex}} = 230 - 350$  nm (25 excitation wavelengths) and  $\lambda_{\text{em}} = 250 - 565$  nm (64 emission wavelengths) with 5 nm intervals in both directions, gain = 500.

The time required for a complete analysis of one sample in Publication I did not exceed 15 minutes and in Publication II, 5 minutes.

### **3.2.2 Capillary electrophoresis**

Three different capillary electrophoresis instruments were utilized during studies. One was a commercial device and the other two were in-house built instruments.

#### **3.2.2.1 Herbal medicine analysis**

The measurements for Publication II were made on an Agilent 3D capillary electrophoresis instrument equipped with a diode array detector (DAD) (Agilent Technologies, Waldbronn, Germany).

CE experiments for polyphenolic analysis in herbal medicines were carried out according to the method by Helmja et al.<sup>107</sup>. A fused silica capillary (60 x 0.005 cm, Polymicro Technology, Phoenix, AZ, USA) with an effective length of 51.5 cm was used. A 50 mM sodium tetraborate solution (pH 9.3) was utilised as BGE. The applied voltage for the separation was +25 kV. The sample solutions were introduced at the anodic end of the capillary at a 50 mbar pressure for 5 s.

Prior to use, the capillary was rinsed with a 1.0 M NaOH solution, water and e BGE, 5 min each. The diode array detector range was set to 200–400 nm (Publication II).

### 3.2.2.2 Drug abuse analysis in saliva

Publications III and IV employed the in-house built instruments equipped with different detectors for illegal drug analysis in saliva samples.

Cannabinoids (THC, CBD) analysis was carried out using the in-house built CE (TTU, Estonia) coupled with the LED-induced fluorescence detector<sup>108</sup> (LDI AS, Estonia).



**Figure 9. CE-LED-induced fluorescence detector (TUT and LDI AS, Estonia)**

UV-LED with an excitation wavelength  $\lambda = 280$  nm (spectrum half width 15 nm) and power output of 0.5 mW was used as the fluorescence excitation source. The classical angle fluorescence was utilized for fluorescence registration using a photon counting PMT (integration time up to 10,000 ms). LED operation was stabilized using an external cooling module with a programmable temperature controller (accuracy  $\pm 0.5$  °C). There were three emission filters to choose from among: one with a wavelength of  $307 \pm 10$  nm, the other with a wavelength  $326 \pm 10$  nm, and a wideband filter with a wavelength from 341 to 600 nm. The most suitable emission filter for detection of fluorescence of THC and CBD was the one with a wavelength of 307 nm, which was used to register the fluorescence signal of analytes of interest.

CE experiments were conducted using a fused silica capillary (60 x 0.0075 cm, Polymicro Technology, Phoenix, AZ, USA) with an effective length of 45 cm according to the method by Backofen et al<sup>23</sup>. A highly basic electrolyte system with 2.5 mM sodium hydroxide dissolved in an acetonitrile-methanol solution (1:1): was used as BGE for separation of cannabinoids (THC, CBD) and internal standard (bicalutamide) in saliva. The applied voltage for the separation was +17

kV. The hydrodynamic ( $\Delta = 20$  cm) injection was used during 30 s. Prior to use, the new capillary was activated with a 1.0 M NaOH solution and water. Between analyses, the capillaries were rinsed with an electrolyte solution for 2 minutes (Publication III).

GHB abuse determination was performed using the in-house built CE coupled with C<sup>4</sup>D (TUT, Estonia)<sup>109</sup> and combined with an Agilent 3D capillary electrophoresis instrument with DAD for indirect UV absorbance detection (Figure 10).

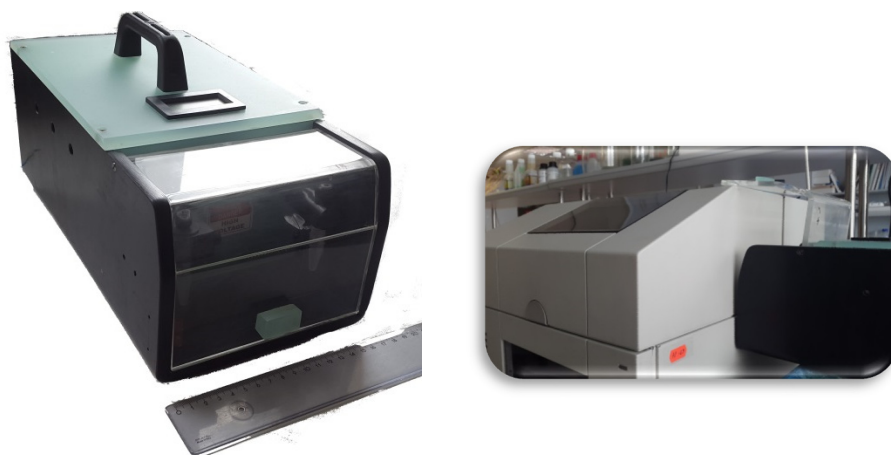


**Figure 10 In-house built portable CE device coupled to C<sup>4</sup>D (TUT, Estonia)**

CE measurements were made using an uncoated fused silica capillary (Agilent Technologies, USA) with a total length of 65 cm, an effective length of 45 cm to C<sup>4</sup>D and 56.5 cm to DAD (i.d. 50  $\mu$ m, o.d. 360  $\mu$ m). The C<sup>4</sup>D frequency was set to 150 Hz. The indirect UV absorbance (ABS) was recorded at  $\lambda_{\text{ABS}} = 210$  nm. The methodology proposed by Hauser et al.<sup>110</sup> for GHB analysis in urine and serum samples was modified and optimised for analysis of saliva samples and the current system. The stock BGE solution consisted of 10 mM maleic acid, 20 mM Arg and 300  $\mu$ M CTAB, the pH was adjusted to 7.35. As an organic modifier, 15% acetonitrile was added to the stock BGE, with a slight adjustment of the final pH to 7.65 and decreasing the BGE components content as follows: to 8.5 mM maleic acid, 17 mM Arg and 255  $\mu$ M CTAB. The final BGE was ultrasonicated (Bandelin electronic, Germany) for 10 minutes, degassed by 10% at 30 °C and then filtered through a 20  $\mu$ m cellulose filter (Sartorius Stedim Biotech, Germany). The applied voltage was set at  $-19$ kV. The plug was conducted hydrodynamically for 10 s at 35 mbar. Prior to CE analysis, the capillary was activated and washed every day with 1 mM NaOH and Milli-Q water for 10 minutes and with BGE for 15 minutes. Between the experiments, the capillary was rinsed with BGE for 3 minutes. Moreover, the capillary was washed with methanol for 10 minutes, Milli-Q water for 10 minutes and BGE

for 15 minutes, at least after 20 analyses in order to prevent adsorption on the capillary surface. (Publication IV).

### **3.2.3 HPLC-DAD-MS**

Herbal medicines (HMs) were analysed by the reference method HPLC-DAD-MS in Publication II. The methanolic extracts of HM were analyzed using HPLC Agilent 1200 Series coupled with DAD and mass Agilent 6300 Series detector equipped with an electrospray ionisation system and controlled by Agilent LC/MSD trap software (Agilent Technologies, Waldbronn, Germany). Nitrogen was used as a nebulizing gas at a pressure of 413.7 kPa (60 psi) and the flow rate was adjusted to 12 L/min. The nebulizer temperature was 350 °C. The full scan mass spectra of compounds were measured from 100 to 1000 m/z. MS data were obtained in the negative ionisation mode and MS/MS data in the automatic mode.

The samples (10 µL) were separated on an Agilent Zorbax SB C-18 column (150 mm x 4.6 mm i.d., particle size 5 µm). The mobile phase consisted of two solvents: solvent A was a 0.1% solution of formic acid, and solvent B was 100% acetonitrile. Gradient elution was performed as follows: initially 100% of solvent A was eluted, followed by elution of 0% to 30% of solvent B in 25 min, 95% of B at 40 min and held for 5 min, and then returned to 0% of B at 50 min. The flow rate was 0.8 mL/min and the column temperature was 25 °C.

Spectral data from all peaks were accumulated in the range of 240–400 nm and UV-VIS chromatograms were recorded at 254 nm. Compounds in plant extracts were identified by comparing DAD spectra and MS and MS/MS data (Publication II).

## 4 RESULTS AND DISCUSSION

The results presented in this dissertation are based on four studies.

The first two studies, discussed in Publication I and Publication II, cover the application of the spectral fluorescence signature (SFS) method coupled to different supervised and unsupervised expert systems:

- for illegal drugs detection in street samples by ANNs, and
- for rapid screening and evaluation of fingerprints and polyphenolic content of herbal medicines by PCA-PARAFAC/CA.

In addition, Publication II presents the results of analysis of electrophoretic and chromatographic fingerprints of HMs.

Publications III and IV present the proof of principle for determination of illegal drugs in saliva samples by capillary electrophoresis for on-site use:

- THC and CBD determination in saliva, and
- GHB determination in saliva samples.

Publications I, III and IV are dealing with methodology validations according to the requirements set for forensic science laboratories, specifically for determination of illegal drugs in seizures and drug abuse determination in biological samples.

An overview of the results is presented in Chapters 4.1.1, 4.1.2, 0 and 4.2.2 of Publications I, II, III and IV.

### **4.1 Spectral Fluorescence Signature method coupled to chemometric techniques as a tool for the rapid and reliable determination of drugs and fingerprints in herbs and solid samples**

#### **4.1.1 Qualitative detection of illegal drugs (cocaine, heroin and MDMA) in seized street samples based on SFS data and ANN: validation of method (Publication I)**

The determination of illegal drugs such as cocaine, heroin and 3,4-methylenedioxy-N-methylamphetamine (MDMA) in bulk street samples by the spectral fluorescence signature method coupled with the pattern recognition technique, the multilayer perceptron artificial neural networks (SFS-MLP-ANN), is discussed in Publication I. The aim of Publication I was to validate the expert system MLP-ANN on a backpropagation learning algorithm used for illegal drugs qualitative analysis by the SFS method according to the requirements of Eurachem (A Focus for Analytical Chemistry in Europe), the

International Conference on Harmonisation of Technical Requirements for Registration of Pharmaceuticals for Human Use/ United States Pharmacopeia (ICH/USP), the Scientific Working Group for the Analysis of Seized Drugs (SWGDRUG) and the United Nations Office on Drugs and Crime (UNODC).

One of the advantages of ANN implementation in comparison to linear regression, principal component and/or partial least squares regressions is its ability to analyse and generalise highly nonlinear, strongly coupled and multivariable systems. Indeed, SFS fingerprints are one of the representatives. In fact, the composition of the samples seized in streets, which contain illegal drugs as one of the substitutes, is unpredictable. Moreover, dealing with illegal drugs that have been synthesized using different synthesis routes leads to the presence of various by-products in the final product. One example of illegal sample's variability is heroin. The nature of exogenous components found in heroin samples from different countries leads to extremal differences in SFS fingerprints (Figure 11).

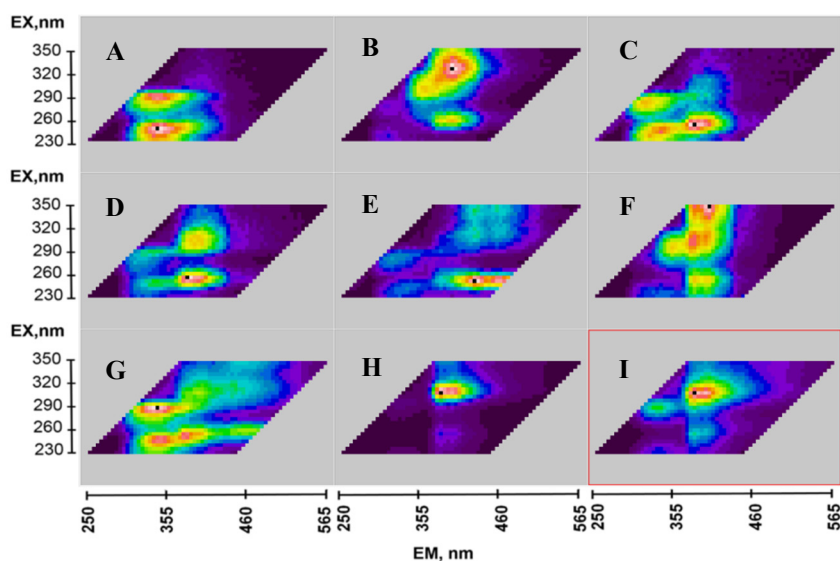


**Figure 11. SFS fingerprints of heroin samples from different countries: A – F – North Carolina, USA; G - Estonia; H – Portugal; I – Switzerland.**

In addition to sample components variability, SFS fingerprint depended on the concentration level of substituents. Figure 1 in Publication I presents the SFSs of analytes at low (5% (w/w)) and the highest concentration levels (100% (w/w)). It is obvious that the inner filter effect occurs for cocaine hydrochloride, morphine and MDMA. However, the inner filter effect should be minimized using the front-face approach for high density samples, but it is not always possible for substances that have very high absorption and small Stock shift. As a result, the re-absorption of emission occurs at high concentration levels, disturbing the

emission spectra. To conclude the above observations, SFS fingerprints are nonlinear, strongly coupled and multivariate systems that can be analysed using nonlinear methods. Therefore, ANN is one of the tools that can be beneficial for SFS fingerprints analysis and prediction.

A comprehensive database, consisting of 4300 different laboratory mixtures and more than 4000 street samples, was used for the further development of ANN and improvement of validation. The qualitative information, based on a binary response (detected/not detected), was directly obtained through the response of an expert system. The qualitative method validation included evaluation of the following parameters:

- range of application:
  - limit of detection (LoD) in the mixture of inert matrix,
  - threshold limit ( $CC\beta$ ) in the mixture of inert matrix,
  - upper range of application;
- selectivity/matrix effects:
  - Threshold limits ( $CC\beta$ ) in the mixture of adulterants/diluents,
  - uncertainty region for each interference;
- robustness (expressed as reliability% at the threshold value \* 1.5);
- precision (repeatability, reproducibility).

It was found that the working capability of ANN differs from instrumental detection capability. The evaluation of illegal drugs has shown that the SFS method exhibits lower LoDs in comparison to ANN's detection capability thresholds that were higher (Table 6). Hence, the re-training of ANN was possible, it was evident that too noisy data at the instrumental detection limit can lead to the overfitting of ANN's. It is the risk that ANN has learnt peculiarities /specificities which are characteristic of training samples and has lost the ability to generalise. Consequently, the dataset with an appropriate amount of data at appropriate concentration levels for the application of interest must be used for training ANN. Moreover, the dataset must be balanced considering the variability of positive to negative samples as well as variability of samples with a common SFS of drugs to an untypical SFS of sample (Publication I).

Based on this finding it was suggested that the work efficacy of ANN should be evaluated. One possible way was to investigate a reasonable amount of independent samples presented as independent validation datasets. Although analysis of real street samples gave information about the reliability and false negative and false positive rates of ANN, it was impossible to determine its critical working capability range. Therefore, it was suggested to determine the uncertainty region for each ANN for illegal drugs in the mixture of the most common adulterants and diluents (Table 1).

**Table 6. Comparison of instrumental detection limits (IDL) and ANN threshold limits in the mixture of inert diluent glucose (Figure 5, Publication I).**

<b>Analyte</b>	<b>IDL*, % (w/w)</b>	<b>ANN threshold limit, % (w/w)</b>
Cocaine HCl	0.0017	0.08
Cocaine base	0.017	0.13
Heroin HCl	0.057	0.20
Heroin base	0.50	0.80
MDMA HCl	0.0017	0.005
MDA HCl	0.0028	0.05

Estimation of the uncertainty of qualitative methods is uncommon. Moreover, it is obligatory only in case of quantitative methods and not qualitative methods. The determination of uncertainty region (UR) is necessary and even crucial in determination of illegal drugs in seizures by using screening methods such as SFS or commercial methods like colour tests or immunoassays. Determination of UR is crucial; taking into account that ANN is often associated with ‘black box’ and it is not easy to predict its behaviour even if there exist exact rules between input and output variables.

The approach based on detection capability ( $CC\beta$ ) determination<sup>101</sup> for uncertainty region evaluation for each ANN was used in this study.  $CC\beta$  values were investigated on the fortified adulterants and diluents at and above the instrumental limit of detection. The region, where the false compliant results of ANN were between 5 – 95%, was suggested as an uncertainty region for ANN. At least 20 measurements for at least one concentration level must be conducted to ensure a reliable basis for determination. The detection capability of ANN equalled the false compliant level of  $\leq 5\%$ . Probability-concentration graphs known as power curves<sup>101</sup> provided the information about the detection capability of ANN within the applied concentration range (Figure 12). URs as graphs are presented in Appendix I–IV.

In addition, this study showed that UR evaluation is an excellent approach to understanding ANN’s behaviour and reliability. The obtained results demonstrated that the developed and improved ANN was able to identify heroin, cocaine, MDMA and MDA neat or in mixtures with other substances with high accuracy, using the SFS method. There was good agreement between the results obtained by the SFS combined with ANN and those obtained by GC methods. The main advantage of this approach is that it does not require specific chemical

skills from the operator and can be used on-site, and is also rapid, reliable and accurate.

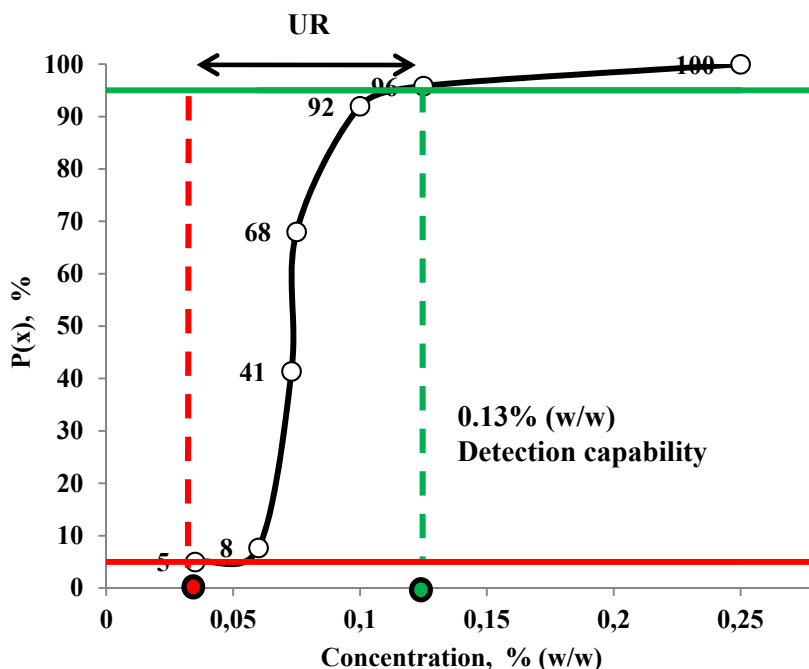


Figure 12. Probability-concentration graph for the proposed cocaine base screening method under optimal conditions. Cut-off values correspond to 95% confidence limits for negative/positive probabilities.

#### 4.1.2 Fluorescence, electrophoretic and chromatographic fingerprints of herbal medicines and their comparative chemometric analysis (Publication II)

The capability of the spectral fluorescence signature method to assess the polyphenolic content in herbal medicines was studied in Publication II. The results presented in Publication I show that SFS fingerprints revealing the unique properties of samples and/or sample groups can be used for determination of samples. Therefore, it was suggested that the SFS method should be capable of determining rapidly and reliably the authenticity of HMs. Moreover, instead of ANN, other chemometric techniques such as PARAFAC in combination with PCA and cluster analysis were utilized for SFS fingerprints.

The application of a novel real-time spectroscopic method such as SFS may be a significant input into the creation of a method of screening herbal medicines

quickly on-site. This method may be especially of value for biologists, as well as phytochemical and chemical analysts. In this thesis, analysis of herbal medicines was performed on concentrated turbid neat/undiluted samples. This was possible due to making front-face mode measurements and was impossible in case of classical fluorescence spectroscopy.

In total, 47 mixtures of air-dried herbal medicines and four herbal tea mixtures were studied. HMs were chosen as they are the most common medicine herbs available in the local market.

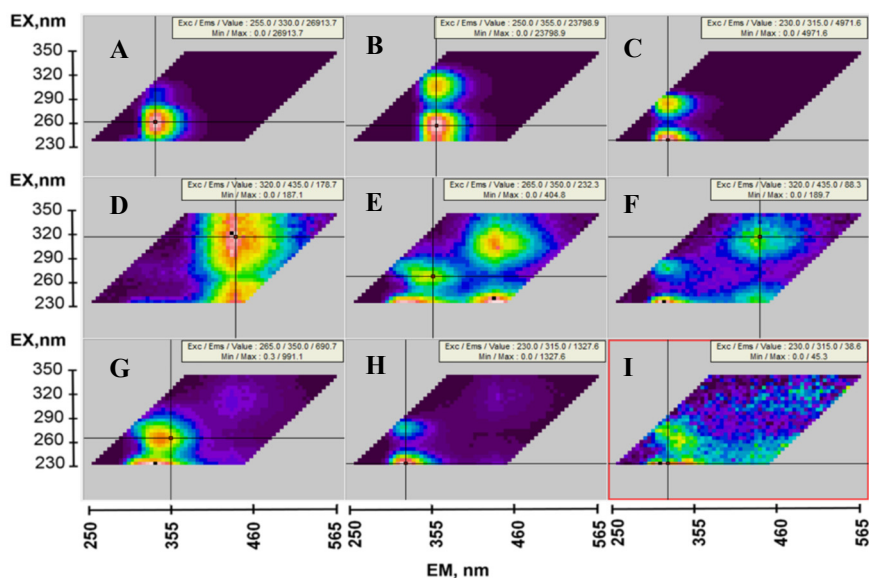


**Figure 13.** SFS fingerprints of HM in methanol: **A** – S36 (*Foeniculum vulgare*); **B** – S41 (*Acorus calamus*); **C** – S38 (*Potentilla erecta* (L)); **D** – S13 (*Tussilago farfara*); **E** – S5 (*Achillea millefolium*); **F** – S25 (*Mentha piperita*); **G** – S16 (*Viscum*); **H** – S22 (*Calluna vulgaris* L. Hull); **I** – S30 (*Cetraria islandica* (L.) Ach).

HMs are complex multicomponent sample matrixes that are used for treatment of different disorders, due to their different pharmacological effects and properties. For instance, some HMs have antibacterial (S1 – *Symphytum officinale*, S3 – *Hypericum perforatum*, etc.), antitumour (S2 – *Chelidonium majus*, S3 – *Hypericum perforatum*, etc.) and anti-inflammatory (S1 – *Symphytum officinale*, S3 – *Hypericum perforatum*, S4 – *Melissa officinalis*, etc.). HMs may also exhibit other favourable effects. HMs contain a large number of different constituents. One of the main groups is polyphenolic compounds. The fluorescence and absorbance characteristics of the main polyphenolic compounds found in herbal medicines under different experimental conditions were determined in Publication II. This information may be especially useful for phytochemists and analysts.

The sequence of chemometric techniques like PARAFAC combined with PCA and/or CA was introduced for an effective authentication of herbal medicines. A comparative study was conducted with well-known separation methods CE-DAD and HPLC-DAD-MS.

The performance characteristics such as IDL, linearity range, intra- and inter-day precision and matrix effect (ME%) were evaluated. The IDLs of three methods were compared. The results showed that the detection capability of SFS was comparable to that of HPLC-DAD in case of syringic and chlorogenic acids. However, the SFS method was much more sensitive, especially for catechin. The IDLs of three methods are given in Table 7, while other parameters can be found in Table 3 in Publication II.

**Table 7. Instrumental detection limits of SFS, CE-DAD and HPLC-DAD methods.**

Analyte	SFS <sup>a</sup> IDL, mg L <sup>-1</sup>	Reference methods IDL, mg L <sup>-1</sup>	
		CE-DAD <sup>b</sup>	HPLC-DAD <sup>c</sup>
Syringic acid	0.058	1.82	0.065
Catechin	0.037	2.56	1.87
Chlorogenic acid	0.136	2.29	0.117
Protocatechuic acid	0.052	1.13	0.56
Ferulic acid	0.256	1.09	1.04
Naringin	No native fluorescence	4.44	0.116
Rutin	No native fluorescence	4.56	0.122

<sup>a</sup> IDL is evaluated at  $\lambda_{EX}/\lambda_{EM}$  as follows: 270/340 nm – syringic acid; 230/310 nm – catechin; 325/435 nm – chlorogenic acid; 250/335 nm – protocatechuic acid; 310/405 nm – ferulic acid.

<sup>b</sup> IDL is evaluated at the detection wavelength of 210 nm (chlorogenic acid at 345 nm).

<sup>c</sup> IDL is evaluated at the detection wavelength of 254 nm.

The SFS fingerprints of HMs can be divided into regions for characterization of polyphenolic compounds: A –flavan-3-ol-like derivatives (the main representative catechin), B – dihydroxybenzoic acid-like derivatives (DHBA), C – flavonol-like derivatives, trihydroxybenzoic acid-like derivatives and tannin-like derivatives, D – stibenoid-like derivatives, E – hydroxycinnamic acid-like derivatives (HCA). Figure 1 in Publication II shows the approximate regions of SFS fingerprints of polyphenolic compounds found in HMs.

The SFS method has demonstrated an excellent detection capability for recognition of HMs according to their polyphenolic content. The exploratory analysis was performed using an expert system that was a combination of several chemometric techniques. The SFS fingerprints reflected the content of

polyphenolic compounds and other constituents in HMs. Figure 13 depicts the SFS fingerprints of some HMs that can be even visually differentiated from each other.

In this thesis, first of all, PARAFAC was applied for reduction of dimensionality and identification of feature vectors. PARAFAC loadings (Figure 2, Publication II) showed excitation and emission profiles of PARAFAC components and scores showed the concentration profile for each HM. PARAFAC scores were fed to PCA and cluster analysis for explanatory analysis. As a result, four PARAFAC components were able to divide HMs into the groups: HMs with a very high/low concentration of catechin-like compounds, HMs with a low/high content of DHBA-like compounds, HMs with a low /high content of HCA-like compounds, and HMs with a low content of fluorescent polyphenolic compounds. Figure 3 C in Publication II presents the results of CA for PARAFAC scores. In the figure the separation of HMs into groups and subgroups according to the content of catechin-like, HCA-like and DHBA-like derivatives is shown.

For better result visualization, the unity-based normalization was performed on PARAFAC scores for every PARAFAC component. The abundance of catechin-like compounds was established in S38 (*Potentilla erecta* (L.)) (Figure 13 C) and S18 (*Vaccinium vitis-idaea*). The overall content of catechin-like compounds in S18 and S38 was greater than 80% of their normalized maximum-minimum content in the investigated HMs (Figure 14 A).

The content of HCA-like compounds was found to be the highest in S5 (*Achillea millefolium*) (Figure 13 E), S2 (*Chelidonium majus*) and S6 (*Veronica officinalis*) unlike the other HMs under study (Figure 14 B). A high content of HCA-like compounds (caffeic, sinapic, ferulic acids, etc.) and a low content of other compounds were observed in *Tussilago farfara* (S13 in Figure 13 D).

Four HMs such as S16 (*Viscum*) (Figure 13 G), S2 (*Chelidonium majus*), S21 (*Malva L.*), S42 (*Taraxacum officinale*) were grouped by the high content of DHBA-like compounds. The overall content of DHBA-like compounds was greater than 50% of their normalized maximum-minimum content in the HMs under study (Figure 14 C).

S47 (*Fucus vesiculosus*), S30 (*Cetraria islandica* (L.) Ach.) (Figure 13 I) and S35 (*Carum carvi*) were characterised by the low content of fluorescent polyphenolic compounds, whose overall concentration in these HMs was less than 10% of their normalized maximum-minimum content in the investigated HMs (Figure 14 D).

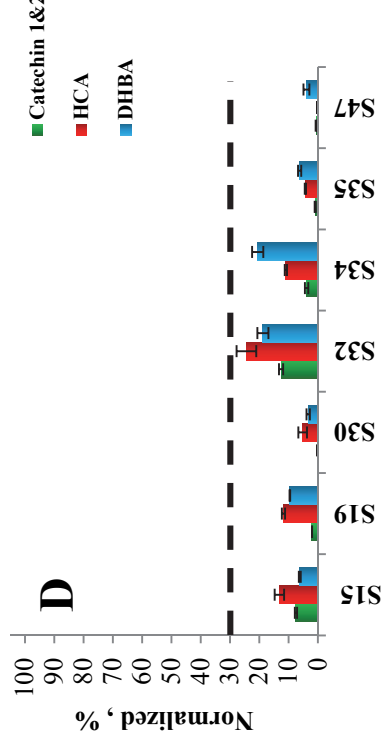
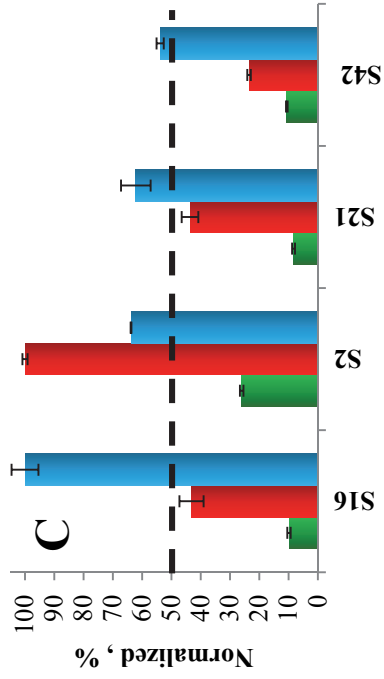
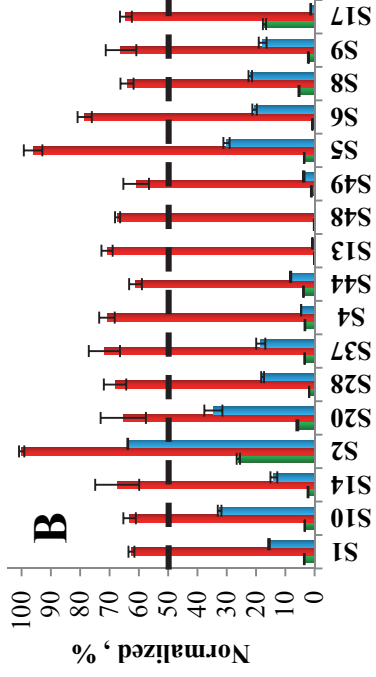
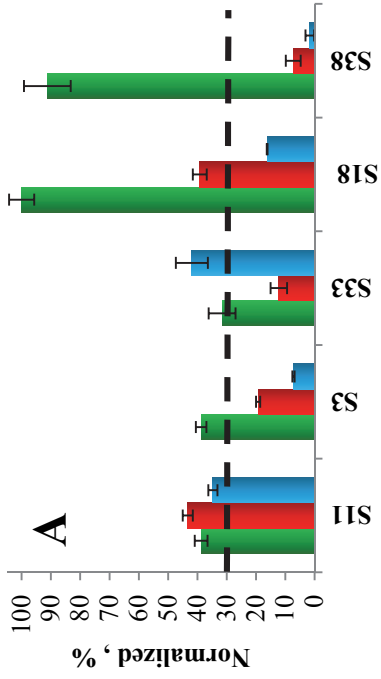


Figure 14. Normalized PARAFAC components scores on HM with A – high content of catechin-like derivatives; B – high content of HCA-like derivatives; C – high content of DHBA-like derivatives; D – low content of all fluorescent polyphenolic compounds.

The performance of the PARAFAC-PCA/CA model was assessed by an independent validation set containing 27 HMs under investigation. The average accuracy and precision of the model as determined by the set were 97.4% (range 85.2–100%) and 89.6% (range 66.7–100%), respectively. PARAFAC-PCA/CA was shown to be capable of identifying HMs on the basis of polyphenolic content.

The reference methods of separation were based on the absorbance properties of polyphenolic compounds. The electrophoretic and chromatographic fingerprints obtained by PARAFAC-PCA/CA, i.e. recognition of HMs on the basis of polyphenolic content, were in good agreement with the SFS fingerprints obtained by chemometric techniques. Table 4 in Publication II compares the results of three methods. In addition, polyphenolic compounds were identified by MS/MS and the results are shown in Table A1 and Figure A3 in Publication II.

Apart from the successful application of SFS to the illegal drug detection as shown in Publication I, it proved to be a rapid, sensitive and reliable tool also for the investigation of fingerprints and prediction of the composition of HMs as demonstrated in Publication II. Moreover, the SFS technique was useful in gathering fingerprints of authentic herbal medicine extracts, requiring neither pre-treatment nor dilution of samples.

## **4.2 Capillary electrophoresis as a tool for drug abuse determination in saliva**

There is a high necessity for simple, rapid and sensitive screening methods with performance parameters similar to those of the confirmation techniques used on-site. One of such methods, whose instrumentation can be simply miniaturized and effectively utilized on-site, is capillary electrophoresis. Moreover, the combination of capillary electrophoresis with different detection techniques makes this method advantageous over others. The pluses of CE are also small sample quantities (as low as nLs) needed for analysis, and short analysis time.

### **4.2.1 Determination of cannabinoids in oral fluid (Publication III)**

The proof of the principle for determination of cannabis abuse in saliva samples by non-aqueous capillary electrophoresis (NACE) coupled to fluorescence detection is discussed in Publication III. Having knowledge of cannabis products and cannabinoids as natively fluorescing substances (Figure 15), fluorescence was suggested as one of the most promising techniques for detection of cannabis abuse due its high sensitivity and specificity. The fluorescence properties of analytes enable optimum excitation and emission wavelengths to be chosen, which improves the selectivity or analysis.). Thus, it gives the possibility to eliminate non-targeted substituents of sample matrixes from the detection range.

Moreover, the utilization of a separation technique as CE in combination with fluorescence allows separation of analytes with similar fluorescence properties, increasing the selectivity of the method as a whole.

The NACE technique was used for several reasons. First of all, THC and CBD are almost insoluble in water and, therefore, separation media containing organic solvents are preferable to aqueous solutions, improving the solubility of analytes. Moreover, non-aqueous media reduce the current, allowing for the application of high field strength, thus decreasing the separation time. Furthermore, the pKa values of analytes must be taken into account. The pKa values of THC and CBD pKa are above 9.5 and 10.5, respectively. Thus, cannabinoids are deprotonated in highly basic electrolytes and they migrate as anions towards the cathode. Consequently, highly basic electrolyte systems are preferable for analysis of cannabinoids.

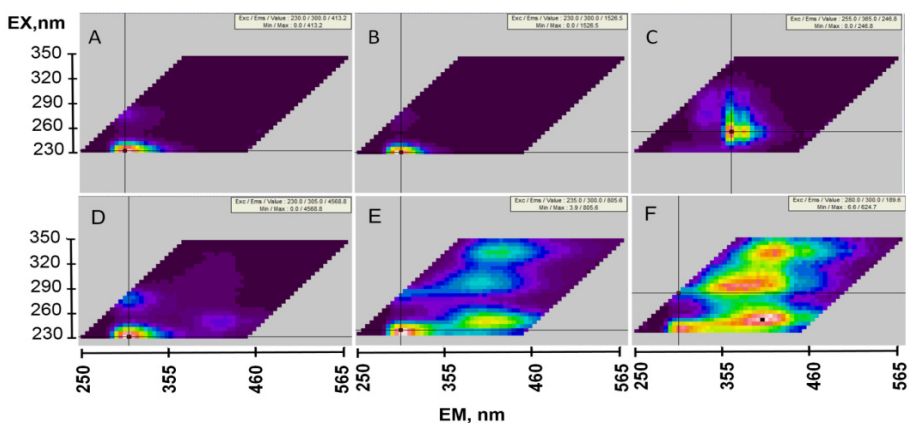


**Figure 15. SFS of cannabinoids and cannabis products in ethanol: A –  $\Delta^9$ -THC; B – CBD; C – CBN; D – hemp; E – marijuana; F – hashish.**

The fluorescence spectra of two main markers of cannabis abuse, THC and CBD, are similar. The excitation maximums are located at 230 and 280 nm and the fluorescence maximum at 300 nm. The availability of the CE device coupled to the LED detector with an excitation wavelength of 280 nm was suitable for detection of the second maximum, but not optimal for detection for THC and CBD, taking into account the higher quantum yield of THC and CBD at  $\lambda_{ex}/\lambda_{em}=230/300$  nm (Figure 16).

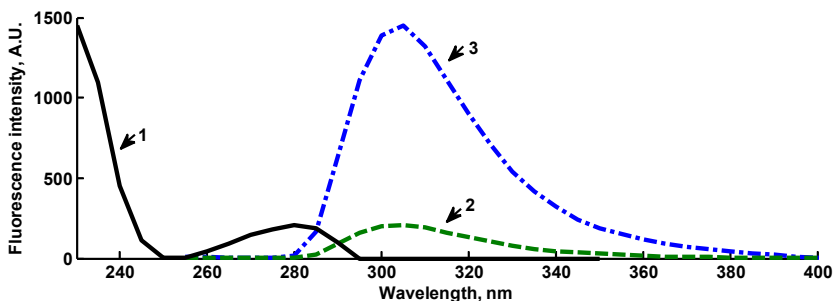


**Figure 16. Fluorescence spectra of THC and CBD: 1 (solid line) – THC excitation spectrum registered at  $\lambda=305$  nm; 2 (dashed line) – THC emission spectrum excited at  $\lambda=280$  nm; 3 (dash-dotted line) – THC emission spectrum excited at  $\lambda=230$  nm.**

Nevertheless, promising results were achieved by the available LED-induced fluorescence detector. The CE methodology for cannabinoids was optimised for saliva matrix using a simple and efficient combined-in step collection/preparation/pre-concentration procedure employing the Salivette® sampling device. Therefore, no separate precipitation of proteins and/or derivatisation was required. The recovery of both tested cannabinoids from the collection pads was greater than 80% at 2.5 mg/mL.

The CE separation of the two cannabinoids was achieved in less than 7 min (Figure 17 – G: peak #2 and peak #3). The NACE methodology utilizing the LED system was validated. The LoD was 0.19 and 0.17  $\mu\text{g/mL}$  for THC and CBD, respectively. The inter-day precision was less than 6% for all analytes. No matrix effect was found for saliva samples. The specificity study was conducted on common pharmaceuticals (listed in Publication III). Moreover, the endogenous saliva components (Figure 17) and exogenous substituents after prescribed drugs use (Figure 4 in Publication III) were assessed for possible peaks co-migration. No false positive results were found during the specificity studies. Furthermore, the proposed methodology was able to differentiate the licit cannabis products consumption using CBD as a marker as CBD migrates separately from THC.

Moreover, the controlled *ad libitum* smoking was conducted and the cannabis abuse was determined after 20 minutes (Figure 18). However, the current CE-LED system lacked sensitivity for THC impairment determination. It is believed that the new detector construction with an excitation wavelength at 230 nm can resolve this issue. The project on cannabis abuse determination by CE is on-going further.

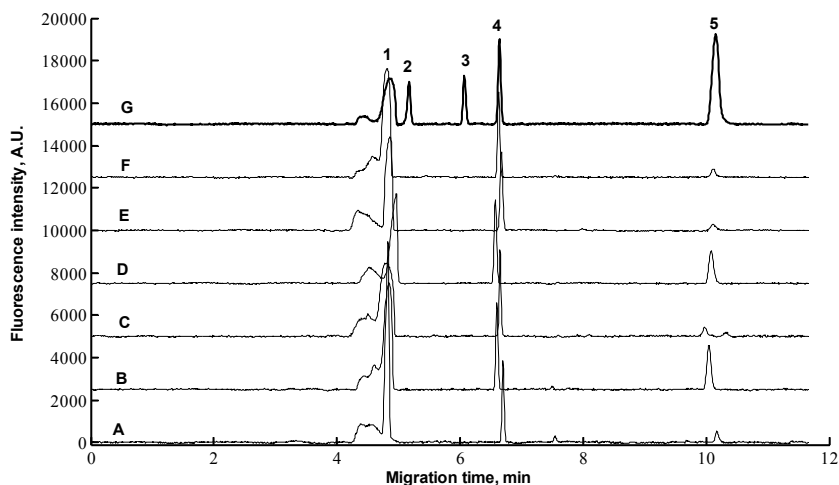


**Figure 17. Assessment of the endogenous matrix effect. Electropherograms: A-F – OF samples from six volunteers, G – OF sample spiked with standards of CBD, THC and IS. Peaks: 1 – neutral compound from a Salivette® swab, 2 – CBD, 3 – THC, 4 – IS, 5 – saliva endogenous compound. Experimental conditions as in Figure 2 in Publication III.**

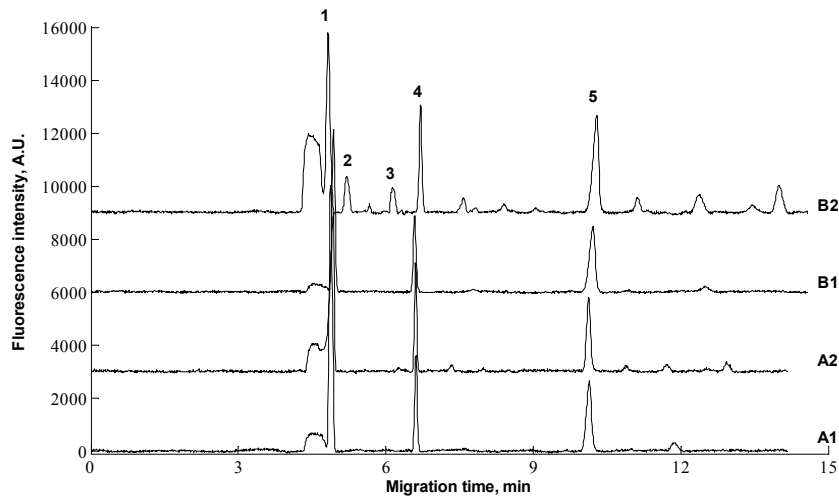


**Figure 18. CE analysis of real OF specimens. Electropherograms: A1, B1 – blank OFs, A2 – saliva sample after the smoking of one “LM blue” cigarette, B2 – saliva sample after the smoking of one cannabis cigarette. Peaks: 1 – neutral compound from a Salivette® swab, 2 – CBD, 3 – THC, 4 – IS, 5 – saliva endogenous compound. Experimental conditions as in Figure 2 in Publication III.**

#### 4.2.2 Determination of $\gamma$ -hydroxybutyric acid in oral fluid (Publication IV)

$\gamma$ -Hydroxybutyric acid (GHB) is a well-known drug that naturally occurs in the human body as a GABA metabolite, facilitating sexual assault. Therefore, the differentiation between the exogenous and endogenous concentrations of GHB is of utmost importance. GHB is a small polar molecule with weak absorbance and without native fluorescence characteristics. Therefore, electrochemical detection such as conductivity is believed to be suitable for detection of GHB in biological samples. Generally, GHB abuse needs a complicated and time-consuming sample preparation, including the derivatisation procedure. Moreover, the half-life of GHB is merely 20-50 minutes. Therefore, the sample collection must be performed as soon as possible after drug abuse suspicion.

The aim of the current study was to show that it is possible to detect GHB and determine its exogenous and endogenous concentrations in saliva samples by CE-C<sup>4</sup>D-ABS. No simple and reliable method had been proposed till now for detection of GHB abuse in saliva samples by CE-C<sup>4</sup>D.

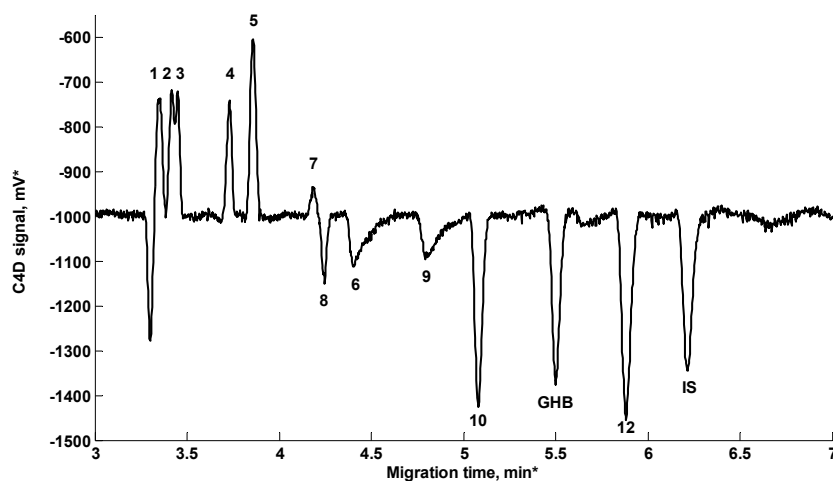


**Figure 19.** Analytes: 1 – chloride (5 mg/L); 2 – nitrite (10 mg/L); 3 – nitrate (10 mg/L); 4 – sulfate (10 mg/L) and sulfite (5 mg/L); 5 – thiocyanate (40 mg/L); 6 – tartrate (120 mg/L); 7– succinate (80 mg/L); 8 citrate (– 120 mg/L); 9 – hydrogen phosphate (20 mg/L); 10 – lactate (20 mg/L); 11 – GHB (20 mg/L); 12 –glutamate (20 mg/L); 13 – PMPA (IS).

**Applied CE conditions.** BGE: 8.5 mM maleic acid, 17 mM Arg and 255  $\mu$ M CTAB, 15% ACN, pH=7.65; capillary length, 65.0 cm; temperature, 21°C; voltage, -19 kV; hydrodynamic injection, 35 mbar for 10 s; contactless conductivity detection, frequency 150 Hz; sample acetonitrile ratio, 1:3.

CE-C<sup>4</sup>D-ABS was also suitable for determination of different anions present in saliva samples (Figure 19 for C<sup>4</sup>D and Figure 1 – II in Publication IV for indirect ABS). The performance characteristics of the CE-C<sup>4</sup>D-indirect UV methodology was validated according to the European Medicines Agency’s Guideline on validation of bioanalytical method (EMA/275542/2014)<sup>57</sup>. The IDL and IQL were 0.49 and 1.6 mg/L for C<sup>4</sup>D, respectively. The LoD and LoQ were 2.0 and 6.5 mg/L, respectively. The IDL and IQL for indirect UV absorbance were 5.1 mg/L and 17.0 mg/L, respectively. The inter-day precisions were within 2.3–5.7% and intra-day precisions were within 1.6–9.0% for C<sup>4</sup>D. The inter-day and intra-day precisions for indirect UV were within 2.1–9.3% and 5.6–10.1%, respectively.

The recovery values were within 87.2–104.4%. The matrix effects were +53.2% for small concentrations up to 25 mg/L for C<sup>4</sup>D and +23.6% for concentrations up to 75 for mg/L for the indirect UV detection. No matrix effects were observed for higher concentration levels. Moreover, six blank saliva samples were tested and no peak overlapping was observed (Figure 20).

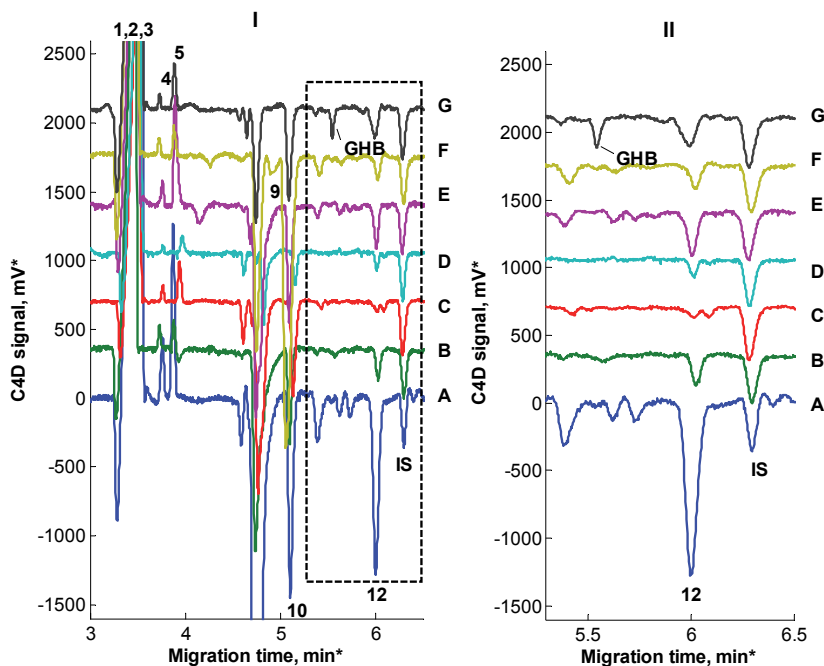


**Figure 20.** I – Electropherograms of saliva blanks. II – Zoomed region of electropherogram from 5.3 to 6.5 min: A – saliva of volunteer #5; B – saliva of volunteer #1; C – saliva of volunteer #3; D – saliva of volunteer #2; E – saliva of volunteer #4; F – saliva of volunteer #6; G – saliva of volunteer #3 spiked with 10 mg L<sup>-1</sup> GHB. Applied working conditions and symbols as in Figure 19.

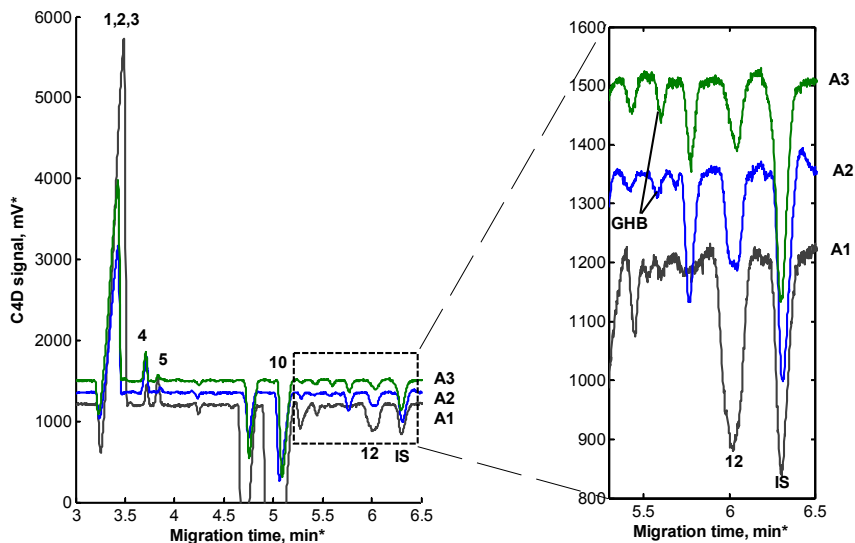


**Figure 21. CCE-C4D electropherograms of saliva samples after drinking red wine and a zoomed region of electropherogram from 5.3 to 6.5 min: A1 – blank saliva of volunteer #5; A2 – saliva of volunteer #5 after drinking 30 cl of “Vina Maipo Vitral”; A3 – saliva of volunteer #5 spiked with 10 mg/L GHB (#11) after drinking 30 cl of “Vina Maipo Vitral”. Applied working conditions as in Figure 19.**

Figure 21 shows electropherograms of saliva samples after wine drinking. The saliva sample containing wine remains is a complex sample matrix with different wine constituents, including phenolic compounds that can be recorded by C<sup>4</sup>D. The small increase of GHB peak was observed after red wine drinking.

In conclusion, it is expected that there will be no difficulties in determination of GHB abuse in forensic and patient saliva samples. Moreover, the proposed methodology will be applied for real GHB abuse cases in the on-going research. CE-C<sup>4</sup>D-indirect-UV as a forensic screening tool can offer rapidness, accuracy, sensitivity and definiteness in the determination of GHB abuse in saliva samples.

## 5 CONCLUSIONS

The main goal of this dissertation was to develop and optimize quick on-site screening methods such as the spectral fluorescence signature method and capillary electrophoresis for determination of drugs in different sample matrixes.

The results of the work demonstrate that SFS and in particular CE are very promising techniques to be considered for the rapid on-site detection of illicit drugs instead of the existing qualitative assays. It was demonstrated that both the methods can use saliva as a body fluid for detection of abuse of illicit drug, thus liberating law enforcement officers from the need to collect more common yet more inconvenient-to-take urine and blood samples.

However, it was demonstrated that advantages of SFS and CE can be made use of only by capable and sophisticated data processing chemometric tools.

The results of the study can be summarized as follows:

- ✓ The SFS method with ANN as an expert system and optimized methodologies for illegal drugs detection was successfully validated.
- ✓ The SFS-ANN database was extended and the working capability of ANNs was improved.
- ✓ The approach for evaluation of uncertainty region for the artificial intelligence system was proposed and proven to be effective for understanding the working capability of ANN in the mixtures of different adulterants and diluents.
- ✓ The SFS method combined with PARAFAC-PCA-cluster analysis as a rapid and sensitive method for qualitative and quantitative analysis of different types of herbal medicines was applied for the first time ever.
- ✓ The SFS-PARAFAC-PCA/CA method for determining the polyphenolic content of HMs can be used as a screening method on-site or in laboratory.
- ✓ The front-face SFS method is capable of analyzing directly the authentic fluorescent fingerprints of neat/undiluted herbal medicine extracts and does not interfere with the Rayleigh scattering due to the special measurement window.
- ✓ The NACE-LED system was capable of detecting THC abuse in saliva samples after smoking a cannabis joint. Moreover, it was possible to

differentiate the licit cannabis use from the illicit one via detection of CBD.

- ✓ The CE-C<sup>4</sup>D system was capable of differentiating the exogenous and endogenous concentrations of GHB in saliva samples.
- ✓ CE-C<sup>4</sup>D was successfully applied for determination of GHB in saliva samples after drinking red wine.
- ✓ CE analysis time was within 10 minutes in determination of THC and CBD and within 6 minutes in determination of GHB.

## REFERENCES

1. UNODC. *World Drug Report 2015*; 978-92-1-148282-9; United Nations: New York, May 2015, 2015.
2. EMCDDA. *European Drug Report 2015: Trends and Developments*; EMCDDA: Luxembourg, 2015.
3. UNODC. *World Drug Report 2014*; 978-92-1-148277-5; United Nations: New York, June 2014, 2014.
4. EMCDDA. Data and statistics: Price, purity and potency. [WWW] <http://www.emcdda.europa.eu/data/stats2015> (accessed 11.11.2015).
5. Broseus, J., Gentile, N., Bonadio Pont, F., Garcia Gongora, J. M., Gaste, L., Esseiva, P. Qualitative, quantitative and temporal study of cutting agents for cocaine and heroin over 9 years. *Forensic Sci. Int.* **2015**, *257*, 307-313.
6. Schneider, S., Meys, F. Analysis of illicit cocaine and heroin samples seized in Luxembourg from 2005-2010. *Forensic Sci. Int.* **2011**, *212* (1-3), 242-246.
7. Evrard, I., Legleye, S., Cadet-Tairou, A. Composition, purity and perceived quality of street cocaine in France. *Int. J. Drug Policy* **2010**, *21* (5), 399-406.
8. Cole, C., Jones, L., McVeigh, J., Kicman, A., Syed, Q., Bellis, M. Adulterants in illicit drugs: a review of empirical evidence. *Drug Test Anal.* **2011**, *3* (2), 89-96.
9. Erowid Ecstasy Data tests [WWW] [www.ecstasydata.org](http://www.ecstasydata.org) (accessed 11.11.2015).
10. Protocol amending the Single Convention on Narcotic Drugs, 1961. *Bull Narc* **1972**, *24* (3), 1-6.
11. Ramaekers, J. G., Berghaus, G., van Laar, M., Drummer, O. H. Dose related risk of motor vehicle crashes after cannabis use. *Drug Alcohol Depend.* **2004**, *73* (2), 109-19.
12. Dussy, F. E., Hamberg, C., Luginbühl, M., Schwerzmann, T., Briellmann, T. A. Isolation of  $\Delta^9$ -THCA-A from hemp and analytical aspects concerning the determination of  $\Delta^9$ -THC in cannabis products. *Forensic Sci. Int.* **2005**, *149* (1), 3-10.
13. Sharma, P., Murthy, P., Bharath, M. M. Chemistry, metabolism, and toxicology of cannabis: clinical implications. *Iran J. Psychiatry* **2012**, *7* (4), 149-56.
14. Mathre, M. L. *Cannabis In Medical Practice : a Legal, Historical, and Pharmacological Overview of the Therapeutic Use of Marijuana*. McFarland & Company, Inc.: North Carolina, U.S., 1997.
15. Huestis, M. A. Human Cannabinoid Pharmacokinetics. *Chem. Biodiversity* **2007**, *4* (8), 1770-1804.
16. Drummer, O. H., Gerostamoulos, J., Batziris, H., Chu, M., Caplehorn, J., Robertson, M. D., Swann, P. The involvement of drugs in drivers of motor vehicles killed in Australian road traffic crashes. *Accid. Anal. Prev.* **2004**, *36* (2), 239-48.
17. Musshoff, F., Madea, B. Review of biologic matrices (urine, blood, hair) as indicators of recent or ongoing cannabis use. *Ther. Drug Monit.* **2006**, *28* (2), 155-163.
18. Verstraete, A. G. Detection times of drugs of abuse in blood, urine, and oral fluid. *Ther. Drug Monit.* **2004**, *26* (2), 200-5.
19. Odell, M. S., Frei, M. Y., Gerostamoulos, D., Chu, M., Lubman, D. I. Residual cannabis levels in blood, urine and oral fluid following heavy cannabis use. *Forensic Sci. Int.* **2015**, *249*, 173-80.
20. Vindenes, V., Boix, F., Koksæter, P., Strand, M. C., Bachs, L., Morland, J., Gjerde, H. Drugged driving arrests in Norway before and after the implementation of per se law. *Forensic Sci. Int.* **2014**, *245*, 171-177.
21. Huestis, M. A., Cone, E. J. Relationship of Delta 9-tetrahydrocannabinol concentrations in oral fluid and plasma after controlled administration of smoked cannabis. *J. Anal. Toxicol.* **2004**, *28* (6), 394-9.
22. Fabritius, M., Chtioui, H., Battistella, G., Annoni, J.-M., Dao, K., Favrat, B., Fornari, E., Lauer, E., Maeder, P., Giroud, C. Comparison of cannabinoid concentrations in oral fluid and whole blood

- between occasional and regular cannabis smokers prior to and after smoking a cannabis joint. *Anal. Bioanal. Chem.* **2013**, *405* (30), 9791-9803.
23. Backofen, U., Matysik, F.-M., Lunte, C. E. Determination of cannabinoids in hair using high-pH<sup>□</sup> non-aqueous electrolytes and electrochemical detection: Some aspects of sensitivity and selectivity. *J. Chromatogr. A* **2002**, *942* (1-2), 259-269.
24. Giroud, C., Ménétrey, A., Augsburger, M., Buclin, T., Sanchez-Mazas, P., Mangin, P.  $\Delta$ 9-THC, 11-OH- $\Delta$ 9-THC and  $\Delta$ 9-THCCOOH plasma or serum to whole blood concentrations distribution ratios in blood samples taken from living and dead people. *Forensic Sci. Int.* **2001**, *123* (2-3), 159-164.
25. Schwöpe, D. M., Karschner, E. L., Gorelick, D. A., Huestis, M. A. Identification of Recent Cannabis Use: Whole-Blood and Plasma Free and Glucuronidated Cannabinoid Pharmacokinetics following Controlled Smoked Cannabis Administration. *Clin. Chem.* **2011**, *57* (10), 1406-1414.
26. Vindenes, V., Jordbru, D., Knapskog, A. B., Kvan, E., Mathisrud, G., Stordal, L., Morland, J. Impairment based legislative limits for driving under the influence of non-alcohol drugs in Norway. *Forensic Sci. Int.* **2012**, *219* (1-3), 1-11.
27. Huestis, M. A., Henningfield, J. E., Cone, E. J. Blood cannabinoids. I. Absorption of THC and formation of 11-OH-THC and THCCOOH during and after smoking marijuana. *J. Anal. Toxicol.* **1992**, *16* (5), 276-82.
28. Saytzeff, A. Über die Reduction des Succinylchlorids". *Liebigs Annalen der Chemie* **1874**, *171*, 258-290.
29. Laborit, H. Sodium 4-Hydroxybutyrate. *Int. J. Neuropharmacol.* **1964**, *3*, 433-51.
30. Carter, L. P., Pardi, D., Gorsline, J., Griffiths, R. R. Illicit *gamma*-hydroxybutyrate (GHB) and pharmaceutical sodium oxybate (Xyrem®): Differences in characteristics and misuse. *Drug Alcohol Depend.* **2009**, *104* (1-2), 1-10.
31. Mazarr-Proo, S., Kerrigan, S. Distribution of GHB in tissues and fluids following a fatal overdose. *J. Anal. Toxicol.* **2005**, *29* (5), 398-400.
32. Elian, A. A. Determination of endogenous *gamma*-hydroxybutyric acid (GHB) levels in antemortem urine and blood. *Forensic Sci. Int.* **2002**, *128* (3), 120-2.
33. Andresen, H., Sprys, N., Schmoltdt, A., Mueller, A., Iwersen-Bergmann, S. *Gamma*-hydroxybutyrate in urine and serum: additional data supporting current cut-off recommendations. *Forensic Sci. Int.* **2010**, *200* (1-3), 93-9.
34. Elliott, S. P. *Gamma*-hydroxybutyric acid (GHB) concentrations in humans and factors affecting endogenous production. *Forensic Sci. Int.* **2003**, *133* (1-2), 9-16.
35. De Paoli, G., Walker, K. M., Pounder, D. J. Endogenous *gamma*-hydroxybutyric acid concentrations in saliva determined by gas chromatography-mass spectrometry. *J. Anal. Toxicol.* **2011**, *35* (3), 148-52.
36. Schrock, A., Hari, Y., König, S., Auwärter, V., Schurch, S., Weinmann, W. Pharmacokinetics of GHB and detection window in serum and urine after single uptake of a low dose of GBL - an experiment with two volunteers. *Drug Test. Anal.* **2014**, *6* (4), 363-366.
37. Kintz, P., Gouille, J. P., Cirimele, V., Ludes, B. Window of detection of *gamma*-hydroxybutyrate in blood and saliva. *Cli. Chem.* **2001**, *47* (11), 2033-4.
38. Brenneisen, R., Elshohly, M. A., Murphy, T. P., Passarelli, J., Russmann, S., Salamone, S. J., Watson, D. E. Pharmacokinetics and excretion of *gamma*-hydroxybutyrate (GHB) in healthy subjects. *J. Anal. Toxicol.* **2004**, *28* (8), 625-30.
39. Abanades, S., Farre, M., Segura, M., Pichini, S., Pastor, A., Pacifici, R., Pellegrini, M., de la Torre, R. Disposition of *gamma*-hydroxybutyric acid in conventional and nonconventional biologic fluids after single drug administration: issues in methodology and drug monitoring. *Ther. Drug Monit.* **2007**, *29* (1), 64-70.
40. Haller, C., Thai, D., Jacob, P., Dyer, J. E. GHB Urine Concentrations After Single-Dose Administration in Humans. *J. Anal. Toxicol.* **2006**, *30* (6), 360-364.
41. Borgen, L. A., Okerholm, R., Morrison, D., Lai, A. The influence of gender and food on the pharmacokinetics of sodium oxybate oral solution in healthy subjects. *J. Clin. Pharmacol.* **2003**, *43* (1), 59-65.
42. WHO. *Gamma-hydroxybutyric acid (GHB) Critical Review Report*; 4-8 June, 2012, 2012.

43. Roberts, D. M., Smith, M. W. H., Gopalakrishnan, M., Whittaker, G., Day, R. O. Extreme  $\gamma$ -Butyrolactone Overdose With Severe Metabolic Acidosis Requiring Hemodialysis. *Ann. Emerg. Med.* **2011**, *58* (1), 83-85.
44. M. Helrich, T. C. McAslan, Skolnick, S., Bessman, S. P. Correlation of blood levels of GHB with state of consciousness. *Anesthesiology* **1964**, *25*, 771-775.
45. Brailsford, A. D., Cowan, D. A., Kicman, A. T. Pharmacokinetic properties of *gamma*-hydroxybutyrate (GHB) in whole blood, serum, and urine. *J. Anal. Toxicol.* **2012**, *36* (2), 88-95.
46. Busardo, F. P., Jones, A. W. GHB Pharmacology and Toxicology: Acute Intoxication, Concentrations in Blood and Urine in Forensic Cases and Treatment of the Withdrawal Syndrome. *Curr. Neuropharmacol.* **2015**, *13* (1), 47-70.
47. Divry, P., Baltassat, P., Rolland, M. O., Cotte, J., Hermier, M., Duran, M., Wadman, S. K. A new patient with 4-hydroxybutyric aciduria, a possible defect of 4-aminobutyrate metabolism. *Clin. Chim. Acta* **1983**, *129* (3), 303-9.
48. Dai, J., Mumper, R. J. Plant phenolics: extraction, analysis and their antioxidant and anticancer properties. *Molecules* **2010**, *15* (10), 7313-52.
49. Harborne, J. B. *Phytochemical methods. A guide to modern techniques of plant analysis*. 3 ed.; Chapman & Hall: London, UK, 1998.
50. Bishayee, A. Cancer Prevention and Treatment with Resveratrol: From Rodent Studies to Clinical Trials. *Cancer Prev. Res.* **2009**, *2* (5), 409-418.
51. Grootaert, C., Kamiloglu, S., Capanoglu, E., Van Camp, J. Cell Systems to Investigate the Impact of Polyphenols on Cardiovascular Health. *Nutrients* **2015**, *7* (11), 9229-9255.
52. Shimizu, M., Shirakami, Y., Sakai, H., Kubota, M., Kochi, T., Ideta, T., Miyazaki, T., Moriwaki, H. Chemopreventive potential of green tea catechins in hepatocellular carcinoma. *Int. J. Mol. Sci.* **2015**, *16* (3), 6124-39.
53. Spencer, J. P., Abd El Mohsen, M. M., Minihane, A. M., Mathers, J. C. Biomarkers of the intake of dietary polyphenols: strengths, limitations and application in nutrition research. *Br. J. Nutr.* **2008**, *99* (1), 12-22.
54. Rocha, L. D., Monteiro, M. C., Teodoro, A. J. Anticancer Properties of Hydroxycinnamic Acids. *J. Cancer Clin. Oncol.* **2012**, *1* (2).
55. Lall, R. K., Syed, D. N., Adhami, V. M., Khan, M. I., Mukhtar, H. Dietary polyphenols in prevention and treatment of prostate cancer. *Int. J. Mol. Sci.* **2015**, *16* (2), 3350-76.
56. SWGDRUG. *Scientific working group for the analysis of seized drugs (SWGDRUG) recommendations*; SWGDRUG 2014.
57. EMA. Guideline on bioanalytical method validation. Committee for Medicinal Products for Human Use: London, UK, 2011.
58. Markert, H., Ring, J., Campbell, N., Grates, K. *A Comparison of Four Commercially Available Portable Raman Spectrometers*; National Forensic Science Technology Center: 2011.
59. Hill, H. H., Simpson, G. Capabilities and limitations of ion mobility spectrometry for field screening applications. *Field Anal. Chem. Technol.* **1997**, *1* (3), 119-134.
60. Moeller, K. E., Lee, K. C., Kissack, J. C. Urine drug screening: practical guide for clinicians. *Mayo Clin. Proc.* **2008**, *83* (1), 66-76.
61. Grates, K. M., Ring, J. G., Savage, K. A., Denicola, T. A., Beall, V. M., Dovyak, J. L., Schlomer, E. M. *Conclusion of Validation Study of Commercially Available Field Test Kits for Common Drugs of Abuse*; NFSTC.
62. Institoris, L., Toth, A. R., Molnar, A., Arok, Z., Kereszty, E., Varga, T. The frequency of alcohol, illicit and licit drug consumption in the general driving population in South-East Hungary. *Forensic Sci. Int.* **2013**, *224* (1-3), 37-43.
63. Simonsen, K. W., Steentoft, A., Hels, T., Bernhoft, I. M., Rasmussen, B. S., Linnet, K. Presence of psychoactive substances in oral fluid from randomly selected drivers in Denmark. *Forensic Sci. Int.* **2012**, *221* (1-3), 33-8.
64. Bosker, W. M., Huestis, M. A. Oral Fluid Testing for Drugs of Abuse. *Clin. Chem.* **2009**, *55* (11), 1910-1931.
65. DRUID. *Analytical evaluation of oral fluid screening devices and preceding selection procedures*; 2010.

66. Schütz, H., Paine, A., Erdmann, F., Weiler, G., Verhoff, M. Immunoassays for drug screening in urine. *Forens. Sci. Med. Pathol.* **2006**, *2* (2), 75-83.
67. Schulze, H., Schumacher, M., Urmeew, R., Auerbach, K., Alvarez, J. *Driving Under the Influence of Drugs, Alcohol and Medicines in Europe — findings from the DRUID project*; EMCDDA: Luxembourg: Publications Office of the European Union, 2012; p 57.
68. Guilbault, G. G. *Practical fluorescence; theory, methods, and techniques*. M. Dekker: New York, 1973; p 664.
69. Babichenko, S., Poryvkina, L., Orlov, Y., Persiantsev, I., Rebrik, S. *Fluorescent Signatures in Environmental Analysis*. John Wiley & Sons Inc.: New York, 1999; Vol. 8.
70. Babichenko, S., Leeben, A., Poryvkina, L., van der Wagt, R., de Vos, F. Fluorescent screening of phytoplankton and organic compounds in sea water. *J. Environ. Monit.* **2000**, *2* (4), 378-83.
71. Babichenko, S., Erme, E., Ivkina, T., Poryvkina, L., Sominsky, V. A portable device and method for on-site detection and quantification of drugs. Google Patents: 2005, WO2005111586A1.
72. Poryvkina, L., Babichenko, S. In *Detection of illicit drugs with the technique of spectral fluorescence signatures (SFS)*. Proc. SPIE, 2010; p 11.
73. Poryvkina, L., Tsvetkova, N., Sobolev, I. Evaluation of apple juice quality using spectral fluorescence signatures. *Food Chem.* **2014**, *152*, 573-577.
74. Tiselius, A. A new apparatus for electrophoretic analysis of colloidal mixtures. *J. Chem. Soc. Faraday Trans.* **1937**, *33*, 524-531.
75. Hjerten, S. Free zone electrophoresis. *Chromatogr. Rev.* **1967**, *9* (2), 122-219.
76. Jorgenson, J. W., Lukacs, K. D. High-Resolution Separations Based on Electrophoresis and Electroosmosis. *J. Chromatogr.* **1981**, *218* (1-3), 209-216.
77. Terabe, S., Otsuka, K., Ichikawa, K., Tsuchiya, A., Ando, T. Electrokinetic Separations with Micellar Solutions and Open-Tubular Capillaries. *Anal. Chem.* **1984**, *56* (1), 111-113.
78. Altria, K. D. *Capillary Electrophoresis Guidebook: Principles, Operation and Applications*. Humana Press Inc.: United States of America, 1996.
79. Acunha, T., Ibanez, C., Garcia-Canas, V., Simo, C., Cifuentes, A. Recent advances in the application of capillary electromigration methods for food analysis and Foodomics. *Electrophoresis* **2015**.
80. Joul, P., Lees, H., Vaher, M., Kobrin, E. G., Kaljurand, M., Kuhtinskaja, M. Development of a capillary electrophoresis method with direct UV detection for the analysis of thiodiglycol and its oxidation products. *Electrophoresis* **2015**, *36* (9-10), 1202-1207.
81. Buchberger, W. W. Current approaches to trace analysis of pharmaceuticals and personal care products in the environment. *J. Chromatogr. A* **2011**, *1218* (4), 603-618.
82. Kuban, P., Seiman, A., Makarotseva, N., Vaher, M., Kaljurand, M. In situ determination of nerve agents in various matrices by portable capillary electropherograph with contactless conductivity detection. *J. Chromatogr. A* **2011**, *1218* (18), 2618-25.
83. Kubáň, P., Kobrin, E.-G., Kaljurand, M. Capillary electrophoresis – A new tool for ionic analysis of exhaled breath condensate. *J. Chromatogr. A* **2012**, *1267* (0), 239-245.
84. Ban, E., Yoo, Y. S., Song, E. J. Analysis and applications of nanoparticles in capillary electrophoresis. *Talanta* **2015**, *141*, 15-20.
85. Anastos, N., Barnett, N. W., Lewis, S. W. Capillary electrophoresis for forensic drug analysis: A review. *Talanta* **2005**, *67* (2), 269-279.
86. Posch, T. N., Putz, M., Martin, N., Huhn, C. Electromigrative separation techniques in forensic science: combining selectivity, sensitivity, and robustness. *Anal Bioanal Chem* **2015**, *407* (1), 23-58.
87. Elbashir, A. A., Aboul-Enein, H. Y. Applications of capillary electrophoresis with capacitively coupled contactless conductivity detection (CE-C<sup>4</sup>D) in pharmaceutical and biological analysis. *Biomed. Chrom.* **2010**, *24* (10), 1038-44.
88. Tamizi, E., Jouyban, A. The potential of the capillary electrophoresis techniques for quality control of biopharmaceuticals. *Electrophoresis* **2015**, *36* (6), 831-858.
89. Cole, M. D. *The Analysis of Controlled Substances*. John Wiley & Sons, Ltd.: England, 2003.
90. Quirino, J. P., Terabe, S. Sample stacking of cationic and anionic analytes in capillary electrophoresis. *J. Chromatogr. A* **2000**, *902* (1), 119-35.

91. Shihabi, Z. K. Stacking in capillary zone electrophoresis. *J. Chromatogr. A* **2000**, *902* (1), 107-117.
92. Guo, J., Chen, Q., Wang, C., Qiu, H., Liu, B., Jiang, Z. H., Zhang, W. Comparison of two exploratory data analysis methods for classification of *Phyllanthus* chemical fingerprint: unsupervised vs. supervised pattern recognition technologies. *Anal. Bioanal. Chem.* **2015**, *407* (5), 1389-401.
93. Zhang, H., Chen, H. Correction of migration time of *Paeoniae Radix* in capillary electrophoresis by powerful one-marker technology. *Anal. Methods* **2011**, *3* (3), 745-750.
94. Pearson, K. LIII. On lines and planes of closest fit to systems of points in space. *Philos. Mag.* **1901**, *2* (11), 559-572.
95. Abdi, H., Williams, L. J. Principal component analysis. *Comput. Stat.* **2010**, *2* (4), 433-459.
96. Bro, R. PARAFAC. Tutorial and applications. *Chemometr. Intell. Lab.* **1997**, *38* (2), 149-171.
97. Schmidt, B., Jaroszewski, J. W., Bro, R., Witt, M., Staerk, D. Combining PARAFAC analysis of HPLC-PDA profiles and structural characterization using HPLC-PDA-SPE-NMR-MS experiments: Commercial preparations of St. John's wort. *Anal. Chem.* **2008**, *80* (6), 1978-1987.
98. Papik, K., Molnar, B., Schaefer, R., Dombovari, Z., Tulassay, Z., Feher, J. Application of neural networks in medicine. *Med. Sci. Monitor* **1998**, *4* (3), 538-546.
99. Amato, F., Lopez, A., Pena-Mendez, E. M., Vanhara, P., Hampl, A., Havel, J. Artificial neural networks in medical diagnosis. *J. Appl. Biomed.* **2013**, *11* (2), 47-58.
100. Maltarollo, V. G., Honório, K. M., Borges Ferreira da Silva, A. Applications of Artificial Neural Networks in Chemical Problems. Suzuki, K., Ed. Intech: 2013
101. EC. 2002/657/EC Commission Decision of 12 August 2002 implementing Council Directive 96/23/EC concerning the performance of analytical methods and the interpretation of result. OJC, 2002; p 36.
102. Ermer, J., Burgess, C., Kleinschmidt, G., McB. Miller, J. H. Performance Parameters, Calculations and Tests. In *Method Validation in Pharmaceutical Analysis*, Wiley-VCH Verlag GmbH & Co. KGaA: 2005; pp 21-194.
103. Caban, M., Migowska, N., Stepnowski, P., Kwiatkowski, M., Kumirska, J. Matrix effects and recovery calculations in analyses of pharmaceuticals based on the determination of  $\beta$ -blockers and  $\beta$ -agonists in environmental samples. *J. Chromatogr. A* **2012**, *1258* (0), 117-127.
104. Ferrer, C., Lozano, A., Agüera, A., Girón, A. J., Fernández-Alba, A. R. Overcoming matrix effects using the dilution approach in multiresidue methods for fruits and vegetables. *J. Chromatogr. A* **2011**, *1218* (42), 7634-7639.
105. EURACHEM/CITAC *Guide: The Expression of Uncertainty in Qualitative Testing*; LGC: Teddington, UK, 2003.
106. NarTest website [WWW] [www.nartest.com](http://www.nartest.com) (accessed 11.11.2015).
107. Helmja, K., Vaher, M., Pussa, T., Raudsepp, P., Kaljurand, M. Evaluation of antioxidative capability of the tomato (*Solanum lycopersicum*) skin constituents by capillary electrophoresis and high-performance liquid chromatography. *Electrophoresis* **2008**, *29* (19), 3980-3988.
108. Kulp, M., Bragina, O., Kogerman, P., Kaljurand, M. Capillary electrophoresis with led-induced native fluorescence detection for determination of isoquinoline alkaloids and their cytotoxicity in extracts of *Chelidonium majus* L. *J. Chromatogr. A* **2011**, *1218* (31), 5298-5304.
109. Seiman, A., Jaanus, M., Vaher, M., Kaljurand, M. A portable capillary electropherograph equipped with a cross-sampler and a contactless-conductivity detector for the detection of the degradation products of chemical warfare agents in soil extracts. *Electrophoresis* **2009**, *30* (3), 507-14.
110. Gong, X. Y., Kuban, P., Scholer, A., Hauser, P. C. Determination of *gamma*-hydroxybutyric acid in clinical samples using capillary electrophoresis with contactless conductivity detection. *J. Chromatogr. A* **2008**, *1213* (1), 100-104.

## ACKNOWLEDGEMENTS

The research presented in this thesis was carried out at the Chair of Analytical Chemistry of the Department of Chemistry at Tallinn University of Technology and the Estonian private company NarTest AS located in Tallinn.

Hereby, I would like to express my sincere gratitude and appreciation to all people who assisted and encouraged me in various ways during my PhD studies and at the time of preparing this work.

First of all, I would like to express special thanks to both of my supervisors, Dr. **Larisa Poryvkina** and **Prof. Mihkel Kaljurand**, who supported me during all these years and encouraged me to discover and join in the impressive world of science. I am deeply grateful to Larisa, co-developer of SFS, for providing the opportunity to carry out this research using the modern and first-class technology Spectral Fluorescence Signature at NarTest AS, for her patience, understanding and kind support. I would like to thank the Professor, who is, with no doubt, a Noteworthy contributor to the world of capillary electrophoresis, and who inspired me to discover the “charms” of capillary electrophoresis and chemometrics.

I would like to thank my first BSc and MSc supervisor, **Jelena Gorbatsova**, for her scientific enthusiasm and constant help during my PhD studies. I am certain my life in the lab would have been different without Jelena’s exceptional ability to solve issues which arose from nowhere or nohow and her skill to make things go on.

This work would not have been possible without my wonderful current and former colleagues at Laser Diagnostic Instruments AS, NarTest AS and the Chair of Analytical Chemistry; Tallinn University of Tehnology. Special thanks go to my former colleague **Valeri Aleksejev**, who is a guru in ANN, for his persistence, patience, *especially patience*, invariable support, and contribution to the development of ANN. I wish to thank **Sergei Shchemelyov** for his endless enthusiasm and Dr. **Sergei Babichenko**, co-founder of SFS, for his motivation during my study.

I would like to thank separately my colleagues at the Chair of Analytical Chemistry, **Merike Vaher** for her honest opinions and constructive remarks, objectivity and extraordinary kindness, **Maria Kulp** and **Maria Kuhtinskaja** for their fruitful advice and comments. I am thankful to **Piret Saar-Reismaa** for her ability to understand my *crazy* ideas, and her willingness to help.

I would like to **thank other colleagues** who are not mentioned here, but beyond doubt, their support is highly appreciated.

My very special gratitude belongs to the CEO of NarTest AS, **Kaisa Uiibo**, for her encouraging support, kindness and firm confidence in my ability to succeed. I would like to thank **Endel Siff** for his understanding and giving me the possibility to conduct my PhD study.

I would like to acknowledge the Estonian Forensic Science Institute for cooperation, especially **Peep Rausberg** and **Irina Grebennikova**, for their helpful advice and insightful comments.

I would like to convey special thanks to my high school chemistry teacher, **Margarita Chaushskaya**, for her ability to encourage me to deal with chemistry.

I thank all **my friends** for their support and for always being there for me!

**Most importantly**, none of this would have been possible without the love and patience of **my family**. My family, to whom this dissertation is dedicated to, has been a constant source of love, concern, support and strength during all these years. I would like to express my heart-felt gratitude to my lovely **Andrei and his parents**, whose marvellous support encouraged me not to give up during my PhD studies and always to move on.

I acknowledge the financial support from the Estonian Science Fund (Grant ETF9106), and the Estonian Research Council (Institutional Research Fund No. 33-20 "Advancing analytical and computational chemistry methods for regulatory decisions") and Ministry of Interior (Internal Security Fund).

This work was partially supported by the Graduate School of Functional Materials and Processes receiving funding from the European Social Fund through the project 1.2.0401.09-0079 in Estonia, and was also supported by the European Social Fund's Doctoral Studies and Internationalisation Programme DoRa, which is carried out by the Archimedes Foundation.

## ABSTRACT

Illegal drug abuse and addiction is a globally recognized phenomenon encountering thousands of victims every year. It is reported that there were estimated 187,100 drug-related deaths only in 2013. The widespread use of illegal drugs causes the need for development of new analytical methods targeted at the ability to identify the narcotics used by drivers/criminals as quickly as possible, so that appropriate preventive measures can be taken. Without a doubt, the global epidemic of drug abuse and addiction can be compared to the plague, which contracted millions of victims. Nowadays the diversification of drugs is extremely difficult to stop. New legal “highs” are continuously coming to the market. There have been already registered more than 450 new psychoactive substances via the EU Early Warning System, 101 of which were notified in 2014. Therefore, the implementation of new technologies for the rapid determination of illegal drugs and timeliness sharing of information within and between countries is a priority for border control, law enforcement officers and organizations fighting against this global problem. Cocaine, heroin, and marijuana are under international control and scheduled according to the 1961 Convention (48th Ed. 2008). Marijuana is the most widely used illegal substance in the world. Cocaine is the most trafficked drug in the world after herbal cannabis and cannabis resin. Heroin is the third most frequently mentioned illegal drug in emergency-room episodes within the US and East Europe. Other well-known and popular drugs of abuse among teens and young adults are MDMA known as ‘Ecstasy’ and  $\gamma$ -hydroxybutyric acid (GHB) known as “Liquid Ecstasy”.

This study was aimed to evaluate the efficacy and accuracy of detecting cocaine/heroin/MDMA in the form of powder, solid crystals or solid chunks of material by the spectral fluorescence signature (SFS) method combined with Artificial Neural Networks (ANN). Validation was not only required for the method with optimized methodology, but also for the application of advanced statistical methods and intelligence methodologies for data analysis. Moreover, the SFS method coupled to PARAFAC-PCA/cluster analysis was utilized for the herbal medicines (HM) profiling known as traditional drugs used for treatment of different disorders. This study explored the possibility of application of capillary electrophoresis for determination of drug abuse. The methodologies for determination of marijuana and GHB abuse in saliva were developed, optimized and validated. Saliva was chosen as an alternative sample matrix as it is less invasive, painless and easier to collect than blood and urine and can be used as a screening sample matrix on-site, giving more accurate representation of the processes going on in the body. The utilized methods such as SFS coupled to different pattern recognition techniques and CE coupled to different detectors for illegal drugs identification in seized samples, profiling of HMs according to the polyphenolic content and determination of drug abuse in saliva were proved to be reliable and accurate.

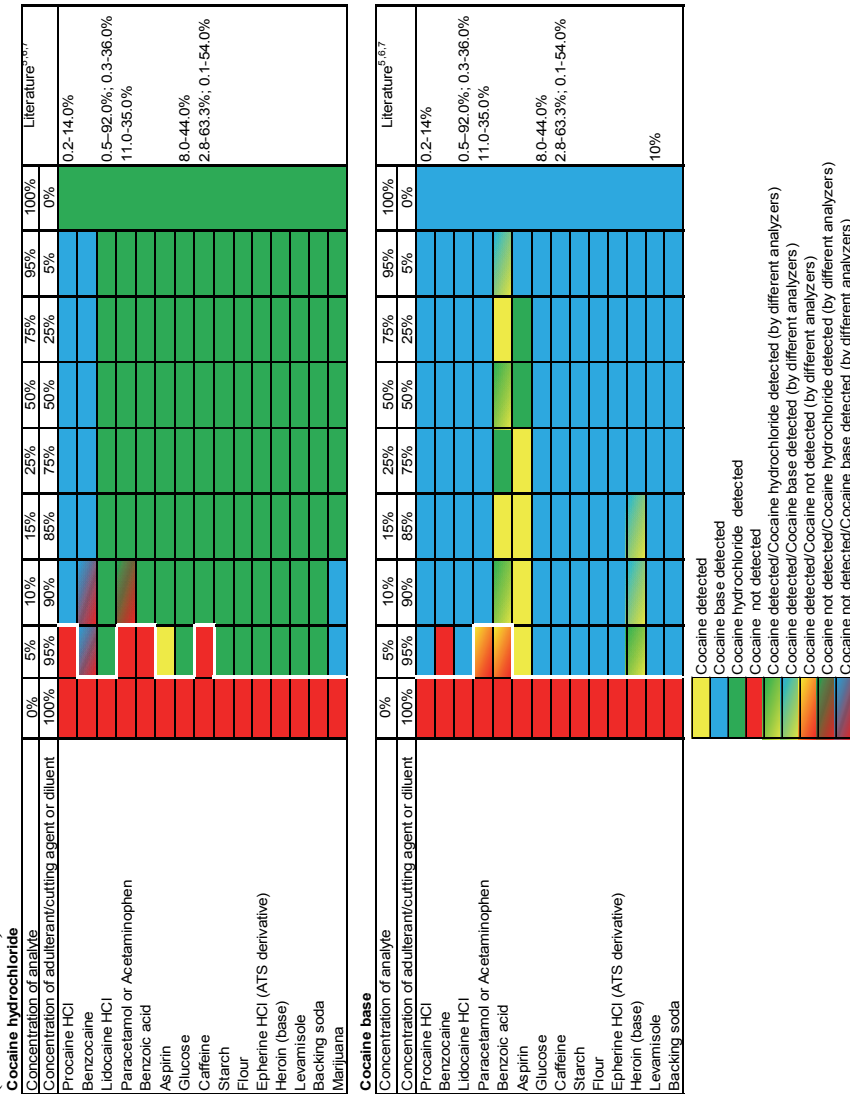
## KOKKUVÕTE

Keelatud narkootiliste ja psühhotroopsete ainete joove ja sõltuvus on ülemaailmne probleem, mis tabab tuhandeid ohvraid igal aastal.

Vastavalt hiljuti avaldatud Euroopa Narkootikumide ja Narkomaania Seirekeskuse (EMCDDA) aruandele lisandus 2014. a turule erakordselt suur arv uusi psühhotroopseid aineid – 101, saavutades sellega uue rekordilise arvu – 450, mis on nüüdseks registreeritud Euroopa Liidu Varajase Hoiatamise süsteemis (*EU Early Warning System*). Viimased andmed näitavad, et narkootikumide tarbimine maailmas on praegu saavutanud kõigi aegade kõrgeima taseme. Ka Eestis ei ole narkootikumide kasutamise osas vähenemise tendentsi märgata. Narkomaania on üks tõsisematest probleemidest, mille lahendamine on oluline nii riiklikul kui ka rahvusvahelisel tasandil. Uute narkootiliste ainete lisamine kontrollitavate ainete nimekirja on keeruline ja aeganõudev protsess. Üks olulisematest etappidest on ainete identifitseerimine, mis omakorda nõuab uue meetodika väljatöötamist, selle optimeerimist ning valideerimist. Äärmiselt oluline on ka ekpressdiagnostika meetodite väljatöötamine nii uute narkootikumide kui ka klassikaliste narkootiliste ainete tuvastamiseks. Kõige levinumad narkootilised ained on kokaiin, heroiin ja kanepi produktid (marihuaana, hašiš). Muuhulgas, kanep on üks enim tarbitavaid uimasteid. EMCDDA aruande järgi on iga neljas Euroopa Liidu elanik proovinud kanepit vähemalt üks kord oma elus. Seejuures tuleb silmas pidada, et kokaiini ja heroini tarbimisega kaasnevad eriti rasked sotsiaalsed probleemid, kuna need uimastid tekitavad tugeva sõltuvuse ja muudavad põhjalikult, isegi pöördumatult inimese elu, tuues sageli kaasa fataalseid tagajärgi. Lisaks on noorte seas ülipopulaarsed ka teised narkootilised ained nagu MDMA (tuntud 'Ecstasy' nime all) ja GHB ehk 'korgijook'.

Käesoleva uurimistöö eesmärgiks oli hinnata alternatiivina või täiendavalt traditsioonilistele meetoditele uusi meetodeid narkootiliste ainete tuvastamiseks nii tahketes, tänaval konfiskeeritud kui ka bioloogilistes proovides. Vere ja uurini asemel uuriti narkootiliste ainete marihuaana ja GHB joobe tuvastamist süljes, mis on efektiivne tõendusmaterjal ja mille proovide võtmine on lihtne, vähem ebameeldiv ja ka valutu ning ei nõua eritingimusi. Selleks töötati välja, optimeeriti ja valideeriti erinevate detektoritega kombineeritud kapillaarelektroforeesi (KE) meetodikad narkojoobe kiireks ja usaldusväärseks tuvastamiseks süljes. Lisaks hinnati kemomeetriliste meetoditega kombineeritud spektraalse fluorestsentskujutise (*Spectral Fluorescence Signature, SFS*) meetodi võimet kiiresti ja usaldusväärsest tuvastada kokaiin, heroiin ja MDMA pulbrites lisandainete juuresolekul, ning võimet kaardistada ravimtaimede sõrmejälgi polüfenoolsete ühendite sisalduse alusel. Käesoleva uurimistöö eesmärgid on saavutatud ja hüpoteesid tõestatud. Kasutatud meetodid koos uudsete meetodikatega andsid väga häid ja usaldusväärseid tulemusi, võimaldades narkootilisi aineid erinevates proovimaatriksites efektiivselt analüüsida ning ka ravimtaimi profileerida.

## Appendix I. Uncertainty region of ANN for cocaine salt and cocaine base in the mixture with different diluents and adulterants (Publication I).



**Appendix II. Uncertainty region of ANN for heroin in the mixture with different diluents and adulterants (Publication I).**

Concentration of analyte	0%	5%	10%	15%	25%	35%	50%	75%	90%	95%	100%	Literature <sup>5,6</sup>
Concentration of adulterant/cutting agent or diluent	100%	95%	90%	85%	75%	65%	50%	25%	10%	5%	0%	
Procaine HCl	Heroin detected	2.2-27.0%										
Lidocaine HCl	Heroin detected	4.8-11.2%										
Paracetamol or Acetaminophen	Heroin detected	0.9-36.1%; 0.2-53.0%										
Aspirin	Heroin detected	<6-40.0%										
Sugars (glucose)	Heroin detected	18.7-44.5%; 0.2-41%; 35.0-55.0										
Caffeine	Heroin detected	≤10%										
Quinine HCl (50 ug/ml or 2.5% (w/w))	Heroin detected	≤10%										
Quinine HCl (200 ug/ml or 10% (w/w))	Heroin detected											
Quinine HCl (2000 ug/ml or 100% w/w)	Heroin detected											
Starch	Heroin detected											
Flour	Heroin detected											
Cocaine HCl	Heroin detected											
Methamphetamine HCl (ATS derivative)	Heroin detected											
Nicotinamide	Heroin detected											
Morphine HCl	Heroin detected											
Codeine phosphate	Heroin detected											
6-MAM (200 ug/ml or 10% (w/w))	Heroin detected											
3-MAM oxalate (400 ug/ml or 20% (w/w))	Heroin detected											
Hydromorphone HCl (200 ug/ml or 10% (w/w))	Heroin detected											
Norfentanyl HCl (200 ug/ml or 10% (w/w))	Heroin detected											
Fentanyl (6.3%)	Heroin detected											
3-methylfentanyl (6.1%)	Heroin detected											
Backing soda	Heroin detected											

Heroin detected  
Heroin not detected

**Appendix III. Uncertainty region of ANN for MDA in the mixture with different diluents and adulterants (Publication I).**

Concentration of analyte	0%	1%	2%	3%	4%	5%	6%	10%	75%	95%	100%	Literature <sup>9</sup>
Concentration of adulterant/cutting agent or diluent	100%	99%	98%	97%	96%	95%	94%	90%	25%	5%	0%	
Procaine HCl	Red	2.0-66.7%										
Benzocaine	Red	44.4%										
Lidocaine HCl	Red	2.9-95.2%										
Paracetamol	Red	4.5%										
Benzoic acid	Red	1.0-96.8%										
Aspirin	Red											
Glucose	Red											
Caffeine	Red											
Starch	Red											
Flour	Red											
Amphetamine sulphate	Red	1.6-25.4%										
Methamphetamine HCl	Red	0.4-90.9%										
Ephedrine HCl (ATS derivative)	Red	1.8-83.3%										
Heroin (base)	Red											
Heroin HCl	Red											
MDMA HCl	Yellow	0.9-99.0%										
Cocaine HCl	Red	3.5-33.3%										
Baking soda	Red											
Ketamine HCl	Red	1.5-93.0%										
Nicotinamide	Red											
BZP	Red	4.2-60.0%										
TMFPP/BZP	Red	4.2-73.2%										
Dextromethorphan HBr	Red	3.2-90.0%										
m CPP HCl	Red	9.8%										
2C-B	Red	16.7%										
Phentermine HCl	Red	33.3%										
Fentanyl	Red											
3-methylfentanyl	Red											

**Appendix IV. Uncertainty region of ANN for MDMA (MDMA) in the mixture with different diluents and adulterants (Publication I)**

Concentration of analyte	0%	1%	2%	5%	10%	15%	25%	50%	75%	85%	90%	95%	98%	99%	100%	Literature <sup>a</sup>	
Concentration of adulterant/cutting agent or diluent	0%	99%	98%	95%	90%	85%	75%	50%	50%	5%	1%	5%	1%	5%	100%	0%	
Procaine HCl	Red	Red	2.0-66.7%														
Benzocaine	Red	Red	44.4%														
Lidocaine HCl	Red	Red	2.9-95.2%														
Paracetamol	Red	Red	4.5%														
Benzoic acid	Red	Red	1.0-96.8%														
Aspirin	Red	Red															
Glucose	Red	Red															
Caffeine	Red	Red															
Starch	Red	Red															
Flour	Red	Red															
Amphetamine sulphate	Red	Red	1.6-25.4%														
Methamphetamine HCl	Red	Red	0.4-90.9%														
Ephedrine HCl (ATS derivative)	Red	Red	1.8-83.3%														
Heroin (base)	Red	Red															
Heroin HCl	Red	Red															
MDA HCl	Red	Red	1.8-90.9%														
Cocaine HCl	Red	Red	3.5-33.3%														
Backing soda	Red	Red															
Ketamine HCl	Red	Red	1.5-93.0%														
Nicotinamide	Red	Red															
BZP	Red	Red	4.2-60.0%														
TMFP/BZP	Red	Red	4.2-73.2%														
Dextromethorphan HBr	Red	Red	3.2-90.0%														
mCPP	Red	Red	9.8%														
2C-B	Red	Red	16.7%														
Phentermine HCl	Red	Red	33.3%														
Fentanyl	Red	Red															
3-methylfentanyl	Red	Red															



# LIST OF ORIGINAL PUBLICATIONS

## 1.1. - 4 publications

Mazina, J., Vaher, M., Kuhtinskaja, M., Poryvkina, L., Kaljurand, M. Fluorescence, electrophoretic and chromatographic fingerprints of herbal medicines and their comparative chemometric analysis. *Talanta*, **2015**,139, 233 – 246 .

Mazina, J., Saar-Reismaa, P., Kulp, M., Poryvkina, L., Kaljurand, M., Vaher, M. Determination of  $\gamma$ -hydroxybutyric acid in saliva by capillary electrophoresis coupled with contactless conductivity and indirect UV absorbance detectors . *Electrophoresis*, **2015**, doi: 10.1002/elps.201500293.

Mazina, J., Špiljova, A., Vaher, M., Kaljurand, M., Kulp, M. Rapid capillary electrophoresis method with LED-induced native fluorescence detection for the analysis of cannabinoids in oral fluid. *Analytical methods*, **2015**, 7(18), 7741 – 7747.

Mazina, J., Aleksejev, V., Ivkina, T., Kaljurand, M., Poryvkina, L. Qualitative detection of illegal drugs (cocaine, heroin and MDMA) in seized street samples based on SFS data and ANN: validation of method. *Journal of Chemometrics*, **2012**, 26, 442 – 455.

## 1.2. - 1 publications

Mazina, J., Gorbatoeva, J. Sample preparation for CE-DAD analysis of the water soluble vitamins in food products. *Procedia Chemistry*, **2010**, 2(S1), 46 – 53.

## 5.2. - 12 publications

Kaljurand, M., Mazina, J., Saar, P., Jõul, P., Lees, H., Špiljova, A., Kulp, M., Vaher, M. Detection of banned chemicals in various matrices (saliva, sediments) by capillary electrophoresis. In: ITP2015/NoSSS2015 Final Program and Book of Abstracts: Helsinki, Finland: Helsinki University Press, **2015**, p. 36.

Mazina, J., Kulp, M., Kaljurand, M., Porõvkina, L. Detection By Fluorescence Signature Method And Non-Aqueous Spectral Capillary Electrophoresis Combined With Fluorescence Detector In Abstract book: The 22nd Analysdagarna (Analytical Days), Nordic Separation Science Society 7th Conference, Djurönäset, Juuni 9 – 11, **2014**.

Mazina, J., Aleksejev, V., Kaljurand, M., Porõvkina, L. Determination Of Synthetic Drugs By Sfs-Mlp-Ann Method: Validation Of The Procedure In: 13th Conference o Methods and Applications of Fluorescence (MAF13) teaduskonverents, Genova, September 9 – 11, **2013**.

Mazina, J., Aleksejev, V., Ivkina T., Kaljurand, M., Porõvkina, L. Determination Of Synthetic Drugs By SFS-MLP-ANN Method: Validation Of The Procedure. In: TÜ ja

TTÜ doktorikooli “Funktsionaalsed materjalid ja tehnoloogiad” IV teaduskonverents, Tallinn, Märts 7 – 8, **2013**.

Mazina, J., Aleksejev V., Kaljurand, M., Porõvkina, L. Determination Of Cannabis and its products by SFS-MLP-ANN method: Validation Of The Procedure. In: TÜ ja TTÜ doktorikooli “Funktsionaalsed materjalid ja tehnoloogiad” III teaduskonverents, Tartu, Vebruar 29 – Märts 1, **2012**.

Mazina, J., Vaher, M., Borissova, M., Kaljurand M. Comparative Fingerprint Of Medicinal Herb Polyphenols And Chemometric Analysis. In: ISC 2012, Abstract book 29th international Symposium on Chromatography, Torun, Poland, September 9 – 13, **2012**. (Toim.) B. Buszewski, J. Kowalska. ISBN 978-83-7780-440-7.

Mazina, J., Ivkina T., Porõvkina, L., Kaljurand, M. Qualitative detection of illegal drugs (cocaine, heroin) in seized street samples based on excitation emission matrix data and artificial neural networks: validation of the procedure. In: SSC12, Abstract book: 12th Scandinavian Symposium on Chemometrics, Billund, Taani, Juuni 8 – 10, **2011**. (Toim.) Rinnan, Å.

Mazina, J., Porõvkina, L., Kaljurand, M. Metoodika valideerimine: Kvalitatiivne analüüs kokaiini (vaba alusena ja soola vormis) määramiseks konfiskeeritud tänavaproovides fluoretsentspektroskoopia meetodil. In: TTÜ keemiainstituudi doktorantide teaduskonverents: teeside kogumik: Tallinn, Aprill 8, **2011**.

Mazina, J., Porõvkina, L., Kaljurand, M. Detection Of Illegal Drugs In Seized Street Samples Using Excitation Emission Matrix Spectroscopy Combined With Parallel Factor Analysis. In: TÜ ja TTÜ doktorikooli “Funktsionaalsed materjalid ja tehnoloogiad” I teaduskonverents, Tallinn, Märts 3 – 4, **2011**.

Mazina, J., Knjazeva, T., Gorbatoova, J., Hälvin, K., Kaljurand, M. B-rühma vitamiinide analüüs reaalsetes proovides kapillaarelektroforeesi meetodil. In: XXXI Eesti Keemiapäevad/31st Estonian Chemistry Days; Tallinn, **2010**.

Mazina J., Gorbatoova J., Knjazeva T., Kaljurand M. Simultaneous determination of water-soluble by capillary electrophoresis combined with MALDI-TOF In: NoSSS2009, Abstract book: 5th Conference on Separation and Related Techniques by Nordic Separation Science Society, Tallinn, Estonia, August 26 – 29, **2009**, 117. (Toim.) Vaher M., Borissova M.

Mazina J., Gorbatoova J., Knjazeva T., Kaljurand M., Simultaneous determination of water-soluble vitamins in food samples by CE coupled with MALDI. In: Natural Products 2009, Abstract book: Zing - Natural Products Conference, The Jolly Beach, Antigua, March 1 – 4, **2009**, 40. (Toim.) Leadlay Willis Chris, P.

# CURRICULUM VITAE

## 1. Personal data

Name	Jekaterina Mazina
Date and place of birth	30.01.1986, Tallinn, Estonia
Citizenship	Estonian
E-mail address	jekaterina.mazina@gmail.com

## 2. Education

<b>Educational institution</b>	<b>Graduation year</b>	<b>Education (field of study/degree)</b>
Tallinn University of Technology	2010	Applied chemistry and biotechnology, MSc, (cum laude)
Tallinn University of Technology	2008	Applied chemistry and biotechnology, BSc
Tallinn Central Russian Gymnasium	2005	Secondary education, gold medallist

## 3. Language competence/skills (fluent, average, basic skills)

<b>Language</b>	<b>Level</b>
Russian	Native
Estonian	Professional working proficiency
English	Professional working proficiency

## 4. Special courses

<b>Period</b>	<b>Educational or other organisation</b>
13-15.10.2015	ISO 9001:2015, internal audit, ISO 14001:2015 and OHSAS 18001:2007 courses, Bureau Veritas, Tallinn
08.2015	Refresher and updating assessor courses (Estonian Accreditation Centre), Tallinn
06.02.2015	Wastewater treatment. EU requirements for devices and methods (Arenguline OÜ), Tallinn
28.08.2013	Refresher and updating assessor courses (Estonian Accreditation Centre), Tallinn
08.2012	ISO 17025 Assessor courses (Estonian Accreditation Centre), Paatsalu, 14 – 17.08.2012
06.2011	"Techniques for On-line Application of Multivariate Monitoring Systems" course, Perceptive Engineering Ltd), Billund, Denmark
02.2011	Chemometrics course, Department of Chemistry, TUT, Rakvere, Estonia
09.2010	"Multiway analysis" courses, University of Copenhagen, Denmark
04.2010	Quality assurance in laboratory: AAS method, TUT
02.2010	Chemometrics course, St.Peterburg; Russia
03.2009	Food and Feed Quality and Safety, Estonian Research Institute of Agriculture and Tallinn University of Technology

## 5. Professional employment

<b>Period</b>	<b>Organisation</b>	<b>Position</b>
01.10.2015 – ...	Tallinn University of Technology, Department of Chemistry	Scientist
01.10.2014 – ...	AS NarTest	Senior Researcher
01.10.2013 – ...	AS Laser Diagnostic Instruments	Senior Researcher
01.03.2011 – 1.10.2013	AS Laser Diagnostic Instruments	Researcher
01.03.2010 – 1.10.2014	AS NarTest	Researcher
01.01.2009 – 31.12.2010	Tallinn University of Technology, Department of Chemistry project ETF7818	Investigator
06.2009 – 08.2009	Health Protection Inspectorate	Chemist-analyst
06.2008 – 08.2008	Health Protection Inspectorate	Chemist-analyst

## 6. Research activity, including honours and thesis supervised

### *Theses supervised*

Piret Saar-Reismaa, MSc, 2015, (sup) Jekaterina Mazina, GHB analysis in saliva and exhaled breath condensate by capillary electrophoresis, Department of Chemistry Tallinn University of Technology

Piret Saar, BSc, 2012, (sup) Jekaterina Mazina, Simultaneous spectrophoto- and spectrofluorometric analysis of petroleum products in water. Department of Chemistry, Tallinn University of Technology

### *Honors and activities*

2009, Jekaterina Mazina, diploma, State Competition of Students' Scientific Works, diploma

2009, SA Archimedes. DORA framework 8: poster presentation Natural Products 2009 Conference, The Jolly Beach, Antigua, March 1 – 4, 2009

2010, SA Archimedes. DORA framework 8: poster presentation -"WSC7" and courses on Chemometrics, St. Petersburg, Russia, February 15 – 19, 2010

2011, Conference of UT and TUT Graduate school "Functional materials and technologies" (GSFMT), poster presentation " SSC12" and courses "Techniques for On-line Application of Multivariate Monitoring Systems", Perceptive Engineering Ltd., Billund, Denmark, June 7 – 10, 2011

2012, Awarded poster: Determination of Cannabis and Its Products by SFS-MLP-ANN method: Validation of the Procedure. At: 3rd Conference of UT and TUT Graduate school "Functional materials and technologies" (GSFMT), Tartu, February 29 – March 1, 2012.

## ELULOOKIRJELDUS

1. Isikuandmed  
Ees- ja perekonnanimi Jekaterina Mazina  
Sünniaeg ja -koht 30.01.1986, Tallinn, Eesti  
Kodakondsus Eesti  
E-posti aadress jekaterina.mazina@gmail.com

### 2. Hariduskäik

<b>Õppeasutus (nimetus lõpetamise ajal)</b>	<b>Lõpetamise aeg</b>	<b>Haridus (eriala/kraad)</b>
Tallinna Tehnikaülikool	2010	rakenduskeemia ja biotehnoloogia/ magistrikraad <i>cum laude</i>
Tallinna Tehnikaülikool	2008	rakenduskeemia ja biotehnoloogia/ bakalaureusekraad
Tallinna Kesklinna Vene Gümnaasium	2005	Keskharidus, kuldmedal

### 3. Keelteoskus (alg-, kesk- või kõrgtase)

<b>Keel</b>	<b>Tase</b>
vene keel	emakeel
eesti keel	kõrgtase
inglise keel	kõrgtase

### 4. Täiendusõpe

<b>Õppimise aeg</b>	<b>Täiendusõppe korraldaja nimetus</b>
13-15.10.2015	ISO 9001:2015 ülevaade, siseadiitor ja ISO 14001:2015 ja OHSAS 18001:2007 koolitus, Bureauveritas, Tallinn
08.2015	Assessorite täiendkoolitus (Eesti Akrediteerimiskeskus), Tallinn
06.02.2015	7-h seminar Reoveepuhastus. Seadmed ja meetodid. Euroopa Liidu nõuded (Areniline OÜ), Tallinn
28.08.2013	Assessorite täiendkoolitus (Eesti Akrediteerimiskeskus), Tallinn
08.2012	ISO 17025 assessorite koolitus (Eesti Akrediteerimiskeskus), Paatsalu, 14. – 17. august 2012 a.
06.2011	Koolitus "Techniques for On-line Application of Multivariate Monitoring Systems" (by Perceptive Engineering Ltd.)
02.2011	Koolitus kemomeetrias, Keemiainstituut, Rakvere
09.2010	Koolitus "Multiway analysis", Kopenhaageni ulikool, Taani
04.2010	Koolitus Kvaliteedi tagamine laboris: AAS meetod
02.2010	Koolitus kemomeetrias, St.Peterburg, Venemaa
03.2009	Food and Feed Quality and Safety, Eesti Maaviljeluse Instituut ja Tallinna Tehnikaülikool

## 5. Teenistuskäik

Töötamise aeg	Tööandja nimetus	Ametikoht
01.10.2015 – ...	Tallinna Tehnikaülikool, Keemiainstituut	teadur
01.10.2014 – ...	AS NarTest	vanemteadur
01.10.2013 – ...	AS Laser Diagnostic Instruments	vanemteadur
01.03.2011 – 1.10.2013	AS Laser Diagnostic Instruments	teadur
01.03.2010 – 1.10.2014	AS NarTest	teadur
01.01.2009 – 31.12.2010	Tallinna Tehnikaülikool, matemaatika- loodusteaduskond, projekt ETF7818	täitja
06.2009 – 08.2009	Tervisekaitseinspeksioon	keemik
06.2008 – 08.2008	Tervisekaitseinspeksioon	keemik

## 6. Teadustegevus, sh tunnustused ja juhendatud lõputööd

### *Juhendatud väitekirjad*

Piret Saar-Reismaa, magistrikraad, 2015, (juh) Jekaterina Mazina, GHB analüüs süljes ja väljahingatavas õhus kapillaarelektroforeesil, Tallinna Tehnikaülikool, Keemiainstituut

Piret Saar, bakalaureusekraad, 2012, (juh) Jekaterina Mazina, Samaaegne spektrofoto- ja spektrofluoromeetiline naftasaaduste analüüs vees. Tallinna Tehnikaülikool, Keemiainstituut

### *Saadud uurimistoetused ja stipendiumid*

2009, SA Archimedes. DORA programmi tegevus 8: esinemine poster - ettekanne rahvusvahelisel konverentsil "Natural Products 2009", The Jolly Beach, Antigua, 1. – 4. märts 2009.

2009, Jekaterina Mazina; Üliõpilaste teadustööde riiklik konkurss loodusteaduste ja tehnika valdkonnas rakenduskõrgharidusõppe ja bakalaureuseõppe üliõpilaste astmes, diplom.

2010, SA Archimedes. DORA programmi tegevus 8: rahvusvahelisel konverentsil "WSC7" ning koolitusel osalemine, St. Petersburg, Venemaa, 15. – 19. veebruar 2010

2011, TÜ ja TTÜ doktorikoolis "Funktsionaalsed materjalid ja tehnoloogiad" : rahvusvahelisel konverentsil "SSC12" ja koolitusel "Techniques for On-line Application of Multivariate Monitoring Systems" (Perceptive Engineering Ltd., Inglismaa) osalemine, Billund, Taani, 7 – 10. juuni 2011.

2012, Jekaterina Mazina, auhinnatud stendiettekanne: Determination of Cannabis and Its Products by SFS-MLP-ANN Method: Validation of the Procedure. TÜ ja TTÜ doktorikooli "Funktsionaalsed materjalid ja tehnoloogiad" III teaduskonverents, Tartu, 29. veebruar – 1. märts 2012.



## PUBLICATION I

**Mazina, J.,** Aleksejev, V., Ivkina, T., Kaljurand, M., Poryvkina, L. Qualitative detection of illegal drugs (cocaine, heroin and MDMA) in seized street samples based on SFS data and ANN: validation of method. *Journal of Chemometrics* **2012**, 26, 442 – 455 <sup>1</sup>.

<sup>1</sup>Copyright © 2012 John Wiley & Sons, Ltd.



# Qualitative detection of illegal drugs (cocaine, heroin and MDMA) in seized street samples based on SFS data and ANN: validation of method

Jekaterina Mazina<sup>a\*</sup>, Valeri Aleksejev<sup>b</sup>, Tatjana Ivkina<sup>c</sup>, Mihkel Kaljurand<sup>d</sup> and Larissa Poryvkina<sup>e</sup>

**In this paper, the validation procedure of spectral fluorescence signature (SFS) method combined with multilayer perceptron artificial neural networks (MLP-ANNs) for detection of illegal drugs (cocaine, heroin and 3,4-methylenedioxy-N-methylamphetamine) in street samples is proposed. The qualitative information, based on a binary response (detected/not detected), was directly obtained through the response of an expert system. The performance parameters (limit of detection, selectivity/matrix effects, threshold value and robustness) were evaluated according to the requirements for qualitative method. Copyright © 2012 John Wiley & Sons, Ltd.**

**Keywords:** artificial neural networks; validation; spectral fluorescence signature; narcotics; excitation–emission matrices

## 1. INTRODUCTION

According to the European Monitoring Centre for Drugs and Drug Addiction report, published in May 2011, the number and diversity of new drugs are not only increasing rapidly but are also becoming widespread [1]. Evidently, there is a strong necessity of synergic cooperation of different laboratories and law enforcement forces internationally. For quick and efficient battle against drug trafficking, simplicity, reliability and efficiency of the selected instruments and methods for drug detection is expected. Without a doubt, modern hyphenated techniques such as gas chromatography/liquid chromatography-mass spectrometry (GC/LC-MS) are powerful methods for detection of illegal drugs, but the operation requires well-trained technicians in the interpretation of the obtained results, and the equipment, because of its complexity, can only be used indoors. The alternative methods such as Fourier transform infrared (FT-IR) spectroscopy [2], Raman spectroscopy [3], ion-mobility spectrometry [4] and colour tests [5] are used for onsite tests. Although these methods are simple to operate, none of them could be sufficiently selective, accurate and reliable for illicit drug detection in multicomponent street samples [6–11].

The innovative approach of using the spectral fluorescence signature (SFS) method for detection of illegal drugs in seized street samples is proposed [12–14]. This method is based on the measurements and analysis of two-dimensional fluorescence matrixes where the intensity is a function of excitation and emission wavelengths, and concentration  $C$  of an analyte ( $\lambda_{\text{exc}}$ ,  $\lambda_{\text{em}}$  and  $C$ ). The crucial part of analysis is the data interpretation. One of the options is using chemometric techniques for data analysis. Chemometric methods have proven to be powerful tools for mathematical extraction of the latent structures of multicomponent spectroscopic data and are used more and more for the interpretation of spectral matrixes [15].

Artificial neural networks (ANNs) are powerful mathematical tools that can be related to biological neural network models. The use of the ANNs for data processing (interpretation) has significantly increased during the last 20 years. ANNs are being successfully used to resolve several issues in finance, medical diagnosis, process control, physics, weather forecasting and analytical chemistry [16]. The real advantage of using the ANNs in the spectroscopic data analysis is the option to automatise the analysis. The new approach to combine the SFS technique with ANNs proposed [12–14,17,18] in a forensic science is unique. The chemometric tools coupled to spectroscopy make the analysis highly valuable in the present situation when the need of illegal drug detection counts to the minute in order to stop the next crime and also prevents the possibility of drug trafficking in the future.

One of the critical tasks for analysts is to ascertain that the selected method fulfils the desirable needs and works accurately to solve the issue. In particular, when the goal of chemometric

\* Correspondence to: Jekaterina Mazina, Tallinn University of Technology/NarTest AS, Tallinn, Estonia  
E-mail: jatak@msn.com

a J. Mazina  
Tallinn University of Technology/NarTest AS, Tallinn, Estonia

b V. Aleksejev  
LDI AS, Tallinn, Estonia

c T. Ivkina  
NarTest, Morrisville, NC, USA

d M. Kaljurand  
Tallinn University of Technology, Tallinn, Estonia

e L. Poryvkina  
NarTest AS

analysis is not only exploratory analysis but also a further prediction of unknown samples, the validation procedure must be conducted with extreme care. The European Union directives regulate and offer certain validation parameters for qualitative and quantitative analysis [19,20]. Sometimes, validation of qualitative analysis is frustrating because of the different terminologies for parameters being used in different organisations. This problem was defined by R. Galarini [21]. Indeed, there are numerous useful protocols for method validation defined by different organisations, that is, Food and Drug Administration, National Drug Administration, the United States Pharmacopoeia Convention, the European Network of Forensic Science Institutes, the International Union of Pure and Applied Chemistry (IUPAC) or Eurachem (A Focus for Analytical Chemistry in Europe)/the Clinician Investigator Trainee Association of Canada [22,23].

Qualitative analysis is a primary part of the chemical analysis. Its validation requires the determination of the following performance parameters: specificity/selectivity, limit of detection (LoD), precision (within the laboratory repeatability and/or within the laboratory reproducibility conditions) and stability. Obviously, the important part of the validation is the evaluation of the applied chemometric technique, especially when it is used for routine analysis. Nowadays, more and more chemometric approaches such as ANNs [24] and support vector machines [25] are implemented for data analysis to make the detection more efficient; therefore, human subjective judgement is replaced by the artificial intelligence system's response. With no doubt, the efficacy of the ANNs in the classification of unknown samples must be evaluated. Moreover, it is necessary to determine whether the model used for analysis with generalising ability is overfitted or underfitted [26]. Indeed, there are no special requirements for the artificially intelligent system either in the 2002/657/EC [19] or in the 2007/47/EC [27]. There are a huge number of articles that suggest that the primary parameter for evaluation of prediction performance of an ANN model is a true error on testing the trained network [28], but none of them defines rather the ANN has the uncertainty region (unreliability region), where the outputs of ANN are inconclusive.

This study aims to evaluate the efficacy and accuracy of cocaine, heroin and MDMA detection seized in the form of a powder, solid crystals and chunks of material or tablets by the SFS method combined with ANNs (SFS-MLP-ANN). In this paper, the validation of the method for binary analysis with responses 'detected/not detected' is described. Furthermore, the special approach using uncertainty regions for multicomponent matrixes is proposed for better understanding of the prediction performance of the ANN models. Consequently, validation is required for the SFS method with optimised methodology combined with advanced statistical methods such as ANN, that is, intelligence methodology for data interpretation.

## 2. EXPERIMENTAL

### 2.1. Chemicals and standard solutions

3-Trifluoromethylphenylpiperazine with benzylpiperazine (1:1), 4-bromo-2,5-dimethoxyphenethylamine (2C-B) (about 3%) and marijuana (13% THC) were obtained from the Estonian Forensic Science Institute (EFSI) (Tallinn, Estonia) (Table I). All reagents were of analytical grade. Deionised water was obtained from a Milli-Q water purification system (Millipore, Molsheim, France).

Samples of forensic drug exhibits were obtained from the police departments (nine) [17] in North Carolina, USA, and from EFSI

in Tallinn, Estonia. The validation was performed in EFSI and in NarTest laboratory in North Carolina. The EFSI supplied quantitative analyses of drug content for samples provided by them, along with identification of additional compounds. Another set of samples seized by police in North Carolina, USA, was analysed by the reference methods GC-MS and FT-IR in the laboratory of NarTest Company (NC, USA).

### 2.2. Equipment and analytical conditions

All fluorescence measurements were carried out on a NarTest™ NTX2000 Drug Analyzer (Tallinn, Estonia) that generates excitation–emission matrixes (EEMs) or SFSs. This is a compact spectrofluorometer equipped with a 5 W pulsed xenon lamp and a special 10 mL optical cell. SFSs were measured in front-face optical layout (35°) from the surface. The following experimental parameters were set:  $\lambda_{\text{ex}}=230\text{--}350\text{ nm}$  (25 excitation wavelengths) and  $\lambda_{\text{em}}=250\text{--}565\text{ nm}$  (64 emission wavelengths) with 5 nm intervals in both directions. The spectrofluorometer generated SFS, where the Rayleigh scattering was outside the measuring range. One scanning took 2.3 min. The required time for complete analysis of one sample was not more than 15 min.

#### 2.2.1. Measurement of SFS

The SFS of neat cocaine base, cocaine hydrochloride, MDMA hydrochloride, MDA hydrochloride, heroin and morphine, and also different neat adulterants, binary mixtures and multicomponent drug samples, were recorded. The SFS of neat analytes of interest in the mixture of glucose at two different concentrations (5% w/w and 100% w/w) are presented in Figure 1. Spectral data are corrected on the spectral distribution of Xe-lamp and detector spectral sensitivity. SFS as two-dimensional matrix is normalised on the fluorescence maximum of the analyte of interest that is marked with a black dot in SFS. Different colours at SFS indicate the level of equal fluorescence intensity.

### 2.3. Sample preparation

Stock standard solutions of analyte at a concentration of 2 mg/mL were prepared in deionised water and stored at 4 °C. A concentration of 2 mg/mL is equal to the upper range of application, that is, 100% by weight. The working standard solutions were prepared by appropriate dilution of the stock solution prior to analysis.

Hydrochloric acid (6 N), sodium hydroxide (0.75 M) and OPA-NAC (0.03 M) solutions were also prepared in deionised water, transferred to dropping bottles with 40  $\mu\text{L}$  drops and stored at 4 °C for 6 months.

#### 2.3.1. Contamination check

The test tube, pipette, optical cell and solvent (distilled water) were checked for contamination prior to analysis using NTX2000 analyser. Water (10 ml) was transferred by pipette to the tube. The test tube was capped and shaken several times. Afterwards, the solvent was transferred into the optical cell. If the blank sample was accepted, the analysis would be continued. Otherwise, the blank test was repeated with another 10 ml of water and new consumables (test tube, pipette, optical cell) until the result was satisfactory.

**Table I.** Reagents and cutting agents/adulterants specific for analytes of interest

Drug standards	Cutting agents	Chemicals
Cocaine HCl <sup>a</sup>	1-BZP (Fluka)	Hydrochloric acid (37%) (Fluka)
Cocaine base (Sigma)	3-MAM oxalate <sup>a</sup>	<i>N</i> -Acetyl-L-cysteine (Sigma-Aldrich)
Heroin HCl <sup>a</sup>	3-Methylfentanyl <sup>a</sup> (0.88%)	<i>o</i> -Phthaldialdehyde (Sigma-Aldrich)
Heroin base <sup>a</sup>	6-MAM HCl <sup>a</sup>	Sodium hydroxide (Sigma-Aldrich)
MDMA HCl <sup>a</sup>	Amphetamine sulfate <sup>a</sup>	Cutting agents (local store)
MDA HCl <sup>a</sup>	Benzocaine (Sigma)	Flour (Veski-Mati)
	Benzoic acid (Sigma-Aldrich)	Potato starch (Minu)
	Caffeine (Dolder)	Baking soda (Latplanta)
	Codeine phosphate <sup>a</sup>	Pseudoephedrine (Sudafed <sup>®</sup> )
	Dextromethorphan HBr H <sub>2</sub> O (Fluka)	Paracetamol (Pamol <sup>®</sup> )
	Diltiazem HCl (Sigma)	Aspirin (Bayer HealthCare)
	Ephedrine <sup>a</sup>	
	Fentanyl <sup>a</sup> (6.6%)	
	Glucose <sup>a</sup>	
	Hydromorphone HCl <sup>a</sup>	
	Inositol (Alfa-Aesar)	
	Ketamine HCl (Sigma)	
	Mannitol (Sigma-Aldrich)	
	Methamphetamine HCl <sup>a</sup>	
	Morphine HCl <sup>a</sup>	
	Tetramisole HCl (Sigma)	
	Lidocaine (Sigma)	
	MDEA HCl <sup>a</sup>	
	mCPP HCl (Aldrich)	
	Nicotinamide (Sigma)	
	Norfentanyl HCl (Lipomed)	
	Phentermine <sup>a</sup>	
	Procaine HCl (CPC W.M. GmbH)	
	Quinine (Sigma)	
	Marijuana <sup>a</sup> (13% THC)	

<sup>a</sup>Secondary standard, EFSI.

### 2.3.2. Sample pre-treatment

Solid samples were homogenised prior to analysis, and 20 mg of powder or crushed sample was dissolved in 10 mL of water and checked for contamination. The tube with a sample solution was shaken carefully and left to stand for 1 min until the insoluble particles settled. At the first step, 5 mL of liquid aliquot was transferred to the optical cell. The further analysis was performed according to the instructions of the programme guidance [29].

**2.3.2.1. Cocaine procedure.** In this study, the distinction of cocaine is based on the change of fluorescence intensity at  $\lambda_{\text{ex}}/\lambda_{\text{em}}$  235/315 and  $\lambda_{\text{ex}}/\lambda_{\text{em}}$  275/315 nm of the two chemical forms of cocaine under the treatment with acid solution (Figure 2(b1)).

One drop or 40  $\mu\text{L}$  of 6 N hydrochloric acid was added to 5 mL of sample solution in the second step. If the growth of fluorescence intensity was observed at  $\lambda_{\text{ex}}/\lambda_{\text{em}}$  235/315 and  $\lambda_{\text{ex}}/\lambda_{\text{em}}$  275/315 nm, cocaine base (Figure 1(c and d)) would have been detected. Cocaine salt (Figure 1(a and b)) would have been detected if the quenching was observed. Cocaine differentiation was impossible when the growth or loss of fluorescence intensity was insufficient.

**2.3.2.2. MDMA/MDA procedure.** The analysis of MDMA (known as ecstasy) is based on the detection of SFS with maximums of

$\lambda_{\text{ex}}/\lambda_{\text{em}}$  235/320 and  $\lambda_{\text{ex}}/\lambda_{\text{em}}$  285/320 nm (shown in Figure 1 (i and j)). The ecstasy structural analogue MDA has a similar to MDMA SFS. In order to differentiate MDMA samples (neat or cut) from the samples that contain MDA (neat or cut), one drop of 0.75 M sodium hydroxide and one drop of 0.03 M OPA-NAC were added to 5 mL of sample solution. Formation of isoindole complex between the OPA-NAC reagent and the primary amino group of MDA provides a maximum at  $\lambda_{\text{ex}}/\lambda_{\text{em}}$  335/425 nm [30]. If the isoindole complex was formed, either MDA or MDA in the mixture of MDMA would have been found, and the answer would have been 'MDMA/MDA detected', respectively. Otherwise, MDMA would have been detected in the sample under investigation (Figure 2(d2-1 and d2-2)).

**2.3.2.3. Heroin procedure.** Heroin analysis is based on the detection of morphine in the sample. It is known that the fluorescence of heroin in water (Figure 1(e and f)) is not strong enough to confirm the presence of heroin in the multicomponent samples, but the morphine (Figure 1(g and h)) presence can be easily detected because of its high quantum yield of fluorescence.

The seized sample can contain morphine (scheduled II in Estonia [31]) as one of its constituents and none of heroin. To confirm the presence of heroin in the sample, the fluorescence intensity at  $\lambda_{\text{ex}}/\lambda_{\text{em}}$  285/345 nm in the main sample was compared with fluorescence intensity at the same point of reference sample.

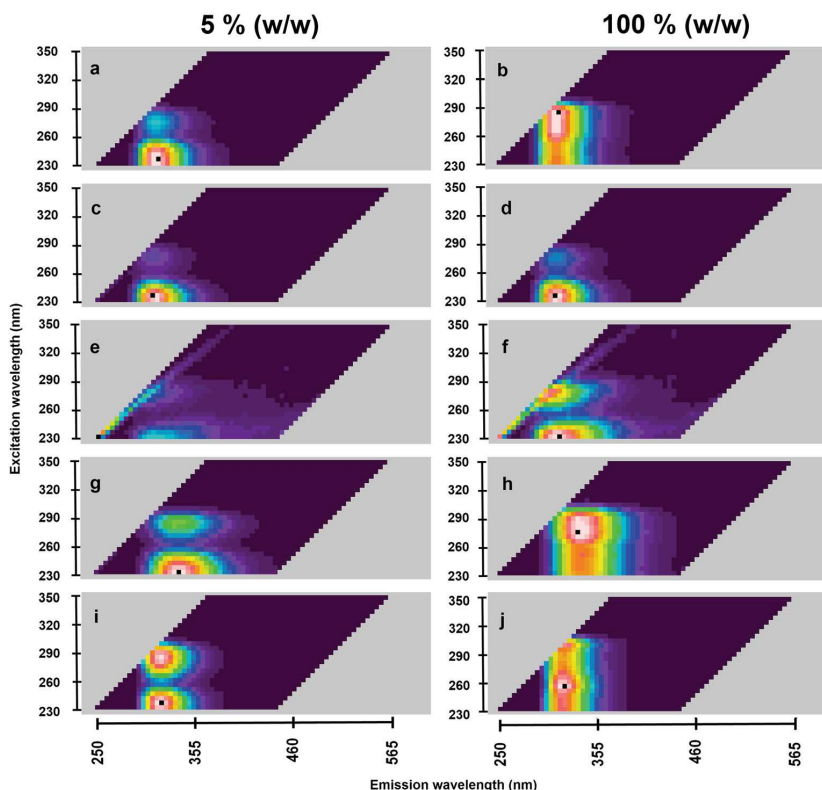


**Figure 1.** SFS of analytes ( $\lambda_{\text{ex}}/\lambda_{\text{emr}}$ ,  $I^*$ ) in deionised water: (a) cocaine hydrochloride (235/315, 7482.5); (b) cocaine hydrochloride (285/315, 6879.5); (c) cocaine base (235/310, 2330.8); (d) cocaine base (235/310, 2770.6); (e) heroin (230/315, 61.0); (f) heroin (230/315, 142.1); (g) morphine (230/340, 636.6); (h) morphine (275/335, 2755.3); (i) MDMA (235/320, 49801.4); (j) MDMA (255/320, 41731.4). \*  $\lambda_{\text{ex}}$ —excitation wavelength, nm;  $\lambda_{\text{em}}$ —emission wavelength, nm;  $I$ —intensity, a.u.

First of all, the reference sample solution was measured. To prepare the reference samples, three drops of 6 N hydrochloric acid and then three drops of 0.75 M sodium hydroxide were added to 5 mL of sample solution.

In order to treat the main sample, three drops of 0.75 M sodium hydroxide were added to 5 mL of sample solution remaining in the test tube. The solution was agitated and left to react for 15 min. Afterwards, three drops of 6 N hydrochloric acid were added to convert morphine into morphine hydrochloride. Morphine hydrochloride has a higher quantum yield of fluorescence in comparison with its base form. For this reason, the conversion of morphine to its salt form is crucial for detection of morphine (Figure 2(c2-1)).

If there had been a sufficient growth of the signal response at  $\lambda_{\text{ex}}/\lambda_{\text{em}}$  285/345 nm, heroin presence would have been confirmed in the sample.

#### 2.4. The methodology of artificial neural networks

Multilayer perceptron (MLP) ANNs based on a backpropagation learning algorithm were employed as a tool for pattern recognition of SFS (or EEMs) for illicit drug detection in seized street samples [18]. Unlike linear regression, principal component regression and partial least squares, ANNs can deal with the highly nonlinear,

strongly coupled, multivariable systems. Moreover, the crucial characteristic of the used chemometric technique is its generalisation ability. However, the most widely used technique for EEM interpretation is parallel factor analysis [32], and this method has also been considered for data analysis; it was not a better solution for the current study. The comparison of different techniques will follow in a later publication.

A comprehensive database has been used to develop the models for drug detection. The data consisted of 4300 different laboratory mixtures (neat drug standards, laboratory mixtures with adulterants, diluents, neat cutting agents, impurities and precursors [17]) and more than 4000 street samples. The data were balanced in the view of variability of positive to negative samples as well as variability of samples with common SFS of drugs to untypical SFS of sample. Moreover, all street samples used for ANN construction were analysed by the reference method, GC-MS.

The balanced data were split into three sets: training, monitoring and validation set with two subsets: the first validation and the second validation subset. The training set consisted of 4126 different samples for cocaine, 2357 samples for heroin and 1970 samples for MDMA/MDA. The aim of the monitoring set was to estimate and select the optimal model. The monitoring set consisted of 4124 different samples for cocaine, 2357 samples for heroin and 1969 samples for MDMA/MDA, and this data

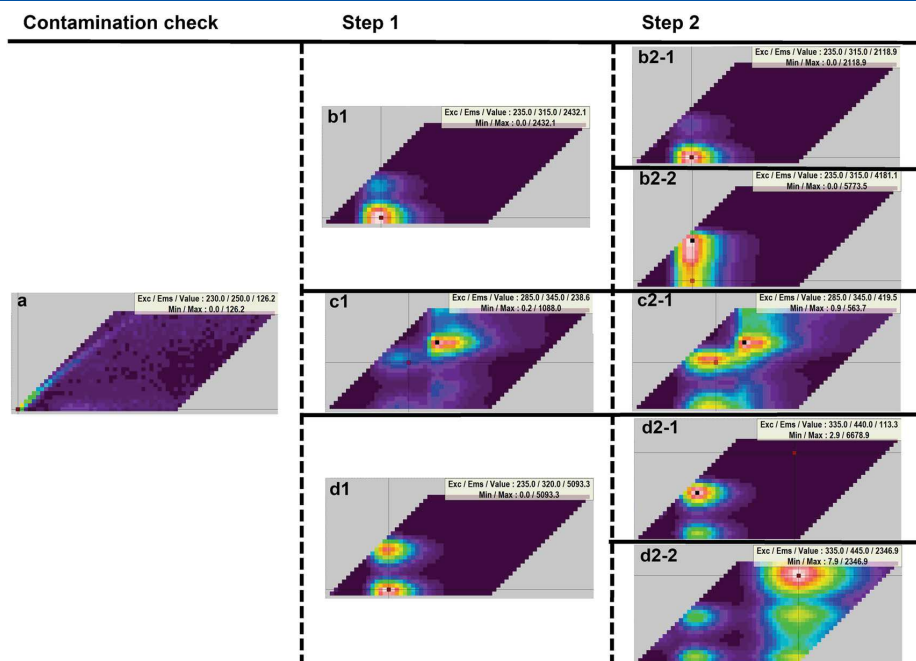


**Figure 2.** Schematics of procedures presented as SFS of analytes at different steps in water and treated by reagents. Pre-analysis: (a) deionised water. Step 1: (b1) cocaine sample in water; (c1) heroin sample treated by reagents (i.e. reference sample); (d1) ecstasy sample in water. Step 2: (b2-1) cocaine under treatment of reagent ('cocaine salt detected'); (b2-2) cocaine under treatment of reagent ('cocaine base detected'); (c2-1) formed morphine under treatment of reagents ('heroin detected'); (d2-1) ecstasy sample under treatment of reagents ('MDMA detected'); (d2-2) ecstasy sample and isoindole complex under treatment of reagents ('MDMA/MDA detected').

did not intersect with the data of the training set. The first validation subset consisted of certain binary laboratory mixtures with a known ratio (w/w) of pure drug standards to pure cutting agents. The following mixtures were prepared:

- Cocaine procedure % (w/w): 5:95, 10:90, 15:85, 25:75, 50:50, 75:25, 95:5;
- Heroin procedure % (w/w): 5:95, 10:90, 15:85, 25:75, 35:65, 50:50, 75:25, 90:10, 95:5;
- MDMA procedure % (w/w): 1:99, 2:98, 3:97, 5:95, 6:94, 10:90, 15:85, 25:75, 50:50, 75:25, 95:5.

The first validation subset was used for evaluation of the efficacy of optimal ANNs. The second validation subset consisted of 628 true positive seized street samples (491 cocaine samples, 26 ecstasy samples and 111 heroin samples) and 625 true negatives for all analytes of interest. This validation subset was performed by different operators and instruments in the different laboratories to evaluate the statistical parameters: false positive rate, false negative rate, sensitivity and specificity [33,18].

The dimensionality of the original dataset was reduced by using feature extraction. The vector of features, which represented an average value of intensities of segments in SFS (Figure 3), was used as input for ANN. The sizes and locations of such segments depended on the certain task. Primarily, they were directly connected with the spectral maximums of the analyte of interest. A well-considered selection of inputs improved the final model, reducing the amount of noisy and interfering components in the input data.

Prior to ANN training, the raw features are submitted to different ways of normalisation preparing the data to be suitable for training. [34] The normalisation rescales the feature or output from one range of values to a new range of values. Three techniques were used for vector rescaling: linear scaling with range [0, 1] or [-1, +1] with or without clipping; linear scaling of mean dispersion to [0, 1] or [-1, +1] with or without clipping; and without scaling. The minimum–maximum values of the feature vector were rescaled to the range from 0 to 1 or from -1 to +1, respectively. The normalised feature lies within the ranges from 0 to 1 or from -1 to +1.

After data normalisation, all variables were in the range of [0, 1] or [-1, +1]. If an out-of-range value was observed, the clipping would be applied to the data. The clipping approach meant that the out-of-range value was set equal to the nearest valid threshold value, that is, 0 or 1; -1 or +1. For instance, if the

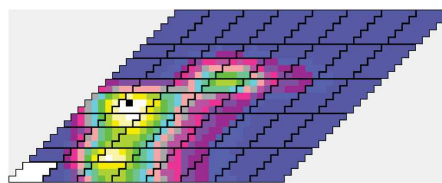


**Figure 3.** Example: one of the masks applied for feature extraction. One segment is highlighted in white

value was higher than the threshold, then the upper threshold value would be assigned to it.

The architecture of ANNs depended on the concrete task and was developed for each procedure independently. The number of input nodes (12–95), hidden layers (1–3) and outputs (1–4) was optimised for each ANN. Generally, the configuration of ANNs was as simple as possible and approached empirically by different possibilities, that is, neurons (approximately 10) in the hidden layer, learning rate ( $\eta = 0.01$ ) and momentum ( $\alpha = 0.9$ ). The most commonly used transfer functions were linear, sigmoidal and hyperbolic tangent. The ANNs were trained with the desired output that was coded in a numerical value by assigning 0 for 'not detected' and 1 for 'detected'. For classification purposes, a threshold value was set to 0.5 (50%). All results with an output less than 0.5 were classified as 'not detected', and results exceeding the threshold value were classified 'detected'.

With no doubt, ANNs can be exposed to data overfitting, that is, the risk that the networks have learnt peculiarities specific for the training samples and lost the ability to generalise. This study attempted to minimise this by using a simple as possible configurations of ANNs, large testing size, two validation subsets and their independency from each other and also by applying constraints as described previously in the procedures. The final choice was performed by selecting the one that provided the best classification accuracy on the monitoring set. Afterwards, the optimal ANNs were verified by validation subsets. Finally, the nets were accepted or rejected and sent to redevelopment if the results did not fit the purpose of validation. ANNs were built using internally developed software based on the Neurowindows library from Ward Systems Group Inc. (Frederick MD, USA).

## 2.5. Validation

Concrete requirements for validation of SFS-MLP-ANN must be fulfilled in order to be categorised as a confirmatory analysis. First of all, the method must provide information on the chemical structure of the substance with the maximum discriminating power, and also sufficient separation must be achieved between the analytes. The method under investigation is not ordinary fluorescence spectroscopy but the combination of two different analytical groups according to the Scientific Working Group for the Analysis of Seized Drugs (SWDRUG): group 2—structural elucidation technique: SFS method and group 4—chemical properties: solubility and specific reactions (conversion of heroin to morphine, derivatisation). Moreover, this study has determined MLP-ANN as the independent group: multivariate analysis technique (chemometrics). Utilising several techniques, in series or combination, has certainly increased the discriminating power of fluorescence spectroscopy that is put into the category C by SWDRUG.

The validation procedure was performed according to the United Nations Office on Drugs and Crime, International Conference on Harmonisation of Technical Requirements for Registration of Pharmaceuticals for Human Use/United States Pharmacopoeia, SWDRUG and Commission Decision 2002/657/EC requirements established for the qualitative analysis. Furthermore, it was found that the better understanding of the work of ANNs was crucial for validation. ANNs are often allied with a 'black box' nature because of its complexity to describe the explicit rules between input and output variables.

Therefore, the uncertainty region for ANN for each compound in the binary mixtures was found to be an ideal tool to determine the ANN behaviour. The following parameters are to be determined in the validation of SFS-MLP-ANN: range of application (LoD in the mixture of inert matrix, threshold limit ( $CC\beta$ ) in the mixture of inert matrix, upper range of application); selectivity/matrix effects ( $CC\beta$ , uncertainty region for each of the interferences); robustness (expressed as reliability% at the threshold value\*1.5); precision (repeatability, reproducibility).

The discriminating power of the SFS-MLP-ANN method was evaluated on the testing of street samples. Statistical parameters (false positive rate, false negative rate, sensitivity and specificity) [35] were obtained by comparison of the results of the SFS-ANN method with GC-MS or FT-IR, well-characterised reference methods. The previous statistics from 2005 to 2009 (I) was published in *SPIE* proceedings [17,18], and up-to-date statistics (2009–2011) are presented in the current study.

## 3. RESULTS AND DISCUSSION

### 3.1. Training of ANNs

The data for construction of ANNs were divided into four different sets, as described previously: training (TRN), test set (TST) and two validation sets (VAL1 and VAL2). The training was repeated with several random restarts to find the best suitable model. The training of normalised data lasted until no improvement of the statistical parameters was observed during 1000 epochs. As mentioned previously, all systems were trained using a back propagation algorithm. The objective was to minimise the instantaneous value of total error energy. Errors of training (TRN) were defined as average error energy and were found according to the following equations [36]:

$$E^n = \frac{1}{2} \sum (d_j^n - y_j^n)^2$$

$$E_{av} = \frac{1}{N} \sum_{n=1}^N E^n \quad (3.1-1)$$

where  $n$  is the number of iteration,  $E^n$  the instantaneous value of total error energy,  $E_{av}$  the average error energy,  $N$  the total number of training pattern,  $d_j^n$  the target output for neuron  $j$  and  $y_j^n$  the network output of neuron  $j$ .

Several (about 10) best trained networks were tested on the monitoring sets, and the best ones were chosen for more precise investigation on the validation subsets. Figure 4 presents only the results for optimum ANNs used for the current validation procedure. The best ones were chosen according to the following criterion:

- None of the false positives ( $f_p$ ) were accepted either in the TRN or TST to prevent a mistaken arrest;
- The lowest rate of false negatives was preferable;
- 'Erroneous' classification was acceptable but leads to a minimum value. 'Erroneous' classification meant 'erroneous' identification of forms of the analyte of interest, but the substance was also scheduled, for instance, cocaine salt and cocaine base, MDMA and MDA in the mixture of MDA, and MDEA detected as MDMA.
- The highest efficiency was found according to the following equation:

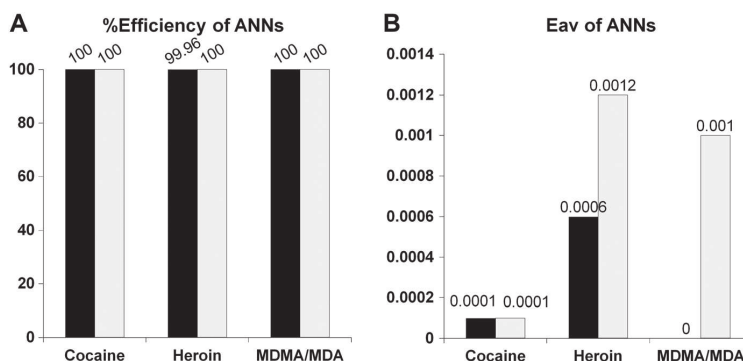


**Figure 4.** Parameters of optimal ANNs: (A) %Efficiency; (B) average error energy ( $E_{av}$ ) (black—TRN; white—TST).

$$\% \text{efficiency} = \frac{t_p + t_n}{t_p + f_n + t_n + f_p} * 100\% \quad (3.1-2)$$

where  $t_p$  is the number of true positives,  $f_p$  the number of false positives,  $t_n$  the number of true negatives and  $f_n$  the number of false negatives.

No false positives were found either on TRN or TST, and only one false negative for the heroin procedure was observed. The erroneous sample was investigated more precisely. It was concluded that the high masking effect of the unknown adulterant and probably low concentration of heroin in the sample gave the invalid suggestion about the sample. The obtained results were suggested as satisfactory, and the trained ANNs were verified by further evaluation by independent validation subsets.

### 3.2. Validation set

Usually, the prediction performance of the ANN model is estimated by efficiency on testing the trained network. Certainly, all methods have their ranges of application, where they are working perfectly. That is why the methods must be verified and validated, showing that they fulfil the scope of investigation. This study showed that efficiency of the ANNs did not depend only on how well the ANNs were trained but also on the data fed to the trained ANN.

Typically, drug street samples are multicomponent complex samples. Multicomponent samples do not only challenge the selectivity of the SFS method, but the phenomena of quenching and masking effects must also be considered when dealing with such samples. Therefore, this study was designed to evaluate the reliability of SFS-MLP-ANN method to detect analytes of interest even in highly adulterated mixtures. The potential for errors ( $f_p$ ,  $f_n$ ) from binary mixtures in the range of 0% to 100% by weight of analyte of interest was examined, and the ratios at which cocaine, heroin or MDMA could be detected were determined. The validation was divided into two subsets: laboratory mixtures and real street samples. Performing testing of trained networks on laboratory mixtures gave primarily the understanding of the range of application of the SFS-MLP-ANN method. The subset containing street samples provided a better understanding of how the SFS-MLP-ANN method was working in a routine analysis.

#### 3.2.1. Calibration curves and limits of detection and quantitation

**3.2.1.1. Limit of detection and detection capability ( $CC\beta$ ).** There is a variety of terminologies for LoD [37]. According to IUPAC,

LoD is the 'minimum detectable (true) value', and ISO defines it as the 'minimum detectable net concentration'. Moreover, there are more terms, such as limit of decision ( $CC\alpha$ ) and detection capability ( $CC\beta$ ), defined in 2002/657/EC [19].  $CC\alpha$  and  $CC\beta$  are two important performance characteristics of confirmatory methods for banned substances (group A, i.e. substances having anabolic effect and unauthorised substances) [19].

Actually, the method detection limit (LoD) is referred to real matrices [38] and is defined as the 'threshold concentration at which the test becomes unreliable' [23] for qualitative analysis. The LoD was found using the calibration-design-dependent LoD approach with 95% prediction intervals [39,40]. The estimation of LoD was sometimes unfeasible, because the values varied from device to device to a small extent, and certainly depended on instrument settings and the sample matrix. Indeed, it displayed method sensitivity, because the slope of the calibration curve with confidence intervals ( $p = 95\%$ ) was used for the LoD calculation, but it did not show the sensitivity of ANNs.

It was obvious that for qualitative analysis coupled with ANNs, it was necessary to find  $CC\beta$  or 'the lowest concentration at which a method was able to detect truly contaminated samples with statistical certainty of  $1 - \beta'$ ' [19].  $CC\beta$  or the threshold concentration showed the sensitivity of the intelligence system and therefore the actual limit of the optimised system.

Indeed,  $CC\beta$  for screening and confirmation methods must be as low as possible for detection of banned substances such as cocaine, heroin or MDMA in bulk materials. Moreover, Commission Decision 2002/657/EC requirement for qualitative methods must be fulfilled, that is, the false compliant rate ( $CC\beta$ ) must be  $<5\%$  ( $\beta$ -error) at the level of interest. In other words, the method should be able to identify the analyte in 95% of the cases at the  $CC\beta$  [41].

Therefore, the  $CC\beta$  was defined not only by decomposing the spectral patterns in SFS but also by the capabilities of the ANN expert system used for analysis. The  $CC\beta$  was defined by a probability-concentration graph by investigating the spiked blank material at and above the LoD, where at least 20 independent replicates were performed for each point (Figure 6). Glucose was chosen as the blank material, that is, a compound that does not have either a native fluorescence or quenching effect on the analytes of interest. Also inositol, lactose, sucrose and other compounds were suitable.

The LoD and  $CC\beta$  values are summarised in Figure 5. It is obvious that LoDs are much higher than the threshold ( $CC\beta$ ). In order to improve the threshold values, SFS with a desirable concentration could be fed up to the training set and the ANN retrained. But

the risk of overfitting must be taken into account if too noisy data due to the low concentration of analyte in sample are applied for retraining of ANN. Consequently, SFSs with reasonable concentration range should be only used for retraining. In this study, the retraining was only required for heroin. The first results found for the heroin procedure showed that the threshold value for heroin HCl was 3.13% (w/w) and for heroin base was 6.25% (w/w). It was decided to overtrain the ANN adding SFSs containing 0.2%, 0.5%, 0.8% and 1% (w/w) of heroin hydrochloride. The efficiency% on TRN and TST remained the same. The final results of the threshold value for the heroin procedure were the following: 0.2% for heroin hydrochloride and 0.8% for heroin base, respectively (Figure 6).

### 3.2.2. Selectivity

Selectivity is one of the important parameters that must be evaluated in the validation of qualitative method. It shows how accurately the method with optimised methodology distinguishes the analytes in the mixtures with different compounds found in the sample matrixes. Moreover, the study of mixtures provides the possibility to determine substances that can lead to false negative results, false positive and also erroneous classification. It also shows the substances that have quenching effects on the analytes of interest. In order to obtain realistic results, the most common drug combinations must be determined. According to 'Guide to Adulterant, Bulking agents and other Contaminants Found in Illicit Drugs' (Claire Cole, Lisa Jones and others) [42] the following adulterants/cutting agents are mainly found in seized heroin samples: caffeine, quinine, sugars (sucrose, lactose, dextrose, mannitol), procaine, phenobarbital, paracetamol, lead-contamination, clenbuterol, chloroquine (an antimalarial drug) and phenolphthalein (a laxative). The most frequently found are procaine, paracetamol, sugars and caffeine. According to the European Monitoring Centre for Drugs and Drug Addiction annual report 2010, the most often found adulterants/cutting agents for cocaine samples are tetramisole, benzocaine, pharmacologically active adulterants including analgesics (e.g. paracetamol), local anaesthetics (e.g. lidocaine), antihistamines (e.g. hydroxyzine), diltiazem and atropine, and phenacetin [43–45]. The statistics about the MDMA and MDA adulteration can be obtained from [www.ecstasydata.org](http://www.ecstasydata.org). According to this database, the main adulterants found with MDMA are procaine, caffeine, paracetamol, ketamine, dextromethorphan,

methamphetamine, 3-trifluoromethylphenylpiperazine, benzylpiperazine, pseudoephedrine, 2C-B and other MDMA analogues such as 3,4-methylenedioxyamphetamine (MDA) and 3,4-methylenedioxy-N-ethylamphetamine (MDE).

However, the statistics on the common concentration of excipients is available; the certain ratios of compounds' combinations with cocaine, heroin or ecstasy are not guaranteed. The reason is obvious; it is unknown whether the drug dealers mix the different compounds in certain proportions for purpose or randomly. Moreover, the sample combinations vary geographically. The main peculiarity of the presented method is the absence of the analysis separation. That is why the uncertainty region for the expert system must be found for each of the excipients specific for the analyte of interest. It is especially crucial when the sample consists of two or even more native and highly fluorescent compounds in the region specific for cocaine, heroin or MDMA. Because of spectral overlap, the analyte of interest could be completely hidden in the sample matrix, and it would lead to a false negative result. The extremely adulterated samples can be found on the streets, but the probability of their presence is quite low. Nevertheless, this possibility cannot be completely ignored. On the other hand, the absence of the separation system is a benefit of the method, because it saves time and simplifies the operation.

**3.2.2.1. Binary mixtures.** The results containing binary mixtures are summarised in Table II. It gives an overview of the ratios of compounds that could be easily detected by the SFS-MLP-ANN method. It also describes the uncertainty region, where the results of the expert system are not conclusive, and the ratio of excipient to analyte of interest (the lowest range of application), where the false negative results appear. Generally, the presence of the excipients (glucose, inositol, mannitol, lactose, starch and flour) that did not generate either a fluorescence signal or quenching had no effect on the detection of the controlled substances. Other compounds had either a fluorescent masking effect and/or a quenching effect on the analyte of interest (for example, benzocaine, procaine, caffeine, lidocaine and nicotinamide), but it was not so drastic as to prevent the detection of analytes of interest in the matrix.

In general, the detection of cocaine was not problematic in the samples, where adulteration reached 95% (median) of excipient,

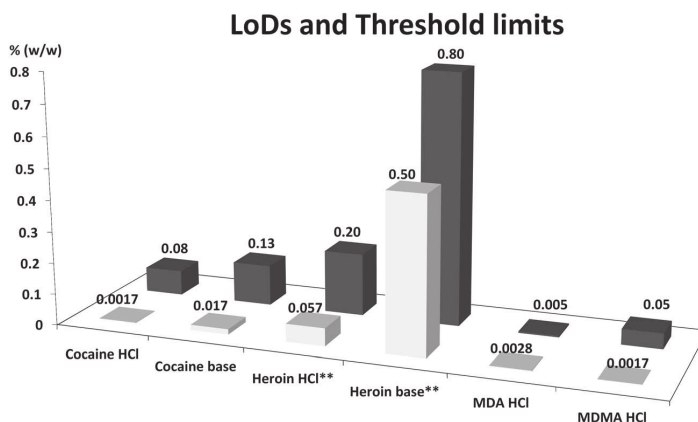


**Figure 5.** LoDs and threshold limits for analytes of interest in the mixture of glucose (black—threshold value; white—LoD value).

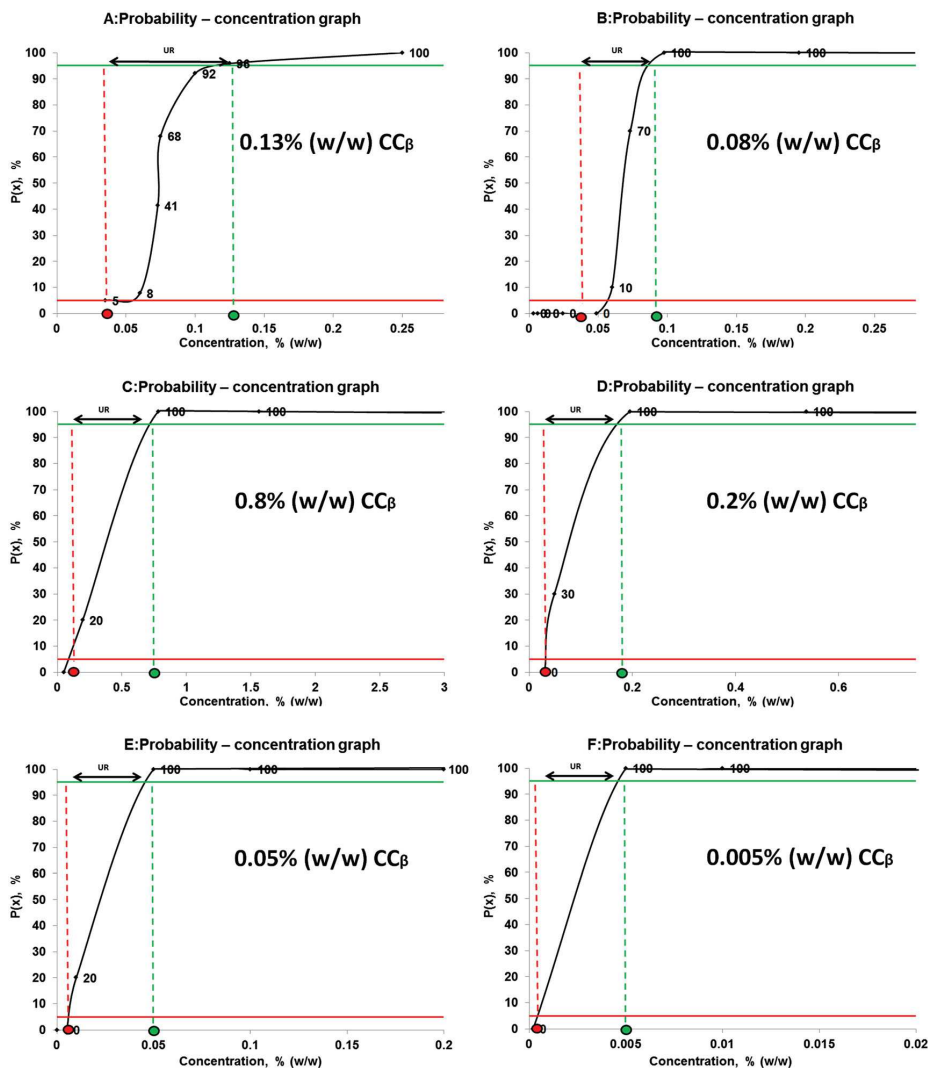


**Figure 6.** Probability–concentration graphs: (A) cocaine base, (B) cocaine hydrochloride, (C) heroin base, (D) heroin hydrochloride, (E) MDMA hydrochloride, (F) MDA hydrochloride. Cut-off values correspond to 95% confidence limits for negative/positive probabilities, where UR is the uncertainty region.

excluding some excipients, where the expert system was not sufficiently confident (Table II). The  $CC\beta$  of cocaine HCl in the mixture of paracetamol and benzocaine was between 10% and 15% and in the mixture of marijuana (THC 13%) was between 15% and 30%. In case cocaine was presented in the mixture of procaine or benzocaine, cocaine base would be detected. The reason of 'erroneous' classification laid on the growth of signal response at  $\lambda_{ex}/\lambda_{em} = 275/315$  nm under the treatment of reagent. So it was found that the differentiation between the cocaine salt and cocaine base in the mixture of procaine or benzocaine was not successful. Overall, the SFS-MLP-ANN method displayed adequate sensitivity to allow the detection of cocaine at commonly encountered concentrations in street samples. Actually, the mean purity of cocaine in Europe ranged between 18% and 51.3% in 2009 [44].

For heroin detection, aspirin had the most drastic masking effect, entirely blocking the detection of the analyte. The  $CC\beta$  of heroin was between 35% and 40% in the mixture of aspirin. In the case of cocaine and heroin mixtures, the  $CC\beta$  of cocaine was lower than 5% in the mixture of heroin, and the  $CC\beta$  of heroin was between 5% and 10% (w/w), respectively. This meant that both substances could be detected in the bulk samples but separate procedures; that is, cocaine procedure and heroin procedure must be applied. Moreover, structurally very close compounds to heroin (i.e. 3-MAM, 6-MAM, codeine, hydromorphone and morphine) were investigated. It was determined that 3-MAM, 6-MAM and morphine base (Schedule II) can give 'erroneous classification' for heroin identity. According to the statistical bulletin 2011, the mean purity of heroin in Europe ranged between 14.3% and 50.3% in 2009 [46].

**Table II.** Threshold values for binary mixtures of analytes in the mixture of known excipients (at least three independent replicates, at least two instruments, at least two operators and at least two laboratories)

No.	Procedure Excipient	Cocaine (salt/base)		MDMA/MDA		Heroin
		CoH	CoB	MDMA	MDA	HH
1	1-BZP	n.a.	n.a.	≥1%	≥1%	n.a.
2	2C-B 3%	n.a.	n.a.	≥1% to <2% (MDMA/MDA) ≥2% (MDMA)	≥1%	n.a.
3	3-MAM 20%	n.a.	n.a.	n.a.	n.a.	≥5%
4	3-methylfentanyl 0.88%	n.a.	n.a.	≥1%	≥1%	≥5%
5	6-MAM 10%	n.a.	n.a.	n.a.	n.a.	≥5%
6	Amphetamine	n.a.	n.a.	≥1% (MDMA/MDA)	≥1%	n.a.
7	Aspirin	≥5%	≥5%	>1% to ≤2%	>1% to ≤2%	>35% to ≤40%
8	Baking soda	≥5%	≥5%	≥1%	≥1%	≥5%
9	Benzocaine	>10% to ≤15%	>5% to ≤10%	≥1%	≥1%	n.a.
10	Benzoic acid	>5% to ≤10%	>5% to ≤10%	≥1%	≥1%	n.a.
11	Caffeine	>5% to ≤10%	≥5%	≥1%	≥1%	≥5%
12	Cocaine (salt)	—	—	≥1%	≥1%	>5% to ≤10%
13	Codeine	n.a.	n.a.	n.a.	n.a.	>15% to ≤20%
14	DXM	n.a.	n.a.	>2% to ≤5%	>2% to ≤3%	n.a.
15	Ephedrine	≥5%	≥5%	≥1%	≥1%	n.a.
16	Fentanyl 6.6%	n.a.	n.a.	≥1%	≥1%	≥5%
17	Flour	≥5%	≥5%	≥1%	≥1%	≥5%
18	Glucose	≥0.08%	≥0.13%	≥0.05%	≥0.005%	≥0.2%
19	Heroin (base)	≥5%	≥5%	>1% to ≤2%	≥1%	—
20	Heroin (salt)	n.a.	n.a.	≥1%	≥1%	—
21	Hydromorphone 10%	n.a.	n.a.	n.a.	n.a.	≥5%
22	Inositol	≥5%	≥5%	≥1%	≥1%	≥5%
23	Ketamine	n.a.	n.a.	≥1%	≥1%	n.a.
24	Lactose	≥5%	≥5%	≥1%	≥1%	≥5%
25	Lidocaine	≥5%	≥5%	≥1%	≥1%	≥5%
26	Mannitol	≥5%	≥5%	≥1%	≥1%	≥5%
27	Marijuana (THC 14%)	>15% to ≤30%	n.a.	n.a.	n.a.	n.a.
28	mCPP	n.a.	n.a.	≥1% to <5% (MDMA/MDA) ≥5% (MDMA)	≥1%	n.a.
29	Methamphetamine	n.a.	n.a.	≥1% to <2% (MDMA/MDA) ≥2% (MDMA)	≥1%	≥5%
30	Morphine	n.a.	n.a.	n.a.	n.a.	>15% to ≤20%
31	Nicotinamide	n.a.	n.a.	≥1%	≥1%	≥5%
32	Norfentanyl 10%	n.a.	n.a.	n.a.	n.a.	≥5%
33	Paracetamol	>10% to ≤15%	>5% to ≤10%	≥1% to <10% (MDMA/MDA) ≥10% (MDMA)	≥1%	>10% to ≤15%
34	Phentermine	n.a.	n.a.	≥1%	≥1%	n.a.
35	Procaine	>5% to ≤10%	≥5%	>1% to ≤2%	>1% to ≤2%	>5% to ≤10%
36	Quinine	n.a.	n.a.	n.a.	n.a.	≥5%
37	Starch	≥5%	≥5%	≥1%	≥1%	≥5%
38	Tetramisole	n.a.	≥5%	n.a.	n.a.	n.a.
39	TMFPP/BZP (1:1)	n.a.	n.a.	>2% to ≤5%	>1% to ≤2%	n.a.
Min%		≥0.08	≥0.13	≥0.05	≥0.005	≥0.2
Max%		≤30	≤10	≥10	≤3	≤40

n.a.—not analysed (because the excipient is not specific for the analyte of interest); CoH—cocaine hydrochloride; CoB—cocaine base; DXM—dextromethorphan; HH—heroin hydrochloride.

The best results were aligned to MDMA in the binary mixtures with different substances because of a high fluorescent yield of MDMA and its analogues MDA and MDEA. The ANNs were able to identify MDMA and its structural analogue presence, even in the highly adulterated samples, by a median >99% (w/w) adulterated by one compound. The system was not adjusted to

separate and identify MDA alone. In the case of the mixtures MDMA with MDA or MDA alone with excipients, the expert system identifies the sample as MDMA/MDA. Additionally, it was determined that the mixtures of MDMA with amphetamine would always generate an MDMA/MDA answer ('erroneous classification') because of the isoindole formation with the primary amino group

of amphetamine. For conclusive identification of MDMA in the mixtures of 2C-B, methamphetamine, mCPP or paracetamol, the  $CC\beta$  of MDMA is lower (between 1% and 15%; see Table II) than for the rest of the excipients. Moreover, the MDMA structural analogues MDE and MDEA (Schedule I) behaved as MDMA, and therefore, they were detected by the expert system as MDMA. This answer was suggested as an 'erroneous classification'. These facts must be taken into consideration. The mean purity of ecstasy found in Lithuania and Austria ranged between 20% and 41.1% (given in % of MDMA) in 2009 [44].

The rate of false positives was evaluated in the neat licit compounds with the maximum concentration available. In total, three independent measurements were performed for each of the compounds. Neither of the compounds was determined as positive. Therefore, the false positive rate for all methodologies for cocaine, heroin and MDMA/MDA was considered to be 0%. True negative samples were used in reproducibility and repeatability studies. Two laboratories, six spectrofluorometers and two analysts participated in the studies. Reproducibility was 100%, and repeatability was also 100%. Moreover, the independent estimation of the threshold value for cocaine base in the mixture of glucose was used as a control for reproducibility. Two laboratories defined the  $CC\beta$  for cocaine base identically, that is, 0.13% cocaine base.

Compared with alternative methods [4,7–11], SFS-MLP-ANN has shown better threshold values for MDMA, cocaine and heroin in the mixture of excipients. In most cases, it was possible to detect the analyte of interest at levels down to approximately 5% (w/w) or 100 mg/L (w/v). The upper range of application was set to the maximum concentration, that is, 100% (w/w) or 2000 mg/L (w/v). Overall, the results were suggested to be satisfactory for fulfilling the purposes of the method.

**3.2.2.2. Multicomponent mixtures.** With no doubt, the design of the experiments for analysis of mixtures that contain more than two compounds is more complex. It was decided to investigate the mixtures that contain caffeine and paracetamol in the mixture of analytes of interest. The substances were chosen because both substances have native fluorescence and also because caffeine is a known quencher. Moreover, the combination of paracetamol with caffeine is a common painkiller medicine. The following mixtures were analysed:

- Cocaine HCl, caffeine, paracetamol (5%, 45%, 50%; 10%, 45%, 45%; 15%, 45%, 40%);
- Heroin HCl, caffeine, paracetamol (5%, 45%, 50%);
- MDMA HCl, caffeine, paracetamol (5%, 45%, 50%; 10%, 45%, 45%);
- MDA HCl, caffeine, paracetamol (1%, 49%, 50%)

The following uncertainty regions were determined for detection of the analytes of interest in the mixture of two selected excipients: cocaine HCl >10% to ≤15%, if paracetamol >45% to ≤50% and caffeine >45% to ≤50%; heroin HCl ≥5%, if paracetamol ≤50% and caffeine ≤45%; MDA HCl ≥1%, if paracetamol ≤50% and caffeine ≤49%; MDMA HCl >5% to ≤10%, if paracetamol >45% to ≤50% and caffeine ≤45%. The obtained results were in concordance with  $CC\beta$  values presented in Table II for binary mixtures.

### 3.2.3. Robustness

Robustness is a parameter that shows the method's ability to remain unaffected by small but deliberate changes in method

variables [19]. It also indicates the method reliability during normal operation. Through experimental design, it is possible to define the performance limits for critical variables that influence the reliability of responses of ANN. This parameter is definitely crucial for subsequent validation to show that the response does not depend on external/intrinsic factors, because the tests methods are often handled by a nonprofessional operator. With no doubt, the robustness depends on the concentration, where the robustness is examined. In case the examined concentration equals the threshold value ( $CC\beta$ ), the robustness will have lower results. The United Nations Office on Drugs and Crime proposes the ranges for the robustness to be examined:  $1.25 \times CC\beta$  and  $2 \times CC\beta$ , where 1.25 and 2 are coefficients [22]. One of the possible experimental designs is the Youden approach suggested by European Decision 2002/657/EC of 12 August 2002, implementing Council Directive 96/23/EC, concerning the performance of analytical methods and the interpretation of results. The Youden approach is a fractional factorial design developed by Plackett–Burman [47]. It keeps the required time and effort to a minimum. Only eight experiments ( $N = 8$ ) are required for evaluation of the influence of  $N - 1$  factors. Therefore, the number of factors under investigation can vary from three to seven.

Firstly, all possible variables were defined for each of the procedures. The main factors are weight of sample, volume of solvent, amount of reagents added in the procedures, volume of aliquot solution in optical cell and reaction time. The design of experiments with factors from five to seven, and their levels ('–' low and '+' high) are presented in Table III. There were in total seven factors found for heroin, six factors with one dummy factor for MDMA/MDA and five factors with two dummy factors for the cocaine procedure. The concentration of analytes used in these experiments equalled the  $CC\beta$  of analytes in glucose multiplied by 1.5. Consequently, the following concentrations were prepared for robustness tests: for cocaine hydrochloride 0.12% (w/w), cocaine base 0.19% (w/w), heroin base 1.2% (w/w), heroin hydrochloride 0.3% (w/w), MDMA hydrochloride 0.1% (w/w) and MDA hydrochloride 0.01% (w/w), respectively. Glucose was used for sample preparations as a diluent.

In dealing with the qualitative method, it was suggested to evaluate robustness via reliability%. The reliability or the proportion of right answers was found according to Eq. 3.2-1 [48].

$$\text{Reliability}(\%) = 100\% - \text{Fn}(\%) - \text{Fp}(\%) \quad (3.2-1)$$

'Erroneous' classification between MDMA or MDMA/MDA, cocaine base or salt was aligned as the correct answer. The obtained results are summarised in Table III.

The obtained results showed that heroin, cocaine or MDMA would be detected in the range of ± 50% from the nominal value. The method was found to be 100% reliable if the concentration of analyte of interest exceeded its threshold. If the concentration was suggested to be below the  $CC\beta$ , a lower reliability was found as expected (run nos 2 and 5). The determined critical variables at lower concentrations were the following: ratio of weight of the sample to volume of solvent. It was suggested that a nonprofessional operator allowed that variations would be ± 25% from the nominal value. Moreover, it is recommended to fulfil the following criteria: the ratio of the weight to solvent volume must be 2:1. Therefore, it was claimed that the SFS-MLP-ANN method was robust to the variations that could happen during the sample analysis.

**Table III.** Results of robustness tests for cocaine, MDMA/MDA, heroin procedures

Run no.	Factors							Reliability%					
	$A_{(1,2,3)}$	$B_{(1,2,3)}$	$C_{(1,2,3)}$	$D_{(1,2,3)}$	$E_{(1,2,3)}$	$F_{(2,3)}$	$G_{(3)}$	CoH	CoB	MDMA	MDA	HH	HB
1	+	+	+	-	+	-	-	100	100	100	100	100	100
2	-	+	+	+	-	+	-	20	100	100	100	20	100
3	-	-	+	+	+	-	+	100	100	100	100	100	100
4	+	-	-	+	+	+	-	100	100	100	100	100	100
5	-	+	-	-	+	+	+	20	100	100	100	20	100
6	+	-	+	-	-	+	+	100	100	100	100	100	100
7	+	+	-	+	-	-	+	100	100	100	100	100	100
8	-	-	-	-	-	-	-	100	100	100	100	100	100
Low level	10	5	0	2.5	20 (80 <sup>a</sup> )	20 (80 <sup>a</sup> )	10 <sup>a</sup>						
High level	30	15	2	7.5	80 (160 <sup>a</sup> )	80 (160 <sup>a</sup> )	20 <sup>a</sup>						

1—cocaine procedure (CoH—cocaine HCl; CoB—cocaine base); 2—MDMA/MDA procedure (MDMA; MDA); 3—heroin procedure (HH—heroin HCl; HB—heroin base);  $A_1, A_2, A_3$ —sample weight, mg;  $B_1, B_2, B_3$ —solvent volume, mL;  $C_1$ —reaction time, min;  $C_2$ —reaction time at step 2, min;  $C_3$ —reaction time at step 1, min;  $D_1$ —solution volume in optical cell, mL;  $D_2$ —solution volume in optical cell, mL;  $D_3$ —solution volume in optical cell, mL;  $E_1$ —volume of 6 N HCl,  $\mu$ L;  $E_2$ —volume of 0.03 M OPA-NAC,  $\mu$ L;  $E_3$ —volumes of 6 N HCl and 0.75 M NaOH,  $\mu$ L;  $F_2$ —volume of 0.75 M NaOH,  $\mu$ L;  $F_3$ —volumes of 0.75 M NaOH and 6 N HCl,  $\mu$ L;  $G_3$ —reaction time at step 2, min.

<sup>a</sup>Valid for heroin procedure only.

### 3.2.4. Detection of seized street samples

A total of 1253 street samples seized by North Carolina police in USA and Estonian police in Estonia were then analysed to evaluate the ability of the SFS-MLP-ANN method to detect and identify the analytes of interest in the real samples. There were 628 samples containing at least one analyte of interest, and 625 samples were true negative for all analytes of interest. Seven from 491 samples containing cocaine were assumed to be false negative. These samples showed the fluorescence signal under the threshold limit of the method, that is, under 300 a.u. at  $\lambda_{ex}/\lambda_{em}$  235/315 nm. One sample from 762 samples was found to be false positive for cocaine, and it contained ecgonine benzyl ester hydrochloride (scheduled substance as preventative of ecgonine ester). Three false positive samples were found from 1142 true negative samples for heroin that contained 6-MAM, 3-MAM or morphine base (Schedule II), giving false positives. Two samples from 111 heroin samples were assumed to be false negative because of insufficient increase in the fluorescence signal. Neither false positives (1227 true negative samples for MDMA) nor false negatives (true positives 26 samples) were observed for the MDMA/MDA procedure. The obtained results are summarised in Table IV.

The determination of the chemical composition of cocaine provided important information from a forensic science point of view, because the possession of cocaine varied according

to the drug form. [49] Various methods for the differentiation of cocaine forms have been considered (e.g. IR, the use of silver nitrate) [50]. In total, 449 cocaine samples were supplied by reference methods with additional information concerning the form of cocaine presented in the sample, that is, base or salt. They were used for the evaluation of the ability of cocaine methodology to differentiate forms of cocaine. Remarkable results were obtained; that is, 98.7% of samples were correctly identified by the SFS-MLP-ANN method. 'Erroneous' differentiation was primarily connected to excipients as benzocaine or procaine presented in these samples. If the mixture of cocaine salt and base was presented in the sample, cocaine base would be detected.

## 4. CONCLUSION

The results of the validation clearly demonstrated the suitability of the SFS technique combined with ANN for qualitative analysis of cocaine, heroin and MDMA/MDA in the street samples. The main advantage of this approach was that it did not require a specific chemical background from the operator and could be used onsite as a rapid, reliable and accurate method. The application of ANN as an expert system with a unique learning ability provides permanent improvement of method reliability with a reduction of false results to a minimum. The study surveyed a number of

**Table IV.** Statistics 2009–2011

Parameter/procedure	Cocaine	MDMA/MDA	Heroin	Min.	Max.	Median	MAD <sup>a</sup>
Specificity, %	99.9	100	99.7	99.7	100	99.9	0.6
Sensitivity, %	98.6	100	98.2	98.2	100	98.6	1.7
False negative rate, %	1.4	0.0	1.8	0.0	1.8	1.4	1.7
False positive rate, %	0.1	0.0	0.3	0.0	0.3	0.1	0.6

<sup>a</sup>MAD or median average deviation,  $p = 99.7\%$ .

different materials, and the detection of analytes of interest was possible in highly adulterated mixtures at concentrations down to 5% (w/w) of analyte.

## Acknowledgements

The authors acknowledge the EFSI for cooperation. This work has been partially supported by the Graduate School of Functional Materials and Processes receiving funding from the European Social Fund through project 1.2.0401.09-0079 in Estonia. The corresponding author is thankful to NarTest AS [51] and patent holders Dr S. Babichenko, Dr L. Poryvkina, Dr V. Sominsky, Mr E. Erme and Mrs T. Ivkina for providing the opportunity to run this study as part of a future dissertation.

## REFERENCES

- EMCDDA. *EMCDDA-EUROPOL annual report reviews new drugs entering market*. EMCDDA: Lisbon, Portugal, 2011.
- Kenji T. Development of an on-site screening system for amphetamine-type stimulant tablets with a portable attenuated total reflection Fourier transform infrared spectrometer. *Anal. Chim. Acta* 2008; **608**: 95–103.
- Eliasson C, Macleod NA, Matousek P. Non-invasive detection of cocaine dissolved in beverages using displaced Raman spectroscopy. *Anal. Chim. Acta* 2008; **607**: 50–53.
- Jennifer R, Verkouteren J, Staymates L. Reliability of ion mobility spectrometry for qualitative analysis of complex, multicomponent illicit drug samples. *Forensic Sci. Int.* 2011; **206**: 190–196.
- Zolotov YA, Ivanov VM, Amelin VG. Test methods for extra-laboratory analysis. *Trac-Trend Anal Chem.* 2002; **21**: 302–318.
- Detulleo AM, Galat PB, Gay ME. Detecting heroin in the presence of cocaine using ion mobility spectrometry. *IJMS* 2000 **3**: 38–42.
- Verkouteren JR, Staymates JL. Reliability of ion mobility spectrometry for qualitative analysis of complex multicomponent illicit drug samples. *J. Forensic Sci.* 2011; **206**: 190–196.
- Dussy FE, Berchtold C et al. Validation of an ion mobility spectrometry (IMS) method for detection of heroin and cocaine on incriminated material. *J. Forensic Sci.* 2008; **177**: 105–111.
- Weyermann C, Mimoune Y et al. Application of a transportable Raman spectrometer for the in situ detection of controlled substances at border controls. *J. Forensic Sci.* 2011; **209**: 21–28.
- Ryder AG, O'Connor GM, Glynn TJ. Identifications and quantitative measurements of narcotics in solid mixtures using near-IR Raman spectroscopy and multivariate analysis. *J. Forensic Sci.* 1999; **44**: 1013–1019.
- Grates KM, Ring JG, Savage KA. *Conclusion of Validation Study of Commercially Available Field Test Kits for Common Drugs of Abuse*. NFSTC: USA, 2008.
- Babichenko S, Erme E, Ivkina T, Poryvkina L, Sominsky V. A portable device and method for onsite detection and quantification of drugs. *Espacenet*, (WO2005111586), 2007.
- Babichenko S, Ivkina T, Poryvkina L, Sominsky V. Method for On-Site drug detection in illicit drug samples. *Espacenet*, (WO2008040386), 2008.
- Babichenko S, Ivkina T, Poryvkina L, Sominsky V. Method for on-site drug detection in illicit drug samples. *Espacenet*, (WO2010003447 (A1)), 2010.
- Gómez V, Callao, MP. Analytical applications of second-order calibration methods. *Anal. Chim. Acta* 2008; **627**: 169–183.
- Marini F. Artificial neural networks in foodstuff analyses: trends and perspectives. *Anal. Chim. Acta* 2009; **635**: 121–131.
- Poryvkina L, Babichenko S. Detection of illicit drugs with the technique of spectral fluorescence signatures (SFS). *Proc. SPIE* 2010; **7838**: 78380S.
- Poryvkina L, Aleksejev V, Babichenko S, Ivkina T. Spectral pattern recognition of controlled substances in street samples using artificial neural network system. *Proc. SPIE* 2011; **8055**: 80550R.
- European Commission. 2002/657/EC. Commission Decision of 12 August 2002 implementing Council Directive 96/23/EC concerning the performance of analytical methods and the interpretation of result. *OJC* 2002; **221**: 8–36.
- Taverniers I, De Loose M, Van Bockstaele E. Trends in quality in the analytical laboratory. II. Analytical method validation and quality assurance. *Trac-Trend Anal Chem* 2004; **23**: 535–552.
- Galarini R, Buratti R, Fioroni L, Contiero L, Lega F. Development, validation and data quality assurance of screening methods: a case study. *Anal. Chim. Acta* 2011; **700**: 2–10.
- UNODC. *Guidance for the validation of analytical methodology and calibration of equipment used for testing of illicit drugs in seized materials and biological specimens*. UN: New York, USA, 2009.
- Eurachem. *The Fitness for Purpose of Analytical Methods. A Laboratory Guide to Method Validation and Related Topics*. LGC: Teddington, UK, 1998.
- Molnar L. A neural network based classification scheme for cytotoxicity predictions: validation on 30,000 compounds. *Bioorg. Med. Chem. Lett.* 2006; **16**: 1037–1039.
- Rabelo Baccharini LM. SVM practical industrial application for mechanical faults diagnostic. *Expert Syst. Appl.* 2011; **38**: 6980–6984.
- Cozzoline D, Cynkar WU, Shah N, Damberg RG, Smith PA. A brief introduction to multivariate methods in grape and wine analysis. *Aust J Grape Wine R* 2009; **1**: 123–130.
- European Commission. Directive 2007/47/EC of the European Parliament and of the Council. *OJC* 2007; **247**: 21–55.
- Hernandez-Caballo EA, Marco-Parra LM. Direct analysis of blood serum by total reflection X-ray fluorescence spectrometry and application of an artificial neural networks approach for cancer diagnosis. *Spectrochim Acta B* 2003; **58**: 2205–2213.
- NarTest AS. *Procedures for illicit drug detection* (vol 1). NarTest: Tallinn, Estonia, 2012, 61–64.
- Herraez-Hernandez R, Falco PC. Derivatization of ephedrine with o-phthalaldehyde for liquid chromatography after treatment with sodium hypochlorite. *J. Chromatogr. A* 2000; **893**: 69–80.
- The Riigiteataja Website. Narkootiliste ja psühhotroopsete ainete ning nende lähteainete seadus. <https://www.riigiteataja.ee/akt/12947070?leiaKehtiv> [1 January 2012].
- Bro R. PARAFAC. Tutorial and applications. *Chemometr Intell Lab.* 1997; **38**: 149–171.
- EURACHEM/CITAC. *Guide: The Expression of Uncertainty in Qualitative Testing*. 2003, LGC: Teddington, UK, 2003, 48.
- Jayalakshmi T, Santhakumaran A. Statistical normalization and back propagation for classification. *IJCTE* 2011; **3**: 89–93.
- Pulido A, Ruisa'nchez I, Boque R, Rius FX. Uncertainty of results in routine qualitative analysis. *Trac-Trend Anal Chem* 2003; **22**: 647–654.
- Manda S, Sivaprasad PV, Venugopal S, Murthy KNP. Artificial neural network to evaluate and predict the deformation behaviour of stainless steel type AISI 304L during hot torsion. *ASCI* 2009; **9**: 237–244.
- Lavagnini I, Magno F. A statistical overview on univariate calibration, inverse regression, and detection limits: application to gas chromatography/mass spectrometry technique. *Mass Spectrom. Rev.* 2007; **26**: 1–18.
- Thomsen V, Schatzlein D, Mercurio D. Limits of detection in spectroscopy. *Spectroscopy* 2003; **18**: 112–114.
- Ermer J, Miller JH. *Method Validation in Pharmaceutical Analysis*. WILEY-VCH: Weinheim, Germany, 2005, 101–119.
- Hubaux A, Vos G. Decision and detection limits for linear calibration curves. *Anal. Chem.* 1970; **42**: 849–855.
- The European Commission Website. Document SANCO/2004/2726 rev 4 (2008). Guidelines for the implementation of decision 2002/657/EC. [http://ec.europa.eu/food/food/chemicalsafety/residues/cons\\_2004-2726rev4\\_en.pdf](http://ec.europa.eu/food/food/chemicalsafety/residues/cons_2004-2726rev4_en.pdf) [1 September 2011].
- Cole C, Jones L, McVeigh J, Kicman A, Syed Q, Bellis MA. *Guide to Adulterant, Bulking Agents and Other Contaminants Found in Illicit Drugs*. Centre of Public Health: Liverpool, Great Britain, 2010.
- EMCDDA. *General Report of Activities 2010*. EMCDDA: Luxembourg, 2011.
- Bernardo NP, Siqueira ME, De Paiva MJN, Maia PP. Caffeine and other adulterants in seizures of street cocaine in Brazil. *Int. J. Drug Policy* 2003; **14**: 331–334.
- Andersen MF. Adulterants and diluents in heroin, amphetamine and cocaine found on the illicit drug market in Aarhus, Denmark. *Open Forensic Sci J.* 2009; **2**: 16–20.

46. The EMCDDA Website. Statistical Bulletin 2011. <http://www.emcdda.europa.eu/stats11> [01 September 2011].
47. Dejaegher B, Heyden YV. Ruggedness and robustness testing. *J. Chromatogr. A* 2007; **1158**: 138–157.
48. Aguilera E, Lucena R, Cardenas S, Valcarcel M. Robustness in qualitative analysis: a practical approach. *Trac-Trends Anal Chem.* 2006; **25**: 621–627.
49. The EMCDDA Website. Threshold quantities for drug offences. <http://www.emcdda.europa.eu/html.cfm/index99321EN.html> [25 June 2010].
50. Logan BL, Nichols HS, Safford DT. A simple laboratory test for the determination of the chemical form of cocaine. *J. Forensic Sci.* 1989; **34**: 678–681.
51. The NarTest Website. <http://www.nartest.com/> [20 March 2012].

## PUBLICATION II

**Mazina, J.**, Vaher, M., Kuhtinskaja, M., Poryvkina, L., Kaljurand, M. Fluorescence, electrophoretic and chromatographic fingerprints of herbal medicines and their comparative chemometric analysis. *Talanta* **2015**, 139, 233 – 246<sup>2</sup>.

<sup>2</sup>Copyright © 2015 Elsevier B.V. All rights reserved.





# Fluorescence, electrophoretic and chromatographic fingerprints of herbal medicines and their comparative chemometric analysis



Jekaterina Mazina<sup>a,b,\*</sup>, Merike Vaher<sup>a</sup>, Maria Kuhtinskaja<sup>a</sup>, Larisa Poryvkina<sup>b</sup>, Mihkel Kaljurand<sup>a</sup>

<sup>a</sup> Department of Chemistry, Tallinn University of Technology, Akadeemia tee 15, 12816 Tallinn, Estonia

<sup>b</sup> NarTest AS, Koplianna 49, 11713 Tallinn, Estonia

## ARTICLE INFO

### Article history:

Received 16 December 2014

Received in revised form

17 February 2015

Accepted 24 February 2015

Available online 5 March 2015

### Keywords:

Herbal fingerprinting

Chemometric methods

Herbal medicine

Spectral fluorescence signature

Capillary electrophoresis-diode array detector

High-performance liquid chromatography-diode array detector-mass spectrometer

## ABSTRACT

The aim of the present study was to compare the polyphenolic compositions of 47 medicinal herbs (HM) and four herbal tea mixtures from Central Estonia by rapid, reliable and sensitive Spectral Fluorescence Signature (SFS) method in a front face mode. The SFS method was validated for the main identified HM representatives including detection limits ( $0.037 \text{ mg L}^{-1}$  for catechin,  $0.052 \text{ mg L}^{-1}$  for protocatechuic acid,  $0.136 \text{ mg L}^{-1}$  for chlorogenic acid,  $0.058 \text{ mg L}^{-1}$  for syringic acid and  $0.256 \text{ mg L}^{-1}$  for ferulic acid), linearity (up to  $5.0\text{--}15 \text{ mg L}^{-1}$ ), intra-day precision (RSDs = 6.6–10.6%), inter-day precision (RSDs = 6.4–13.8%), matrix effect (–15.8 to +5.5) and recovery (85–107%). The phytochemical fingerprints were differentiated by parallel factor analysis (PARAFAC) combined with hierarchical cluster analysis (CA) and principal component analysis (PCA). HM were clustered into four main clusters (catechin-like, hydroxycinnamic acid-like, dihydrobenzoic acid-like derivatives containing HM and HM with low/very low content of fluorescent constituents) and 14 subclusters (rich, medium, low/very low contents). The average accuracy and precision of CA for validation HM set were 97.4% (within 85.2–100%) and 89.6% (within 66.7–100%), respectively. PARAFAC-PCA/CA has improved the analysis of HM by the SFS method. The results were verified by two separation methods CE-DAD and HPLC-DAD-MS also combined with PARAFAC-PCA/CA. The SFS-PARAFAC-PCA/CA method has potential as a rapid and reliable tool for investigating the fingerprints and predicting the composition of HM or evaluating the quality and authenticity of different standardised formulas. Moreover, SFS-PARAFAC-PCA/CA can be implemented as a laboratory and/or an onsite method.

© 2015 Elsevier B.V. All rights reserved.

## 1. Introduction

The use of herbal medicines (HM) for health promotion purposes has been known for ages. Unlike synthetic drugs, HM are complex mixtures of substances that might be responsible for their therapeutic effects. Indeed, how many constituents and which of them, in complexes with other constituent(s), are responsible for the therapeutic mechanism has not been well defined for any HM. Therefore, it is important to define as many constituents in HM as possible to understand and explain their bioactivity.

Various techniques have been proposed for identification of the authenticity of HM. These include high performance liquid chromatography (HPLC) combined with mass spectrometry (MS) [1,2] or UV–vis spectrophotometric detection [3,4], gas chromatography (GC) [5,6], capillary electrophoresis (CE) [7–9], paper-based

colorimetric assays [10,11], and infrared [12] and fluorescence spectroscopy [13]. Nowadays, there is an increasing need to exploit methods that are quick, reliable and efficient and, moreover, can be easily automated for on-site analysis. Indeed, one of these methods is fluorescence spectroscopy. It has been shown to be a rapid and accurate method for identifying plant materials [14,15], oil in water [16], illegal drugs [17] and polyphenols in wines [18].

Recently, an innovative approach was proposed by Babichenko et al. [19], which is known as the spectral fluorescence signature method (SFS). SFS could be described as a 2D coloured pattern where colours represent the intensity of fluorescence or a 3D fluorescence matrix, where fluorescence is a function of excitation and emission wavelengths. SFS is a sum of all profiles of intrinsic fluorophores and, therefore, could also be suggested as unique fingerprints of the sample under investigation. SFS does not interfere with Rayleigh scattering due to a special measuring window, where the Rayleigh scattering is outside the measuring range. Therefore, the fluorescent fingerprints do not interfere with Rayleigh scattering that is a frequent issue for the conventional

\* Corresponding author at: Department of Chemistry, Tallinn University of Technology, Akadeemia tee 15, 12816 Tallinn, Estonia. Tel.: +372 620 4322.

E-mail address: [jekaterina.mazina@gmail.com](mailto:jekaterina.mazina@gmail.com) (J. Mazina).

excitation emission matrix (EEM) spectroscopy, where the signal of compounds can be totally hidden in the intensive scattering.

Actually, fluorescence spectroscopy may be divided into two types: classical angle and front-face fluorescence analysis. The first one has a crucial disadvantage over the last approach. The classical angle fluorescence requires the dilution of samples with an appropriate solvent. Indeed, it is necessary to measure those samples whose absorbance is not greater than 0.05 [20]. Unfortunately, the dilution affects the composition of herbal samples. As a result, the fluorescence signal of one constituent can start to predominate over others in the SFS image. In the worst case, other constituents can disappear in the SFS image. Therefore, the authentic SFS fingerprinting of HM can be totally lost.

As proposed by Genot et al. [21], this problem can be overcome using the front-face fluorescence spectroscopy, which enables the analysis of turbid untreated samples such as herbal medicines extracts. Therefore, utilisation of SFS method in the front-face mode for the analysis of undiluted HM extracts is of utmost importance. Unfortunately, there are more fluorescence-affecting factors such as quenching, concentration, and molecular environment. Therefore, the correct experimental conditions must be found for analysis of HM samples.

Undoubtedly, herbal medicines are very complex sample matrices, containing up to thousands of different compounds, e.g. polyphenols such as flavonoids, and non-flavonoid compounds. Although many compounds present in herbs have been thoroughly studied and quantified, there are still a lot of unknown chemical constituents in plants that need to be identified and investigated. The well-known compounds found in herbs can be grouped as simple polyphenols, catechins, anthocyanins, flavonoid glycosides and aglycones, theaflavins, chalcones and anthraquinone derivatives [16]. However, many chemical standards are unavailable or/and are too expensive to be applied to the identification of components present in HM. In this case, it is impossible or economically unreasonable to conduct the identification of every HM constituent. Therefore, the spectral data obtained by several detection methods such as UV–vis absorbance spectroscopy, the excitation emission matrix spectroscopy and the MS detection challenges the benefit making it possible to predict the substance group and/or identify the unknown substances in HM.

Despite the optimised experimental conditions, data analysis is of utmost importance for the final result. The application of chemometric techniques such as principal components analysis (PCA), hierarchical cluster analysis (CA) is very popular for interpretation of chromatographic and electrophoretic HM fingerprints. Several studies have shown good results to be obtained for differentiation of salad vegetables by different polyphenols [22], Oolong tea *Camellia sinensis* from different sources by different polyphenols and alkaloids [23], hops chemical screening by proanthocyanidins [24] and others studies [25–28]. In case of multi-way data such as diode array detector or SFS data, multi-way chemometric techniques must be used. One commonly used approach for EEM data analysis is Parallel Factor Analysis (PARAFAC) [29]. It has proven to be effective for analysis of complex food matrices [18].

The aim of the present study was to evaluate the capability of the SFS method in the front face mode combined with chemometric techniques such as PARAFAC, PCA and hierarchical cluster analysis for the authentication of HM available in the local Estonian market. The results were compared with two independent well-known reference methods, CE-DAD and HPLC-DAD-MS. The reference methods were also combined with PARAFAC-PCA/CA. The comparative study of HM discrimination by three independent methods was conducted. The performance characteristics of SFS method were evaluated and detection capabilities of three methods were compared. Additionally, some of the main chemical constituents in plant extracts were identified by MS/MS.

## 2. Experimental

### 2.1. Reagents and samples

The air dried samples of HM (moisture content 7–8%) were obtained from OÜ Kubja Ürt (Central Estonia, 73302 Karinu, Järvamaa, GPS: 59.0360289, 25.9611146) harvested in 2011 (three samples of each HM). HM grow in a natural environment. The mineral and chemical fertilizers are not used. The list of HM with their respective identification number is presented in Table 1.

Vanillic acid, protocatechuic acid, gallic acid, tannic acid, ferulic acid, caffeic acid, *p*-coumaric acid, chlorogenic acid, sinapic acid, syringic acid, *trans*-resveratrol, catechin, quercetin, myricetin, kaempferol, apigenin, luteolin, quercitrin, and rutin were purchased from Sigma-Aldrich (Germany). MS grade acetonitrile and formic acid (Sigma-Aldrich, Germany) were used for the HPLC-DAD-MS analysis. Deionised water was purified by the Milli-Q system (Millipore, Bedford, MA, USA). Sodium tetraborate decahydrate, sodium hydroxide and methanol were of analytical grade from Sigma-Aldrich (Germany).

### 2.2. Sample preparation

The herbal extracts of 51 samples were prepared using 80% (v/v) methanol. The plant material was ground into powder. The extracts were prepared by weighing 0.5 g of a plant sample, leaching with 10 mL methanol for 2 h at room temperature and extracting in an ultrasonic bath at a temperature of 35–40 °C for 0.5 h. The extract was centrifuged for 10 min at 5000 rpm and stored at –18 °C.

### 2.3. Fluorescence spectroscopy

All fluorescence measurements were carried out on a portable NarTest NTX2000<sup>®</sup> Drug Analyser (Nartest AS, Estonia), which generates special excitation emission matrixes (EEMs) or spectral fluorescence signatures (SFSS). This is a compact spectrofluorometer equipped with a 5 W pulsed Xenon lamp and a special 10 mL optical cell. SFSS were measured in a front-face optical layout (35°) from the surface at room temperature. The following experimental parameters were set:  $\lambda_{\text{ex}}=230\text{--}350$  nm and  $\lambda_{\text{em}}=250\text{--}565$  nm with 5 nm intervals in both directions, gain=500. One scanning took 2.3 min.

### 2.4. CE-DAD

All CE experiments were carried out using an Agilent 3D capillary electrophoresis instrument (Agilent Technologies, Waldbronn, Germany) equipped with a diode array detector (DAD) according to the method by Helmja et al. [30]. The separation of polyphenols was performed in a fused silica capillary (60 × 0.005 cm<sup>2</sup>, Polymicro Technology, Phoenix, AZ, USA) with an effective length of 51.5 cm. Prior to use, the capillary was rinsed with a 1.0 M NaOH solution, water and a background electrolyte (BGE) for 5 min of each. A 50 mM sodium tetraborate solution (pH 9.3) was used as a BGE. The applied voltage for the separation was +25 kV. The diode array detector range was set to 200–400 nm.

The sample solutions were introduced at the anodic end of the capillary with 50 mbar pressure for 5 s. The peaks of polyphenols (peaks in the electropherogram) were identified by the standard addition method and by comparing UV spectra.

### 2.5. HPLC-DAD-MS

Analysis of methanolic extracts was performed on HPLC equipment of the Agilent 1200 series with a diode array detector (DAD) (Agilent Technologies, Waldbronn, Germany). The samples (10 µL) were separated on an Agilent Zorbax SB C-18 column (150 mm × 4.6 mm i.d., 5 µm particle size). The mobile phase

**Table 1**  
HM and mixtures of HM under investigation.

Sample# (S#)	Name and part of HM	Latin name	Order	Family
1	Comfrey leaves	<i>Symphytum officinale</i>	(unplaced)	Boraginaceae
2	Celandine herb	<i>Chelidonium majus</i>	Ranunculales	Papaveraceae
3	St.-Johns wort	<i>Hypericum perforatum</i>	Malpighiales	Hypericaceae
4	Balm leaves	<i>Melissa officinalis</i>	Lamiales	Lamiaceae
5	Milfoil flower	<i>Achillea millefolium</i>	Asterales	Asteraceae
6	Veronica herb	<i>Veronica officinalis</i>	Lamiales	Plantaginaceae
7	Hawthorn flower	<i>Crataegus</i>	Rosales	Rosaceae
8	Field horsetail herb	<i>Equisetum arvense</i> L.	Equisetales	Equisetaceae
9	Motherwort herb	<i>Leonurus villosus</i>	Lamiales	Lamiaceae
10	Oregano herb	<i>Origanum vulgare</i>	Lamiales	Lamiaceae
11	Lime - tree flower	<i>Tilia cordata</i>	Malvales	Malvaceae
12	Stinging-nettle herb	<i>Urtica dioica</i>	Rosales	Urticaceae
13, 48 <sup>a</sup> , 49 <sup>b</sup>	Coltsfoot flower	<i>Tussilago farfara</i>	Asterales	Asteraceae
14	Coneflower flower	<i>Echinacea purpurea</i>	Asterales	Asteraceae
15	Birch leaves	<i>Betula</i>	Fagales	Betulaceae
16	Mistletoe herb	<i>Viscum</i>	Santalales	Santalaceae
17	Thyme herb	<i>Thymus vulgaris</i>	Lamiales	Lamiaceae
18	Cowberry leaves	<i>Vaccinium vitis-idaea</i>	Ericales	Ericaceae
19	Common lady's-mantle	<i>Alchemilla vulgaris</i> L.	Rosales	Rosaceae
20	Wormwood	<i>Artemisia absinthium</i>	Asterales	Asteraceae
21	Mallow	<i>Malva</i> L.	Malvales	Malvaceae
22 <sup>a</sup> , 22 <sup>b</sup>	Heather flowers	<i>Calluna vulgaris</i> L. Hull	Ericales	Ericaceae
23	Everlasting flowers	<i>Helichrysum</i>	Asterales	Asteraceae
24	Primula flowers	<i>Primula veris</i>	Ericales	Primulaceae
25	Peppermint leaves	<i>Mentha piperita</i>	Lamiales	Lamiaceae
26	Calendula flowers	<i>Calendula officinalis</i>	Asterales	Asteraceae
27	Salvia leaves	<i>Salvia</i>	Lamiales	Lamiaceae
28, 51 <sup>c</sup>	Camomile flower	<i>Chamomilla recutita</i>	Asterales	Asteraceae
29	Bearberry	<i>Arctostaphylos uva-ursi</i> L.	Ericales	Ericaceae
30	Iceland moss	<i>Cetraria islandica</i> (L.) Ach.	Lecanorales	Parmeliaceae
31	Fungus	<i>Piptoporus betulinus</i>	Polyporales	Fomitopsidaceae
32	Hop strobilus	<i>Humulus lupulus</i>	Rosales	Cannabaceae
33	Hip	<i>Rosa majalis</i>	Rosales	Rosaceae
34	Linseed	<i>Linum usitatissimum</i>	Malpighiales	Linaceae
35	Caraway seeds	<i>Carum carvi</i>	Apiales	Apiaceae
36	Fennel seeds	<i>Foeniculum vulgare</i>	Apiales	Apiaceae
37	Burdock root	<i>Arctium lappa</i>	Asterales	Asteraceae
38	Tormentil root	<i>Potentilla erecta</i> (L.)	Rosales	Rosaceae
39	Chicory root	<i>Cichorium intybus</i>	Asterales	Asteraceae
40	Elecampane root	<i>Imula helenium</i> L.	Asterales	Asteraceae
41	Calamus root	<i>Acorus calamus</i>	Acorales	Acoraceae
42	Dandelion root	<i>Taraxacum officinale</i>	Asterales	Asteraceae
43	Evening Primrose herb	<i>Onagraceae</i>	Myrtales	Onagraceae
47	Kelp	<i>Fucus vesiculosus</i>	Fucales	Fuaceae
#	<b>Name of HM's mixtures</b>	<b>HM</b>		
44	"Kurgutee"	<i>Plantaginis folium</i> , <i>Tussilago farfara</i> (S13, 48, 49), <i>Hyssopus officinalis</i> L., <i>Filipendula ulmaria</i> , <i>Monarda folium</i> , <i>Petasites</i>		
45	"Kõhatee aniisiga"	<i>Tussilago farfara</i> (S13, 48, 49), <i>Malva</i> L.(S21), <i>Illicium verum</i> , <i>Mentha piperita</i> (S25), <i>Rosa majalis</i> (S33)		
46	"Paastutee"	<i>Taraxaci</i> (S42), <i>Aroniae fr.</i> , <i>Carum carvi</i> (S35), <i>Ribes cynosbati</i> L., <i>Frangulae cortex</i> , <i>Rubi idaei cornus</i>		
50	"Külmetuse tee"	<i>Hyssopus officinalis</i> L., <i>Calluna vulgaris</i> L. Hull (S22), <i>Mentha piperita</i> (S25), <i>Tussilago farfara</i> (S13, 48, 49), <i>Achillea millefolium</i> (S5)		

<sup>a</sup> OÜ "Loodustooide" (Estonia).

<sup>b</sup> "Lekarset" (Russia).

<sup>c</sup> Wilken Tee GmbH (Germany).

consisted of two solvents: solvent A was a 0.1% solution of formic acid, and solvent B was 100% acetonitrile. Gradient elution was performed as follows: initially 100% of solvent A, followed by 0% to 30% B in 25 min, 95% B at 40 min and hold for 5 min, and then returned to 0% B at 50 min. The flow rate was 0.8 mL/min, and the column temperature was 25 °C. Spectral data from all peaks were accumulated in the range 240–400 nm and UV–vis chromatograms were recorded at 254 nm.

Compounds in plant extracts were identified by comparing DAD spectra and MS and MS/MS data. The mass detector (Agilent 6300 Series LC/MSD Trap; Agilent Technologies, Waldbronn, Germany) was equipped with an electrospray ionisation system and controlled by Agilent LC/MSD trap software (Agilent Technologies, Waldbronn, Germany). Nitrogen was used as nebulising gas at a pressure of 60 psi and the flow rate was adjusted to 12 L/min. The nebuliser temperature was 350 °C. The full scan mass spectra of compounds were measured from 100 to 1000 *m/z*. MS data were

obtained in the negative ionisation mode and MS/MS data in the automatic mode.

## 2.6. Methods performance characteristics

The performance characteristics of methods were investigated prior to the HM authentication study by chemometric techniques. The main method for HM analysis was SFS method under investigation. The SFS method was validated with respect to its range of application, including instrument detection limit (IDL), linearity range, matrix effect% (ME%) [31,32] and intra-day and inter-day precision (RSD%). The IDL was defined using 95% prediction interval of the regression line [33], taking into account that this approach was moderately sensitive to large regression ranges (upper concentration point maximally 10–20xIDL) and required a sufficient number of determinations (5 concentration levels and 8 replicates for each level). The ME% effect was evaluated along a

range of concentrations using the slope of calibration curves in the solvent and in the sample matrix S18 for ferulic acid and chlorogenic acid, and sample matrix S48 for syringic acid, catechin and protocatechuic acid). No matrix effect is observed, if the matrix effect remains in the range of  $\pm 20\%$ , medium matrix effect within  $\pm 20$ –50% and strong one higher than  $\pm 50\%$  [31]. ME% was calculated using the following equation:

$$ME\% = \left( \frac{\text{slope}_B}{\text{slope}_A} - 1 \right) * 100\%, \quad (1)$$

where  $\text{slope}_A$  is the slope of calibration curve of the analyte for the standard solution,  $\text{slope}_B$  is the slope of calibration curve of the analyte recorded for the sample spiked with the target compound after extraction.

The intra-day and inter-day precisions were evaluated as a relative standard deviation (%) at three different concentrations of analyte (six replicates for each level during the same day and three consecutive days,  $n=18$ ). The accuracy of the SFS method was demonstrated by recovery values for three concentration levels, i.e. at low, medium and high concentration levels of the linearity range (for each level six replicates). The recovery was found using the following equation:

$$\text{Rec}\% = \left( \frac{B - C}{A} \right) * 100\%, \quad (2)$$

where  $A$  is the amount of the analyte added to the spiked sample,  $B$  is the amount of the compound found in the spiked sample and  $C$  is the amount of the analyte in the non-spiked sample. The acceptance criteria for precision (RSD%) and accuracy (recovery) of SFS method should be within  $\pm 15\%$ , except for the lower concentration level which should not exceed  $\pm 20\%$ .

## 2.7. Chemometric techniques

### 2.7.1. Data preparation

Because of the great diversity of herbal samples included in this study, significant differences between the constituents of fingerprints were expected. Moreover, due to capillary or column aging, the shifting of peaks in time axes was considered possible. Therefore, the results of fingerprints analysis by chemometric techniques can be affected or even totally ruined.

Indeed, it was observed that the reproducibility of CE fingerprints was poor. This observation was based on the reproducibility of the electroosmotic flow (EOF) and internal standard (IS), i.e. gallic acid. Some samples, in whose case extreme time shifts were observed ( $t_{\text{EOF}}$  and/or  $t_{\text{IS}} > 1\%$ ), were excluded from the chemometric analysis. The electropherograms were aligned using IS and EOF in the software Chemstation (Agilent Technologies, Waldbronn, Germany).

As compared to the reproducibility of peaks in CE, that of HPLC was not as drastic. Therefore, HPLC chromatographic fingerprints did not need any alignment prior to chemometric analysis. Consequently, all fingerprints of the samples were exploited.

### 2.7.2. Parallel factor analysis

The data arranged into a 3-way array ( $I \times J \times K$ ) were modelled using PARAFAC [29] as follows:

$$x_{ijk} = \sum_{r=1}^R a_{ir} b_{jr} c_{kr} + e_{ijk} \quad (3)$$

where  $I$  is the number of samples,  $J$  is the number of emission wavelengths,  $K$  is the number of excitation wavelengths, and  $R$  is the number of components applied to the model. PARAFAC decomposes the SFS into a number of tri-linear components where the output results are presented in excitation, emission spectra

loadings (vectors  $b$  and  $c$ ) and scores (vector  $a$ ) that are directly related to the relative concentration of each component. Non-negativity constraints were applied to all three modes to ensure that each model had a physical interpretation.

### 2.7.3. Principal component analysis

Principal component analysis (PCA) is one of the most popular oldest methods used for data analysis [34,35]. PCA compresses the size of data by simplifying and extracting and keeping only important information. PCA creates linear combinations of the original variables called the principal components, which describes the systematic patterns of variation between the samples. The PCs are orthogonal and the number of PCs is less than or equal to the number of original variables. The first principal component has the largest possible variance. PCA is a decomposition of the original 2D-matrix  $X$ , i.e. representation it as the product of two 2D-matrices  $T$  and  $P$ :

$$X = TP^T + E \quad (4)$$

where  $T$  is a matrix of scores,  $P$  is a matrix of loadings and  $E$  is a matrix of residuals.

### 2.7.4. Cluster analysis

Cluster analysis (CA) is an unsupervised pattern recognition technique that can be used instead of PCA or in combination with PCA. Cluster analysis is divided into two approaches, namely non-hierarchical and hierarchical algorithms. Furthermore, a large variety of hierarchical algorithms exists, e.g. average linkage, complete linkage, single linkage and Ward's linkage. The hierarchical cluster analysis using Ward's linkage was chosen in this study as the algorithm showed the best results for SFS, CE-DAD and HPLC-DAD data. This method started with  $N$  clusters, each containing one object. This algorithm differs from others by utilising the variance approach to evaluate the distance between clusters, instead of using distance metrics or measures of association. Ward's linkage attempts to minimise the sum of squares (SSE) of any two hypothetical clusters that can be formed at each step. This was applied to the scores of PARAFAC models. The error sum of squares (SSE) was defined as follows:

$$SSE = \sum_{i=1}^K \sum_{j=1}^{n_i} (y_{ij} - \bar{y}_i)^2 \quad (5)$$

where  $y_{ij}$  is the  $j$ th object in the  $i$ th cluster and  $n_i$  is the number of objects in the  $i$ th cluster.

The validation of clustering was performed using independent validation set. The validation clustering results were compared to the training clustering results. The accuracy and precision were evaluated using the following equations:

$$\text{Accuracy}\% = \frac{\text{True\_positives} + \text{True\_negatives}}{\text{Total\_positives} + \text{Total\_negatives}} * 100\% \quad (6)$$

$$\text{Precision}\% = \frac{\text{True\_positives}}{\text{True\_positives} + \text{False\_positives}} * 100\% \quad (7)$$

### 2.7.5. Data analysis flowchart

First of all, the data for each method were separately stacked to form a 3-way array  $\underline{X}$ . As a result, three arrays were produced, i.e.  $\underline{X}_{\text{SFS}}$  for SFS,  $\underline{X}_{\text{CE-DAD}}$  for CE-DAD and  $\underline{X}_{\text{HPLC-DAD-MS}}$  for HPLC-DAD-MS.

**2.7.5.1. SFS data.** The non-negativity constraint was applied in all modes, conducting PARAFAC on  $\underline{X}_{\text{SFS}}$ . After the optimal number of PARAFAC components was found, the scores of PARAFAC components were fed to the CA and then to PCA. Before CA and PCA model construction, the PARAFAC scores were auto-scaled. CA helped to find

hidden similarities/dissimilarities between HM samples at a large extent. After CA analysis, better understanding of the PCA plots on PARAFAC scores was achieved.

**2.7.5.2. Separation methods data.** In the case of electrophoretic and chromatographic data, the original data dimension in time axes was reduced prior to chemometric analysis, taking into account every third and sixth point, respectively. The data from the separation methods were segmented and every segment was fed into PARAFAC with the non-negativity in the first and the third modes and unimodality in the second mode. The scores of PARAFAC models, which represent the relative concentration profiles of compounds, were combined into one new matrix,  $X_{\text{REDUCED-CE-DAD}}$ , and  $X_{\text{REDUCED-HPLC-DAD}}$ , respectively. The mean-centred matrixes  $X_{\text{REDUCED}}$  were further analysed by CA and PCA, as previously performed on SFS data.

### 2.7.6. Software

Data were processed with a PLS toolbox 6.2 (Eigenvector Research) in Matlab R2011b (Mathworks) and Chemstation (Agilent Technologies, Waldbronn, Germany).

## 3. Results and discussion

Different techniques for evaluating the identity of HM originating from Estonia were used, namely the spectral fluorescence signature (SFS) method and hyphenated techniques such as HPLC-DAD-MS and CE-DAD.

### 3.1. Spectral fluorescence signature method (EEM spectroscopy)

#### 3.1.1. Identity of polyphenolic compounds

HM contain a wide range of naturally occurring fluorescent compounds (coumarins, catechins, hydroxycinnamic acids), making it possible to use SFS for pattern recognition. The SFS of a HM is the sum of individual native fluorophores. In order to interpret

regions appearing in the SFS, some of the polyphenol standards prepared in methanol were measured (Table 2).

The SFS can be divided into five main regions: A – a catechin derivatives-like region (flavan-3-ol), B – a dihydroxybenzoic acid derivatives-like region (DHBA), C – a flavonol derivatives-like, trihydroxybenzoic acid derivatives-like and tannin derivatives-like region, D – a stilbenoid derivatives-like region, and E – a hydroxycinnamic acid-like derivatives region. Fig. 1 represents the approximate and representative boundaries of regions specific for the autofluorophores found in HM. Fluorescence of flavonols such as quercetin, myricetin, kaempferol and quercetin glucoside's representative rutin was not observed in the set measurement window. Indeed, only quercitrin was detected at  $\lambda_{\text{ex}} 230/\lambda_{\text{em}} 340$  nm. Nevertheless, Rodriguez-Delgado et al. [36] defined that quercetin, quercitrin, myricetin and kaempferol could be observed in the range of  $\lambda_{\text{ex}} 260\text{--}268/\lambda_{\text{em}} 370\text{--}426$  nm. Actually, flavonol representatives can be characterised by dual fluorescence [37], i.e. emission of a compound depends on the solvent and sample matrix.

#### 3.1.2. Method performance characteristics

The performance characteristics of SFS method were evaluated for identification of HM polyphenolic compounds. The representatives of different regions defined in the identity study such as catechin (region A), syringic acid (region C), protocatechuic acid (region B), ferulic acid (region E) and chlorogenic acid (region E) were used for validation study. Moreover, the instrument detection limits obtained by SFS method were compared to the well-known separation methods CE-DAD and HPLC-DAD utilised as the reference methods in this study. Additionally, the instrument detection limits of naringin and rutin by CE-DAD and HPLC-DAD were evaluated.

Overall, SFS method showed the excellent detection capability of catechin (50 times better than HPLC-DAD), protocatechuic acid (10 times better than HPLC-DAD) and ferulic acid (4 times better than HPLC-DAD). The detection capability of chlorogenic acid and syringic acid by SFS method were comparable to HPLC-DAD results. The detection capability of polyphenolic compounds by CE-DAD

**Table 2**

Excitation, emission and absorbance wavelengths of polyphenolic compounds under investigation conditions.

Region	Polyphenol's class	Compound	FWHM <sup>a</sup> $\lambda_{\text{ex}}/\lambda_{\text{em}}$ nm	Maximums $\lambda_{\text{ex}}/\lambda_{\text{em}}$ nm	Absorbance maximums, nm (pH 2.6)	Absorbance maximums, nm (pH 9.3)
A	Flavan-3-ol derivatives	Catechin and its derivatives	230–290/ 295–320	230,280/ 315	280 (catechin, epicatechin) 274–280 <sup>b</sup>	239sh, 284 (catechin) 284–286
B	Dihydroxybenzoic acid derivatives	Protocatechuic acid	230–320/ 330–385	235,310/ 355	260(max), 294	264, 296
C	Flavonol derivatives	Vanillic acid	230–300/ 305–355	250,295/ 350	260(max), 294	255, 290 (max)
		Quercitrin	230–240/ 330–370	230/ 340	256 (max), 352	268, 325sh, 380
D	Trihydroxybenzoic acid derivatives	Syringic acid	230–295/ 315–370	260/ 335	276	265sh, 300
		Gallic acid	230–265/ 325–395	240/ 350	272	218, 277
		Tannins	230–315/ 345–405	230,290/ 375	277	226, 304
E	Stilbenoid derivatives	<i>trans</i> -Resveratrol	230–340/ 360–450	230,310/ 395	306	225sh, 325
		Hydroxycinnamic acid derivatives	Caffeic acid	230–350/ 405–470	230,260,305,350/ 435	324 (max), 296
E	Hydroxycinnamic acid derivatives	Ferulic acid	230–350/ 380–455	250,305,350/ 430	324 (max), 296	344
		Sinapic acid	230–350/ 400–470	230,245,310,335/ 430	324	240, 330
		<i>p</i> -Coumaric acid	230–350/ 420–465	235,330/ 435	310	288(max), 330sh
		Chlorogenic acid	230–350/330–485	245,310/445	326 (max), 300sh	222, 255sh, 301sh, 345
		Quercetin	No native fluorescence	No native fluorescence	210, 254, 365	268, 322sh, 380
		–	Flavonol and its derivatives	Kaempferol	No native fluorescence	No native fluorescence
–	–	Rutin	No native fluorescence	No native fluorescence	256 (max), 356	268, 324sh, 380
–	–	Myricetin	No native fluorescence	No native fluorescence	264sh, 302sh, 355	244, 328
–	–	Quercetin	No native fluorescence	No native fluorescence	254,298sh,355	270, 320, 396

<sup>a</sup> Full width at half maximum.

<sup>b</sup> depends on structural analogue of the polyphenol's class.

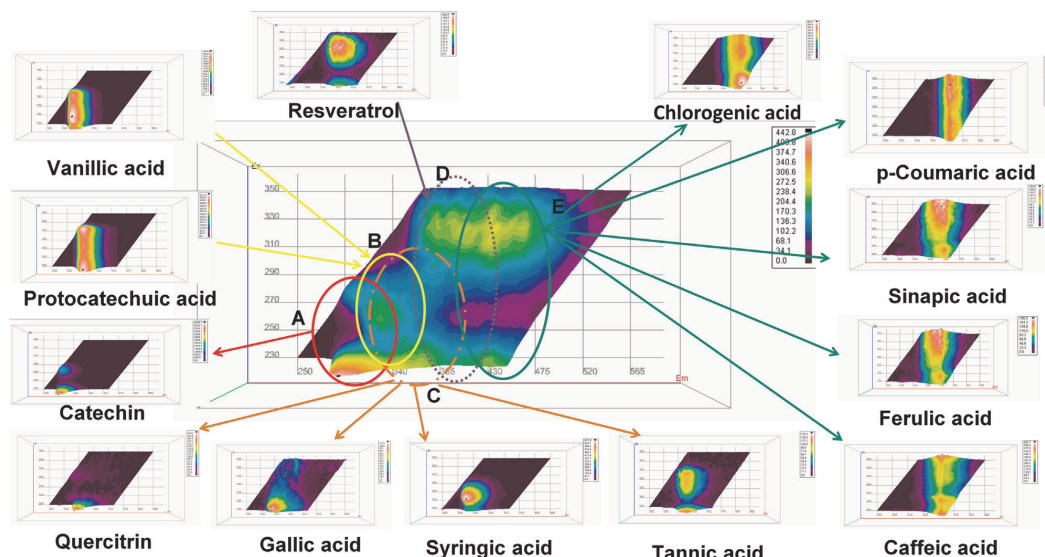


Fig. 1. The fluorescence fingerprint corresponding to one of the HM extracts in methanol (S51), indicating the fluorescent properties of typical fluorophores of HM.

was worse in 4 times (ferulic acid) up to 70 times (catechin). The comparative limits of detection of three methods are given in Table 3. Nevertheless, all three methods were capable of detecting polyphenolic compounds in the HM.

The linearity ranges of polyphenolic compounds were up to  $10 \text{ mg L}^{-1}$  for chlorogenic acid and protocatechuic acid, and up to  $5 \text{ mg L}^{-1}$  for catechin and ferulic acid. Two linear ranges were found for syringic acid from 0.1 to 1.0 and from 1.0 up to  $15 \text{ mg L}^{-1}$ . The intra-day precision were in the ranges of 6.6–10.6% (RSD%) and inter-day from 6.4–13.8% (RSD%). No matrix effect was considered as the values of ME% were in the range of  $\pm 20\%$  for all polyphenols under investigation. The results of this validation confirmed the suitability of the SFS method for reliable and accurate determination of polyphenolic substances in HM. The validation study results are summarised in Table 3.

### 3.1.3. HM exploratory analysis by chemometric techniques

In total, 153 SFSs were measured, i.e. 51 HM with 3 replicates for each sample. Each SFS was of the same size,  $25 \times 63$ , where 25 was the number of excitation wavelengths and 63 was the number of emission wavelengths, respectively. The SFSs of samples were stacked to form a 3-way array ( $X_{\text{SFS}}$ ) with dimensions of  $153 \times 63 \times 25$ . The non-negativity constraint was set on all modes. PARAFAC was applied for the exploratory analysis of HM fluorescence fingerprints. After a preliminary study, the data were divided into calibration ( $77 \times 63 \times 25$ ) and validation ( $76 \times 63 \times 25$ ) sets. Split-half analysis was applied to assess the correct number of components. The results of such analysis performed separately on the calibration and validation set also indicated that four components should be used as scores, and the loadings from the two resulting models were very alike (data not shown). The suggestion was also based on good core consistency diagnostics (CORCONDIA), i.e. 99%.

The results obtained showed that the SFS of *Acorus calamus* (S41) and *Foeniculum vulgare* (S36) greatly differed from those of other HM. S41 and S36 mainly contained one predominant peak in their electropherograms and chromatograms. The UV–vis absorbance spectra of predominant peaks and MS/MS data determined the presence of  $\beta$ -asarone in S41 and *trans*-anethole in S36,

respectively. Therefore, PARAFAC component 1 (PC1) was assigned to asarone-like compound ( $\lambda_{\text{ex}}/\lambda_{\text{em}}$  250, 305/360 nm) and, further used as a fluorescent chemomarker for *Acorus calamus*. *Foeniculum vulgare* (S36) was characterised by PC2 with maximums at  $\lambda_{\text{ex}}/\lambda_{\text{em}}$  255, 300/335 nm, and was assigned to anethole-like compounds. PC3 was attributed to catechin-like derivatives with maximums at  $\lambda_{\text{ex}}/\lambda_{\text{em}}$  230, 280/320 nm. Indeed, the standard of catechin was measured and the spectra of the latter were similar to PC3. Finally, PC4 ( $\lambda_{\text{ex}}/\lambda_{\text{em}}$  230, 320/435 nm) was assigned to one of the derivatives of hydroxycinnamic acids-like compounds such as caffeic acid, sinapic acid, *p*-coumaric acid, chlorogenic acid and/or ferulic acid. The PARAFAC excitation and emission loadings are shown in Fig. 2 (A and B). Since PC1 and PC2 described 90% of the dataset in the first model and assigned only for S41 and S36, respectively, it was suggested that further analysis of the data be made without these two HM. Moreover, the influence plot (not presented) also showed that *Acorus calamus* (S41) and *Foeniculum vulgare* (S36) should be removed from the dataset.

The second model was constructed using 147 samples (three replicates for each sample). The optimal number of components was again found to be four. Four components (Fig. 2C and D) described 98.3% of the data and CORCONDIA showed good results (89%). PC1 and PC2 were assigned to catechin-like derivatives, PC3 to hydroxycinnamic acid-like compounds (caffeic acid, sinapic acid, *p*-coumaric acid, chlorogenic acid and/or ferulic acid), and PC4 to dihydroxybenzoic acid-like derivatives (DHBA) such as protocatechuic acid-like and/or vanillic acid-like compounds.

Hierarchical cluster analysis (CA) was applied as an alternative approach to PCA. CA was conducted on the autoscaled scores of the second model of PARAFAC. The number of clusters depends on the tree cut. The tree was firstly cut around 20 (variance weighed distance between cluster centres) for main clusters and then around 5 for subclusters. As a result, CA separated HM into 4 main clusters and 14 subclusters presented as a dendrogram in Fig. 3C.

S18 and S38 were easily separated into two distinct clusters. S18 was characterised by  $\text{PC2}_{\text{PARAFAC}}$  linked to catechin-like compounds. S38 was described by both profiles of catechin-like compounds, i.e.  $\text{PC1}_{\text{PARAFAC}}$  and  $\text{PC2}_{\text{PARAFAC}}$ . Moreover, S3 was separated from S33 and S11. S3 was described by  $\text{PC1}_{\text{PARAFAC}}$  (catechin-like compounds),

**Table 3**  
Performance characteristics of SFS method for polyphenolic compounds analysis in HM.

Analyte	$\lambda_{\text{exc}}/\lambda_{\text{em}}$	Linearity, mg L <sup>-1</sup>	R <sup>2</sup>	Regression equation	Intra-day RSD% (n=6)	Inter-day RSD% (n=18)	ME% (n=18)	Concentration added: Recovery%	SFS IDL, mg L <sup>-1</sup>	Reference methods: IDL, mg L <sup>-1</sup>	
										CE-DAD <sup>b</sup>	HPLC-DAD <sup>c</sup>
Syringic acid	270/340	0.1–10; 1.0–15.0	0.9949; 0.9974	$y = 144.4x + 6.78$ ; $y = 402.1x + 271.1$	9.6	11.8	5.5	0.25 mg L <sup>-1</sup> ; 110.5 ± 14.7 0.5 mg L <sup>-1</sup> ; 108.1 ± 9.8 1.0 mg L <sup>-1</sup> ; 103.7 ± 3.9	0.058	1.82	0.065
Catechin	230/310	0.050–5.0	0.9991	$y = 1405.1x + 19.0$	6.6	13.8	-7.8	0.05 mg L <sup>-1</sup> ; 81.3 ± 5.1 1.0 mg L <sup>-1</sup> ; 84.5 ± 5.4	0.037	2.56	1.87
Chlorogenic acid	325/435	0.500–10.0	0.9942	$y = 17.9x + 5.98$	10.5	7.4	-8.9	5.0 mg L <sup>-1</sup> ; 88.5 ± 5.0 1.0 mg L <sup>-1</sup> ; 97.3 ± 8.4 5.0 mg L <sup>-1</sup> ; 91.7 ± 7.7	0.136	2.29	0.117
Protocatechuic acid	250/335	0.050–10.0	0.9987	$y = 226.6x + 4.76$	7.2	6.4	-14.6	10.0 mg L <sup>-1</sup> ; 94.0 ± 6.3 0.1 mg L <sup>-1</sup> ; 86.5 ± 6.0 0.5 mg L <sup>-1</sup> ; 92.3 ± 10.7	0.052	1.13	0.56
Ferulic acid	310/405	0.050–5.0	0.9936	$y = 15.7x + 5.36$	10.6	8.5	-15.8	1.0 mg L <sup>-1</sup> ; 87.8 ± 3.1 1.0 mg L <sup>-1</sup> ; 94.5 ± 7.5 2.5 mg L <sup>-1</sup> ; 87.6 ± 4.4 5.0 mg L <sup>-1</sup> ; 91.5 ± 3.7	0.256	1.09	1.04
Naringin	No native fluorescence									4.44	0.116
Rutin	No native fluorescence									4.56	0.122

<sup>a</sup> ME% is evaluated using the calibration curve slopes in solvent and in sample matrices (S48 and S18).

<sup>b</sup> IDL is evaluated at the detection wavelength 210 nm (chlorogenic acid at 345 nm).

<sup>c</sup> IDL is evaluated at the detection wavelength.

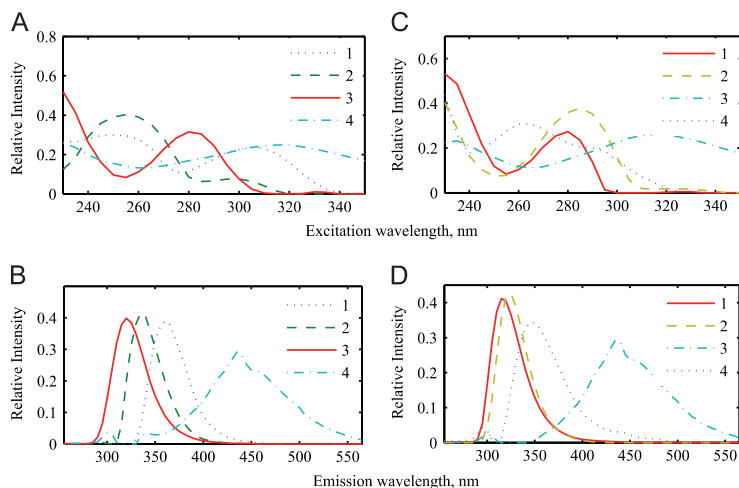


Fig. 2. A, C – PARAFAC excitation loadings; B, D – PARAFAC emission loadings; A, B – PARAFAC model with 153 samples; C, D – PARAFAC model with 147 samples.

but a lower content of  $PC4_{PARAFAC}$  (DHBA). In addition to S13, S48, S49, S5 and S6, other HM (S1, S10, S14, S20, S28, S37, S4, S44, S8 and S9) were characterised by hydroxycinnamic acid-like compounds. Moreover, there were higher contents of DHBA in S5, S10 and S20 in comparison to the others. S42 and S21 were separated from S16. The last HM (S16) was differentiated by the high impact of the  $PC4_{PARAFAC}$  profile (DHBA) compared to S42 and S21. Moreover, there was a significant impact of  $PC4_{PARAFAC}$  found in S2. Therefore, the latter was also clustered together with S42, S21 and S16. Applying CA, it was possible to detect the presence of similarities and dissimilarities between HM, grouping them according to their content of phenolic compounds. The identified clusters were further used for a better understanding of PCA results.

Next to CA analysis, PARAFAC scores were fed to PCA. CA helped to better understand PCA plots and the hidden similarities/dissimilarities between HM samples. It also helped to identify those compounds and/or group(s) of compounds which had the highest differentiation power within the entire dataset. Before PCA model construction, the PARAFAC scores were autoscaled. The  $PC1_{PCA}$ ,  $PC2_{PCA}$ ,  $PC3_{PCA}$  and  $PC4_{PCA}$  explained 38.99%, 28.59%, 20.31% and 12.02% of the total variance, respectively. The loading of  $PC1_{PCA}$  revealed that it was positively influenced by PARAFAC scores of  $PC1_{PARAFAC}$  and  $PC2_{PARAFAC}$  and negatively by  $PC3_{PARAFAC}$  and  $PC4_{PARAFAC}$ . Therefore,  $PC1_{PCA}$  showed good separation of catechin-like compounds. Higher scores indicated a higher content of the latter.  $PC2_{PCA}$  was positively influenced by all scores of PARAFAC PCs, but to a greater extent of the  $PC4_{PARAFAC} > PC3_{PARAFAC} > PC2_{PARAFAC} > PC1_{PARAFAC}$ . Therefore, a bi-plot of  $PC1_{PCA}$  versus  $PC2_{PCA}$  showed good differentiation power among HM containing higher contents of catechin-like compounds or higher contents of hydroxycinnamic acid-like and DHBA derivatives, but lower than the first ones. The loading of  $PC3_{PCA}$  differentiated HM according to the influence of DHBA versus catechin-like and hydroxycinnamic acid-like derivatives.  $PC4_{PCA}$  was described by positive  $PC1_{PARAFAC}$ , but negative  $PC2_{PARAFAC}$ , mainly separating two different profiles of catechin-like derivatives. The loadings of  $PC_{PCA}$  are shown in Fig. 3B.

PCA analysis of PARAFAC scores simplified the characterisation of HM by naturally fluorescent polyphenols present in the plants. S38 (*Potentilla erecta* (L.)) and S18 (*Vaccinium vitis-idaea*) were characterised by a rich content of catechin-like compounds. Additionally, S3 (*Hypericum perforatum*), S11 (*Tilia cordata*) and S33 (*Rosa majalis*) were defined by catechin-like compounds, but with a lower content

of the latter. S13, S48, S49 (*Tussilago farfara*), S5 (*Achillea millefolium*) and S6 (*Veronica officinalis*) were grouped by the high content of hydroxycinnamic acid-like compounds (caffeic, sinapic and ferulic acids and other hydroxycinnamic acids). A low content of hydroxycinnamic acid-like derivatives was observed in  $S19 > S15 > S34 > S33 > S38 > S30 > S35 > S47$  (lowest content). S16 (*Viscum*)  $>$  S2 (*Chelidonium majus*)  $>$  S21 (*Malva* L.)  $>$  S42 (*Taraxacum officinale*) were defined by the high content of DHBA-like derivatives described by  $PC4_{PARAFAC}$ . S47 (*Fucus vesiculosus*), S30 (*Cetraria islandica* (L.) Ach.) and S35 (*Carum carvi*) were characterised by a low content of fluorescent polyphenolic compound.

The clustering helped to analyse the bi-plots of PARAFAC-PCA and determine those groups that were not initially obvious. The most significant separation between classes was achieved by  $PC1_{PCA}$  versus  $PC2_{PCA}$  (Fig. 3A). The HM clustering results are presented in Table 4.

The performance of the PARAFAC-PCA/CA model was assessed by independent validation set, containing 27 HM under investigation (three extracts for each HM, two replicates for each). The validation set ( $X_{VAL\_SFS}$  with the size of  $162 \times 63 \times 25$ ) was explained by 96.13% by the second PARAFAC model. The PARAFAC scores of  $VAL\_SFS$  were used for PCA/CA analysis. The new clusters were used to identify the samples as belonging to one or more classes that were defined previously.

Validation set of HM was clustered into 13 clusters. Two clusters were compared to each other. The accuracy and precision for binary classification were evaluated. Two binary classes were suggested, i.e. clustered as previously or 'correct' clustering and clustered in the new/another cluster or 'erroneous' clustering. The average accuracy and precision of cluster analysis was 97.4% and 89.6%, respectively. The accuracy range was from 85.2% to 100% and the precision range from 66.7% to 100%, respectively. The 'erroneous' clustering has occurred for S43 and S46, which occurred in two different clusters. S46 was mainly characterized by DHBA derivatives, but S43 was mainly described by HCA. S5 and S20 were clustered into the main cluster 'DHBA derivatives rich HM' and mainly described by DHBA compounds in the mixture of high content of HCA. S35 was clustered into the class of low fluorescent compounds, containing predominantly low content of HCA derivatives, but not into the cluster of very low fluorescent compounds as previously. The clustering has shown that the 'erroneous' clustering has occurred with samples that could be described by several constituents, i.e. HM contained as high/moderate content of HCA as high/moderate DHBA. Nevertheless, the validation set showed

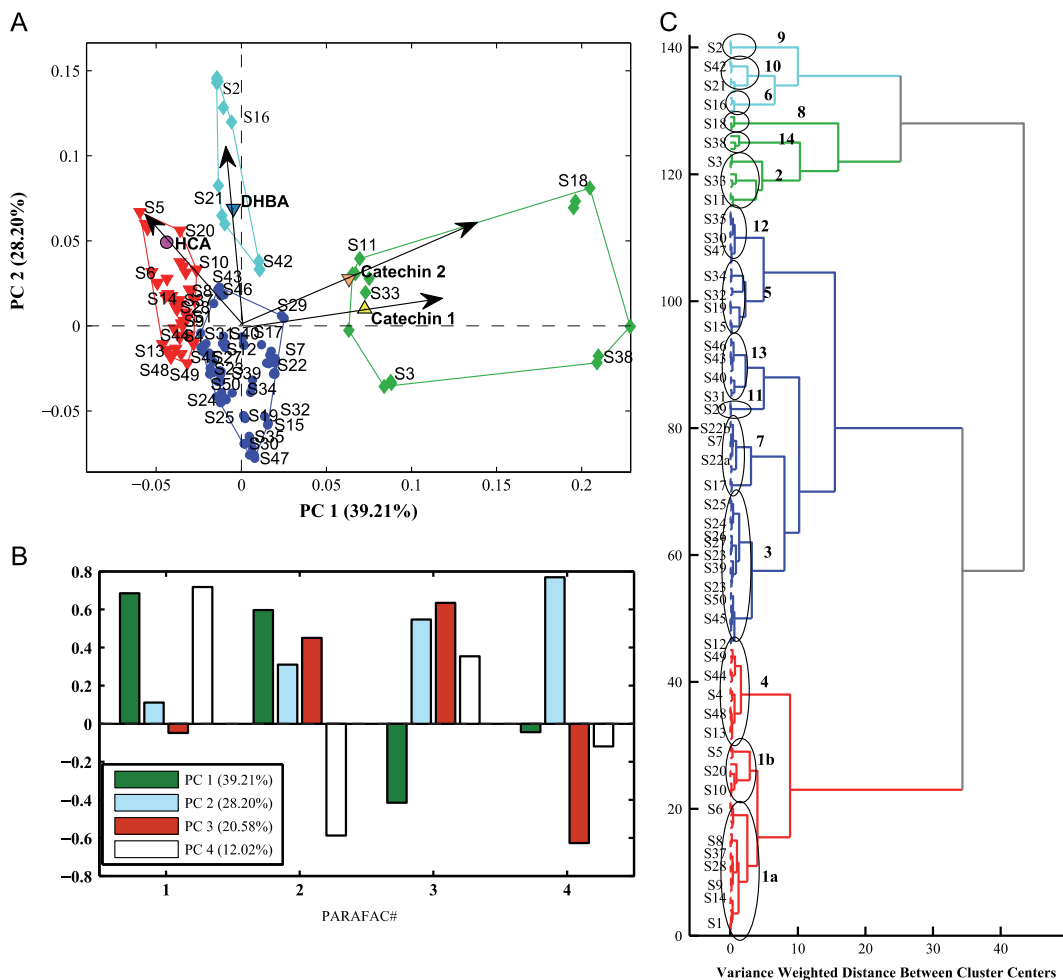


Fig. 3. Chemometric analysis results on SFS data: (A) biplot of PC1 vs PC2 of PCA on PARAFAC scores. (B) loadings of PCA model on PARAFAC scores; (C) dendrogram of CA on PARAFAC scores.

the main trend for evaluation of HM has remained and could be divided by their constituents content or catechin-like derivatives rich HM, DHBA derivatives rich HM, HCA derivatives rich HM and very low or low fluorescent compound content.

The analysis of HM by the SFS-PARAFAC-PCA method is quick, efficient and non-destructive. Indeed, it is an excellent method for the preliminary analysis of the authenticity of HM. It provides rough estimates to distinguish between HM using the different polyphenolic compounds present in plants. Unfortunately, front-face fluorescence spectroscopy is not a widely used technique for the evaluation of HM; however, the potential of this method to evaluate polyphenolic content can clearly be seen from the results. Other well-known techniques such as CE-DAD and HPLC-DAD-MS were used as reference methods for evaluation of polyphenol content of the HM under investigation.

3.1.4. Reference methods

Results of the SFS-PARAFAC-PCA method were further compared with two reference separation methods: CE-DAD and HPLC-DAD-MS/MS coupled with PARAFAC-PCA/CA. SFS method results

showed that not all of the analytes under investigation were natively fluorescing compounds. However, compounds such as quercetin, myricetin, kaempferol, apigenin, luteolin and rutin had no fluorescent properties under the studied conditions; they have absorbance spectra in the UV-vis range. Therefore, it was possible to investigate HM in the wider range of characteristics using the absorbance properties of polyphenolic compounds. However, the overlapping spectra and very similar profiles of the polyphenolic compounds must be taken into account and, indeed, are crucial for data interpretation. Therefore, the separation techniques combined with other detection methods could be of utmost importance for the current study. The different detection techniques helped to differentiate HM based on the combination of their spectral properties and migration/retention time profiles. Moreover, the MS/MS data were very important for compounds identification.

3.1.4.1. CE-DAD. The original data size  $105 \times 5926 \times 41$  was reduced to  $95 \times 1976 \times 41$ , where 95 is the number of wavelengths (between  $\lambda$  210 and 400 nm), 1976 is the migration time (min),

**Table 4**  
Comparative chemometric results of HM by SFS, CE-DAD and HPLC-DAD-MS and main chemomarkers of HM.

S#	SFS		CE-DAD		HPLC-DAD	
	Cluster #	Description	Cluster #	Description	Cluster #	Description
1	1a	High content of HCA and DHBA	n.a.	n.a.	H5	A large amount of HCA flavanols and derivatives. Predominants compound is rosmarinic acid and quercetin glycosides. (H5 – rosmarinic acid; H12 – kaempferol glucoside; H23 – quercetin glucoside)
2	9	High content of HCA, DHBA and catechin	n.a.	n.a.	H12	
3	2	Moderate content of HCA, DHBA, low catechin	n.a.	n.a.	H15	
4	4	High content of HCA, but low DHBA	n.a.	n.a.	H9	Rich by flavanol glycosides (H9 – quercetin galactoside; H15 – rutin; H23 – quercetin glucoside)
5	1b	High content of HCA and DHBA (higher content DHBA)	n.a.	n.a.	H15	
6	1a	High content of HCA and DHBA	n.a.	n.a.	H23	
7	7	High content of catechin and HCA, low DHBA	C20	Rich by flavone derivatives (C25 – vitexin derivative), flavanol derivatives (C20 – quercetin derivatives), and HCA derivatives (C28–chlorogenic acid).	H5	High level of predominant compound HCA ester (H5 – rosmarinic acid)
8	1a	High content of HCA and DHBA	C25		H20	High level of HCA derivatives (dicafeoylquinic acid isomer) (H20 – chlorogenic acid) and flavanones, apigenin derivatives
9	1a	High content of HCA and DHBA	C28		H17	Rich by iridoid derivatives (H17 – verminoside and H18 – verprosode)
10	1b	High content of HCA and DHBA (higher content DHBA)	C29	Rich by HCA derivatives (C29 – quercetin derivatives (C20)).	H18	
11	2	Moderate content of HCA, DHBA, low catechin	C6	Rich by HCA derivatives (C8 – caffeic acid derivatives) and quercetin derivatives (C6 – isorhamnetin derivative)	H7	Rich by HCA derivatives (caffeylquinic acid derivatives) (H20 – chlorogenic acid), flavanol derivatives (quercetin and its glycosides; H9 – quercetin galactoside; H23 – quercetin glucoside), and flavone glycosides (H7 – vitexin)
12	3	Low concentration of fluorescent compounds. Predominantly, HCA derivatives.	C8	Rich by HBA derivatives (C5) and HCA derivatives (rosmarinic acid (C7)).	H9	Rich by flavanol derivatives, quercetin glucoside is predominant compound (H23 – quercetin glucoside)
13, 48 <sup>a</sup> , 49 <sup>b</sup>	4	High content of HCA, but low DHBA	C20	Rich by HBA derivatives (C24 – protocatechuic acid) and quercetin derivatives (C20).	H23	High content of HCA derivatives, flavanols (H24 – n.i. HCA derivative)
14	1a	High content of HCA and DHBA	C24		H5	Rich by HCA derivatives and DHBA (H5 – rosmarinic acid)
15	5	Low content of HCA	C1	Low content of UV abs phenolic compounds. Predominant compounds are HCA derivatives (C8; C28 – chlorogenic acid). Small amount of catechin (C1) and quercetin derivatives (C20).	H3	Rich by flavanol derivatives (H23 – quercetin glucoside and kaempferol glycoside) and DHBA (H3 – protocatechuic acid)
16	6	Highest content of DHBA	C1		H15	Rich by HCA derivatives (H19 – caffeic acid derivative; H20 – chlorogenic acid) and flavanol (H15 – rutin)
17	7	High content of catechin and HCA, low DHBA	C8		H20	
18	8	High concentration of catechin derivatives	C26		H1	Predominantly HCA derivatives (H1 – dicafeoylquinic acid derivatives; H20 – chlorogenic acid). (H12 – kaempferol glucoside; H23 – quercetin glucoside)
19	5	Low content of HCA	C11	High content of HCA derivatives (C11) and HBA derivatives.	H20	High content of HCA derivative (H25 – caffeic acid)
20	1b	High content of HCA and DHBA (higher content DHBA)	C7	Rich by HCA derivatives (C7 – rosmarinic acid; C18 – salvanolic acid derivative), Contains flavone derivatives (C14 – luteolin derivatives).	H9	High content of flavanol derivatives (H9 – quercetin glycosides) and HCA derivatives (dicafeoylquinic acid derivatives; H20 – chlorogenic acid)
21	10	High content of DHBA	C1	High level of flavanol derivatives (C13 – quercetin derivatives), catechin derivatives (C1) and HBA derivatives (C15).	H20	Rich by HCA derivatives (caffeylquinic acid derivatives) (H20 – chlorogenic acid). Rich by HCA derivatives, predominantly by rosmarinic acid (H5). Contains flavone derivatives (H6–luteolin – glucuronide and glucoside)
			C15		H9	High level of flavanol derivatives (H9 – quercetin galactoside) and catechin derivatives
			C20	High level of flavanol derivatives (C20 – quercetin derivatives).	H22	
			C28	High content of HCA derivatives (C28 – chlorogenic acid, C31)	H25	High level of flavanol derivatives (quercetin derivatives) and DHBA derivatives (H25)
			C31	High content of HCA derivatives (C28 – chlorogenic acid, C31)	H20	High content of HCA derivatives (dicafeoylquinic acid derivatives; H20 – chlorogenic acid)

22 <sup>a</sup> , 22 <sup>b</sup>	7	High content of catechin and HCA, low DHBA	C21	Low level of UV abs compounds. Characteristic compounds are flavanol derivatives.	H9	Characteristic compounds are flavanol and flavone glycoside (Low level)
23	3	Low concentration of fluorescent compounds. Predominantly, HCA derivatives.	C28 C4 C17	High level of HCA derivatives (C28 – chlorogenic acid), flavanol and flavanone derivatives (C21) High level of flavanol glycosides (C4) and flavanone derivatives (C17 – naringenin derivatives).	H20 H12 H9	High level of HCA derivatives (H20 – chlorogenic acid), flavanol glycosides (H9 – quercetin galactoside), and flavones High level of flavanol glycosides (H9 – quercetin derivative, H12 – kaempferol) and flavones
24	3	Low concentration of fluorescent compounds. Predominantly, HCA derivatives.	n.a.		H19	Moderate content of HCA derivative (H19 – caffeic acid derivative)
25	3	Low concentration of fluorescent compounds. Predominantly, HCA derivatives.	C7 C14	Rich by HCA derivatives (C7 – rosmarinic acid). Contains flavone derivatives (C14 – luteolin derivatives).	H5 H6	High level of flavone derivatives (H6 – luteolin derivatives). Eriocitrin and HCA derivative rosmarinic acid (H5)
26	3	Low concentration of fluorescent compounds. Predominantly, HCA derivatives.	n.a.		H8	High level of isorhamnetin derivatives (H8 – methylated flavonols)
27	3	Low concentration of fluorescent compounds. Predominantly, HCA derivatives.	C7 C18	Rich by HCA derivatives (C7 – rosmarinic acid; C18 – salvianolic acid derivative).	H5	Predominant compound is rosmarinic acid (H5), HCA ester
28, 51 <sup>c</sup>	1a	High content of HCA and DHBA	C19	High level of n.i. compound (C19) and HCA derivatives.	H20	Rich content of polyphenolic compounds. High level of HCA derivatives (ferulic acid derivatives, H20 – chlorogenic acid and other dicaffeoylquinic acids)
29	11	High content of DHBA and catechin	C1	Rich by tannins derivatives (C1).	H2	High level of catechin derivatives (H2 – flavan-3-ols)
30	12	Very low content of all compounds	n.a.		-	Low level of UV abs polyphenolic compounds
31	13	Low/moderate content of HCA and DHBA	-	Low level of UV abs polyphenolic compounds.	-	Low level of UV abs polyphenolic compounds
32	5	Low content of HCA	-	Low level of UV abs polyphenolic compounds. Predominant flavanol glycosides (quercetin glycosides)	H12 H23	Predominant flavanol glycosides (H23 – quercetin glucoside and H12 – kaempferol glycosides)
33	2	Moderate content of HCA, DHBA, low catechin	-	Low level of UV abs polyphenolic compounds.	-	Low content of UV abs phenolic compounds
34	5	Low content of HCA	-	Low concentration of UV abs polyphenolic compounds. Predominant compound is carvone (C22).	H10	Low content of UV abs phenolic compounds
35	12	Very low content of all fluorescent compounds	C22		-	Predominant compound is carvone (H10).
36	Separated	Anethole derivatives	C23	Low concentration of UV abs polyphenolic compounds. Predominant compound is carvone (C22).	H16	Predominant compound is anethole (H16)
37	1a	High content of HCA and DHBA	C10 C28	High content of HCA derivatives (C10 – dicaffeoylquinic acid derivatives, C28 – chlorogenic acid).	H20	High content of HCA derivatives (dicaffeoylquinic acid: H20 – chlorogenic acid)
38	14	Very high content of catechin-like and low HCA and DHBA	C2 C9	High level of flavan-3-ol derivatives (C2 – catechin derivatives) or tannins constituents and ellagic acid derivatives (C9).	H21	High level of flavan-3-ol derivatives, proanthocyanidin, tannins constitute (H21 – ellagic acid derivatives)
39	3	Low concentration of fluorescent compounds. Predominantly, HCA derivatives.	-	Low level of UV abs polyphenolic compounds.	H20	Predominantly HCA derivatives (Dicaffeoylquinic acid isomers: H20 – chlorogenic acid)
40	13	Low/moderate content of HCA and DHBA	-	Low level of UV abs polyphenolic compounds.	H20	Moderate/Low content of HCA derivatives (dicaffeoylquinic acid isomers: H20 – chlorogenic acid)
41	Separated	Asarone derivatives	-		H4	Predominant compound is asarone (H4)
42	10	High content of DHBA	-	Low content of UV abs phenolic compounds. Predominantly, HCA derivatives (chlorogenic acid) and flavan-3-ols (catechin derivative)	H20	Low content of UV abs phenolic compounds. Predominantly, HCA derivatives (H20 – chlorogenic acid) and flavan-3-ols (catechin)
43	13	Low/moderate content of HCA and DHBA	C30	Moderate content of flavanol derivatives (C30 – quercetin derivatives).	H9	Moderate content of flavanol derivatives (H9 – quercetin glycosides) and HCA derivatives (H20 – chlorogenic acid)
47	12	Very low content of all fluorescent compounds	-	Very low content of UV abs phenolic compounds.	H20	Low content of UV abs phenolic compounds
44	4	High content of HCA, but low DHBA	C12 C16 C28	High content of HCA derivatives (C12, C16 – dicaffeoylquinic acid derivatives; C28 – chlorogenic acid)	H1 H5 H20	High content of HCA derivatives (H1, H5 – dicaffeoylquinic acid isomers and H20 – chlorogenic acid; H5 – rosmarinic acid).
45	3	Low concentration of fluorescent compounds. Predominantly, HCA derivatives.	C12 C27 C28	High content of HCA derivatives (C27, C12 – dicaffeoylquinic acid; C28 – chlorogenic acid), flavanols derivatives (C20 – quercetin derivative).	H5 H20	High content of HCA derivatives (dicaffeoylquinic acid; H5 – rosmarinic acid), flavanones (H6 – luteolin derivative) and flavonols (H12 – kaempferol glycoside) derivatives
46	13	Low/moderate content of HCA and DHBA	-	Low content of UV abs phenolic compounds.	H5 H20	High content of HCA derivatives (H5 – rosmarinic acid; H20 – chlorogenic acid)

Table 4 (continued)

S#	SFS		CE-DAD		HPLC-DAD	
	Cluster #	Description	Cluster #	Description	Cluster #	Description
50	3	Low concentration of fluorescent compounds. Predominantly, HCA derivatives.	C9 C25 C28	High content of HCA derivatives (C25 – dicaffeoylquinic acid; C9 – ellagic acid derivatives), flavone derivatives (C25)	H1 H5 H6 H21	High content of HCA derivatives (H1 – dicaffeoylquinic acid isomer; H5-rosmarinic acid), flavanones (H6 – luteolin derivative) and tannins constitute (H21 – ellagic acid derivatives) derivatives

n.a.–not analysed; HCA – hydroxycinnamic acid; DHBA – dihydroxybenzoic acid; HBA – hydroxybenzoic acid; UV abs – UV absorbance.

and 41 is the number of samples. Then, the  $X_{CE\_DAD}$  array was divided into 35 segments from 4.0 to 25.0 min.  $X_{CE\_DAD}$  was finally fed into parallel factor analysis (PARAFAC). PARAFAC models were conducted on each segment with the non-negativity in the first and the third modes and unimodality in the second mode. Each model contained a maximum of 5 PARAFAC components. The scores of PARAFAC models, which represent the relative concentration profiles of compounds, were combined into one new matrix  $X_{REDUCED\_CE\_DAD}$  ( $41 \times 84$ ). Moreover, the loadings of electrophoretic migration and absorption profiles were also obtained from PARAFAC models. The absorbance spectra could not be compared directly to the absorbance spectra obtained by HPLC-DAD, because of the bathochromic shifts of spectra for polyphenolic compounds in the alkaline conditions (pH 9.3). The mean-centred matrix  $X_{REDUCED\_CE\_DAD}$  was further analysed by PCA and Hierarchical Cluster Analysis, as it was previously performed on SFS data.

Only 31 compounds from 84 found by PARAFAC were defined as reasonable chemical profiles for HM investigation by PCA/CA. These chemical profiles were assigned as HM chemomarkers. PARAFAC-PCA analysis of CE fingerprints was also able to distinguish between S18 and S38. The results correlate with those of SFS-PARAFAC-PCA analysis, i.e. S18 was attributed to a catechin-like derivative as its chemomarker. CE-DAD has defined S38 by ellagic acid derivatives. S7 was described by vitexin derivatives (flavone glucosides). S9 was characterised by the rich content of HCA and quercetin derivatives. S13, S48 and S49 predominantly contained HCA derivatives, i.e. different dicaffeoylquinic acid derivatives at very high levels. The chemical profiles for HM obtained by PCA are presented in Table 4. Fig. A.1 shows the biplot of PC1 versus PC3 versus PC5 of PCA on PARAFAC scores and the cascade dendrograms of CA for HM identification. Unfortunately, the determination of structural analogues of chemomarkers was complicated because of the similarity between UV-vis spectra and the absence of polyphenolic standards. The absorbance characteristics of identified compounds in HM are shown in and Fig. A.2. Moreover, the electrophoretic fingerprinting data requires a special time-consuming alignment procedure, making the data interpretation more difficult. Therefore, further analysis using HPLC-DAD-MS was extremely valuable.

**3.1.4.2. HPLC-DAD-MS.** In contrast to CE fingerprints, in which migration time shifts were significant, HPLC elution shifting was not as drastic. Therefore, all HPLC fingerprints of 47 HM and fingerprints of four additional mixtures were analysed by PARAFAC. The original data size  $81 \times 7515 \times 51$  was reduced to  $81 \times 1200 \times 51$ , where 81 is the number of wavelength points, 1200 is the number of time points and 51 is the number of samples. Then  $X_{HPLC\_DAD}$  array was divided into 39 segments from 3.9 to 38.3 min. PARAFAC models were conducted on each segment with the non-negativity in the first and the third modes and unimodality in the second mode. Each model contained a maximum of 6 PARAFAC components. Moreover, two of the components were specific to solvent background and were therefore excluded from each model. The scores of PARAFAC models, which represent the relative concentration profiles of compounds, were combined into one new matrix:  $X_{REDUCED\_HPLC}$  ( $51 \times 83$ ). Moreover, the loadings of chromatographic profile and absorption profiles were also obtained from PARAFAC models. The absorbance spectra were used for the characterisation of polyphenolic compounds by possible polyphenolic groups (dihydroxybenzoic acid or hydroxycinnamic acid derivatives, flavanols, flavones, flavan-3-ols and others). Furthermore, the MS/MS data helped to identify compounds. The mean-centred matrix  $X_{REDUCED}$  was further analysed by PCA and Hierarchical Cluster Analysis, as previously performed on SFS data.

The PARAFAC-PCA analysis differentiated HM into groups and the absorbance chemomarkers for each group of HM and/or representative of HM were defined. *Tussilago farfara* (S13, S48, S49) was successfully characterised by the rich content of dicaffeoylquinic acid isomers, including chlorogenic acid. The same result was found by analysis of CE-DAD data. Moreover, the HM mixture S44 containing *Tussilago farfara* was also grouped to S13, S48 and S49 by the same chemomarkers; S29 was described by different flavan-3-ol derivatives. The SFS method showed also that S29 was rich with catechin-like compounds, i.e. flavan-3-ol structural analogues. The absorbance spectra of all flavan-3-ols were around 280 nm with shifts by 4–6 nm to the shorter wavelength for analogues esterified by gallate. *Tilia cordata* (S11) and *Alchemilla vulgaris* L. (S19) were grouped by phenolic compounds eluted at 10 min with absorbance spectral bands at 260 and 294 nm specific to protocatechuic acid. The MS/MS analysis proved this suggestion,  $[M-H]^- 153 \rightarrow 109$ . S41 and S36 were characterised by the predominant absorbance of the compounds asarone ( $\lambda_{\text{abs}}=254, 303$  nm) and anethole ( $\lambda_{\text{abs}}=259, 294$  nm), respectively, comparable to SFS method results. Another HM S35, which was previously grouped as HM containing a low content of fluorescent compounds, was described by carvone ( $\lambda_{\text{abs}}=240$  nm). S1, S4, S10, S17, S25 and S27 were grouped by rosmarinic acid ( $t_r=23.8$  min) ( $\lambda_{\text{abs}}=300\text{sh}, 328(\text{max})$ ). Moreover, the highest PARAFAC scores (that equal to absorbance, a.u.) of rosmarinic acid, and, therefore, comparable to the content, was found in *Origanum vulgare* (S10) > *Melissa officinalis* (S4) > *Salvia* (S27) > *Thymus vulgaris* (S17) > *Symphytum officinale* (S1) > *Mentha piperita* (S25). All of these HM (except S1) belong to the *Lamiaceae* family and notably contain rosmarinic acid. S1 belongs to the *Boraginaceae* family; it is also known that this family contains rosmarinic acid. In addition, rosmarinic acid was found in the mixtures of HM S44, S45, S46 and S50. All of these HM mixtures contain at least one HM belonging to the *Lamiaceae* family. S25 (*Mentha piperita*) was identified in the herbal tea mixtures, namely S45 and S50, by luteolin rhamnoglucoside.

S15 (*Betula*) was characterised by numerous quercetin derivatives. The predominant quercetin derivative eluted at 20 min was identified as quercetin-3-O-galactoside (hyperoside) ( $[M-H]^- 463 \rightarrow 301,179$ ). S23 (*Helichrysum*) was characterised by isosalipurposide ( $433 \rightarrow 313,271,151$ ), different naringenin and apigenin derivatives. S6 (*Veronica officinalis*) is rich in iridoid derivatives (verminoside, verprosoid), while S3 (*Hypericum perforatum*) contained the highest content of rutin and hyperoside, and was therefore distinguished by these flavanols from other HM under investigation. S12 (*Urtica dioica*) was characterised by caffeic acid derivatives ( $\lambda_{\text{abs}}=298\text{sh}, 329$  nm) eluted at 17.3 min. The presence of chlorogenic acid was defined in the majority of HM under investigation: S5, S7, S12, S13&S48&S49, S15, S20, S22, S23, S28&S51, S36, S37, S39, S40, S42, S43, S44, S45, S46 and S50. S18 was characterised by the high level of flavanol derivatives (quercetin derivatives) and catechin derivatives. S38 contained a high level of flavan-3-ol derivatives, proanthocyanidin, and tannins (ellagic acid derivatives). The results were comparable to the SFS results; S38 and S18 were also described by the high content of catechin-like derivatives.

The HPLC-DAD-MS method, as for SFS and CE-DAD combined with chemometric techniques, was also able to distinguish between S38 and S18. Moreover, the exact chemomarker was identified; namely S38 was characterised by an ellagic acid derivative and S18 by quercetin rhamnoside, respectively. HPLC-DAD-MS (/MS) data has also shown that S38 contains catechin and also epicatechin. Catechin derivatives were also determined by the SFS method. S18 contains different derivatives of quercetin. S10, S17, S27, S25 are characterised by rosmarinic acid. S36 and S41 were distinguished by all methods as these HM contain anethole and asarone, respectively. The unique fingerprint was successfully identified for S35 both by CE-DAD and HPLC-DAD-MS. S35 was also suggested by the SFS method as one of the HM with a low

content of polyphenolic compounds. This suggestion was proven by separation methods. It was confirmed by both CE-DAD and HPLC-DAD-MS. S29 was characterised by tannins using both separation techniques. CE-DAD determined S19 by the quercetin derivative. HPLC-DAD-MS (/MS) identified a chemomarker of S19, i.e. quercetin glucuronide. This compound was also determined in S15 and S43 by HPLC-DAD-MS (/MS). The summary of chemical profiles for HM obtained by PCA is presented in Table 4. The MS/MS and absorbance characteristics of identified compounds in HM are shown in Table A.1 and Fig. A.3. Fig. A.4 shows the biplot of PC1 versus PC3 versus PC5 of PCA on PARAFAC scores and the dendrogram of CA for HM identification.

It should be pointed out that unlike CE-DAD and SFS, HPLC-DAD-MS was able to identify the chemical profiles of HM in mixtures S44, S45, S46 and S50. This can be explained by the high selectivity of HPLC and the good reproducibility of retention time of peaks. The electrophoretic conditions set for CE-DAD do not work for all samples. Therefore, it is better to optimise conditions according to the sample under analysis, but comparable fingerprints might be lost in this case.

#### 4. Conclusion

In this paper, spectral fluorescence signature (SFS) method in front face mode combined with the chemometric techniques PARAFAC, CA and PCA were applied to authentication HM (Central Estonia) found in an Estonian market. The results showed that SFS-PARAFAC-PCA/CA is rapid, sensitive and reliable tool for the investigation of fingerprints and prediction of the composition of HM. SFS-PARAFAC-PCA/CA enables only classes of chemical constituents to be suggested, not identified with certainty and, hence, quantified, but can be easily used for the rapid evaluation of polyphenolic compounds content in the HM. Moreover, the polyphenolic rich or poor HM can be reliably defined. The biggest advantage of the SFS method in front face mode is the ability to analyse undiluted HM extracts. Therefore, the unique fingerprint of HM can directly be obtained from the surface of sample extracts, i.e. unique chemical composition of constituents is not lost during dilution. The results obtained by the SFS-PARAFAC-PCA/CA method are in good agreement with the results obtained by the CE-DAD and HPLC-DAD-MS methods.

#### Acknowledgements

The authors acknowledge the financial support from the Estonian Science Fund (Grant ETF9106), the Estonian Research Council (Institutional Research Fund No. 33-20 "Advancing analytical and computational chemistry methods for regulatory decisions") for financial support of this research. This work has been partially supported by the Graduate School of Functional Materials and Processes receiving funding from the European Social Fund through project 1.2.0401.09-0079 in Estonia and also supported by European Social Fund's Doctoral Studies and Internationalisation Programme DoRa, which is carried out by Foundation Archimedes. We are also grateful to OÜ Kubja Ürt, Estonia, for providing samples and to AS Laser Diagnostics Instruments, Tallinn, Estonia to NarTest AS, Tallinn, Estonia.

#### Appendix A. Supplementary material

Supplementary data associated with this article can be found in the online version at <http://dx.doi.org/10.1016/j.talanta.2015.02.050>.

## References

- [1] A. Wojdylo, J. Oszmianski, R. Czemerzys, *Food Chem.* 105 (2007) 940–949.
- [2] M. Yang, J. Sun, Z. Lu, G. Chen, S. Guan, X. Liu, B. Jiang, M. Ye, D.A. Guo, *J. Chromatogr. A* 1216 (2009) 2045–2062.
- [3] X. Liang, L. Zhang, X. Zhang, W. Dai, H. Li, L. Hu, H. Liu, J. Su, W. Zhang, *J. Pharm. Biomed. Anal.* 51 (2010) 565–571.
- [4] M. Sajewicz, D. Staszek, M.S. Wróbel, M. Waksmundzka-Hajnos, T. Kowalska, *Chromatogr. Res. Int.* 2012 (2012) 1–8.
- [5] S.Y. Xue, Z.Y. Li, H.J. Zhi, H.F. Sun, L.Z. Zhang, X.Q. Guo, X.M. Qin, *Biochem. Syst. Ecol.* 41 (2012) 6–12.
- [6] V. Kaskoniene, P. Kaskonas, A. Maruska, O. Ragazinskiene, *Acta. Physiol. Plant* 33 (2011) 2377–2385.
- [7] R. Gotti, *J. Pharm. Biomed.* 55 (2011) 775–801.
- [8] M. Kulp, O. Bragina, P. Kogerman, M. Kaljurand, *J. Chromatogr. A* 1218 (2011) 5298–5304.
- [9] K. Helmja, M. Vaher, M. Kaljurand, *Electrophoresis* 32 (2011) 1094–1100.
- [10] M. Vaher, M. Kaljurand, *Anal. Bioanal. Chem.* 404 (2012) 627–633.
- [11] M. Vaher, M. Borissova, A. Seiman, T. Aid, H. Kolde, J. Kazarjan, M. Kaljurand, *Food Chem.* 143 (2014) 465–471.
- [12] Y.A. Woo, H.J. Kim, J. Cho, H. Chung, *J. Pharm. Biomed. Anal.* 21 (1999) 407–413.
- [13] D.M. Anderson, T.L. Danielson, S.M. Obeidat, G.D. Rayson, R.E. Estell, B. Bai, E.L. Fredrickson, *Open Agric.* 1, 5 (2011) 1–9.
- [14] S.M. Obeidat, T. Glasser, S.Y. Landau, D.M. Anderson, G.D. Rayson, *Talanta* 72 (2007) 682–690.
- [15] M. Lang, F. Stober, H.K. Lichtenthaler, *Radiat. Environ. Biophys.* 30 (1991) 333–347.
- [16] S. Babichenko, L. Poryvkina, Y. Orlov, I. Persiantsev, S. Rebrik, *Fluorescent Signatures in Environmental Analysis*, John Wiley & Sons Inc., New York, 1999.
- [17] J. Mazina, V. Aleksejev, T. Ivkina, M. Kaljurand, L. Poryvkina, *J. Chemom.* 26 (2012) 442–455.
- [18] D. Airado-Rodríguez, I. Duran-Meras, T. Galeano-Díaz, J.P. Wold, *J. Food Compos. Anal.* 24 (2011) 257–264.
- [19] S. Babichenko, E. Erme, T. Ivkina, L. Poryvkina, V. Sominsky, *A portable device and method for on-site detection and quantification of drugs*, Google Patents, 2005.
- [20] G.G. Guilbault, *Practical Fluorescence; Theory, Methods, and Techniques*, Marcel Dekker, New York, 1973.
- [21] C. Genot, F. Tonetti, T. Montenaygarestier, R. Drapron, *Sci. Aliment.* 12 (1992) 199–212.
- [22] R. Llorach, A. Martínez-Sánchez, F.A. Tomás-Barberán, M.I. Gil, F. Ferreres, *Food Chem.* 108 (2008) 1028–1038.
- [23] J. Olšovská, Z. Kameník, P. Čejka, M. Jurková, A. Mikyška, *Talanta* 116 (2013) 919–926.
- [24] Y. Wang, Q. Li, Q. Wang, Y. Li, J. Ling, L. Liu, X. Chen, K. Bi, *J. Agric. Food Chem.* 60 (2011) 256–260.
- [25] C. Dall'Asta, M. Cirlini, E. Morini, G. Galaverna, *J. Chromatogr. A* 1218 (2011) 7557–7565.
- [26] C. Tistaert, B. Dejaegher, G. Chataigne, C. Riviere, N.N. Hoai, M.C. Van, J. Quetin-Leclercq, Y. Vander Heyden, *Anal. Chim. Acta.* 721 (2012) 35–43.
- [27] F. Gong, B.T. Wang, Y.Z. Liang, F.T. Chau, Y.S. Fung, *Anal. Chim. Acta.* 572 (2006) 265–271.
- [28] V. Kaskoniene, P. Kaskonas, M. Jalinskaitė, A. Maruska, *Chromatographia* 73 (2011) S163–S169.
- [29] R. Bro, *Chemometr. Intell. Lab* 38 (1997) 149–171.
- [30] K. Helmja, M. Vaher, T. Püssa, P. Raudsepp, M. Kaljurand, *Electrophoresis* 29 (2008) 3980–3988.
- [31] M. Caban, N. Migowska, P. Stepnowski, M. Kwiatkowski, J. Kumirska, *J. Chromatogr. A* 1258 (2012) 117–127.
- [32] C. Ferrer, A. Lozano, A. Agüera, A.J. Girón, A.R. Fernández-Alba, *J. Chromatogr. A* 1218 (2011) 7634–7639.
- [33] J. Ermer, C. Burgess, G. Kleinschmidt, J.H. McB. Miller, in: J. Ermer, J.H. McB. Miller (Eds.), *Method Validation in Pharmaceutical Analysis: A Guide to Best Practice*, Wiley-VCH Verlag GmbH & Co. KGaA, Weinheim, FRG, 2005. 10.1002/3527604685.ch2.
- [34] K. Pearson, *Philos. Mag. Ser. 6* (2) (1901) 559–572.
- [35] H. Abdi, L.J. Williams, *Wiley Interdiscip. Rev. Comput. Stat.* 2 (2010) 433–459.
- [36] M.A. Rodríguez-Delgado, S. Malovana, J.P. Perez, T. Borges, F.J. Garcia Montelongo, *J. Chromatogr. A* 912 (2001) 249–257.
- [37] A. Banerjee, P.K. Sengupta, *Chem. Phys. Lett.* 424 (2006) 379–386.

## PUBLICATION III

**Mazina, J., Špiljova, A., Vaher, M., Kaljurand, M., Kulp, M.** Rapid capillary electrophoresis method with LED-induced native fluorescence detection for the analysis of cannabinoids in oral fluid. *Analytical methods* **2015**, *7*, 7741-7747 <sup>3</sup>.

<sup>3</sup>Reproduced by permission of The Royal Society of Chemistry





Cite this: DOI: 10.1039/c5ay01595b

## A rapid capillary electrophoresis method with LED-induced native fluorescence detection for the analysis of cannabinoids in oral fluid†

Jekaterina Mazina,‡ Anastassija Spiljova,‡ Merike Vaher, Mihkel Kaljurand and Maria Kulp\*

In the present study, a capillary electrophoresis method with native fluorescence detection for the quantification of two main marijuana cannabinoids, tetrahydrocannabinol (THC) and cannabidiol (CBD), in oral fluid is described. The reported CE method makes it possible to assess illegal cannabis use in approximately 10 min, including saliva sample collection, pre-treatment procedures and capillary electrophoresis (CE) analysis. The proof of the principle, demonstrated on a home-made lab scale instrument, has potential to be easily translated onto a truly portable instrument for on-site measurements. The saliva sample collection/preparation/pre-concentration procedure was combined into one step using a Salivette® sampling device. No separate precipitation of proteins and/or derivatisation was required. The baseline CE separation of the two cannabinoids was achieved in less than 7 min by applying a non-aqueous background electrolyte (BGE), composed of 2.5 mM sodium hydroxide in a methanol–acetonitrile mixture (1 : 1). Cannabinoids were detected at their second  $\lambda_{\text{ex}}/\lambda_{\text{em}}$  maximum (280/307 nm) with LOD values of 0.19 and 0.17  $\mu\text{g mL}^{-1}$  for THC and CBD, respectively. The recovery of the cannabinoids from the collection pad was greater than 80% for both cannabinoids tested at 2.5  $\mu\text{g mL}^{-1}$ , and the inter-day precision was less than 6% for all analytes. The procedure was applied to oral fluid specimens after the controlled *ad libitum* smoking of one cannabis cigarette.

Received 21st June 2015  
Accepted 22nd July 2015

DOI: 10.1039/c5ay01595b

www.rsc.org/methods

### 1. Introduction

Cannabis (marijuana) is the most widely used illegal substance in the world.<sup>1,2</sup> Humans smoke or ingest cannabis for its psychotropic effects. Tetrahydrocannabinol (THC) is the primary psychoactive compound in cannabis and its confirmation is an important element in assessing drug exposure in the workplace, while driving or during drug treatment. Cannabidiol (CBD), the other natural cannabinoid found in relatively high concentration in cannabis, contributes little to cannabis's psychotropic activity; quite the contrary, it may have antipsychotic properties.<sup>3</sup> Its concentration relative to THC can be useful in distinguishing the smoking of cannabis from the administration of cannabinoid-containing pharmacotherapies.<sup>4</sup>

The widespread use of illegal cannabis is generally the reason that cannabinoids are intensively studied and that the search for possible new methods for determining usage is still very active.<sup>5,6</sup> The quest for the development of an analytical method is targeted at the ability to identify the narcotics used by drivers/

criminals as quickly as possible, so that appropriate preventive measures can be taken. For such a method to be useful, several factors have to be considered, including non-invasive sampling and sample preparation time, the portability of instruments, instrument start-up time, and actual analysis time.

The use of oral fluid (OF) as an alternative biological matrix for drug abuse testing has received increased attention in forensic and clinical chemistry. Saliva sample collection, compared to blood sampling, is easy, non-invasive and does not require any special training. In addition, for drug abuse control, saliva is available at any time and a sample can be collected in public view to prevent adulteration or sample substitution. An OF clean matrix contains approximately 98% water, with electrolytes, mucus, proteins and small molecules. Oral fluid contains predominately the parent drug rather than drug metabolites, and therefore is a good indicator of intoxication states.<sup>7</sup> During cannabis smoking, oral mucosa is immediately contaminated with cannabinoids contained in cannabis vapour and THC concentrations in saliva often exceed 1000  $\mu\text{g L}^{-1}$  for a short time after smoking.<sup>8,9</sup>

To date, the assessment of illicit cannabis use, based on oral fluid analysis, has employed on-site screening tests and, in the case of positive results, follow-up confirmatory analysis in the lab. For on-site testing, such immunoassay devices as DrugWipe®, Cozart® RapiScan, Rapid STAT®, Dräger

Tallinn University of Technology, Department of Chemistry, Akadeemia tee 15, Tallinn, Estonia, 12618. E-mail: maria@chemnet.ee; Fax: +372 620 2828; Tel: +372 620 4349

† Electronic supplementary information (ESI) available. See DOI: 10.1039/c5ay01595b

‡ These authors contributed equally to this work.

DrugTest® 5000, Oratect XP saliva kits, *etc.* are available commercially. The main drawbacks of immunoassay tests are cross-reactivity and poor analyte recovery from the device, which lead to low diagnostic sensitivity (about 60%) and often to inadequate performance.<sup>10,11</sup> In the next step of the assessment of narcotic intoxication, chromatographic separation techniques play a dominant role. Usually, GC and HPLC are coupled to a mass spectrometer (MS),<sup>12–15</sup> because these detection techniques provide very reliable identification of separated compounds. Each of these techniques has advantages and drawbacks for on-site analysis. For instance, GC can be made portable and the separation times are relatively short.<sup>16</sup> However, the analysis typically requires derivatization steps because cannabinoids are insufficiently volatile. HPLC, on the other hand, cannot readily be made portable and thus requires the sample to be delivered to an analytical laboratory. In addition, despite the lower amounts of proteins found in OF with respect to blood, extensive sample preparation is needed in order to avoid relevant matrix effects.<sup>17</sup> This is generally carried out using solid phase<sup>15,18</sup> or liquid–liquid extraction modes.<sup>19</sup> The recovery values of these techniques often decrease up to 50% and the accuracy of the methods suffers.

Capillary electrophoresis (CE) and related techniques are increasingly being employed in forensic analysis, as documented in several recent reviews.<sup>20–22</sup> The exceptional power of separation and resolution, short analysis time, economical use of reagents, and minimum sample requirements make CE an attractive methodology for forensic laboratories. CE can easily be miniaturized, unlike GC or HPLC.<sup>23</sup> CE start-up time is significantly shorter than that of HPLC, because there is no need for lengthy equilibration of the separation column with an eluent. In addition, CE analysis times are unquestionably the shortest of the available separation techniques. In contrast to these advantages, the primary disadvantage limiting its use is its poor concentration sensitivity, particularly when applied with on-column ultraviolet (UV) absorbance detection, due to low sample-injection volume and short optical path length. More adequate detection limits for abused drugs in the context of miniaturized analytical techniques can be obtained by light-emitting diode (LED) induced fluorescence detection.<sup>24,25</sup> The combination of extremely high stability, long lifetime, small size, low cost and commercial availability at wavelengths ranging from deep-UV to near-IR regions makes LEDs an attractive light source.<sup>26–29</sup>

In this study, we propose the hypothesis that the capillary electrophoresis method with a native LED-induced fluorescence detector (LED-IF) is an alternative analytical technology to laboratory GC/LC-MS and roadside drug tests. The proof of the principle was demonstrated on a home-made lab scale instrument, with the goal of transforming it further to a portable format for on-site measurements. The LED-fluorescence detector used in this work was operated at a deep UV wavelength, providing the detection of the two main marijuana cannabinoids, THC and CBD, at their excitation/emission maximum without the need for derivatization. A saliva sample collection/preparation/pre-concentration procedure was combined into one step using the Salivette® sampling device

and was carried out in several minutes. A rapid and effective clean-up was carried out with good recovery values. The electrophoretic conditions obtained with a non-aqueous background electrolyte allowed for good separation of analytes in only 6 min. The developed method was thoroughly validated and used for the analysis of real oral fluid specimens after controlled marijuana smoking.

## 2. Materials and methods

### 2.1. Chemicals and reagents

Tetrahydrocannabinol and cannabidiol standard solutions 10 mg mL<sup>-1</sup> and 1 mg mL<sup>-1</sup> and powders were purchased from Lipomed AG (Switzerland). Internal standard (IS) bicalutamide (BCT) and potential interferents, including ethanol, acetaldehyde, nicotine, cotinine, caffeine and ibuprofen, were obtained from Sigma-Aldrich (USA). Other drugs, including analgetics (acetylsalicylic acid, paracetamol, ibuprofen, metamizole, diclofenac, meloxicam, flupirtine, tramadol, and codeine), antibiotics (doxycycline, amoxicillin, clindamycin, azithromycin, metronidazole, nitrofurantoin, sulfamethoxazole, and trimethoprim), histamine antagonists (loratadine, cetirizine, and levocetirizine), psychoactive drugs (phenobarbital, alprazolam, citalopram, escitalopram, venlafaxine, carbamazepine, and olanzapine), and others (doxazosin, finasteride, ambroxol, metoprolol, omeprazole, dydrogesterone, loperamide, warfarin, enalapril, glucosamine, sildenafil, and levothyroxine) were purchased from a pharmacy. Non-aqueous background electrolyte compounds, including sodium hydroxide, methanol and acetonitrile (ACN), were obtained from Sigma-Aldrich (USA). All of the chemicals were of ACS grade and the organic solvents were of HPLC grade.

Cannabis cigarettes with concentrations of THC and CBD of 25 and 20 mg, respectively, were made from medical marijuana Bediol (Bedrocan, Switzerland) and LM Blue cigarettes.

### 2.2. Calibrator and quality control solutions

THC 10 mg mL<sup>-1</sup> in ethanol and CBD 1 mg mL<sup>-1</sup> in methanol standard solutions were diluted with acetonitrile to prepare 100 µg mL<sup>-1</sup> stock solutions, which were stored at –20 °C. A stock solution 100 µg mL<sup>-1</sup> of bicalutamide used as IS was prepared in acetonitrile. Fresh OF samples for the preparation of the working and quality controls (QCs) were donated by staff personnel, and collected with the Salivette® device (Sarstedt, Numbrecht, Germany). Calibration solutions 0.5, 1.0, 2.0, 5.0 and 10.0 µg mL<sup>-1</sup> were prepared by the addition of the appropriate amount of the cannabinoid stock solutions and IS (0.5 µg mL<sup>-1</sup>) to blank oral fluid samples, with the following sample preparation. QC solutions were prepared in the same way from different cannabinoid standard lots than those used for the calibrators.

### 2.3. Oral fluid collection and sample preparation

Fresh OF samples were collected with the Salivette® device and centrifuged at 10 000 rpm for 1 minute. The centrifugate was discarded and 1000 µL of acetonitrile was added to the pad. The Salivette tube was centrifuged again under the same conditions

and the obtained centrifugate was injected for CE analysis. The collected samples were stored at  $-20\text{ }^{\circ}\text{C}$ .

## 2.4. CE apparatus and analysis

The LED-fluorescence detector for CE used for the determination of cannabinoids was designed and constructed by Laser Diagnostic Instruments AS (LDI), Estonia. It was described in detail in our previous study.<sup>25</sup> A UV-LED (Roithner Lasertechnik, Austria) was used as the fluorescence excitation source ( $\lambda = 280\text{ nm}$ ). An interference filter of 307 nm (Andover Corporation, USA) was used to block reflected UV radiation and select the required spectral region for fluorescence signal registration.

The CE apparatus was constructed in-house. Uncoated, fused-silica capillaries, i.d. 75  $\mu\text{m}$  and o.d. 360  $\mu\text{m}$  (Polymicro Technologies, Phoenix, AZ, USA), were used for the analyses. The total capillary length was 60 cm with the detection zone placed at 15 cm from the capillary end. Prior to injection, the capillary was rinsed sequentially with 0.1 M NaOH and the background electrolyte for 2 min each. The samples were injected into the capillary by hydrodynamic flow at a height differential of 20 cm for 30 seconds. Separations were performed at +17 kV. Before the measurements, new capillaries were conditioned by rinsing them sequentially with 1 M sodium hydroxide and Milli-Q water. Between analyses, the capillaries were rinsed with the electrolyte solution for 2 min.

## 2.5. Method validation

The developed CE method was evaluated for linearity, limits of detection and quantification (LOD and LOQ), selectivity, inter-day precision, accuracy, carry-over, extraction recovery and matrix effects (ME).

Calibration was performed by the method of standard additions. For this, blank OF samples were spiked at five different concentration levels and each concentration level was injected five times. Analyte responses were normalized to an internal standard and quantified by linear least-squares regression. Bicalutamide (BCT) was utilized as the IS. Linearity was checked from 0.5 to 10  $\mu\text{g mL}^{-1}$  for both cannabinoids, THC and CBD. The correlation coefficient ( $R^2$ ) was required to be at least 0.99, and residuals <20% at the LOD and <15% at the other concentrations.

LOD and LOQ were determined by measuring a series of decreasing concentrations of fortified saliva samples. LOD was determined as the lowest analyte concentration with an S/N ratio of at least 3 for both cannabinoids, with acceptable peak shapes. LOQ was the lowest concentration that could be quantified with acceptable precision (%CV < 20%) of the target concentration.

Selectivity was defined as the ability to identify and quantify an analyte in the presence of potential endogenous or exogenous interferents. Potential endogenous interferents were assessed by the analysis of six OF samples from volunteers fortified with IS. Exogenous interferents were assessed by the analysis of OF samples fortified with 45 common drugs and alcoholic beverages listed above. Moreover, exogenous

interference caused by the smoking of common tobacco cigarettes was also evaluated.

Precision and accuracy were assessed at low (0.5  $\mu\text{g mL}^{-1}$ ), medium (2.5  $\mu\text{g mL}^{-1}$ ) and high (10  $\mu\text{g mL}^{-1}$ ) QC concentrations in an oral fluid matrix. Precision and accuracy were studied by analysing three replicates on ten different days ( $n = 30$ ). The experimental precision was expressed as the relative standard deviation. Accuracy was calculated as the difference between mean and target concentrations ( $C_t$ ) ( $A\% = \text{mean}/C_t \times 100$ ).

Fortified OF samples exceeding the linear range for THC and CBD (100  $\mu\text{g mL}^{-1}$ ) were extracted and analysed to evaluate carry-over. Blank samples containing IS were injected after each carry-over challenge to quantify potential carry-over from the previous injection.

Extraction recovery ( $R\%$ ) was calculated at two concentration levels (2.5 and 10  $\mu\text{g mL}^{-1}$ ) by comparing mean peak areas in blank samples fortified with the analytes and IS before (A) and after (B) extraction with the Salivette® device ( $n = 5$ ). Accordingly,  $R\% = A/B \times 100$ . The interference of the matrix with the S/N ratio of each analyte was calculated as the slope ratios of the calibration curves obtained in solvent (ACN) and in OF.

# 3. Results and discussion

## 3.1. Method development

**3.1.1. Fluorescence emission spectra of cannabinoids.** The fluorescence emission spectra of THC and CBD were first investigated to estimate the feasibility of this method. It was found that both cannabinoids emitted fluorescence wavelengths around 307 nm when excited at 230 and 280 nm. Therefore, it was possible to use a 280 nm light-emitting diode with an interference filter 307 nm to detect them in CE without the need for fluorescence derivatization. The use of the first  $\lambda_{\text{ex}}/\lambda_{\text{em}}$  maximum of cannabinoids (230/307 nm) would provide a higher quantum yield (Fig. 1S in the ESI†) and therefore, detection sensitivity; however, the absence of the commercially available 230 nm LEDs restricted the possibility of their use for this application.

**3.1.2. CE conditions.** The cannabinoids studied in the present work represent weakly acidic molecules with hydroxyl groups attached to unsaturated aromatic hydrocarbon rings, and they exhibit  $\text{p}K_{\text{a}}$  values above 9.5 and 10.5 for CBD and THC, respectively (see Fig. 1). Thus, in very basic electrolytes, cannabinoids are deprotonated at the oxygen atom and migrate as anions towards the cathode. THC and CBD are almost insoluble in water and the use of organic solvents for separation media has many advantages compared to aqueous CE. Besides the improved solubility for water-insoluble compounds, a non-aqueous medium in CE provides increased selectivity and reduced currents, which allow for the application of high field strengths to achieve rapid separation.<sup>30</sup> The application of a very basic electrolyte system consisting of sodium hydroxide dissolved in methanol-acetonitrile for the analysis of acidic species was first proposed by K. Altria *et al.*<sup>30</sup> and confirmed by U. Backofen<sup>31</sup> *et al.* for the determination of cannabinoids in hair. In the present study, both cannabinoids and IS (bicalutamide) were separated in 2.5 mM NaOH dissolved in a

## Analytical Methods

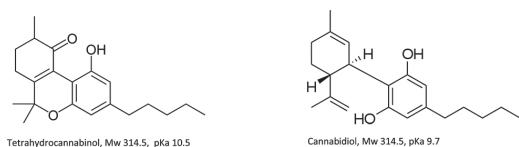


Fig. 1 The chemical formulae, molecular masses and  $pK_a$  of studied cannabinoids.  $pK_a$  values can change depending on the environment.

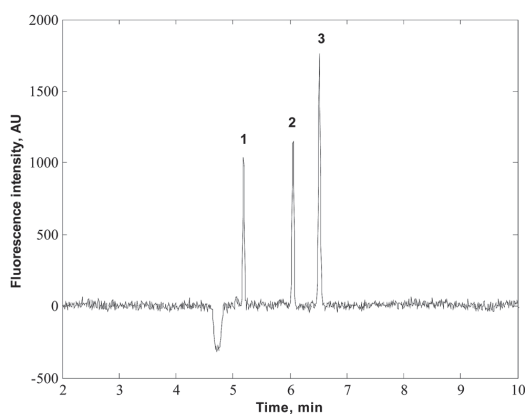


Fig. 2 Separation on tetrahydrocannabinol (THC) and cannabidiol (CBD) standards by non-aqueous CE with a LED-fluorescence detector. Experimental conditions: capillary I.D. 75  $\mu\text{m}$ ; running electrolyte 2.5 mM sodium hydroxide dissolved in methanol–acetonitrile (1 : 1); separation field 283  $\text{V cm}^{-1}$ ;  $\lambda_{\text{ex/em}}$  = 280/305 nm. Peaks: 1 – CBD ( $2 \mu\text{g mL}^{-1}$ ), 2 – THC ( $2 \mu\text{g mL}^{-1}$ ), and 3 – IS ( $1 \mu\text{g mL}^{-1}$ ).

methanol–acetonitrile (1 : 1) mixture (Fig. 2). It is interesting to note that CBD, which has two phenol moieties and the same mass, migrated faster than THC. This can be explained by the fact that in strongly basic media, CBD is oxidized to a quinone, and becomes less charged than THC.<sup>32</sup>

**3.1.3. Optimization of the extraction procedure.** A careful optimization of the extraction step was needed, particularly to achieve the best sensitivity for the detection of cannabinoids in OF. As was mentioned above, during cannabis smoking, oral mucosa is contaminated with cannabinoids contained in cannabis vapour. In the present study, we exploited the strong adsorption of oral mucosa with cannabinoids to Salivette® cotton swabs, which allowed us to use the Salivette® device for sample collection, analyte pre-concentration and extraction. First, a Salivette® tube, containing the collected OF sample was centrifuged and the obtained oral fluid was withdrawn. Then, cannabinoids were extracted by the addition of a certain amount of ACN to the swab, providing denaturation of the mucosa proteins and release of the analytes, followed by centrifugation. The sampling/extraction procedure was examined in terms of the remaining amount of OF in the swab and the loading volume of ACN for maximum extraction efficiency, while the sampling time was kept constant (1 min) according to the Salivette® producer recommendations. For this, blank and

Table 1 Performance characteristics of the CE-LED method for the quantification of THC and CBD in saliva

Analytes	Linear range, $\mu\text{g mL}^{-1}$	Equation ( $\text{area}_{\text{analyte}}/\text{area}_{\text{IS}}$ )	$R^2$	LOD, $\mu\text{g mL}^{-1}$	LOQ, $\mu\text{g mL}^{-1}$	Inter-day precision ( $n = 30$ ), RSD/%	Accuracy $\pm$ SD, % ( $n = 30$ )	Extraction recovery $\pm$ SD, ( $n = 30$ )	Matrix effect (ME)
CBD	0.5–10	$y = (0.127 \pm 0.002)x + (0.006 \pm 0.009)$	0.9955	0.17	0.36	0.5 : 5.6, 2.5 : 5.2, 10 : 4.0	108 $\pm$ 3, 98 $\pm$ 2, 100 $\pm$ 3	83 $\pm$ 4, 81 $\pm$ 3	1.26
THC	0.5–10	$y = (0.158 \pm 0.003)x + (0.013 \pm 0.013)$	0.9943	0.19	0.41	0.5 : 2.8, 2.5 : 5.6, 10 : 3.7	107 $\pm$ 5, 100 $\pm$ 3, 100 $\pm$ 6	81 $\pm$ 3, 80 $\pm$ 3	1.40

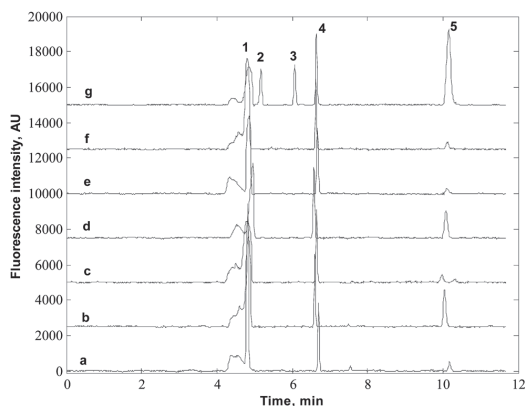


Fig. 3 Assessment of the endogenous matrix effect. Experimental conditions as in Fig. 2. Electropherograms (a–f) represent the CE analysis of OF samples from six volunteers, (g) OF sample spiked with standards of CBD, THC and IS. Peaks: 1 – neutral compound from Salivette® swab, 2 – CBD, 3 – THC, 4 – IS, 5 – saliva endogenous compound.

fortified ( $1 \mu\text{g mL}^{-1}$  of each cannabinoid) OF samples from six volunteers were extracted and analysed. The amount of the saliva obtained after the first centrifugation varied, depending on the person, from 0.1 to 1.5 mL. However, the remaining amount of oral fluid in the swab after the first centrifugation was constant,  $0.33 \pm 0.03 \text{ mL}$  ( $n = 6$ ), providing normalization of the sampling procedure. The ACN loading volume was varied from 0.5 to 2 mL. The addition of decreased amounts of ACN to the swab produced lower recovery and peak broadening, caused by the weak stacking effect, while an increased amount of ACN led to sample dilution and lower sensitivity. The best extraction

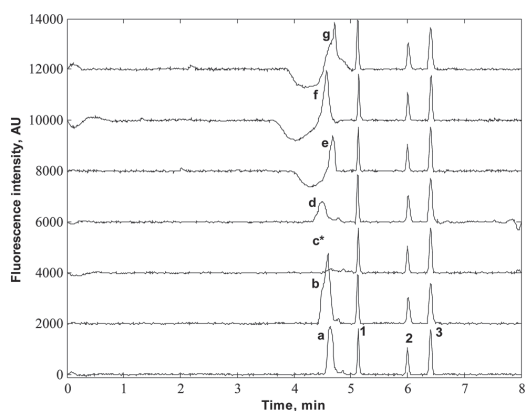


Fig. 4 Assessment of the exogenous matrix effect. Experimental conditions as in Fig. 2. Peaks: a – tramadol, b – metoprolol, c\* – omeprazole peak at 14 min, d – venlafaxine, e – escitalopram, f – tsitalopram and g – codeine ( $1 \mu\text{g mL}^{-1}$  of each drug); 1 – CBD ( $1 \mu\text{g mL}^{-1}$ ), 2 – THC ( $1 \mu\text{g mL}^{-1}$ ) and 3 – IS ( $0.5 \mu\text{g mL}^{-1}$ ).

recovery values (over 80%) with minimum sample dilution were obtained when 1 mL of ACN was added to the swab (Table 1).

**3.1.4. Method validation.** The data of the method validation are summarized in Table 1. The calibration curves were generated using an unweighted least-square regression model. A linear relationship was obtained between the concentration injected and the corrected peak area for both cannabinoids within the range  $0.5\text{--}10 \mu\text{g mL}^{-1}$ . The calibration curve  $R^2$  always exceeded 0.994. Limits of detection and quantification of  $0.19 \mu\text{g mL}^{-1}$  and  $0.41 \mu\text{g mL}^{-1}$  for THC, and  $0.17 \mu\text{g mL}^{-1}$  and  $0.36 \mu\text{g mL}^{-1}$  for CBD were achieved. In spite of that, the GC-MS technique for the analysis of cannabinoids still outperformed the proposed CE protocol in LOD; the real concentrations of cannabinoids in saliva were usually much higher ( $1\text{--}5 \mu\text{g mL}^{-1}$ ) for a short time after smoking than the declared cut-offs.<sup>9</sup> Therefore, the proposed CE technique can be successfully applied for confirmation analysis during the intoxication period (0–3 hours after cannabis use<sup>33,34</sup>).

The selectivity of the method was proven by the evaluation of endogenous and exogenous matrix effects. Endogenous matrix effects were determined in the OF fortified with IS collected from six drug-free volunteers. There were no endogenous signal contributions for any analyte of interest (Fig. 3).

Exogenous interferences were assessed by fortifying QC samples with forty-five potential interfering drugs. Under applied CE separation conditions, only tramadol, codeine, citalopram, escitalopram, venlafaxine, metoprolol and omeprazole peaks were observed on the electropherograms. The analysis of the drug-fortified ( $1 \mu\text{g mL}^{-1}$ ) OF samples confirmed that these drugs do not contribute to the measured concentrations of THC and CBD in OF (Fig. 4). All drugs, except omeprazole, co-migrated with the EOF peak. The omeprazole migration time was about 14 min (electropherogram (c), peak not shown).

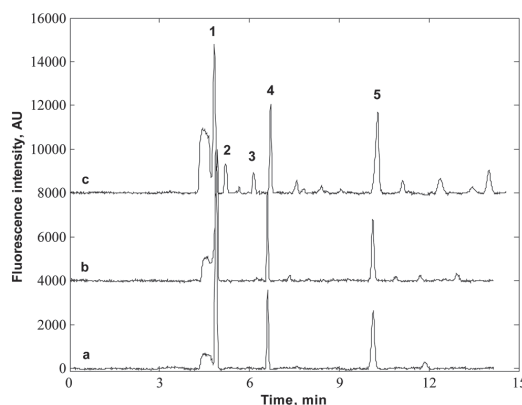


Fig. 5 CE analysis of real OF specimens. Experimental conditions as in Fig. 2. Electropherograms: a – blank OF, b – saliva sample after the smoking of one “LM blue” cigarette, c – saliva sample after the smoking of one cannabis cigarette. Peaks: 1 – neutral compound from a Salivette® swab, 2 – CBD, 3 – THC, 4 – IS, 5 – saliva endogenous compound.

Exogenous interferents caused by the smoking of tobacco cigarettes were also evaluated. Fig. 5(a) and (b) demonstrate a volunteer's blank OF sample and saliva sample analyses after the smoking of one "LM blue" cigarette. No quantifiable peaks were detected at the specific retention time for both analytes.

Inter-day reproducibility (precision) and accuracy were assessed using a fortified drug-free matrix at three concentration levels (Table 1). Inter-day reproducibility results expressed as residual standard deviation (RSD%) were constantly <6%. Accuracy calculated as the percent difference between mean and target concentrations of each analyte ranged from 98 to 108% for all concentration levels.

Extraction recovery was calculated by comparing mean corrected peak areas ( $n = 5$ ) of analytes in drug-free OF fortified prior to and after the extraction procedure with the Salivette® device. Mean extraction efficiencies ranged between 80 and 85%, which are very good compared to LLE (70%)<sup>4</sup> or MEPS (50%)<sup>35</sup> saliva pre-treatment methodologies.

With regard to the matrix effect in neat OF, both CBD and THC showed fluorescence signal enhancement: +26% and +40%, respectively (Table 1). Therefore, the quantitative determination of these cannabinoids in saliva must be conducted by a standard addition method into a sample matrix.

Negative samples injected immediately after samples containing  $100 \mu\text{g mL}^{-1}$  of THC and CBD showed no evidence of carry-over (the signal was below the LOD for both analytes).

**3.1.5. Application to real OF specimens.** The developed CE-LED-IF method was employed to quantify THC and CBD in OF specimens collected with the Salivette® device after the controlled *ad libitum* smoking of one cannabis cigarette containing approximately 20 mg THC and 15 mg CBD. The protocols were approved by the National Medical Research Ethics Committee, and the participants provided written informed consent. OF was collected 10 min before (blank) and 20 min after the start of smoking. A representative electropherogram demonstrating a selective separation of analytes from a participant's OF after smoking is presented in Fig. 5(c). The measured concentrations of THC and CBD were  $3.04 \mu\text{g mL}^{-1}$  and  $4.05 \mu\text{g mL}^{-1}$ , respectively.

## 4. Conclusions

A rapid and simple method of CE with ultraviolet light-emitting diode-induced native fluorescence (UV-LEDIF) detection was presented to determine THC and CBD in OF. The proposed separation protocol in combination with highly selective native fluorescence detection made it possible to quantify these cannabinoids in a biological matrix with a minimum sample pretreatment. No separate precipitation of proteins or derivatization was needed. The procedure of saliva sample collection and clean-up was accomplished with the Salivette® sampling device and the whole analysis, including CE separation of analytes, took 10 minutes.

The validation results show that the detection limits of the CE-LEDIF method are less reliable than GC-MS LODs, but can be considered acceptable for the determination of cannabinoids in OF during a short time after smoking (a couple of

hours). Moreover, the lack of detection sensitivity can be overcome by using an excitation source at the first  $\lambda_{\text{ex}}/\lambda_{\text{em}}$  maximum of cannabinoids (230/307 nm). The implementation, for example, of a miniature flash Xe-lamp instead of an LED for the excitation of analytes provides an approximate 50-fold increase in sensitivity. With respect to the simplified operating conditions, excellent selectivity and miniaturization benefits of the proposed CE technology, it seems to be a very promising and reliable alternative to conventional laboratory GC/LC-MS for on-site analysis of drug abuse. The construction of a novel portable CE instrument with a 230 nm excitation source would be an interesting direction for further development.

## Acknowledgements

The Estonian Research Council (institutional Research Fund No. 33-20) is acknowledged for financial support. The authors have declared no conflict of interest.

## References

- 1 SAMHSA, *Results from the 2013 National Survey on Drug Use and Health: Summary of National Findings, NSDUH Series H-48, HHS Publication No. (SMA)*, Substance Abuse and Mental Health Services Administration, Rockville, MD, 2014, pp. 14–4863.
- 2 European Monitoring Centre for Drugs and Drug Addiction (EMCDDA), *European Drug Report*, 2015.
- 3 C. D. Schubart, I. E. C. Sommer, P. Fusar-Poli, L. de Witte, R. S. Kahn and M. P. M. Boks, *Eur. Neuropsychopharmacol.*, 2014, **24**, 51–64.
- 4 A. Molnar, S. L. Fu, J. Lewis, D. J. Allsop and J. Copeland, *Forensic Sci. Int.*, 2014, **238**, 113–119.
- 5 N. Ferreiros, *Bioanalysis*, 2013, **5**, 2713–2731.
- 6 N. Battista, M. Sergi, C. Montesano, S. Napoletano, D. Compagnone and M. Maccarrone, *Drug Test. Anal.*, 2014, **6**, 7–16.
- 7 L. F. Martins, M. Yegles and R. Wennig, *J. Chromatogr. B*, 2008, **862**, 79–85.
- 8 D. Lee and M. A. Huestis, *Drug Test. Anal.*, 2014, **6**, 88–111.
- 9 G. Milman, D. M. Schwope, D. A. Gorelick and M. A. Huestis, *Clin. Chim. Acta*, 2012, **413**, 765–770.
- 10 A. Pehrsson, T. Blencowe, K. Vimpari, K. Langel, C. Engblom and P. Lillsunde, *J. Anal. Toxicol.*, 2011, **35**, 211–218.
- 11 N. A. Desrosiers, D. Lee, D. M. Schwope, G. Milman, A. J. Barnes, D. A. Gorelick and M. A. Huestis, *Clin. Chem.*, 2012, **58**, 1418–1425.
- 12 L. Anzillotti, E. Castrignanò, S. S. Rossi and M. Chiarotti, *Sci. Justice*, 2014, **54**, 421–426.
- 13 N. A. Desrosiers, G. Milman, D. R. Mendu, D. Lee, A. J. Barnes, D. A. Gorelick and M. A. Huestis, *Anal. Bioanal. Chem.*, 2014, **406**, 4117–4128.
- 14 M. Míguez-Framil, J. Á. Cocho, M. J. Tabernero, A. M. Bermejo, A. Moreda-Piñeiro and P. Bermejo-Barrera, *Microchem. J.*, 2014, **117**, 7–17.
- 15 G. Milman, A. J. Barnes, R. H. Lowe and M. A. Huestis, *J. Chromatogr. A*, 2010, **1217**, 1513–1521.

- 16 B. A. Eckenrode, *J. Am. Soc. Mass Spectrom.*, 2001, **12**, 683–693.
- 17 V. Samanidou, L. Kovatsi, D. Fragou and K. Rentifis, *Bioanalysis*, 2011, **3**, 2019–2046.
- 18 C. Moore, S. Rana and C. Coulter, *J. Chromatogr. B*, 2007, **852**, 459–464.
- 19 A. Molnar, J. Lewis, P. Doble, G. Hansen, T. Prolov and S. L. Fu, *Forensic Sci. Int.*, 2012, **215**, 92–96.
- 20 T. N. Posch, M. Putz, N. Martin and C. Huhn, *Anal. Bioanal. Chem.*, 2015, **407**, 23–58.
- 21 J. P. Pascali, F. Bortolotti and F. Tagliaro, *Electrophoresis*, 2012, **33**, 117–126.
- 22 C. Cruces-Blanco and A. M. Garcia-Campana, *Trends Anal. Chem.*, 2012, **31**, 85–95.
- 23 P. Kubáň, A. Seiman, N. Makarõtševa, M. Vaher and M. Kaljurand, *J. Chromatogr. A*, 2011, **1218**, 2618–2625.
- 24 C. C. Tsai, J. T. Liu, Y. R. Shu, P. H. Chan and C. H. Lin, *J. Chromatogr. A*, 2006, **1101**, 319–323.
- 25 A. Alnajjar, J. A. Butcher and B. McCord, *Electrophoresis*, 2004, **25**, 1592–1600.
- 26 M. Kulp, O. Bragina, P. Kogerman and M. Kaljurand, *J. Chromatogr. A*, 2011, **1218**, 5298–5304.
- 27 M. Kulp and O. Bragina, *Anal. Bioanal. Chem.*, 2013, **405**, 3391–3397.
- 28 M. Macka, T. Piasecki and P. K. Dasgupta, *Annu. Rev. Anal. Chem.*, 2014, **7**, 183–207.
- 29 D. A. Bui and P. C. Hauser, *Anal. Chim. Acta*, 2015, **853**, 46–58.
- 30 K. D. Altria and S. M. Bryant, *Chromatographia*, 1997, **46**, 122–130.
- 31 U. Backofen, F. M. Matysik and C. E. Lunte, *J. Chromatogr. A*, 2002, **942**, 259–269.
- 32 R. Mechoulam, Z. Ben-Zvi and Y. Gaoni, *Tetrahedron*, 1968, **24**, 5615–5624.
- 33 R. L. Hartman and M. A. Huestis, *Clin. Chem.*, 2013, **59**, 478–492.
- 34 R. A. Sewell, J. Poling and M. Sofuoglu, *The American Journal on Addictions*, 2009, **18**, 185–193.
- 35 M. Sergi, C. Montesano, S. Odoardi, L. M. Rocca, G. Fabrizi, D. Compagnone and R. Curini, *J. Chromatogr. A*, 2013, **1301**, 139–146.



## PUBLICATION IV

**Mazina, J.,** Saar-Reismaa, P., Kulp, M., Poryvkina, L., Kaljurand, M., Vaher, M. Determination of  $\gamma$ -hydroxybutyric acid in saliva by capillary electrophoresis coupled with contactless conductivity and indirect UV absorbance detectors. *Electrophoresis* **2015**, 36, 3042–3049<sup>4</sup>.

<sup>4</sup> Copyright © 2015 WILEY-VCH Verlag GmbH & Co. KGaA, Weinheim



Jekaterina Mazina<sup>1,2</sup>  
Piret Saar-Reismaa<sup>1</sup>  
Maria Kulp<sup>1</sup>  
Mihkel Kaljurand<sup>1</sup>  
Merike Vaher<sup>1</sup>

<sup>1</sup>Department of Chemistry,  
Tallinn University of  
Technology, Tallinn, Estonia  
<sup>2</sup>NarTest AS, Tallinn, Estonia

Received April 28, 2015  
Revised August 24, 2015  
Accepted September 16, 2015

## Research Article

# Determination of $\gamma$ -hydroxybutyric acid in saliva by capillary electrophoresis coupled with contactless conductivity and indirect UV absorbance detectors

The aim of the current study was to optimise and validate the methodology for determination of  $\gamma$ -hydroxybutyric acid (GHB) in saliva by CE combined with a contactless conductivity detector (C<sup>4</sup>D) and indirect UV absorbance detection ( $\lambda_{\text{ABS}} = 210 \text{ nm}$ ). The optimized BGE, consisting of 8.5 mM maleic acid, 17 mM arginine, 255  $\mu\text{M}$  cetyltrimethylammonium bromide (CTAB), and 15% acetonitrile, was evaluated for the separation of GHB in saliva within 6 min. The performance characteristics of the CE-C<sup>4</sup>D-indirect UV methodology was validated. The instrument detection and quantification limits were 0.49 and 1.6 mg/L for C<sup>4</sup>D, and 5.1 mg/L and 17.0 mg/L for indirect UV, respectively. The linearity was obtained over the range from 2.5 to 400 mg/L for C<sup>4</sup>D and from 12.5 to 400 mg/L for indirect UV. The interday precisions were within 2.3–5.7% and intraday precisions were within 1.6–9.0% for C<sup>4</sup>D as well as 2.1–9.3%, 5.6–10.1% for indirect UV in spiked saliva, respectively. The recoveries were within 87.2–104.4%. The matrix effects were +53.2% for small concentrations up to 25 mg/L for C<sup>4</sup>D and +23.6% for concentrations up to 75 mg/L for indirect UV detection. No matrix effects were observed for higher concentration levels. In conclusion, CE-C<sup>4</sup>D-indirect UV can offer a rapid, accurate, sensitive, and definitive method for the determination of GHB abuse in saliva samples as a forensic screening tool.

### Keywords:

CE / Contactless conductivity detection /  $\gamma$ -Hydroxybutyric acid / Indirect UV absorbance detection / Saliva  
DOI 10.1002/elps.201500293



Additional supporting information may be found in the online version of this article at the publisher's web-site

## 1 Introduction

A global epidemic of drug abuse and addiction can be compared to the “Plague,” encountering millions of victims every year. One of the well-known and popular drugs of abuse among teens and young adults is  $\gamma$ -hydroxybutyric acid

(GHB). GHB can be used as a recreational drug or as a drug facilitating sexual assault, robbery, money extortion, and other crimes. Drug-facilitated crime implies that a victim is unable to resist assault due to unconsciousness caused by the influence of substances. GHB is also known as a central nervous system depressant and hypnotic. It occurs naturally in the human body at low levels (saliva 0.15–3.33 mg/L [1], urine 0.64–4.20 mg/L [2], serum 0.62–3.24 mg/L [2]) as a metabolite of GABA ( $\gamma$ -aminobutyric acid) [3]. As an illegal drug, GHB is often abused at bars, “raves” and clubs. It can be consumed orally as a solid white powder or added to different alcoholic beverages. The latter is the predominant method of consumption. GHB analog such as  $\gamma$ -butyrolactone (GBL) and 1,4-butanediol (1,4-BD) can also be used instead of GHB. The analogs are converted to GHB in the human body (1,4-BD to GBL and GBL then to GHB). Therefore, the detection of

**Correspondence:** Jekaterina Mazina, Department of Chemistry, Tallinn University of Technology, Akadeemia tee 15, 12816 Tallinn, Estonia

**E-mail:** jekaterina.mazina@gmail.com

**Abbreviations:** ABS, absorbance; C<sup>4</sup>D, contactless conductivity detector; GHB,  $\gamma$ -hydroxybutyric acid; IDL, instrument detection limit; IQL, instrument quantification limit; IS, internal standard; LLOQ, lower LOQ; ME, matrix effect; MLOQ, medium LOQ; PMPA, pinacolyl methylphosphonic acid; ULOQ, upper LOQ; URT, upper respiratory tract; UV, ultraviolet

**Colour Online:** See the article online to view Figs. 1 and 2 in colour.

GHB is of utmost importance and reflects illegal drug abuse. Although, the different and, even more severe, toxic effects of GHB analogs might be taken into account.

The GHB dose drastically varies from 0.5 g for a slight and up to 4 g for strong or severe one. In the case of regular drink volumes, 100–150 mL, the GHB concentration can be between 3 and 40 g/L in liquids. It is demonstrated that the effects of GHB last for 3–6 h, starting 15–30 min after intake. Nevertheless, GHB is rapidly eliminated from the body (half-life of 10–53 min) [4] and, therefore, the detection window is rather short, that is, approximately 3 h in oral fluids, 5 h in blood samples and less than 12 h in urine samples [4, 5]. Thus, samples should be collected as quickly as possible after intake. It is especially critical for the detection of GHB abuse using oral samples and blood.

Despite the illicit consumption of chemically synthesized compounds, GHB and GBL are fermentation by-products that occur naturally in different beverages such as soya as well as white and red wines. In contrast to the illicit consumption doses, the concentration levels of GHB and GBL are very low. The highest content found in red wines is from 4.1 to 21.4 mg/L [6]. Therefore, wine drinking can increase, to a minor extent, the endogenous GHB content in biological samples. But, the levels of GHB after wine drinking are not comparable to the illicit drug doses, which are several orders higher.

Furthermore, GHB is a well-known prescription drug for the treatment of narcolepsy, alcoholic abuse and catalepsy [7]. Moreover, GHB is also used by body builders as a muscle-growth enhancer [8]. Therefore, the accurate endogenous and exogenous GHB level interpretation in biological samples is critical for point-of-care and drug-abuse testing. The following cut-off limits are proposed to distinguish endogenous from exogenous GHB in clinical samples: 4–10 mg/L in urine [9] and 2–5 mg/L in blood [2].

The above facts make the analysis of GHB challenging in biological samples. Undoubtedly, the accurate and sensitive analysis of the small polar organic molecule with weak UV-absorbing properties is a complex feature for toxicological sample investigation. The main methods for the determination of GHB in biological samples are GC-FID, GC-MS, LC-MS-MS [10], and HPLC-MS/MS [3]. These methods are generally time consuming and require complex sample preparation including derivatization. However, there are a limited number of studies investigating the application of CE for the determination of either endogenous or exogenous GHB levels in biological samples. Most publications using CE as a separation method deal with urine, serum, or blood samples [11], but neither of them utilize saliva samples. Biological samples have mainly been investigated by CE coupled with indirect UV absorbance detection or MS [12], and few of them by contactless conductivity detector ( $C^4D$ ). Nevertheless, the only reported research by Hauser et al. [13] has implied CE- $C^4D$  for the detection of GHB, but only in urine and blood serum samples. Therefore, the current study implements CE- $C^4D$  with sequential indirect UV detection for the first time in the determination of GHB in saliva samples.

Different hyphenated techniques with different methodologies are proposed for the determination and quantification of GHB in urine [13, 14], blood [14], and saliva [1, 15]. Certainly, one of the suitable methods for the detection of weakly or nonabsorbing small organic and inorganic molecules is CE coupled with a  $C^4D$ . The main advantage of CE- $C^4D$  is the miniaturization possibility of the instrument and, therefore, the possibility to conduct measurements on the scene of the crime. CE- $C^4D$  was successfully applied for the detection of simple organic and inorganic compounds in oral fluids, blood serum, urine, exhaled breath condensate, and saliva by Kubáň et al. [16, 17]. Moreover, saliva is a perspective sample matrix containing thousands of compounds that can be suggested as markers for health disorders. Therefore, known markers can be used to monitor metabolism processes in organisms [18]. Despite the marker exploration, saliva is an excellent source for the determination drug of abuse. Saliva has the merit of being easy to collect.

The purpose of the present study was to demonstrate the use of saliva as a sample in the screening of GHB abuse by CE. The feasibility study of the sequential dual detection system using conductivity and indirect UV for biological sample analysis was performed and evaluated. Both detection modes, with the optimized methodology, were validated according to the European Guideline on bioanalytical method validation (EMA/275542/2014) [19].

## 2 Materials and methods

### 2.1 Standards and chemicals

All chemicals were analytical grade. Sodium  $\gamma$ -hydroxybutyrate (GHB) powder and a solution of 1 mg/mL GHB salt in methanol were purchased from Lipomed AG (Germany). ACN (HPLC grade), maleic acid, L-arginine (Arg), CTAB, pinacolyl methylphosphonic acid (PMPA), calcium chloride, potassium nitrate, potassium nitrite, magnesium sulfate, sodium sulfite, sodium thiocyanate, disodium hydrogen phosphate, sodium hydroxide, and succinic, tartaric, citric, lactic acid, and glutamic acid were obtained from Sigma-Aldrich (Germany). Ultrapure water (Milli-Q) (resistivity  $\geq 18 M\Omega cm$ ) was obtained using a Milli-Q integral water purification system (Merck KGaA, Germany). Saliva samples were collected from six volunteers (both male and female, age ranging from 25 to 70). Two red wines “Le Grand Noir” (85% Cabernet/15% of Shiraz, 13% vol, France, 2013) and “Vina Maipo Vitral” (Cabernet Sauvignon, 13.5% vol, Valle del Maipo, Chile, 2011) were purchased at a local store in Estonia.

### 2.2 Separation procedure

The in-house built portable CE device equipped with a  $C^4D$  [20] (Chemistry Department, TUT, Estonia) and an Agilent 3D CE instrument (Agilent Technologies, Waldbronn, Germany) equipped with a DAD were combined in this study.

The conductivity detection cell was incorporated into the Agilent 3D CE capillary cassette. The sample injection, CE analysis was conducted inside Agilent 3D CE instrument. The conductivity signal was registered by in-house built hardware for CE-C<sup>4</sup>D, absorbance signal by Agilent 3D CE instrument hardware, respectively. An uncoated fused silica capillary (Agilent Technologies, USA) with a total length of 65 cm, effective length of 45 cm to the C<sup>4</sup>D and 56.5 cm to the DAD (id 50 μm and od 360 μm) was used to separate the analyte of interest. The applied voltage was −19 kV. The C<sup>4</sup>D frequency was set to 150 kHz. The indirect UV absorbance was recorded at λ<sub>ABS</sub> = 210 nm.

The proposed methodology for GHB analysis in urine and serum samples by Hauser et al. [13] was modified and optimized for saliva samples and the current system. The stock BGE solution consisted of 10 mM maleic acid, 20 mM Arg, and 300 μM CTAB adjusted to pH 7.35. As an organic modifier, 15% acetonitrile was added to the stock BGE, with slight adjustment of the final pH to 7.65 and decreasing the BGE components content to 8.5 mM maleic acid, 17 mM Arg, and 255 μM CTAB. The final BGE was ultrasonicated (Bandelin electronic, Germany) for 10 min, degassed by 10% at 30°C and then filtered through a 20 μm cellulose filter (Sartorius Stedim Biotech, Germany). Prior to CE analysis, the capillary was activated and washed every day with 1 mM NaOH for 10 min, Milli-Q water for 10 min and BGE for 15 min. The injection was conducted hydrodynamically for 10 s at 35 mbar. Between the experiments, the capillary was rinsed for 3 min with BGE. Moreover, the capillary was washed with methanol for 10 min, Milli-Q water for 10 min and BGE for 15 min, at least after 20 analyses in order to prevent adsorption on the capillary surface.

### 2.3 Sample collection and preparation

The GHB salt was dissolved in an acetonitrile/Milli-Q solution (1:1) (5 g/L) and further dilutions were prepared in acetonitrile. Saliva samples were collected prior to analyses and stored in a freezer (−18°C) until used (but not longer than 6 months). A minimum of 400 μL of saliva sample was collected in a 1.5 mL Eppendorf tube. Then, 2 μL of 10 mM PMPA (final 100 μM) in water as internal standard (IS) and 148.5 μL of acetonitrile added to 49.5 μL of the saliva sample. The sample was thoroughly mixed and the supernatant was separated by centrifugation for 10 min at a maximum speed of 6000 rpm in a mini-centrifuge for 1.5 mL Eppendorf tubes (Sarstedt AG&Co, Germany). The supernatant was transferred to a new Eppendorf tube and used for further analysis by CE.

### 2.4 CE data preprocessing

The reproducibility in terms of the migration time is of importance in CE in order to identify the analyte of interest. Therefore, electropherograms were corrected using the

method proposed by Zhang and Chen prior to the analysis of the CE data [21]. Two internal substance components, such as exogenous IS (PMPA) and endogenous IS (chloride ion), were used for correction coefficient evaluation for each electropherogram against the standard, using the following equation:

$$\gamma = \frac{\frac{1}{t_I} - \frac{1}{\widehat{t}_P}}{\frac{1}{t_I} - \frac{1}{t_P}} \quad (1)$$

The new migration time ( $t_x$ ) was found using the calculated correction coefficient  $\gamma$ :

$$t_x = \left[ \frac{1}{t_I} - \frac{1}{\gamma} \left( \frac{1}{\widehat{t}_I} - \frac{1}{\widehat{t}_x} \right) \right]^{-1}, \quad (2)$$

where  $\gamma$  is the correction coefficient,  $t_I$  and  $t_P$  are migration times of the exogenous and endogenous ISs, respectively,  $\widehat{t}_I$  and  $\widehat{t}_P$  are migration times of PMPA and chloride ions, respectively, in the electropherogram under correction;  $t_x$  is the corrected migration time for corrected electropherogram and  $\widehat{t}_x$  is the migration time of the electropherogram under correction.

## 2.5 Validation

Validation of the CE methodology was carried out in concordance to the European Guideline on bioanalytical method validation (EMA/275542/2014) published by the European Medicine Agency in 2009 and adapted in 2012 [19]. This guideline sets the minimum performance parameters for small (MW < 1000 Da), medium (1000 < MW < 10 000 Da), and large molecules (MW > 10 000 Da) that are to be evaluated and set their acceptance criteria. As the GHB ( $M_r = 104.1$  g/mol) is referred to as a small molecule, the following CE performance parameters were evaluated: selectivity, carry-over effect, lower LOQ (LLOQ), calibration curve, accuracy, precision, matrix effect (ME), and efficacy/extraction recovery.

### 2.5.1 Design of experiments

The design of experiments for the robustness study was developed using the Box–Behnken experimental design [22]. Small variations in the BGE composition were investigated in the robustness study using response surface regression analysis [23]. The changes represent typical errors that can occur in daily analyses. The following parameter ranges were used to conduct a Box–Behnken design at three levels: maleic acid  $10 \pm 1$  mM, arginine  $20 \pm 2$  mM, and CTAB  $300 \pm 25$  μM. The levels were coded as −1 for the minimum, 0 for nominal and 1 for the maximum change. The BGE pH remained the same and was always adjusted to 7.35 prior to analysis, using the appropriate amount of aqueous sodium hydroxide solution. Six independent replicates were conducted for each design order.

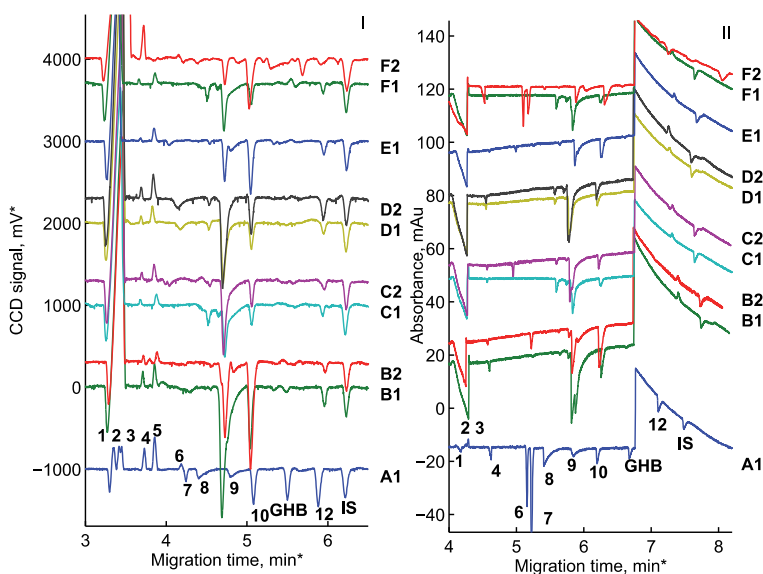


**Figure 1.** Various profiles of saliva samples: (I) CE-conductivity detection; (II) Indirect absorbance detection ( $\lambda_{\text{ABS}} = 210 \text{ nm}$ ). Analytes: 1, Chloride (5 mg/L); 2, Nitrite (10 mg/L); 3, Nitrate (10 mg/L); 4, Sulfate (10 mg/L) and sulfite (5 mg/L); 5, Thiocyanate (40 mg/L); 6, Tartrate (120 mg/L); 7, Succinate (80 mg/L); 8, Citrate (–120 mg/L); 9, Hydrogen phosphate (20 mg/L); 10, Lactate (20 mg/L); 11, GHB (20 mg/L); 12, Glutamate (20 mg/L); 13, PMPA (IS). Applying the working conditions. BGE: 8.5 mM maleic acid, 17 mM Arg, and 255  $\mu\text{M}$  CTAB, 15% ACN, pH = 7.65; capillary length, 65.0 cm; temperature, 21°C; voltage, –19 kV; hydrodynamic injection, 35 mbar for 10 s; contactless conductivity detection, frequency 150 Hz; absorbance detection,  $\lambda_{\text{ABS}} = 210 \text{ nm}$ ; sample acetonitrile ratio, 1:3.

## 2.6 Software

Data were processed with in-lab-made software for peak acquisition (TUT, Chemistry Department, Estonia), Chemstation (Agilent Technologies, Waldbronn, Germany), and PLS toolbox 6.2 (Eigenvector Research) in Matlab R2011b.

## 3 Results and discussion

### 3.1 CE methodology optimization

The preliminary study was conducted using the proposed methodology by Hauser et al. [13]. Unfortunately, the time of analysis was more than 10 min and, therefore, the methodology was not suitable for quick onsite analysis of saliva samples. Therefore, it was decided that the methodology should be optimized for efficient and rapid GHB separation in saliva samples within 10 min. At the BGE pH of 7.65, GHB ( $pK_a$  is 4.71) was negatively charged and migrated as an anion in BGE. Moreover, the high pH value assured that GHB did not convert to the lactone form GBL.

It was found out that the concentration of CTAB, as a cationic modifier, and ACN, as an organic modifier, drastically affected the migration time, resolution ( $R_s$ ), and efficiency in terms of theoretical plates ( $N$ ) of anions naturally occurring in saliva. First, different concentrations of CTAB, such as 30, 100, and 300  $\mu\text{M}$ , were tested. Upon addition of CTAB to the BGE (ACN0%), there was a rapid transition from normal (cathodic) to reversed (anodic) EOF. The increase of CTAB concentration led to the decrease of EOF migration time from 18 min to 6.2 min, indicating the com-

plete EOF reversal in the BGE. A stable baseline and a good resolution ( $R_s > 1.2$ ) between GHB and neighbor peaks, as well as a short separation time, were obtained with 300  $\mu\text{M}$  CTAB in the BGE. Second, the voltage was optimized (–5, –10, –15, and –19 kV). The separation at –19 kV was assumed to be the most suitable, as the separation of GHB in spiked saliva was achieved in 3.6 min (sample: ACN 1:1, BGE + ACN0%) (S – Fig. 1I–A3). The sample preparation was optimized in addition to the optimization of BGE and CE conditions. Whole saliva proteins were precipitated using ACN in ratios of 1:1, 1:2, and 1:3 (sample/acetonitrile). The best resolution, a stable baseline and the most effective precipitation of proteins in saliva were achieved with the ratio of 1:3. Moreover, adding ACN to the saliva sample that contained a high concentration of inorganic ions (chloride presents at about 5 mM in resting and up to 70 mM in stimulated saliva [24]) increased the efficiency of CE separation via a “ACN-salt stacking” effect [25]. The stacking mechanism was similar to the transient isotachopheresis. The salts, due to the limited solubility in ACN, moved rapidly with some water in the front, creating the region with a low field strength and leaving behind a more concentrated zone of ACN (the region with a high field strength), where organic anions were moving faster, slowing down at the region of a low field strength. Furthermore, ACN, as an organic modifier, could affect the capillary surface in the BGE, changing its viscosity by inducing solvent–solute and solute–solute interactions, as well as by modifying the  $pK_a$  of ionization of the silanol group, solute molecules, and analytes—thus resulting in the alteration of electroosmotic and electrophoretic mobility. The addition of ACN to the BGE increased the sensitivity and improved the resolution (Supporting Information

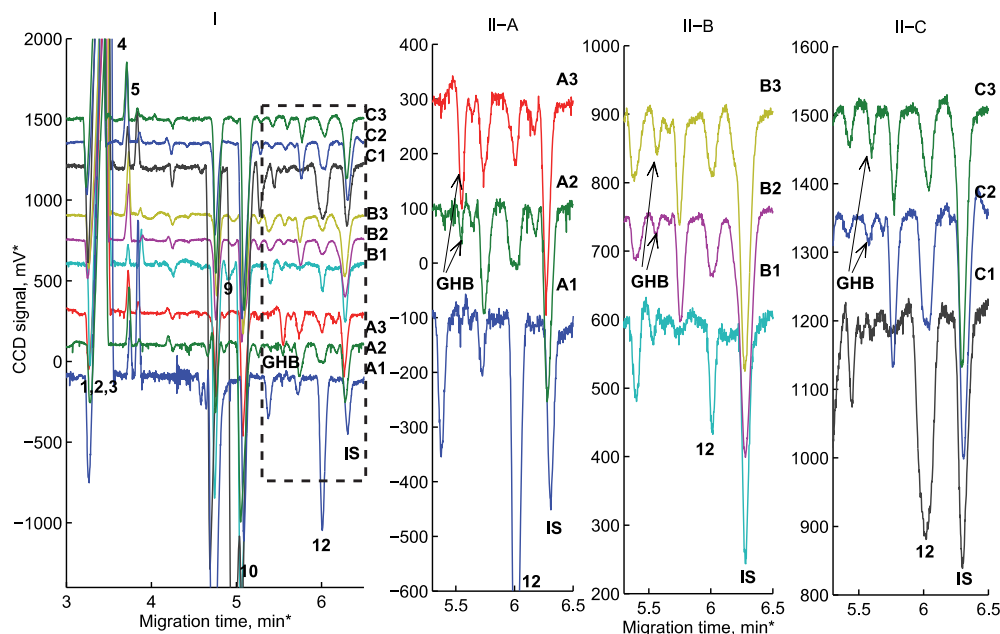


**Figure 2.** (I) CE-C<sup>4</sup>D electropherograms of saliva samples after red wine drinking; (II) Zoomed region of electropherogram from 5.3 to 6.5 min: (A1) Blank saliva of volunteer #5; (A2) Volunteer's #5 saliva after drinking of 40 cl of "Le Grand Noir"; (A3) Volunteer's #5 saliva spiked with 20 mg/L GHB (#11) after drinking of 40 cl of "Le Grand Noir"; (B1) Blank saliva of volunteer #6; (B2) Volunteer's #6 saliva after drinking of 30 cl of "Vina Maipo Vitral"; (B3) Volunteer's #6 saliva spiked with 10 mg/L GHB (#11) after drinking of 30 cl of "Vina Maipo Vitral"; (C1) Blank saliva of volunteer #5; (C2) Volunteer's #5 saliva after drinking of 30 cl of "Vina Maipo Vitral"; (C3) Volunteer's #5 saliva spiked with 10 mg/L GHB (#11) after drinking of 30 cl of "Vina Maipo Vitral."

Fig. 1, Fig. 1II). The best results were achieved with the BGE containing 15% of ACN.  $N_{\text{GHB}}$  was increased from 60 000 (ACN0%) to 120 000 (ACN10%) and, finally, to 255 000 (ACN15%) plates per meter. However, because of the added ACN, the GHB migration time increased to 5.5 min (ACN15%) (CV% uncorrected 7.3–9.4%) due to a lower EOF velocity that was caused by a lower dielectric constant and a higher viscosity. In spite of that, the time required for analysis was within a 10-min timeframe, and the sensitivity improvement (fourfold) was of more importance.

## 3.2 Validation of CE methodology

### 3.2.1 Identification

Saliva consists of 99% water, containing inorganic ions (sodium, chloride, nitrate, nitrite, phosphate, and others) and proteins (enzymes, immunoglobulins, and others). The presence of different substances reflects the metabolism processes in the body and, subsequently, shows the body's health and wellbeing. For example, it was found that physical activity changes the sodium and lactate ion contents [24].

Moreover, saliva can indicate medication or illegal-drug consumption.

Prior to knowledge of possible interferences, the identity of GHB was studied in different samples. The identity study was based on selectivity/specificity, showing the ability of the methodology to distinguish the analyte of interest, GHB, and IS, PMPA ( $t_{\text{mig}} = 6.3$  min), from the endogenous matrix components under the optimized methodology. As the composition of saliva varies from person to person, six samples were analysed for possible interferences. Moreover, the saliva variations under different effects were monitored, including intensive physical training, upper respiratory tract infection (URT) with administration of Ospamox (1000 mg of Amoxicillin, Sandoz GmbH, Austria), long-term tobacco smoking, drinking of orange juice, and the consumption of two red wines. Moreover, the possible anions, such as chloride, nitrate, nitrite, sulfate, sulfite, thiocyanate, succinate, tartrate, citrate, hydrogen phosphate, lactate, and glutamate, that can be found in saliva naturally or occur after the administration of different products (juice, coffee, wine, etc.) were identified. Possible comigration with GHB was studied. All samples were suggested as true-negative samples, except for the red wine, in which GHB can be naturally found.

Table 1. CE-CCD and indirect UV absorbance performance characteristics

Range, mg/L	$n$ , $Tn^*$	$R^2$	Equation (Area <sub>GHb</sub> /Area <sub>Ag</sub> )100%	IDL (IOL)	ILLOQ (IULOQ)	LoD (LoD)	Precision (interday/intraday)	Accuracy (recovery), %	ME %
<b>Conductivity detection</b>									
GHb in water	2.5–400	$n = 6$ ; $Tn = 36$	$y = (3.63 \pm 0.07)x + (-34.5 \pm 10.0)$	0.62	2.5	2.5	2.5: 1.1%/1.6% 7.5: 0.9%/4.3%	2.5: 117.1 ± 1.7 7.5: 100.2 ± 4.8	
GHb in water (small)	2.5–25	$n = 6$ ; $Tn = 36$	$y = (1.97 \pm 0.03)x + (1.13 \pm 0.38)$	(2.1)	(400)	(8.3)	100: 2.2%/6.6% 300: 2.0%/1.5%	100: 106.5 ± 6.4 300: 101.1 ± 1.5	
Saliva	2.5–400	$n = 6$ ; $Tn = 36$	$y = (3.62 \pm 0.03)x + (-12.77 \pm 4.1)$	0.49	2.50	2.0	2.5: 2.6%/5.9% 7.5: 2.4%/3.4%	2.5: 100.1 ± 3.4 7.5: 95.7 ± 4.2	-0.3
Saliva (small)	2.5–25	$n = 6$ ; $Tn = 36$	$y = (3.02 \pm 0.35)x + (6.90 \pm 0.35)$	(1.6)	(400)	(6.5)	00: 5.7%/9.0% 1300: 2.3%/1.6%	100: 87.9 ± 5.6 300: 102.1 ± 2.4	+53.2
<b>UV absorbance-indirect detection (<math>\lambda_{Abs} = 210 \text{ nm}</math>)</b>									
GHb in water	12.5–400	$n = 6$ ; $Tn = 36$	$y = (3.78 \pm 0.08)x + (-44.6 \pm 11.5)$	3.7	12.5	14.8	12.5: 1.7%/2.2% 35: 3.0%/5.9%	12.5: 111.2 ± 1.8 35: 100.3 ± 2.1	
GHb in water (small)	12.5–75	$n = 6$ ; $Tn = 36$	$y = (1.95 \pm 0.06)x + (-6.7 \pm 2.6)$	(12.4)	(400)	(49.7)	100: 1.1%/14.6% 400: 4.8%/3.5%	100: 97.6 ± 12.5 400: 100.3 ± 3.5	
Saliva	12.5–400	$n = 6$ ; $Tn = 36$	$y = (3.86 \pm 0.07)x + (-47.2 \pm 11.6)$	5.1	12.5	20.4	12.5: 4.4%/6.1% 35: 2.1%/5.6%	12.5: 104.4 ± 5.5 35: 95.3 ± 1.9	+2.0
Saliva (small)	12.5–75	$n = 6$ ; $Tn = 36$	$y = (2.41 \pm 0.07)x + (-7.9 \pm 2.2)$	(17.0)	(400)	(68.0)	100: 9.3%/10.1% 400: 2.5%/6.3%	100: 87.2 ± 8.0 400: 101.1 ± 2.5	+23.6

\* $n$ , number of concentration levels and  $Tn$ , total number of measurements used for linear regression construction.

Figure 1 presents the electropherograms of Milli-Q water spiked with different anions found in saliva (A1) and whole saliva blanks (B1, D1, F1) in comparison to saliva after training (D2), long-term tobacco smoker saliva (E1), saliva of a volunteer with a URT infection (C1) and that after treatment (the fourth day of Ospamox administration) (C2) as well as saliva samples after juice (B2) and red wine consumption (F2). There was no migration observed for the analyte of interest, GHB, with the tested substances under the optimized conditions. Moreover, consumption of 10 cl of red wine has not significantly increased the endogenous GHB content in saliva and remained below instrument detection limit (IDL). Therefore, it was concluded that the optimized system has successfully passed the identity study. Moreover, the system was successful for the codetection of thiocyanate, lactate, and glutamate by  $C^4D$ . Furthermore, BGE has proven to be suitable for sequential detection by conductivity and then indirect UV absorbance. It was observed that indirect UV absorbance detection was perfect for tartrate, succinate, citrate, hydrogen phosphate, lactate, glutamate, and GHB (Fig. 1II: A1).  $C^4D$  detection was not so sensitive to tartrate, succinate, citrate, or hydrogen phosphate. As saliva contains a very high concentration of chloride ions, it was impossible to separate chloride from nitrate and nitrite in real samples. Nevertheless, the effective separation of the latter ions was not the aim of the current study, but only an additional observed fact.

### 3.2.2 Limits of detection and quantification

The LOD and LOQ were evaluated in saliva by spiking GHB at different concentration levels in blank saliva: 0, 2.5, 5, 7.5, 10, 12.5, and 25 mg/L for  $C^4D$  and higher concentrations were needed for indirect UV absorbance: from 12.5 to 75 mg/L. At least six independent replicates for each concentration were conducted. The linearity was evaluated with higher concentrations up to 400 mg/L.

Linearity was found up to 400 mg/L for  $C^4D$  and indirect UV absorbance. The IDL was defined using a 95% prediction interval of the regression line [25]. The IDL was 0.49 mg/L and the instrument quantification limit (IQL) was 1.6 mg/L in saliva for  $C^4D$ . The IDL and IQL for indirect detection were lower, as expected, at 5.1 and 17 mg/L in saliva, respectively. Taking into account the sample preparation, the LOD equalled 2.0 mg/L and the LOQ 6.5 mg/L for  $C^4D$  and 20.4 mg/L and 68 mg/L for indirect UV absorbance in saliva, respectively.

Despite the fact that the IQL was sometimes lower than the lowest calibration level (for conductivity), the instrument lower LOQ (ILLOQ) was set to 2.5 mg/L and instrument upper quantification limit was set to 400 mg/L. It was found that the LOQ of 6.5 mg/L for the  $C^4D$  was suitable for accurate differentiation between exogenous and endogenous GHB levels in the case of a 10 mg/L cut-off limit. Unfortunately, the sensitivity of indirect UV absorbance was not enough, but could be used for the quantification of higher concentrations up to

**Table 2.** Box–Behnken design of experiments and response values for robustness study (*number of replicates* = 6)

Run order	Design order	[Maleic acid], mM	[Arginine], mM	[CTAB], $\mu$ M	$R_{U1-GHB}$	$R_{GHB-U2}$	$N_{GHB}$ ( $10^5$ )	$t_{R\ GHB}$ , min
1	1	-1	-1	0	2.2	1.2	1.43	4.3
2	5	0	-1	-1	2.2	1.4	1.46	4.4
3	3	-1	0	1	2.1	1.8	1.19	4.5
4	11	1	0	-1	2.4	1.2	1.24	4.7
5	13	1	1	0	2.4	1.1	0.98	4.4
6	2	-1	0	-1	2.2	1.4	0.77	4.3
7	8	0	1	-1	2.5	1.2	1.15	4.5
8	10	1	-1	0	2.7	1.2	0.90	4.6
9	6	0	-1	1	2.1	1.3	0.69	4.6
10	9	0	1	1	1.6	1.3	0.48	4.5
11	12	1	0	1	1.6	1.7	0.41	4.5
12	4	-1	1	0	1.3	2.3	0.28	4.5
13	7	0	0	0	2.1	1.2	1.07	4.7

257 mg/L of GHB, which can be found in saliva samples after GHB consumption [4].

### 3.2.3 Accuracy and precision

A precision study was carried out to assure the reproducibility of the proposed methodology. The results were expressed as the coefficient of variation (CV%) and evaluated at four levels: LLOQ,  $3 \times$  LLOQ, MLOQ (medium LOQ, 30–50% from calibration range) and at 75% of the upper LOQ (ULOQ) or at the ULOQ for indirect UV absorbance. The interday precision was evaluated using six replicates of spiked blank saliva and Milli-Q for each concentration level and intraday precision was evaluated over 3 days, preparing the same concentration levels. The inter- and intraday precisions (CV%) were below the acceptance level of 15% for the tested concentrations and below 20% for the LLOQ. The interday precision was within 2.3–5.7% and intraday within 1.6–9.0% for C<sup>4</sup>D and 2.1–9.3% or 5.6–10.1% for indirect UV in spiked saliva, respectively. The precision results showed good reproducibility and repeatability.

The accuracy was assessed for samples spiked with GHB before the sample preparation at four concentration levels: LLOQ,  $3 \times$  LLOQ, MLOQ (30–50% from calibration range) and at 75% of ULOQ or at ULOQ for indirect UV absorbance. The accuracy was expressed as the relative recovery (Rec%). Six replicates for each level were conducted over three different days. The accuracy was within  $\pm 20\%$  of the nominal value at the LLOQ and within  $\pm 15\%$  of the nominal value for the other concentration levels. The results for each level are presented in Table 1.

### 3.2.4 Matrix effect

The ME indicates the saliva matrix components effect on GHB signal intensity. The positive ME value emphasizes the enhancement of the signal and the negative one shows the suppression of the signal. The ME was evaluated along a

range of concentrations using the slopes of calibration curve of GHB dissolved in water and in the saliva sample using the following equation [26]:

$$ME\% = \left( \frac{\text{slope}_{\text{matrix}}}{\text{slope}_{\text{solvent}}} - 1 \right) \times 100\%. \quad (3)$$

The ME% in the range of  $\pm 20$  ( $\pm 15$ )% (within accepted intraday precision) was designated as showing no matrix effects, while MEs within  $\pm 20$  ( $\pm 15$ )–50% and higher than  $\pm 50\%$  were assigned to a medium and strong ME, respectively [26].

A medium and strong MEs for the low concentration levels were observed for indirect UV absorbance (ME% of +23.6%) and for conductivity (ME% of +53.2%), respectively. Therefore, the concentration levels between 2.5–25 mg/L of GHB for C<sup>4</sup>D must be evaluated using either the calibration curve constructed by the standard addition method or applying the correction factor to the traditional calibration curve, thus eliminating ME. No MEs (<15%) were observed for the higher concentration levels (Table 1).

### 3.2.5 Robustness study

Since only CE-C<sup>4</sup>D was capable to differentiate the exogenous and endogenous GHB concentrations in saliva, the robustness study for CE-C<sup>4</sup>D was conducted using a saliva sample matrix spiked at the cut-off level of 10 mg/L GHB. The design order was randomized and the run order of the experiments was conducted as shown in Table 2. The responses, such as migration time ( $t_{R\ GHB}$ ) of GHB, the number of theoretical plates ( $N_{GHB}$ ) and the two resolution values between undefined peaks migrated before and after GHB, U1-GHB ( $R_{U1-GHB}$ ), and GHB-U2 ( $R_{U2-GHB}$ ), were recorded and calculated (Table 2). It was found that  $N_{GHB}$  is significantly affected by concentration variations of [CTAB] (+1) and [arginine] (+1) and their interactions [maleic acid]  $\times$  [CTAB] and [maleic acid]  $\times$  [arginine] ( $p$ -value < 0.050). Therefore, CE-C<sup>4</sup>D method is sensitive to small variations of BGE at GHB cut-off level and, therefore, extreme attention must be paid to correct BGE preparation.

### 3.3 Real sample analysis

GHB can be found in food and beverages, that is, in sherry as well as white and red wines. Red wine is a natural source of GHB, and the GHB concentration can be up to 21.4 mg/L (mean 12.6 mg/L) [6]. Therefore, two different red wines (red wine 1 and red wine 2) were chosen for the detection of GHB in saliva samples. The analysis of blank saliva was conducted prior to wine drinking. The GHB endogenous occurrence in saliva was investigated using 10 cl doses of red wine. Each dose was completed during 3–4 min and followed by the new one after sample collection. The saliva sample was collected after 2-min interval of every completed dose. Slight increase of GHB peak height was observed after drinking 30 and 40 cl of red wine. The experiment was finished within 25 min due to short half-life of GHB (10–53 min).

The identity of the GHB peak was further confirmed by spiking GHB into the same sample. It follows that minor quantities in human saliva can be unambiguously detected (Fig. 2). The quantification of GHB was not conducted, as it was below the IQL. But, the detection of the presence of GHB in red wine has proven the possibility to detect GHB in saliva based on CE with C<sup>4</sup>D and indirect UV absorbance detection. The analysis of clinical samples after GHB consumption is to be conducted in further research.

### 4 Concluding remarks

In this paper, CE-C<sup>4</sup>D–indirect absorbance was successfully applied for the determination of GHB in saliva samples. The validation results show that CE-C<sup>4</sup>D has suitable sensitivity for the differentiation of endogenous and exogenous concentrations of GHB in saliva. The biggest advantages of the proposed methodology are the short time of analysis, sensitivity, and simple sample preparation that can be further automated and miniaturised for on-site confirmation analysis.

*The authors acknowledge financial support from the Estonian Science Fund (Grant ETF9106), the Estonian Research Council (Institutional Research Fund No. 33-20 “Advancing analytical and computational chemistry methods for regulatory decisions”). This work has been supported by the European Social Fund’s Doctoral Studies and Internationalisation Programme DoRa, which is carried out by Foundation Archimedes.*

*The authors have declared no conflict of interest.*

### 5 References

- [1] De Paoli, G., Walker, K. M., Pounder, D. J., *J. Anal. Toxicol.* 2011, 35, 148–152.
- [2] Andresen, H., Sprys, N., Schmoltdt, A., Mueller, A., Iwersen-Bergmann, S., *Forensic Sci. Int.* 2010, 200, 93–99.
- [3] Ingels, A.-S. E., Wille, S. R., Samyn, N., Lambert, W., Stove, C., *Anal. Bioanal. Chem.* 2014, 406, 3553–3577.
- [4] Kintz, P., Goulle, J. P., Cirimele, V., Ludes, B., *Clin. Chem.* 2001, 47, 2033–2034.
- [5] Brenneisen, R., Elshohly, M. A., Murphy, T. P., Passarelli, J., Russmann, S., Salamone, S. J., Watson, D. E., *J. Anal. Toxicol.* 2004, 28, 625–630.
- [6] Elliott, S., Burgess, V., *Forensic Sci. Int.* 2005, 151, 289–292.
- [7] Carter, L. P., Pardi, D., Gorsline, J., Griffiths, R. R., *Drug Alcohol Depend.* 2009, 104, 1–10.
- [8] Mason, P. E., Kerns, W. P., *Acad. Emerg. Med.* 2002, 9, 730–739.
- [9] LeBeau, M. A., Christenson, R. H., Levine, B., Darwin, W. D., Huestis, M. A., *J. Anal. Toxicol.* 2002, 26, 340–346.
- [10] Johansen, S. S., Windberg, C. N., *J. Anal. Toxicol.* 2011, 35, 8–14.
- [11] Bortolotti, F., De Paoli, G., Gottardo, R., Trattene, M., Tagliaro, F., *J. Chromatogr. B* 2004, 800, 239–244.
- [12] Baldacci, A., Theurillat, R., Caslavská, J., Pardubská, H., Brenneisen, R., Thormann, W., *J. Chromatogr. A* 2003, 990, 99–110.
- [13] Gong, X. Y., Kuban, P., Scholer, A., Hauser, P. C., *J. Chromatogr. A* 2008, 1213, 100–104.
- [14] Kaufmann, E., Alt, A., *Forensic Sci. Int.* 2007, 168, 133–137.
- [15] De Paoli, G., Bell, S., *J. Anal. Toxicol.* 2008, 32, 298–302.
- [16] Kubáň, P., Kobrin, E.-G., Kaljurand, M., *J. Chromatogr. A* 2012, 1267, 239–245.
- [17] Kubáň, P., Ďurč, P., Bittová, M., Foret, F., *J. Chromatogr. A* 2014, 1325, 241–246.
- [18] Baena, B., Cifuentes, A., Barbas, C., *Electrophoresis* 2005, 26, 2622–2636.
- [19] European Medicines Agency, Committee for Medicinal Products for Human Use, London, UK 2011.
- [20] Makarõtsëva, N., Seiman, A., Vaher, M., Kaljurand, M., *Proc. Chem.* 2010, 2, 20–25.
- [21] Zhang, H., Chen, H., *Anal. Methods* 2011, 3, 745–750.
- [22] Hows, M. E. P., Perrett, D., Kay, J., *J. Chromatogr. A* 1997, 768, 97–104.
- [23] Ragonese, R., Macka, M., Hughes, J., Petocz, P., *J. Pharm. Biomed. Anal.* 2002, 27, 995–1007.
- [24] Guilbault, G. G., Palleschi, G., Lubrano, G., *Biosensors Bioelectronics* 1995, 10, 379–392.
- [25] Ermer, J., Burgess, C., Kleinschmidt, G., McB Miller, J. H., *Method Validation in Pharmaceutical Analysis*, Wiley-VCH Verlag GmbH & Co. KGaA, Weinheim 2005, pp. 21–194.
- [26] Caban, M., Migowska, N., Stepnowski, P., Kwiatkowski, M., Kumirska, J., *J. Chromatogr. A* 2012, 1258, 117–127.

**DISSERTATIONS DEFENDED AT  
TALLINN UNIVERSITY OF TECHNOLOGY ON  
NATURAL AND EXACT SCIENCES**

1. **Olav Kongas**. Nonlinear Dynamics in Modeling Cardiac Arrhythmias. 1998.
2. **Kalju Vanatalu**. Optimization of Processes of Microbial Biosynthesis of Isotopically Labeled Biomolecules and Their Complexes. 1999.
3. **Ahto Buldas**. An Algebraic Approach to the Structure of Graphs. 1999.
4. **Monika Drews**. A Metabolic Study of Insect Cells in Batch and Continuous Culture: Application of Chemostat and Turbidostat to the Production of Recombinant Proteins. 1999.
5. **Eola Valdre**. Endothelial-Specific Regulation of Vessel Formation: Role of Receptor Tyrosine Kinases. 2000.
6. **Kalju Lott**. Doping and Defect Thermodynamic Equilibrium in ZnS. 2000.
7. **Reet Koljak**. Novel Fatty Acid Dioxygenases from the Corals *Plexaura homomalla* and *Gersemia fruticosa*. 2001.
8. **Anne Paju**. Asymmetric oxidation of Prochiral and Racemic Ketones by Using Sharpless Catalyt. 2001.
9. **Marko Vendelin**. Cardiac Mechanoenergetics *in silico*. 2001.
10. **Pearu Peterson**. Multi-Soliton Interactions and the Inverse Problem of Wave Crest. 2001.
11. **Anne Menert**. Microcalorimetry of Anaerobic Digestion. 2001.
12. **Toomas Tiivel**. The Role of the Mitochondrial Outer Membrane in *in vivo* Regulation of Respiration in Normal Heart and Skeletal Muscle Cell. 2002.
13. **Olle Hints**. Ordovician Scolecodonts of Estonia and Neighbouring Areas: Taxonomy, Distribution, Palaeoecology, and Application. 2002.
14. **Jaak Nõlvak**. Chitinozoan Biostratigraphy in the Ordovician of Baltoscandia. 2002.
15. **Liivi Kluge**. On Algebraic Structure of Pre-Operad. 2002.
16. **Jaanus Lass**. Biosignal Interpretation: Study of Cardiac Arrhythmias and Electromagnetic Field Effects on Human Nervous System. 2002.
17. **Janek Peterson**. Synthesis, Structural Characterization and Modification of PAMAM Dendrimers. 2002.
18. **Merike Vaher**. Room Temperature Ionic Liquids as Background Electrolyte Additives in Capillary Electrophoresis. 2002.
19. **Valdek Mikli**. Electron Microscopy and Image Analysis Study of Powdered Hardmetal Materials and Optoelectronic Thin Films. 2003.
20. **Mart Viljus**. The Microstructure and Properties of Fine-Grained Cermets. 2003.
21. **Signe Kask**. Identification and Characterization of Dairy-Related *Lactobacillus*. 2003
22. **Tiiu-Mai Laht**. Influence of Microstructure of the Curd on Enzymatic and Microbiological Processes in Swiss-Type Cheese. 2003.
23. **Anne Kuusksalu**. 2–5A Synthetase in the Marine Sponge *Geodia cydonium*. 2003.
24. **Sergei Bereznev**. Solar Cells Based on Polycrystalline Copper-Indium Chalcogenides and Conductive Polymers. 2003.

25. **Kadri Kriis.** Asymmetric Synthesis of C<sub>2</sub>-Symmetric Bimorpholines and Their Application as Chiral Ligands in the Transfer Hydrogenation of Aromatic Ketones. 2004.
26. **Jekaterina Reut.** Polypyrrole Coatings on Conducting and Insulating Substrates. 2004.
27. **Sven Nõmm.** Realization and Identification of Discrete-Time Nonlinear Systems. 2004.
28. **Olga Kijatkina.** Deposition of Copper Indium Disulphide Films by Chemical Spray Pyrolysis. 2004.
29. **Gert Tamberg.** On Sampling Operators Defined by Rogosinski, Hann and Blackman Windows. 2004.
30. **Monika Übner.** Interaction of Humic Substances with Metal Cations. 2004.
31. **Kaarel Adamberg.** Growth Characteristics of Non-Starter Lactic Acid Bacteria from Cheese. 2004.
32. **Imre Vallikivi.** Lipase-Catalysed Reactions of Prostaglandins. 2004.
33. **Merike Peld.** Substituted Apatites as Sorbents for Heavy Metals. 2005.
34. **Vitali Syritski.** Study of Synthesis and Redox Switching of Polypyrrole and Poly(3,4-ethylenedioxythiophene) by Using *in-situ* Techniques. 2004.
35. **Lee Põllumaa.** Evaluation of Ecotoxicological Effects Related to Oil Shale Industry. 2004.
36. **Riina Aav.** Synthesis of 9,11-Secosterols Intermediates. 2005.
37. **Andres Braunbrück.** Wave Interaction in Weakly Inhomogeneous Materials. 2005.
38. **Robert Kitt.** Generalised Scale-Invariance in Financial Time Series. 2005.
39. **Juss Pavelson.** Mesoscale Physical Processes and the Related Impact on the Summer Nutrient Fields and Phytoplankton Blooms in the Western Gulf of Finland. 2005.
40. **Olari Ilison.** Solitons and Solitary Waves in Media with Higher Order Dispersive and Nonlinear Effects. 2005.
41. **Maksim Säkki.** Intermittency and Long-Range Structurization of Heart Rate. 2005.
42. **Enli Kiipli.** Modelling Seawater Chemistry of the East Baltic Basin in the Late Ordovician–Early Silurian. 2005.
43. **Igor Golovtsov.** Modification of Conductive Properties and Processability of Polyparaphenylene, Polypyrrole and polyaniline. 2005.
44. **Katrin Laos.** Interaction Between Furcellaran and the Globular Proteins (Bovine Serum Albumin  $\beta$ -Lactoglobulin). 2005.
45. **Arvo Mere.** Structural and Electrical Properties of Spray Deposited Copper Indium Disulphide Films for Solar Cells. 2006.
46. **Sille Ehala.** Development and Application of Various On- and Off-Line Analytical Methods for the Analysis of Bioactive Compounds. 2006.
47. **Maria Kulp.** Capillary Electrophoretic Monitoring of Biochemical Reaction Kinetics. 2006.
48. **Anu Aaspõllu.** Proteinases from *Vipera lebetina* Snake Venom Affecting Hemostasis. 2006.

49. **Lyudmila Chekulayeva.** Photosensitized Inactivation of Tumor Cells by Porphyrins and Chlorins. 2006.
50. **Merle Uudsemaa.** Quantum-Chemical Modeling of Solvated First Row Transition Metal Ions. 2006.
51. **Tagli Pitsi.** Nutrition Situation of Pre-School Children in Estonia from 1995 to 2004. 2006.
52. **Angela Ivask.** Luminescent Recombinant Sensor Bacteria for the Analysis of Bioavailable Heavy Metals. 2006.
53. **Tiina Lõugas.** Study on Physico-Chemical Properties and Some Bioactive Compounds of Sea Buckthorn (*Hippophae rhamnoides* L.). 2006.
54. **Kaja Kasemets.** Effect of Changing Environmental Conditions on the Fermentative Growth of *Saccharomyces cerevisiae* S288C: Auxo-accelerostat Study. 2006.
55. **Ildar Nisamedtinov.** Application of  $^{13}\text{C}$  and Fluorescence Labeling in Metabolic Studies of *Saccharomyces* spp. 2006.
56. **Alar Leibak.** On Additive Generalisation of Voronoï's Theory of Perfect Forms over Algebraic Number Fields. 2006.
57. **Andri Jagomägi.** Photoluminescence of Chalcopyrite Tellurides. 2006.
58. **Tõnu Martma.** Application of Carbon Isotopes to the Study of the Ordovician and Silurian of the Baltic. 2006.
59. **Marit Kauk.** Chemical Composition of CuInSe<sub>2</sub> Monograin Powders for Solar Cell Application. 2006.
60. **Julia Kois.** Electrochemical Deposition of CuInSe<sub>2</sub> Thin Films for Photovoltaic Applications. 2006.
61. **Iiona Oja Açıık.** Sol-Gel Deposition of Titanium Dioxide Films. 2007.
62. **Tiia Anmann.** Integrated and Organized Cellular Bioenergetic Systems in Heart and Brain. 2007.
63. **Katrin Trummal.** Purification, Characterization and Specificity Studies of Metalloproteinases from *Vipera lebetina* Snake Venom. 2007.
64. **Gennadi Lessin.** Biochemical Definition of Coastal Zone Using Numerical Modeling and Measurement Data. 2007.
65. **Enno Pais.** Inverse problems to determine non-homogeneous degenerate memory kernels in heat flow. 2007.
66. **Maria Borissova.** Capillary Electrophoresis on Alkylimidazolium Salts. 2007.
67. **Karin Valmsen.** Prostaglandin Synthesis in the Coral *Plexaura homomalla*: Control of Prostaglandin Stereochemistry at Carbon 15 by Cyclooxygenases. 2007.
68. **Kristjan Piirimäe.** Long-Term Changes of Nutrient Fluxes in the Drainage Basin of the Gulf of Finland – Application of the PolFlow Model. 2007.
69. **Tatjana Dedova.** Chemical Spray Pyrolysis Deposition of Zinc Sulfide Thin Films and Zinc Oxide Nanostructured Layers. 2007.
70. **Katrin Tomson.** Production of Labelled Recombinant Proteins in Fed-Batch Systems in *Escherichia coli*. 2007.
71. **Cecilia Sarmiento.** Suppressors of RNA Silencing in Plants. 2008.
72. **Vilja Mardla.** Inhibition of Platelet Aggregation with Combination of Antiplatelet Agents. 2008.

73. **Maie Bachmann.** Effect of Modulated Microwave Radiation on Human Resting Electroencephalographic Signal. 2008.
74. **Dan Hüvonen.** Terahertz Spectroscopy of Low-Dimensional Spin Systems. 2008.
75. **Ly Villo.** Stereoselective Chemoenzymatic Synthesis of Deoxy Sugar Esters Involving *Candida antarctica* Lipase B. 2008.
76. **Johan Anton.** Technology of Integrated Photoelasticity for Residual Stress Measurement in Glass Articles of Axisymmetric Shape. 2008.
77. **Olga Volobujeva.** SEM Study of Selenization of Different Thin Metallic Films. 2008.
78. **Artur Jõgi.** Synthesis of 4'-Substituted 2,3'-dideoxynucleoside Analogues. 2008.
79. **Mario Kadastik.** Doubly Charged Higgs Boson Decays and Implications on Neutrino Physics. 2008.
80. **Fernando Pérez-Caballero.** Carbon Aerogels from 5-Methylresorcinol-Formaldehyde Gels. 2008.
81. **Sirje Vaask.** The Comparability, Reproducibility and Validity of Estonian Food Consumption Surveys. 2008.
82. **Anna Menaker.** Electrosynthesized Conducting Polymers, Polypyrrole and Poly(3,4-ethylenedioxythiophene), for Molecular Imprinting. 2009.
83. **Lauri Ilison.** Solitons and Solitary Waves in Hierarchical Korteweg-de Vries Type Systems. 2009.
84. **Kaia Ernits.** Study of In<sub>2</sub>S<sub>3</sub> and ZnS Thin Films Deposited by Ultrasonic Spray Pyrolysis and Chemical Deposition. 2009.
85. **Veljo Sinivee.** Portable Spectrometer for Ionizing Radiation "Gammamapper". 2009.
86. **Jüri Virkepu.** On Lagrange Formalism for Lie Theory and Operadic Harmonic Oscillator in Low Dimensions. 2009.
87. **Marko Piirsoo.** Deciphering Molecular Basis of Schwann Cell Development. 2009.
88. **Kati Helmja.** Determination of Phenolic Compounds and Their Antioxidative Capability in Plant Extracts. 2010.
89. **Merike Sõmera.** Sobemoviruses: Genomic Organization, Potential for Recombination and Necessity of P1 in Systemic Infection. 2010.
90. **Kristjan Laes.** Preparation and Impedance Spectroscopy of Hybrid Structures Based on CuIn<sub>3</sub>Se<sub>5</sub> Photoabsorber. 2010.
91. **Kristin Lippur.** Asymmetric Synthesis of 2,2'-Bimorpholine and its 5,5'-Substituted Derivatives. 2010.
92. **Merike Luman.** Dialysis Dose and Nutrition Assessment by an Optical Method. 2010.
93. **Mihhail Berezovski.** Numerical Simulation of Wave Propagation in Heterogeneous and Microstructured Materials. 2010.
94. **Tamara Aid-Pavlidis.** Structure and Regulation of BDNF Gene. 2010.
95. **Olga Bragina.** The Role of Sonic Hedgehog Pathway in Neuro- and Tumorigenesis. 2010.

96. **Merle Randrüüt.** Wave Propagation in Microstructured Solids: Solitary and Periodic Waves. 2010.
97. **Marju Laars.** Asymmetric Organocatalytic Michael and Aldol Reactions Mediated by Cyclic Amines. 2010.
98. **Maarja Grossberg.** Optical Properties of Multinary Semiconductor Compounds for Photovoltaic Applications. 2010.
99. **Alla Maloverjan.** Vertebrate Homologues of Drosophila Fused Kinase and Their Role in Sonic Hedgehog Signalling Pathway. 2010.
100. **Priit Pruunsild.** Neuronal Activity-Dependent Transcription Factors and Regulation of Human *BDNF* Gene. 2010.
101. **Tatjana Knjazeva.** New Approaches in Capillary Electrophoresis for Separation and Study of Proteins. 2011.
102. **Atanas Katerski.** Chemical Composition of Sprayed Copper Indium Disulfide Films for Nanostructured Solar Cells. 2011.
103. **Kristi Timmo.** Formation of Properties of  $\text{CuInSe}_2$  and  $\text{Cu}_2\text{ZnSn}(\text{S,Se})_4$  Monograin Powders Synthesized in Molten KI. 2011.
104. **Kert Tamm.** Wave Propagation and Interaction in Mindlin-Type Microstructured Solids: Numerical Simulation. 2011.
105. **Adrian Popp.** Ordovician Proetid Trilobites in Baltoscandia and Germany. 2011.
106. **Ove Pärn.** Sea Ice Deformation Events in the Gulf of Finland and This Impact on Shipping. 2011.
107. **Germo Väli.** Numerical Experiments on Matter Transport in the Baltic Sea. 2011.
108. **Andrus Seiman.** Point-of-Care Analyser Based on Capillary Electrophoresis. 2011.
109. **Olga Katargina.** Tick-Borne Pathogens Circulating in Estonia (Tick-Borne Encephalitis Virus, *Anaplasma phagocytophilum*, *Babesia* Species): Their Prevalence and Genetic Characterization. 2011.
110. **Ingrid Sumeri.** The Study of Probiotic Bacteria in Human Gastrointestinal Tract Simulator. 2011.
111. **Kairit Zovo.** Functional Characterization of Cellular Copper Proteome. 2011.
112. **Natalja Makarytsheva.** Analysis of Organic Species in Sediments and Soil by High Performance Separation Methods. 2011.
113. **Monika Mortimer.** Evaluation of the Biological Effects of Engineered Nanoparticles on Unicellular Pro- and Eukaryotic Organisms. 2011.
114. **Kersti Tepp.** Molecular System Bioenergetics of Cardiac Cells: Quantitative Analysis of Structure-Function Relationship. 2011.
115. **Anna-Liisa Peikolainen.** Organic Aerogels Based on 5-Methylresorcinol. 2011.
116. **Leeli Amon.** Palaeoecological Reconstruction of Late-Glacial Vegetation Dynamics in Eastern Baltic Area: A View Based on Plant Macrofossil Analysis. 2011.
117. **Tanel Peets.** Dispersion Analysis of Wave Motion in Microstructured Solids. 2011.

118. **Liina Kaupmees**. Selenization of Molybdenum as Contact Material in Solar Cells. 2011.
119. **Allan Olsper**. Properties of VPg and Coat Protein of Sobemoviruses. 2011.
120. **Kadri Koppel**. Food Category Appraisal Using Sensory Methods. 2011.
121. **Jelena Gorbatšova**. Development of Methods for CE Analysis of Plant Phenolics and Vitamins. 2011.
122. **Karin Viipsi**. Impact of EDTA and Humic Substances on the Removal of Cd and Zn from Aqueous Solutions by Apatite. 2012.
123. **David Schryer**. Metabolic Flux Analysis of Compartmentalized Systems Using Dynamic Isotopologue Modeling. 2012.
124. **Ardo Illaste**. Analysis of Molecular Movements in Cardiac Myocytes. 2012.
125. **Indrek Reile**. 3-Alkylcyclopentane-1,2-Diones in Asymmetric Oxidation and Alkylation Reactions. 2012.
126. **Tatjana Tamberg**. Some Classes of Finite 2-Groups and Their Endomorphism Semigroups. 2012.
127. **Taavi Liblik**. Variability of Thermohaline Structure in the Gulf of Finland in Summer. 2012.
128. **Priidik Lagemaa**. Operational Forecasting in Estonian Marine Waters. 2012.
129. **Andrei Errapart**. Photoelastic Tomography in Linear and Non-linear Approximation. 2012.
130. **Külliki Krabbi**. Biochemical Diagnosis of Classical Galactosemia and Mucopolysaccharidoses in Estonia. 2012.
131. **Kristel Kaseleht**. Identification of Aroma Compounds in Food using SPME-GC/MS and GC-Olfactometry. 2012.
132. **Kristel Kodar**. Immunoglobulin G Glycosylation Profiling in Patients with Gastric Cancer. 2012.
133. **Kai Rosin**. Solar Radiation and Wind as Agents of the Formation of the Radiation Regime in Water Bodies. 2012.
134. **Ann Tiiman**. Interactions of Alzheimer's Amyloid-Beta Peptides with Zn(II) and Cu(II) Ions. 2012.
135. **Olga Gavrilova**. Application and Elaboration of Accounting Approaches for Sustainable Development. 2012.
136. **Olesja Bondarenko**. Development of Bacterial Biosensors and Human Stem Cell-Based *In Vitro* Assays for the Toxicological Profiling of Synthetic Nanoparticles. 2012.
137. **Katri Muska**. Study of Composition and Thermal Treatments of Quaternary Compounds for Monograin Layer Solar Cells. 2012.
138. **Ranno Nahku**. Validation of Critical Factors for the Quantitative Characterization of Bacterial Physiology in Accelerostat Cultures. 2012.
139. **Petri-Jaan Lahtvee**. Quantitative Omics-level Analysis of Growth Rate Dependent Energy Metabolism in *Lactococcus lactis*. 2012.
140. **Kerti Orumets**. Molecular Mechanisms Controlling Intracellular Glutathione Levels in Baker's Yeast *Saccharomyces cerevisiae* and its Random Mutagenized Glutathione Over-Accumulating Isolate. 2012.
141. **Loreida Timberg**. Spice-Cured Sprats Ripening, Sensory Parameters Development, and Quality Indicators. 2012.

142. **Anna Mihhalevski.** Rye Sourdough Fermentation and Bread Stability. 2012.
143. **Liisa Arike.** Quantitative Proteomics of *Escherichia coli*: From Relative to Absolute Scale. 2012.
144. **Kairi Otto.** Deposition of In<sub>2</sub>S<sub>3</sub> Thin Films by Chemical Spray Pyrolysis. 2012.
145. **Mari Sepp.** Functions of the Basic Helix-Loop-Helix Transcription Factor TCF4 in Health and Disease. 2012.
146. **Anna Suhhova.** Detection of the Effect of Weak Stressors on Human Resting Electroencephalographic Signal. 2012.
147. **Aram Kazarjan.** Development and Production of Extruded Food and Feed Products Containing Probiotic Microorganisms. 2012.
148. **Rivo Uiboupin.** Application of Remote Sensing Methods for the Investigation of Spatio-Temporal Variability of Sea Surface Temperature and Chlorophyll Fields in the Gulf of Finland. 2013.
149. **Tiina Kriščiunaite.** A Study of Milk Coagulability. 2013.
150. **Tuuli Levandi.** Comparative Study of Cereal Varieties by Analytical Separation Methods and Chemometrics. 2013.
151. **Natalja Kabanova.** Development of a Microcalorimetric Method for the Study of Fermentation Processes. 2013.
152. **Himani Khanduri.** Magnetic Properties of Functional Oxides. 2013.
153. **Julia Smirnova.** Investigation of Properties and Reaction Mechanisms of Redox-Active Proteins by ESI MS. 2013.
154. **Mervi Sepp.** Estimation of Diffusion Restrictions in Cardiomyocytes Using Kinetic Measurements. 2013.
155. **Kersti Jääger.** Differentiation and Heterogeneity of Mesenchymal Stem Cells. 2013.
156. **Victor Alari.** Multi-Scale Wind Wave Modeling in the Baltic Sea. 2013.
157. **Taavi Päll.** Studies of CD44 Hyaluronan Binding Domain as Novel Angiogenesis Inhibitor. 2013.
158. **Allan Niidu.** Synthesis of Cyclopentane and Tetrahydrofuran Derivatives. 2013.
159. **Julia Geller.** Detection and Genetic Characterization of *Borrelia* Species Circulating in Tick Population in Estonia. 2013.
160. **Irina Stulova.** The Effects of Milk Composition and Treatment on the Growth of Lactic Acid Bacteria. 2013.
161. **Jana Holmar.** Optical Method for Uric Acid Removal Assessment During Dialysis. 2013.
162. **Kerti Ausmees.** Synthesis of Heterobicyclo[3.2.0]heptane Derivatives *via* Multicomponent Cascade Reaction. 2013.
163. **Minna Varikmaa.** Structural and Functional Studies of Mitochondrial Respiration Regulation in Muscle Cells. 2013.
164. **Indrek Koppel.** Transcriptional Mechanisms of BDNF Gene Regulation. 2014.
165. **Kristjan Pilt.** Optical Pulse Wave Signal Analysis for Determination of Early Arterial Ageing in Diabetic Patients. 2014.
166. **Andres Anier.** Estimation of the Complexity of the Electroencephalogram for Brain Monitoring in Intensive Care. 2014.

167. **Toivo Kallaste**. Pyroclastic Sanidine in the Lower Palaeozoic Bentonites – A Tool for Regional Geological Correlations. 2014.
168. **Erki Kärber**. Properties of ZnO-nanorod/In<sub>2</sub>S<sub>3</sub>/CuInS<sub>2</sub> Solar Cell and the Constituent Layers Deposited by Chemical Spray Method. 2014.
169. **Julia Lehner**. Formation of Cu<sub>2</sub>ZnSnS<sub>4</sub> and Cu<sub>2</sub>ZnSnSe<sub>4</sub> by Chalcogenisation of Electrochemically Deposited Precursor Layers. 2014.
170. **Peep Pitk**. Protein- and Lipid-rich Solid Slaughterhouse Waste Anaerobic Co-digestion: Resource Analysis and Process Optimization. 2014.
171. **Kaspar Valgepea**. Absolute Quantitative Multi-omics Characterization of Specific Growth Rate-dependent Metabolism of *Escherichia coli*. 2014.
172. **Artur Noole**. Asymmetric Organocatalytic Synthesis of 3,3'-Disubstituted Oxindoles. 2014.
173. **Robert Tsanev**. Identification and Structure-Functional Characterisation of the Gene Transcriptional Repressor Domain of Human Gli Proteins. 2014.
174. **Dmitri Kartofelev**. Nonlinear Sound Generation Mechanisms in Musical Acoustic. 2014.
175. **Sigrid Hade**. GIS Applications in the Studies of the Palaeozoic Graptolite Argillite and Landscape Change. 2014.
176. **Agne Velthut-Meikas**. Ovarian Follicle as the Environment of Oocyte Maturation: The Role of Granulosa Cells and Follicular Fluid at Pre-Ovulatory Development. 2014.
177. **Kristel Hälvin**. Determination of B-group Vitamins in Food Using an LC-MS Stable Isotope Dilution Assay. 2014.
178. **Mailis Päre**. Characterization of the Oligoadenylate Synthetase Subgroup from Phylum Porifera. 2014.
179. **Jekaterina Kazantseva**. Alternative Splicing of *TAF4*: A Dynamic Switch between Distinct Cell Functions. 2014.
180. **Jaanus Suurväli**. Regulator of G Protein Signalling 16 (RGS16): Functions in Immunity and Genomic Location in an Ancient MHC-Related Evolutionarily Conserved Synteny Group. 2014.
181. **Ene Viiard**. Diversity and Stability of Lactic Acid Bacteria During Rye Sourdough Propagation. 2014.
182. **Kristella Hansen**. Prostaglandin Synthesis in Marine Arthropods and Red Algae. 2014.
183. **Helike Lõhelaid**. Allene Oxide Synthase-lipoxygenase Pathway in Coral Stress Response. 2015.
184. **Normunds Stivrīnš**. Postglacial Environmental Conditions, Vegetation Succession and Human Impact in Latvia. 2015.
185. **Mary-Liis Kütt**. Identification and Characterization of Bioactive Peptides with Antimicrobial and Immunoregulating Properties Derived from Bovine Colostrum and Milk. 2015.
186. **Kazbulat Šogenov**. Petrophysical Models of the CO<sub>2</sub> Plume at Prospective Storage Sites in the Baltic Basin. 2015.
187. **Taavi Raadik**. Application of Modulation Spectroscopy Methods in Photovoltaic Materials Research. 2015.

188. **Reio Põder**. Study of Oxygen Vacancy Dynamics in Sc-doped Ceria with NMR Techniques. 2015.
189. **Sven Siir**. Internal Geochemical Stratification of Bentonites (Altered Volcanic Ash Beds) and its Interpretation. 2015.
190. **Kaur Jaanson**. Novel Transgenic Models Based on Bacterial Artificial Chromosomes for Studying BDNF Gene Regulation. 2015.
191. **Niina Karro**. Analysis of ADP Compartmentation in Cardiomyocytes and Its Role in Protection Against Mitochondrial Permeability Transition Pore Opening. 2015.
192. **Piret Laht**. B-plexins Regulate the Maturation of Neurons Through Microtubule Dynamics. 2015.
193. **Sergei Žari**. Organocatalytic Asymmetric Addition to Unsaturated 1,4-Dicarbonyl Compounds. 2015.
194. **Natalja Buhhallo**. Processes Influencing the Spatio-temporal Dynamics of Nutrients and Phytoplankton in Summer in the Gulf of Finland, Baltic Sea. 2015.
195. **Natalia Maticiuc**. Mechanism of Changes in the Properties of Chemically Deposited CdS Thin Films Induced by Thermal Annealing. 2015.
196. **Mario Öeren**. Computational Study of Cyclohexylhemicucurbiturils. 2015.
197. **Mari Kalda**. Mechanoenergetics of a Single Cardiomyocyte. 2015.
198. **Ieva Grudzinska**. Diatom Stratigraphy and Relative Sea Level Changes of the Eastern Baltic Sea over the Holocene. 2015.
199. **Anna Kazantseva**. Alternative Splicing in Health and Disease. 2015.
200. **Jana Kazarjan**. Investigation of Endogenous Antioxidants and Their Synthetic Analogues by Capillary Electrophoresis. 2016.
201. **Maria Safonova**. SnS Thin Films Deposition by Chemical Solution Method and Characterization. 2016.